The Dissertation Committee for Md Golam Sarwar Certifies that this is the approved version of the following dissertation:

FINE PARTICLE FORMATION IN INDOOR ENVIRONMENTS: LEVELS, INFLUENCING FACTORS AND IMPLICATIONS

Committee:

_____
Richard L. Corsi, Supervisor

_____
David T. Allen, Co-Supervisor

_____
Howard M. Liljestrand

_____
Desmond F. Lawler

_____
Kerry A. Kinney

FINE PARTICLE FORMATION IN INDOOR ENVIRONMENTS: LEVELS, INFLUENCING FACTORS AND IMPLICATIONS

by

Md Golam Sarwar, B.S., M.S.

Dissertation

Presented to the Faculty of the Graduate School of

The University of Texas at Austin

in Partial Fulfillment

of the Requirements

for the Degree of

Doctor of Philosophy

The University of Texas at Austin

May 2002

Dedicated to my daughter, Tasnia Sarwar

ACKNOWLEDGEMENTS

I would like to express my sincere gratitude to Professor Richard Corsi for his guidance and support throughout my doctoral program. His encouragement and motivation helped me to complete this research on time. I would also like to thank other members of my dissertation committee, Professors David Allen, Howard Liljestrand, Desmond Lawler, and Kerry Kinney, for their encouragement throughout my doctoral program. I like to recognize the Texas Air Research Council for providing financial support for this research.

I would also like to recognize Professor Charles Weschler of UMDNJ for his valuable time and help throughout this project. He was always available for discussion and provided invaluable insight on numerous issues related to indoor air chemistry.

I like to thank David Olson, Paul Tanaka, and Dr. Yosuke Kimura of the Center for Energy and Environmental Resources for their help on many occasions during this project. I like to thank to Dori Eubank of Team Corsi for her administrative assistance during the last two years.

I wish to recognize my wife for her encouragement and for releasing me from many household duties to allow me spend more time on research. I also wish to thank my parents and relatives for their continued encouragement throughout my education.

May 2002

FINE PARTICLE FORMATION IN INDOOR ENVIRONMENTS: LEVELS, INFLUENCING FACTORS AND IMPLICATIONS

Publication No. _____

Md Golam Sarwar, Ph.D.
The University of Texas at Austin, 2002

Supervisors: Richard L. Corsi and David T. Allen

Experiments were conducted in an 11-m^3 stainless steel chamber to investigate secondary particle formation/growth in indoor environments. Experimental results indicate that rapid particle growth occurs due to homogeneous reactions between ozone and terpenes, and subsequent gas-to-particle partitioning of reaction products. Experimental results also indicate that many consumer products can emit significant amounts of terpenes that can serve as precursors to the formation of indoor fine particles.

A new Indoor Chemistry and Exposure Model (ICEM) was used to predict dynamic particle mass concentrations based on detailed homogeneous chemical mechanisms and partitioning of semi-volatile products to particles. The ICEM allows for the simulation of air exchange processes, indoor emissions, chemical reactions, deposition, and variations in outdoor air quality. Predicted indoor secondary particle mass concentrations are in good agreement with experimental results.

Both experimental and model results suggest that secondary particle mass concentrations increase significantly at lower building air exchange rates. This result

is significant given a continuing trend toward building weatherization for purposes of energy conservation. Predicted indoor secondary particle concentrations increase with lower temperatures, higher outdoor particle levels, higher outdoor ozone levels, and higher indoor terpene emission rates. Indoor secondary particle concentrations resulting from reactions between ozone that originates outdoors and terpenes that originate from indoor sources can be higher than indoor particle concentrations resulting from the transport of outdoor particles. If ozone generation air "purifiers" and elevated terpene levels are simultaneously present in indoor environments, the resulting indoor secondary particle mass concentrations can exceed 65 $\mu g/m^3$.

The implications of this study are significant. It appears that it is now possible to reasonably simulate complex indoor chemistry and particle growth dynamics using a state-of-the-art model (ICEM). More importantly, it appears that under some conditions, indoor air chemistry can lead to significant increases in human exposure to fine particles. Such exposure could be reduced by avoiding indoor sources of ozone, e.g., from ozone generators marketed as air "purifiers", or by reducing the use of consumer products that contain terpenes, especially during the summer ozone season.

TABLE OF CONTENTS

LIST OF TABLES

LIST OF FIGURES

1.0 INTRODUCTION

1.1 Problem Statement

Fine particles can penetrate deep into the human lung where scarring of the alveolar region and/or dissolution of toxic chemicals into the blood stream are possible. Recent epidemiological and related studies have linked fine particles to human health and welfare effects including premature mortality (Pope and Dockery, 1996; USEPA, 1997). These findings have prompted the United States Environmental Protection Agency (USEPA) to promulgate a new national ambient air quality standard for fine particles.

While the aforementioned regulations focus entirely on outdoor air quality, the average American spends 18 hours indoors for every hour spent outdoors (Robinson *et al*., 1991). Using results of the three major indoor particle characterization studies in the United States, Wallace (1996) concluded that mean indoor fine particle levels are at least 90% or more of the mean outdoor fine particle levels. Thus, human exposure to fine particles in indoor environments can be a major fraction of total exposure to fine particles. Additionally, based on the results of bioassay experiments involving rats, Long *et al*. (2001) recently concluded that particles generated indoors may be more bioactive than particles generated outdoors.

Santannam *et al*. (1990) reported the results of indoor and outdoor sampling completed at 280 residences in Ohio and Wisconsin. The average "unexplained" percentage of indoor fine particles, i.e., those that could not be attributed to specific sources, ranged from 19 to 42%. Similar results (average of 25% "unexplained" fine particles) were observed during the USEPA's PTEAM study (Wallace, 1996). Wallace concluded that the unexplained fraction of fine particles should be the focus of future studies. Wainman (1999) further reported that the "unknown" indoor fine

particle concentration in the PTEAM study was 8.75 $\mu g/m^3$ during the daytime, and 6.75 $\mu g/m^3$ during nighttime.

Recent studies suggest that indoor air chemistry, particularly as related to reactions between terpenes that originate from indoor sources and ozone (O_3) that originates outdoors, can be an important source of indoor fine particles (Weschler and Shields, 1999; Wainman *et al*., 2000; Long *et al*., 2000; Rohr *et al*., 2001; and Weschler and Shields, 2002). Weschler and Shields (1999) observed this phenomenon by tracking indoor O_3 and particle levels, and through the selective release of limonene in an office building. Long *et al*. (2000) reported evidence that chemical reactions are a potentially important source of ultra-fine particles in residential homes. Wainman *et al*. (2000) conducted experiments in a nested chamber and demonstrated that large-scale particle formation and growth can occur when limonene and O_3 react in indoor environments. Rohr *et al*. (2001) conducted experiments in a plexiglas chamber using α-pinene and O_3, and concluded that fine particle formation and growth can occur in indoor environments due to the interactions between these pollutants. Weschler and Shields (2002) reported that lower air exchange rates shift the resulting secondary particle size distribution toward larger sizes and lead to increased particle mass concentrations.

Such findings, albeit sparse and somewhat preliminary in nature, might provide an explanation for the "unexplained" indoor fine particles reported in previous studies. If O_3/terpene reactions are found to be an important source of indoor fine particles, it may be logical to reduce human exposure to fine particles by reducing precursor compounds such as terpenes in indoor environments. Indoor secondary particles associated with the reactions of α-pinene and limonene with O_3 were the focus of this study.

1.2 Research Objectives

The overall objective of this study was to develop a better understanding of the role of indoor air chemistry on indoor particle levels. Specific objectives included:

(1) Evaluate the role of reactions between α-pinene and O_3, and limonene and O_3, on indoor secondary particle levels in indoor environments.

(2) Evaluate the potential for secondary particle growth following the use of common consumer products in the presence of O_3.

(3) Develop a model that can simulate the complex interactions between indoor and outdoor environments. Incorporate the reaction mechanism for α-pinene leading to fine particle growth.

(4) Use the model to evaluate indoor radical levels under a wide range of outdoor air quality conditions and indoor source scenarios, and evaluate the importance of $OH^{\cdot}$/terpene reactions with respect to indoor particle growth.

(5) Use the model to investigate the effects of selected parameters on indoor secondary particle levels.

(6) Use the model to assess indoor secondary particles in Houston due to O_3/terpene reactions. Assess the relative importance of human exposure to fine particles from indoor and outdoor sources.

1.3 Scope of Research

This study was completed in two phases. The first phase included a series of 27 chamber experiments with pure α-pinene, pure limonene, and six different consumer products. The second phase included the development of an Indoor Chemistry and Exposure Model (ICEM). The ICEM was then used to predict chamber particle mass concentrations due to O_3/terpene reactions. Predicted concentrations were compared to experimental results. The ICEM was used to estimate radical concentrations in indoor air under a wide range of outdoor air quality conditions and indoor source scenarios, and to investigate the effects of selected parameters on indoor secondary particle levels. The model was applied to indoor environments under conditions consistent with the Houston airshed using ambient data available from the Texas Natural Resource Conservation Commission.

1.4 Organization of Dissertation

An overview of the existing literature on indoor particles, O_3, and terpenes as well as a summary of the existing knowledge on indoor chemistry are presented in Chapter 2. Chapter 3 provides an overview of the Statewide Air Pollution Research Center (SAPRC) model, development of ICEM, particle chemistry for α-pinene, a description of the input parameters to ICEM, and limonene reaction mechanism and associated products. The experimental program, experimental systems, sampling and analytical methods, quality assurance procedures, and determination of ozone and particle deposition velocities in the chamber are presented in Chapter 4. Experimental results are presented in Chapter 5. Applications of the model to investigate the effects of selected parameters on indoor secondary particle levels and to predict indoor radical levels are presented in Chapter 6. General implications of indoor secondary particles and application of ICEM to Houston airshed conditions are presented in Chapter 7. Conclusions stemming from this study and recommendations for future research are presented in Chapter 8.

2.0 LITERATURE REVIEW

2.1 Particles in Indoor Environments

Three major indoor particle characterization studies have been completed in the United States: the Harvard Six City study, the New York State study, and the USEPA Particle Total Exposure Assessment Methodology (PTEAM) study (Wallace, 1996). In addition, several smaller investigations have been completed on the relationship between indoor and outdoor particles (Wallace, 1996).

Yocum (1971) measured total suspended particle (TSP) concentrations in multiple buildings and reported that the average indoor TSP levels were only about 50% of outdoor levels. Spengler *et al*. (1981) presented early results of the Harvard Six City study and reported that the annual mean $PM_{3.5}$ (particles with diameters less than 3.5 μm) concentration was slightly higher indoors than outdoors in 35 residences without smokers. Homes occupied by one or two smokers had significantly higher $PM_{3.5}$ concentrations indoors than outdoors. However, data reported by Yocum (1971) and Spengler *et al*. (1981) were collected prior to significant reductions made in building fresh air exchange rates over the past 20 years for purposes of energy conservation.

Li and Harrison (1990) measured indoor and outdoor concentrations of acid gases, ammonia and their associated salts in Essex, UK. Indoor inorganic particle levels were found to correlate well with outdoor particle levels, with an indoor-to-outdoor concentration ratio (I/O) of less than unity. Brauer *et al*. (1991) simultaneously measured indoor and outdoor inorganic acidic aerosols and gases in Boston, Massachusetts. The authors reported that the average I/O ratio for an urban area was very close to unity, and in a suburban area the I/O ratio was 1.52 in summer and 0.87 in winter.

Wallace (1996) presented an excellent review of studies related to fine particles in indoor and outdoor environments. He compared the results of the Harvard Six City study, the New York State study, the PTEAM study, and several smaller studies. The Harvard Six-City study was initiated in 1979 and continued through 1988, during which indoor and outdoor particles were simultaneously measured for 1,400 homes. The mean indoor fine particle concentration ($PM_{2.5}$) was higher than the mean outdoor concentration for most of the cities. The New York State study (Wallace, 1996) was completed in 1986 and involved 433 residences in two counties. The indoor geometric mean $PM_{2.5}$ concentration exceeded the outdoor concentration by approximately a factor of two in each county. The PTEAM study was conducted in 1990 and involved simultaneous measurements of indoor and outdoor particles in 178 homes in California. The mean indoor $PM_{2.5}$ concentration was lower than the outdoor concentration by about 6.0 $\mu g/m^3$. Environmental tobacco smoke and cooking were identified as the two most significant indoor sources of $PM_{2.5}$.

Attempts to explain the origin of indoor fine particles through knowledge of indoor sources, outdoor penetration, and elemental analysis of particles has led to an important finding. Santannam *et al*. (1990) presented the results of indoor and outdoor sampling completed at 280 residences in Ohio and Wisconsin, and reported that 19 to 42% of indoor $PM_{2.5}$ was due to "unexplained" sources. Wallace (1996) reported that an average of 25% of indoor $PM_{2.5}$ in the PTEAM study was due to "unexplained" sources and concluded that this "unexplained" $PM_{2.5}$ should be the focus of future studies.

Tropp *et al*. (1998) reported indoor and outdoor $PM_{2.5}$ concentrations in Houston, Texas. The average indoor $PM_{2.5}$ concentration was only about one-third of

the average outdoor $PM_{2.5}$ concentration. Despite the significant differences in $PM_{2.5}$ concentrations between indoor and outdoor environments, the indoor organic carbon concentration associated with fine particles was comparable to the outdoor organic carbon concentration. The authors did not identify the source of the higher organic content in indoor particles, but suggested that it may be the result of the adsorption of indoor hydrocarbons by indoor particles.

Jones *et al*. (2000) measured simultaneous indoor and outdoor particle concentrations in Birmingham, UK, and reported that the I/O ratio was always greater than unity. Indoor smoking and cooking were identified as the major sources of indoor $PM_{2.5}$. Consistent with the findings of Tropp *et al*. (1998), indoor organic carbon levels were higher than outdoor levels. The authors suggested that cooking and smoking may have contributed to higher indoor carbon levels.

By applying a multiple regression model to measured particle concentrations in four homes, Abt *et al*. (2000) determined the relative contribution of indoor and outdoor sources. The authors concluded that 57-80% of indoor coarse particles (2-10μm) was contributed by indoor sources. In contrast, only 8-37% of indoor fine particles (0.02-0.3μm) was contributed by indoor sources.

Pollutant penetration factor is a unitless parameter that accounts for fractional penetration through the building envelope. Mosley *et al*. (2001) recently conducted experiments to determine outdoor-to-indoor particle penetration factors for simulated indoor environments. Two identical compartments of 19 m^3 were used in the experiments. These compartments were connected by small slits, designed to simulate leakage in buildings. Particles were generated in one compartment and transported to the other by the application of a differential pressure. Particle concentrations were simultaneously measured in both compartments and penetration

factors were determined by solving mass balance equations in each compartment. Penetration factors were found to depend on particle size and applied pressure drop. The authors reported a penetration factor of only 0.02 for particles with aerodynamic diameters of 2 μm and 0.001 for particles with aerodynamic diameters of 5 μm for a pressure difference of 2 Pa. For a pressure difference of 5 Pa, the penetration factor for particles with aerodynamic diameters of 2 μm was 0.4 and the penetration factor was less than 0.1 for an aerodynamic diameter less than 5 μm. Penetration factors for particles with aerodynamic diameters less than 2 μm were markedly higher than for particles with aerodynamic diameters of 2 μm. Penetration factors for particles with aerodynamic diameters less than 2 μm reached close to unity. A pressure differential of 2-5 Pa is common in buildings in moderate and near freezing weather. Liu and Nazaroff (2001) performed a detailed modeling study to estimate penetration factors for particles and reported that essentially all fine particles penetrate through building envelopes.

A summary of reported average indoor and outdoor fine particle concentrations and the corresponding I/O ratios are presented in Table 2.1. The reported I/O ratios for fine particles vary widely, ranging from 0.5 to 1.9. However, most of these studies indicate that average fine particle concentrations are close to, or higher than, corresponding outdoor concentrations, which strongly suggests the presence of indoor sources of fine particles.

There is recent evidence that indoor chemistry, as related to reactions between terpenes that originate from indoor sources and ozone that originates outdoors, can be an important source of indoor fine particles (Weschler and Shields, 1999; Shaughnessy *et al.*, 1999; Long *et al.*, 2000; Wainman *et al.*, 2000; Rohr *et al.*, 2001; and Weschler and Shields, 2002). Weschler and Shields (1999) selectively introduced limonene, α-terpinene and a terpene-based cleaner into two adjacent

unoccupied and identical office buildings. In one of the office buildings, an O_3 generator was operated to raise the indoor O_3 levels to 200-300 ppb. The other office building did not have an O_3 generator; however, outdoor-to-indoor transport lead to indoor O_3 levels of between 2-40 ppb.

Table 2.1. Reported Average Indoor and Outdoor Fine Particle Concentrations

Pollutants	Indoor Levels ($\mu g/m^3$)	Outdoor Levels ($\mu g/m^3$)	I/O (-)	Locations	Reference
$PM_{3.5}$	24.4	21.1	1.2	Homes Six Cities in USA	Spengler *et al*., 1981
$PM_{3.0}$	120.0	64.0	1.9	Homes Arnhem, Netherland	Diemel *et al*., 1981
RSP	25.0	19.0	1.3	Homes Waterbury, Vermont	Sexton *et al*., 1984
$PM_{2.5}$	33.0	24.7	1.3	Homes Houston, Texas	Kim and Stock, 1986
$PM1_{1.0}$	16.0	20.0	0.8	Homes Helsinki, Finland	Wallace, 1996
$PM_{2.5}$	25.7	15.8	1.6	Homes Onondaga, New York	Sheldon *et al*., 1989
$PM_{2.5}$	35.9	18.6	1.9	Homes Suffolk, New York	Sheldon *et al*., 1989
RSP	24.0	14.0	1.7	Commercial Buildings Oregon and Washington	Turk *et al*., 1989
$PM_{2.5}$	35.0	38.0	0.9	Homes (day) Riverside, California	Clayton *et al*., 1993
$PM_{2.5}$	27.0	37.0	0.7	Homes (night) Riverside, California	Clayton *et al*., 1993
RSP	8.0	4.2	1.9	Office Building Rio de Jenario, Brazil	Brickus *et al*., 1998
$PM_{2.5}$	22.0	33.0	0.7	Homes (day) Nashville, Tennessee	Wallace, 1996
$PM_{2.5}$	15.0	32.0	0.5	Homes (night) Nashville, Tennessee	Wallace, 1996
$PM_{2.5}$	11.9	11.1	1.1	Homes Boston, Massachuchates	Long *et al*., 2000

RSP = Respirable Suspended Particulate ($PM_{3.5}$)

Indoor particles were continuously monitored in both offices by optical particle counters. The authors reported a significant increase in particle number concentrations in the sub-micron range in the office with elevated O_3. The increase was highest in the 0.1-0.2 μm size range (lowest detectable range). Increases in particle number concentration were highest during experiments with limonene. A different set of experiments was conducted in which only limonene was introduced into one of the office buildings. None of the office buildings received any additional O_3. Indoor O_3 was present due to outdoor-to-indoor transport and was between 2-40 ppb. The particle number concentration in the 0.1-0.2 μm diameter range was about 10 times as high in the office with limonene as compared to the office without the source of limonene. The difference in the particle mass in the sub-micron range was about 20 $\mu g/m^3$ between the two office buildings. Weschler and Shields (1999) also demonstrated that fine particle formation was greater as building fresh air intake was decreased. The authors attributed the formation and growth of indoor particles to O_3/terpene reactions and condensation of the subsequent by-products.

Shaughnessy *et al.* (1999) demonstrated the potential for heterogeneous reactions between O_3 and indoor materials to form ultra-fine particles. Elevated O_3 concentrations were maintained in a chamber that contained linoleum flooring. The inlet air to the chamber was filtered to maintain a negligible amount of initial particles and organic levels. Very low air exchange rates of 0.01-0.02 hr^{-1} were employed. Increased particle concentrations in the chamber suggest that O_3 reacted with unsaturated organic compounds in linoleum flooring.

Long *et al*. (2000) reported evidence that chemical reactions are a potentially important source of ultra-fine particles in indoor environments. The authors conducted six sampling events in Boston homes during which Pine Sol was used for mopping floors and toilet cleaning. Ozone was not deliberately added to these

homes; however O_3 was present indoors due to outdoor-to-indoor transport. Outdoor O_3 concentrations during these experiments varied between 1 to 52 ppb. Mean air exchange rates varied between 0.50 to 2.02 hr^{-1}. Real time particle number concentrations were monitored using a Scanning Particle Mobility Sizer (SPMS) and an Aerodynamic Particle Sizer (APS). Five of the six sampling events demonstrated significant fine particle formation. Maximum increases in indoor particle number and mass concentrations were 189,881 #/cm^3 and 32 $\mu g/m^3$, respectively. Particle number concentrations increased by 7-10 times relative to the original particle number concentrations. More than 50% of the particles (by volume) generated during these five events were ultra-fine in nature.

A nested dynamic system consisting of an inner and an outer chamber was used by Wainman *et al*. (2000) to investigate indoor particle formation and growth due to O_3/limonene reactions. The volume of the inner chamber was 2.5 m^3 and represented a model indoor environment. The volume of the outer chamber was 25 m^3 and represented the outdoor environment. Air exchange could occur between the inner and outer chambers. Limonene and O_3 were injected into the inner chamber. A laser based particle counter was used to measure particle number concentrations. Increases in particle numbers were observed immediately after the introduction of O_3. The greatest increase was observed in the 0.1-0.2 μm channel (the lowest detectable size). Air exchange rates during these experiments were between 0.52 and 0.65 hr^{-1}. Lower air exchange rates produced higher particle numbers and mass concentrations. Combining the results of this study with the earlier study of Weschler and Shields (1999), the investigators concluded that reactions of terpenes that originate from indoor sources and O_3 that originates outdoors can increase indoor particle mass concentration by more than 20 $\mu g/m^3$.

Rohr *et al.* (2001) recently conducted experiments with α-pinene and O_3 in a plexiglas chamber as part of a mouse bioassay study. Ozone concentrations during these experiments were in the range of 100-400 ppb and α-pinene concentrations were about 100 ppm, both much higher concentrations than typically encountered in indoor environments. Particles were monitored using a SMPS and significant increases in particle number concentrations were reported as a result of α-pinene and O_3 reactions.

Weschler and Shields (2002) also conducted experiments to determine the effects of air exchange rates on indoor secondary particle size distribution and mass concentrations. They introduced limonene into two adjacent unoccupied and identical office buildings. In one of the office buildings, an O_3 generator was operated to raise the indoor O_3 levels to 50-425 ppb. The other office building did not have an O_3 generator. The authors reported that the lower air exchange rates shifted the resulting secondary particle size distribution toward larger sizes and led to increased particle mass concentrations.

In summary, several studies have been completed to better understand the relationship between indoor and outdoor particles. The relationship is clearly complex and is affected by many factors. Past studies indicate that indoor fine particle concentrations are approximately equal to or greater than outdoor particle concentrations. These findings suggest that significant fine particle sources exist in indoor environments. Environmental tobacco smoke and cooking have been identified as two major indoor sources of particles. However, approximately 19-42% of indoor particle mass is due to "unexplained" sources. Recent investigations have shown that O_3/terpene reactions can produce significant indoor particle concentrations and can potentially account for some of these "unexplained" sources.

However, existing information related to indoor secondary organic aerosols is somewhat sparse and highly empirical in nature.

2.2 Terpenes in Indoor Environments

Terpenes are a special group of compounds primarily emitted from biogenic sources in the outdoor environment. However, as discussed later, many sources of terpenes exist in indoor environments. Isoprene (a C_5 compound) constitutes the building block of terpenes. Monoterpenes consist of two isoprenes (C_{10}), sesquiterpenes consist of three isoprenes (C_{15}), diterpenes consist of four isproenes (C_{20}), triterpenes consist of six isoprenes (C_{30}), and tetraterpenes consist of eight isoprenes (C_{40}) (Pitts and Pitts, 2000). Several common indoor terpenes are shown in Table 2.2.

Terpenes contain one or more carbon-carbon double bonds and can react with O_3, and $OH^{\cdot}$. Rate constants (k) for reactions of the common indoor terpenes with O_3 are also shown in Table 2.2. These rate constants are relatively high, and the time scales for indoor ozone/tepene reactions have been shown to be on the same order or less than typical residence times for air in residential and commercial buildings (Weschler and Shields, 1996).

Numerous organic compounds, including terpenes, have been measured in residential and commercial buildings, with indoor concentrations generally being significantly higher than outdoors (Weschler *et al.* 1990; Rothweiller *et al.,* 1992; Brown *et al.*, 1994; Daisy *et al.,* 1994; Fellin and Otson, 1994; Gebefuegi *et al.*, 1995; Brickus *et al.,* 1998). For example, Gebefuegi *et al.* (1995) reported an I/O concentration ratio of 12.4 for α-pinene and 14.7 for limonene. Brown *et al*. (1994) reported I/O values of 23 and 80 for α-pinene and limonene, respectively. Thus,

indoor sources of these terpenes are believed to be far more significant than outdoor-to-indoor transport.

Table 2.2. Common Indoor Terpenes*

Compound	Structure	k_{O3} at 298 °K (cm^3/molecule-sec)
α-Pinene	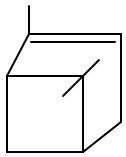	86.6×10^{-18}
β-Pinene	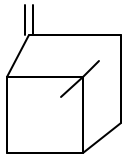	15.0×10^{-18}
Limonene	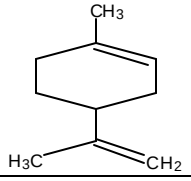	200.0×10^{-18}
α-Terpinene	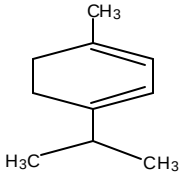	8470.0×10^{-18}
Δ^3-Carene	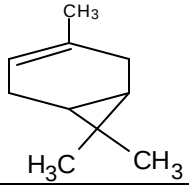	37.0×10^{-18}

* All information from Atkinson (1994)

Indoor sources of terpenes can be grouped into two categories: (1) building materials and (2) consumer products. Many building materials, including natural and engineered wood products (panel board, flooring, cabinetry, furniture, etc.), emit terpenes. For example, Saarela (1999) reviewed emissions from different floor materials and reported that terpenes can be emitted by some of these materials. A summary of the emission rates reported by Saarela (1999) is presented in Tables 2.3

and 2.4. Terpene emissions from building materials are most significant in new or renovated buildings.

Table 2.3. Selected Emission Rates for Different Plain Wood Boards (Saarela, 1999)

Compound	Plain Oak 3 days ($\mu g/m^2h$)	Plain Oak 28 days ($\mu g/m^2h$)	Plain Pine 3 days ($\mu g/m^2h$)	Plain Pine 28 days ($\mu g/m^2h$)
Limonene	5	2	48	10
α-Pinene	28	10	130	17

Table 2.4. Selected Emission Rates of Different Types of Parquets (Saarela, 1999)

Compound	Types of Parquets	Average 3 days ($\mu g/m^2h$)	Maximum 3 days ($\mu g/m^2h$)	Average 28 days ($\mu g/m^2h$)	Maximum 28 days ($\mu g/m^2h$)
Limonene	Varnished	3	4	4	8
α-Pinene	Varnished	15	25	8	19
Limonene	Oiled	5	5	7	8
α-Pinene	Oiled	14	17	10	12
Limonene	Waxed	67	67	40	75
α-Pinene	Waxed	341	1499	286	1371

Terpenes are used as odorants and solvents in a variety of consumer products, including bar soaps, shaving creams, deodorizers, nail colors and removers, air fresheners, perfumes, colognes, dishwashing liquids, liquid wax pastes, and furniture polishes (Wallace *et al.*, 1991; Salthammer, 1999). Wallace *et al.* (1991) tested 31 fragrance products for selected organic compounds; limonene was present in 23 products and α-pinene was present in 12 products.

Brown *et al.* (1994) conducted a review of VOC concentrations in indoor air and presented the overall weighted average geometric mean (WAGM), the 90th and 98th percentile concentrations, and the average maximum concentrations (AMC) of common indoor organic pollutants for established and new buildings. A summary of

the reported indoor limonene and α-pinene concentrations is provided in Table 2.5 (Brown *et al*., 1994). A maximum indoor limonene concentration of 81 ppb (450 $\mu g/m^3$) was reported in established buildings. A 98th percentile indoor α-pinene concentration of 449 ppb (2,500 $\mu g/m^3$) was reported for new dwellings. Indoor limonene concentrations of 175 ppb were also reported by Wainman *et al*. (2000).

Table 2.5. Terpene Concentrations in Indoor Environments (Brown *et al*., 1994).

Compound	Types of Building	WAGM ($\mu g/m^3$)	90th percentile value ($\mu g/m^3$)	98th percentile value ($\mu g/m^3$)	AMC ($\mu g/m^3$)
Limonene	Established Dwelling	21	85	200	450
α-Pinene	New Dwelling	260	1,100	2,500	NA
α-Pinene	New Office	8	32	76	NA
α-Pinene	New School	13	52	120	NA
α-Pinene	New Hospital	3	12	28	NA

The odor thresholds for α-pinene and limonene are each greater than 400 ppb (Molhave *et al*., 2000). Odors of lemon and pine can often be detected following application of many consumer products, indicating that indoor concentrations indeed exceed odor thresholds, especially in close proximity to the source. Indoor concentrations reported in the published literature have typically not been measured during the application of consumer products and are often based on long-term averaging, thereby yielding lower concentrations.

In summary, building materials as well as consumer products can emit terpenes. Terpene concentrations measured indoors are significantly higher than those measured outdoors. Peak indoor α-pinene and limonene concentrations can exceed 400 ppb.

2.3 Ozone in Indoor Environments

A number of researchers have reported on the relationship between indoor and outdoor O_3 concentrations (Sabersky *et al*., 1973; Mueller *et al*., 1973; Shair and Heitner, 1974; Hales *et al*., 1974; Nazaroff and Cass, 1986; Weschler, 1989; Hayes, 1991; Gold *et al*., 1996; and Lee *et al*., 1999). There is general agreement that outdoor to indoor transport is the main source of indoor O_3, and indoor O_3 concentrations typically track outdoor O_3 concentrations (Sabersky and Shair *et al*., 1973).

Sabersky *et al*. (1973) were amongst the first researchers to report elevated levels of indoor ozone. They reported a peak I/O value of 0.80 for a building with a heating, ventilating, and air conditioning (HVAC) system operating with 100% outside air, and a value of 0.65 for a building with an HVAC system operating with 70% outside air. However, indoor O_3 concentrations and associated exposure has received relatively little attention for the last three decades. Increasing attention is now being given to indoor O_3, as a result of growing recognition that indoor inhalation exposure can represent a major fraction of total human exposure (Weschler *et al*., 1989) and can initiate significant indoor chemical reactions (Weschler *et al*., 1997a and Weschler, 2000).

Nazaroff and Cass (1986) were the first to develop a model that included chemistry, ventilation, filtration, surface removal, and indoor emissions. A total of 57 chemical reactions were included in the model. The predicted indoor pollutant levels, including O_3, were found to be in good agreement with measured pollutant levels. The average indoor O_3 concentration was 45% of the average outdoor O_3 concentration.

Weschler *et al*. (1989) conducted simultaneous measurements of indoor and outdoor O_3 levels in three office buildings in Suburban New Jersey. Indoor O_3 levels were found to track outdoor O_3 levels and were between 20-80% of outdoor levels. A simple mass balance model that incorporated the effects of air exchange rates and surface deposition was able to effectively predict indoor O_3 levels from known outdoor O_3 levels. The authors concluded that human exposure to indoor O_3 is greater than exposure to outdoor O_3.

Hayes (1991) performed an extensive modeling study to estimate indoor O_3 levels and reported peak I/O ratios for homes, office buildings, and vehicles. For homes, he predicted a value of 0.65 with windows open, 0.36 with the HVAC system operating, 0.23 with windows closed and no HVAC operation, and 0.05 for energy efficient buildings with windows closed. For office buildings, he predicted a value of 0.82 with the HVAC system operating with 100% outdoor air, 0.60 with a typical HVAC system, and 0.32 with an energy efficient HVAC system. For vehicles with windows closed, he reported a value of 0.41 at 85 miles per hour, 0.33 at 55 miles per hour, and 0.21 at 10 miles per hour. Higher air exchange rates, in general, were accompanied by higher indoor O_3 concentrations.

Gold *et al*. (1999) measured indoor O_3 concentrations at a school in Mexico City where the average outdoor O_3 level was 170 ppb. The authors reported an I/O value of 0.74 with windows/doors open, 0.21 with windows/doors closed and air cleaners off; and 0.17 with windows/doors closed and air cleaners on. Lee *et al*. (1999) measured O_3 deposition rates in 43 Southern California homes and reported a mean I/O value of 0.68 for homes not using an HVAC system and with windows open, and a mean I/O value of less than 0.10 for homes with HVAC systems on.

Weschler (2000) conducted a review of indoor O_3 and stated that indoor O_3 levels depend on outdoor O_3 levels, indoor sources, air exchange rates, surface removal rates, and any possible reactions with common indoor pollutants. Outdoor to indoor transport is the main source of indoor O_3 for most buildings; however, sources of O_3 can also be present in buildings. For example, photocopy machines, laser printers, electrostatic air filters and electrostatic precipitators have been shown to produce O_3 in buildings (Weschler, 2000). Black and Worthan (1999) reported average O_3 emission rates of dry process photocopiers and laser printers of 5.2 and 1.2 mg/hr, respectively. Several companies sell ozone generators for reducing indoor odors. Emission rates of these air "purifiers" can be as high as a few thousand milligrams per hour (Weschler, 2000). In contrast, an episodic summertime O_3 concentration of 200 ppb would produce an outdoor-to-indoor mass flow of 100 mg/hr for a 500 m^3 home with an air exchange rate of 0.5 hr^{-1} at 25 ^oC.

In the absence of indoor O_3 sources and homogeneous chemical reactions in buildings, the steady state value of I/O for ozone can be estimated by:

$$I/O = \lambda / [V_d(A/V) + \lambda] \qquad (2.1)$$

where, I is the indoor O_3 concentration (ppb), O is the outdoor O_3 concentration (ppb), λ is the air exchange rate of the building (hr^{-1}), V_d is the area averaged O_3 deposition velocity to surfaces in the building (m/hr), A is the total surface area (m^2), and V is the volume of the building (m^3).

Indoor O_3 concentrations increase with increased air exchange rates, with asymptotic convergence to the outdoor concentration (I/O = 1) for high air exchange rates. The air exchange rates of homes with HVAC systems are generally lower than homes without HVAC systems (Wallace, 1996). Thus, indoor O_3 levels in homes

without HVAC system tend to be higher than in homes with HVAC systems. Murray and Burmaster (1995) analyzed data on 2,844 residences in the US and estimated a geometric mean air exchange rate of 0.53 hr^{-1} with a geometric standard deviation of 2.3 hr^{-1}. New energy efficient buildings are designed with even lower air exchange rates. Thus, newer energy efficient buildings tend to have lower indoor O_3 levels.

The term $V_d(A/V)$ is commonly known as a surface removal rate and depends on the types of indoor surfaces, mixing conditions of air above those surfaces, and chemical properties. Values of the surface removal rate for O_3 have been measured for many buildings and range from 0.8 to 7.6 hr^{-1}. Buildings with higher surface area-to-volume ratios tend to produce higher surface removal rates and lower indoor O_3 levels. For example, carpet and fleecy furniture can provide relatively high surface areas.

Ozone can rapidly react with nitric oxide (NO), a common indoor air pollutant emitted from gas stoves, heaters, and other combustion sources. Thus, the presence of NO can reduce indoor O_3 levels. Building materials and many consumer products can emit alkenes that also react with indoor O_3.

A summary of the reported I/O values for O_3 in different types of buildings is presented Table 2.6. The reported I/O values vary over a wide range. Typical indoor O_3 levels range between 20-70% of outdoor O_3 levels (Weschler, 2000).

In summary, few sources emit O_3 into indoor environments. Outdoor to indoor transport is the main source of indoor O_3 for most buildings. Indoor O_3 concentrations usually track outdoor O_3 concentrations and increase with increased air exchange rates. Homes with centralized HVAC systems have lower air exchange rates and thereby lower indoor O_3 levels. In contrast, homes without a centralized HVAC system have higher air exchange rates and thereby higher indoor O_3 levels.

Carpets and furniture can increase surface removal rates and can lower indoor O_3 levels. Common indoor pollutants like NO and unsaturated organic compounds can react with O_3 and reduce its indoor concentrations. Indoor O_3 levels typically range between 20-70% of the outdoor O_3 levels.

Table 2.6. I/O Values for O_3 in Different Indoor Environments (Weschler, 2000)

Types of Buildings	Reported I/O Range
Homes with HVAC	< 0.1 - 0.3
Homes without HVAC	0.3 – 1.0
Hospitals	0.5 – 0.7
Offices	0.2 – 0.9
Schools	0.3 – 0.8
Museums	< 0.1 - > 0.67

2.4 Indoor Air Chemistry

2.4.1 Nitrogen Containing Compounds

Nazaroff and Cass (1986) were the first to develop a rigorous indoor air quality model. The model included 57 chemical reactions. The authors applied this model to a California museum and obtained reasonable agreement between predicted and measured indoor pollutant concentrations. Several cases were examined in the study. Comparisons with measured pollutant concentrations were better when detailed chemistry was included in the model. The authors reported that several pollutants, including HNO_2, HNO_3, HNO_4, and $NO_3^{\cdot}$ can be formed in indoor environments at substantial rates due to chemical reactions. Predicted indoor HNO_4 and $NO_3^{\cdot}$ concentrations exceeded outdoor concentrations. Substantial increases in indoor concentrations of HNO_2, HNO_3, HCHO, and H_2O_2 were predicted when a source of indoor organic emissions was included in the model.

Weschler *et al*. (1992a) reported that HNO_3 can be formed in indoor environments via $NO_3^{\cdot}$ initiated reactions. Specifically, O_3 can be transported from

outdoors to indoors and can react with indoor NO_2 to form HNO_3 through reactions 2.2 through 2.4:

$$O_3 + NO_2 \rightarrow NO^{\cdot}_3 + O_2 \quad (2.2)$$

$$NO^{\cdot}_3 + NO_2 \leftrightarrow N_2O_5 \quad (2.3)$$

$$N_2O_5 + H_2O \rightarrow 2HNO_3 \quad (2.4)$$

However, the dominant pathway for indoor HNO_3 was shown to be the reactions of $NO_3^{\cdot}$ with common indoor organic compounds via equation 2.5.

$$RH + NO_3^{\cdot} \rightarrow HNO_3 + R^{\cdot} \quad (2.5)$$

where RH represents some organic compound and $R^{\cdot}$ is the corresponding organic radical after hydrogen abstraction. A simple model was developed that incorporated detailed HNO_3 chemistry, and was applied to homes in the Boston area (Weschler *et al*., 1992a). The HNO_3 chemistry consisted of the reactions of 32 common indoor organic compounds with $NO_3^{\cdot}$ and Reactions 2.2 to 2.4. Reasonable agreement was obtained between predicted and measured indoor HNO_3 concentrations. Typical indoor concentrations of common organic compounds are much higher than outdoor concentrations. Thus, the authors suggested that $NO_3^{\cdot}$ can initiate reactions with these organic compounds via the hydrogen abstraction pathway, and the collective indoor HNO_3 production via this pathway can dominate over the production via Reactions 2.2 to 2.4. Elevated O_3 levels in summer produced higher indoor HNO_3 concentrations than corresponding lower levels in winter.

Wainman (1999) used a nested chamber to study the formation of indoor HNO_3 via reactions between NO_2 with O_3. Gas phase NO_2, NH_3, and O_3 were injected into the inner chamber and particle concentrations were continuously

monitored as a surrogate for HNO_3. Increased particle concentrations were detected, providing evidence that indoor chemistry can produce indoor HNO_3. Indoor HNO_3 concentrations increased with increased relative humidity. The HNO_3 was believed to form via Reactions 2.2 to 2.4 or via Reaction 2.6.

$$N_2O_5 + NH_3 \rightarrow HNO_3 + N_2O + H_2O \quad (2.6)$$

Additional experiments were conducted with NO_2, NH_3, O_3, and acetaldehyde. Increased HNO_3 concentrations were also observed during these experiments due to the reaction between acetaldehyde and $NO_3^{\cdot}$ via Reaction 2.5. The authors suggested that reactions between indoor NO_2 and O_3 can produce particles during periods of elevated indoor ammonia concentrations.

Nitrous acid (HONO) has been shown to affect mucous membranes and lung function (Rasmussen, *et al.*, 1995; Beckett *et al.*, 1995). Wainman (1999) conducted experiments to study indoor HONO formation via the heterogeneous reaction of NO_2 with H_2O (Reaction 2.7):

$$2NO_2 + H_2O \rightarrow HONO + HNO_3 \quad (2.7)$$

Nitrogen dioxide was first injected into the inner chamber and the HONO and NO_2 concentrations were continuously monitored. The results of these experiments reinforced the earlier works of Pitts *et al.* (1985), Brauer *et al.* (1993), and Spicer *et al.* (1993), all of whom concluded that HONO can be formed in indoor environments via Reaction 2.7. The effects of relative humidity and surface materials were also investigated. Carpet and wallpaper were observed to reduce indoor NO_2 levels due to higher surface removal rates and produced higher HONO concentrations. The author

also observed that inert surfaces under elevated relative humidity may become coated with a layer of water vapor and may absorb HONO.

Lee *et al.* (1999) measured indoor and outdoor HONO concentrations in 119 California homes and reported that the average indoor HONO concentration was 5 times as high as the average outdoor concentration. A positive correlation was established between indoor NO_2 and HONO concentrations. Indoor HONO concentrations in homes with humidifiers were higher than in homes without humidifiers. Heterogeneous reactions involving NO_2 and H_2O were believed to be responsible for elevated indoor HONO concentrations.

2.4.2 Hydroxyl Radicals ($OH^{\cdot}$)

The production of $OH^{\cdot}$ inside buildings was predicted as early as 1986 (Nazaroff and Cass, 1986). However, the role of $OH^{\cdot}$ on indoor air quality has not received significant attention until recently. Weschler and Shields (1996) demonstrated that certain alkene/O_3 reactions proceed at rates faster than air exchange rates in typical residential and commercial buildings and thus provide a source of $OH^{\cdot}$ in indoor environments. For example, the reaction of limonene with O_3 can produce indoor $OH^{\cdot}$ via Reaction 2.8:

$$\text{limonene} + O_3 \rightarrow 0.86\ OH^{\cdot} + \ldots\ldots \qquad (2.8)$$

Weschler and Shields (1996) used average indoor concentrations of 39 organic and inorganic compounds to estimate indoor $OH^{\cdot}$ concentrations for an air exchange rate of 1.0 hr^{-1}. Predicted indoor $OH^{\cdot}$ concentrations were lower than typical day-time urban outdoor $OH^{\cdot}$ concentrations, but were higher than typical night-time urban outdoor $OH^{\cdot}$ concentrations.

Weschler and Shields (1997b) also validated the conclusions of their previous studies by performing experiments in a manipulated but realistic indoor setting. The authors measured indoor concentrations of O_3, limonene and 1,3,5-trimethylbenzene, and derived indoor $OH^{\cdot}$ concentrations from the decrease in indoor 1,3,5-trimethylbenzene concentrations. The authors reported indoor $OH^{\cdot}$ concentrations up to 7×10^5 molecules/cm^3 when O_3 and limonene were present at elevated levels. They suggested that the resulting indoor $OH^{\cdot}$ can initiate reactions in which organic compounds may be oxidized to secondary pollutants which may be of greater concern than the original compounds.

2.4.3 Aldehydes

Zhang *et al*. (1994) conducted simultaneous indoor and outdoor measurements of nine different aldehydes (formaldehyde, acetaldehyde, propionaldehyde, 2-furaldehyde, butyraldehyde, benzaldehyde, isovaleraldehyde, n-valeraldehyde, and n-hexaldehyde) in six New Jersey homes in 1992. They reported that indoor concentrations for most of these aldehydes were greater than outdoor concentrations. The arithmetic average total indoor aldehyde concentration was 63 ppb compared to a total outdoor concentration of 19 ppb. Indoor O_3 concentrations were also measured during these experiments. The authors postulated that at least part of the indoor aldehydes was produced through O_3 initiated reactions.

Stabel and Wolkoff (1999) completed a modeling study to evaluate the effect of isoprene chemistry on indoor air quality. The reactions of isoprene with O_3 and $OH^{\cdot}$ were included in the model. The products of the isoprene chemistry included formaldehyde, methacrolein, and methyl vinyl ketone. The authors concluded that the resulting reaction products, under the conditions examined in the study, were not sufficiently elevated to cause airway irritation. The authors, however, implied that

the free radicals produced from the secondary reactions of the isoprene reaction products can contribute to eye and airway irritations.

Wolkoff *et al*. (1999) performed mouse bioassay experiments using O_3/terpene reaction mixtures and measured the reduction in mouse respiratory rates. Three different terpenes used in the experiments were: isoprene, α-pinene, and limonene. Significant reductions in mouse respiratory rates were observed during the experiments, which indicated the formation of strong airway irritants. The authors concluded that consideration of O_3/terpene reactions may be needed in future indoor air quality guidelines.

Clausen *et al*. (2001) performed mouse bioassay experiments using limonene/O_3 reaction mixture. Elevated levels of limonene (initial level 48 ppm) and O_3 (initial level 4 ppm) were allowed to react for only 16 second before being introduced into chambers containing mice. The mean respiratory response of mice decreased by 33%. The authors concluded that the results can only be explained with the formation of strong airway irritants. The authors also measured limonene/O_3 reaction products during the experiments and reported the formation of a series of products including 4-acetyl-1-methyl-cyclohexene, 3-isopropenyl-6-oxoheptanal, formaldehyde, formic acid, acrolein, and acetic acid.

Many companies sell ozone generating devices as air "purifiers". Shaughnessy *et al*. (2001) examined the effects of these air "purifiers" on several saturated and unsaturated organic compounds emitted from environmental tobacco smoke. The organic compounds were exposed to three levels of O_3 in a static chamber. No measurable difference in concentrations of organic compounds was observed when the O_3 level was set to “moderate”. A large reduction in concentrations of the unsaturated organic compounds was observed when the O_3 level

was set to "high". A small reduction in concentrations of some of the saturated organic compounds was also observed during the high O_3 level, presumably due to hydrogen abstraction by OH· radicals generated by the reactions between alkenes with O_3. However, this decrease in concentration was also accompanied by an increase in aldehydes, many of which are considered to be more irritating than their precursors. The most pre-dominant aldehydes included formaldehyde and benzaldehyde.

2.4.4 Hydrogen Peroxide (H_2O_2)

Li *et al*. (2001) performed a series of experiments involving limonene and O_3 and reported the formation of H_2O_2 in a manipulated indoor environment. Indoor H_2O_2 concentrations as high as outdoor concentrations were detected during these experiments. Indoor H_2O_2 concentrations decreased with increased air exchange rates – an observation consistent with other investigations involving indoor secondary pollutants.

Limonene/O_3 reactions also produce elevated particle concentrations. Hydrogen peroxide is water soluble; thus a fraction of the resulting H_2O_2 can be absorbed by the particles and carried to the deep lung where it can cause tissue damage (Weschler, 2001).

2.4.5 Ozone/Carpets

Weschler *et al*. (1992b) used a stainless steel chamber to conduct experiments involving new carpets and O_3. The presence of O_3 in the chamber was observed to decrease the gas phase concentrations of selected organic compounds associated with carpet emissions, and to increase aldehyde concentrations. Total indoor organic concentrations also increased during experiments involving the presence of O_3. The authors explained that the reactions between O_3 and organic compounds emitted by carpets were responsible for increases in aldehydes and total organic compounds in

air. The authors suggested that reactions between O_3 and organic compounds may alter the nature of pollutants present in buildings.

Morrison and Nazaroff (1999) extended the earlier work of Weschler (1992b) by conducting experiments with four different types of carpet. Carpets were exposed to an elevated level of O_3 for several days, during which time selected organic compounds were measured. An increase in concentration of the corresponding aldehydes was detected. Some of the aldehydes were detected well after the termination of O_3 exposure, suggesting that carpets can act as a reservoir for these pollutants. Morrison and Nazaroff (2000) conducted additional experiments with O_3 and carpets, and demonstrated that carpets can remove O_3; thereby reducing overall indoor O_3 concentrations. Four different types of carpet were tested and all of them exhibited similar trends with respect to reduction of O_3. However, the authors cautioned that the reduction in indoor O_3 levels is accompanied by an increase in other reaction products including aldehydes, which may be more irritating than the original products.

2.4.6 Secondary Particles

Indoor secondary particles due to homogeneous reactions between O_3 and terpenes have been studied by several investigators (Weschler and Shields, 1999; Long *et al.*, 2000; Wainman *et al.*, 2000; Rohr *et al*. 2001; and Weschler and Shields, 2002) and were discussed in Section 2.1. Indoor secondary particles due to heterogeneous interactions between O_3 and indoor surfaces have been studied by Shaughnessy *et al.* (1999) and were also discussed in Section 2.1.

Wainman (1999) used the nested chamber described earlier and conducted experiments involving ammonia, acetic acid, and formic acid. The reaction between ammonia and acetic acid did not increase indoor particle concentrations. However,

the reaction between ammonia and formic acid produced a significant increase in indoor particle concentrations.

In summary, indoor chemistry is a nascent but growing field. In the last few years, many investigators have shown the importance of indoor chemistry on indoor air quality. Indoor air chemistry is initiated primarily by O_3, transported from outdoors. Principal products that have been linked to indoor chemistry include secondary particles, aldehydes, $OH^{\cdot}$, H_2O_2, and various nitrogen containing compounds. Air exchange rate has been determined to be the most important building parameter affecting indoor secondary pollutant levels.

3.0 MODEL DEVELOPMENT

An Indoor Chemistry and Exposure Model (ICEM) was developed and used in this study. The starting point for the development of the model was the atmospheric chemistry model of the Statewide Air Pollution Research Center (SAPRC) at the University of California (Carter, 2000). This chapter provides an overview of the SAPRC model, the development of ICEM, the particle chemistry of α-pinene, input parameters to the ICEM, and limonene reaction mechanism and associated products.

3.1 Overview of the SAPRC Model

The SAPRC-99 is the latest version of the SAPRC model. It is written in FORTRAN 77 and contains detailed reaction mechanisms for over 350 common atmospheric pollutants. Reactions are included for inorganic compounds including ground state oxygen atoms (O^3P), excited oxygen atoms (O^1D), oxygen (O_2), ozone (O_3), nitric oxide (NO), nitrogen dioxide (NO_2), nitrate radicals ($NO_3^{\cdot}$), hydroxyl radicals ($OH^{\cdot}$), hydro peroxy radicals ($HO_2^{\cdot}$), hydrogen peroxide (H_2O_2), nitrous acid (HONO), nitric acid (HNO_3), peroxynitric acid (HO_2NO_2), dinitrogen pentoxide (N_2O_5), carbon monoxide (CO), sulfur dioxide (SO_2), and water vapor (H_2O). Reactions are also included for organic compounds, including those involving saturated compounds with $OH^{\cdot}$, and reactions of unsaturated compounds (alkenes and terpenes) with $OH^{\cdot}$, O_3, O^3P, and $NO_3^{\cdot}$. These reaction mechanisms were extensively tested and validated against environmental chamber results (Carter and Lurman, 1991).

Product species that can be formed from the reactions of organic compounds include: formaldehyde (HCHO), acetaldehyde (CH_3CHO), lumped higher aldehydes (RCHO), acetone (ACET), slow reacting ketones (MEK), methanol (MEOH), methyl hydroperoxide (CH_3OOH), lumped higher organic hydroperoxides (ROOH), glyoxal

(GLY), methyl glyoxal (MGLY), biacetyl (BACL), phenol (PHEN), cresols (CRES), nitrophenols (NPHE), benzaldehyde (BALD), methacrolein (METHACRO), methyl vinyl ketone (MVK), lumped isoprene product species (ISO-PROD), fast reacting ketones (PROD2), lumped organic nitrates (RNO_3), uncharacterized aromatic fragmentation product 1 (DCB1), uncharacterized aromatic fragmentation product 2 (DCB2), and uncharacterized aromatic fragmentation product 3 (DCB3).

Reactions of organic compounds also produce organic peroxy radicals. In addition to several lumped peroxy radicals, six explicit organic radicals are used in the SAPRC-99 model: methyl peroxy radicals, acyl peroxy radicals, t-butoxy radicals, phenoxy radicals, nitro phenoxy radicals, and a radical ($HOCOO\cdot$) formed from the reaction of formaldehyde and hydroperoxy radicals. Peroxy radicals can react with NO, NO_2, $HO_2\cdot$, and other radicals. For computational purposes, all organic and inorganic radicals are grouped into active and steady-state species. For active radical species, concentrations are estimated by solving appropriate differential equations. Examples of active radical species include $OH\cdot$, $HO_2\cdot$, $CH_3OO\cdot$, etc. For steady-state radical species, a steady-state approximation is employed and usually includes rapidly reacting radical species (O^3P, O^1D, etc.). Concentrations of steady-state radical species are estimated by assuming that the time rate of change of concentration is zero. Thus, differential equations are not solved for steady-state radical species, saving both computational time and memory.

Three peroxy radical operators are also used in the mechanism: $RO_2\text{-}R\cdot$, $R_2O_2\cdot$, and $RO_2\text{-}N\cdot$. The $RO_2\text{-}R\cdot$ operator represents NO to NO_2 conversion with $HO_2\cdot$ formation. The $R_2O_2\cdot$ operator represents NO to NO_2 conversion without $HO_2\cdot$ formation. The $RO_2\text{-}N\cdot$ operator represents NO consumption with organic nitrate formation. These operators can react with NO, $NO_3\cdot$, $HO_2\cdot$, $CH_3OO\cdot$, as well as with each other.

An airshed may contain hundreds of organic compounds. Thus, lumped species and their associated reactions are included in the model to reduce the explicit treatment of all compounds present in the airshed. The SAPRC-99 model also includes five lumped alkane compounds (ALK1-ALK5), 2 lumped aromatic compounds (ARO1, ARO2), two lumped alkene compounds (OLE1, OLE2), and one lumped terpene compound (TERP).

The SAPRC-99 model contains a base mechanism, which includes the reactions of inorganic compounds, reactions of methane, ethene, isoprene and their reaction products, and reactions of the lumped compounds (ALK1-ALK5, ARO1-ARO2, OLE1-OLE2, and TERP). The model utilizes the Livermore Solver for Ordinary Differential Equations (LSODE). Species concentrations and reaction rates are predicted as a function of time in a single well-mixed volume.

The relationship between various data files and programs of the SAPRC-99 model is shown in Figure 3.1. The main input file to the preparation program is a file named "*model.PRP*". "*Model*" is a user defined file name and "PRP" is the extension of the file. The input file "*model.PRP*" provides the chemical mechanism, associated rate constants, and other data required for a simulation. The preparation program uses the data defined in a "*model.PRP*" file and prepares three files: *model.FTN*, *model.MOD*, and *model.PRO*. The file *model.PRO* is an output file that provides a listing of the chemical mechanisms and related information processed by the preparation program. The file *model.MOD* contains the processed data for the chemical mechanism needed by the airshed program. The file *model.FTN* is a FORTRAN source code needed by the airshed module for solution of the chemical mechanisms. The preparation program also creates several temporary files, which are usually deleted upon termination of the program. Input data needed by the SAPRC-

99 model includes initial conditions, temperature, relative humidity, location, date and time of simulation, emission rates, and deposition rates. Photolysis rate constants are estimated using solar intensity, absorption cross-section, and quantum yields. Absorption cross-section and quantum yields are defined in different files in the model, and solar intensity is estimated from the prescribed location, date and time of simulation.

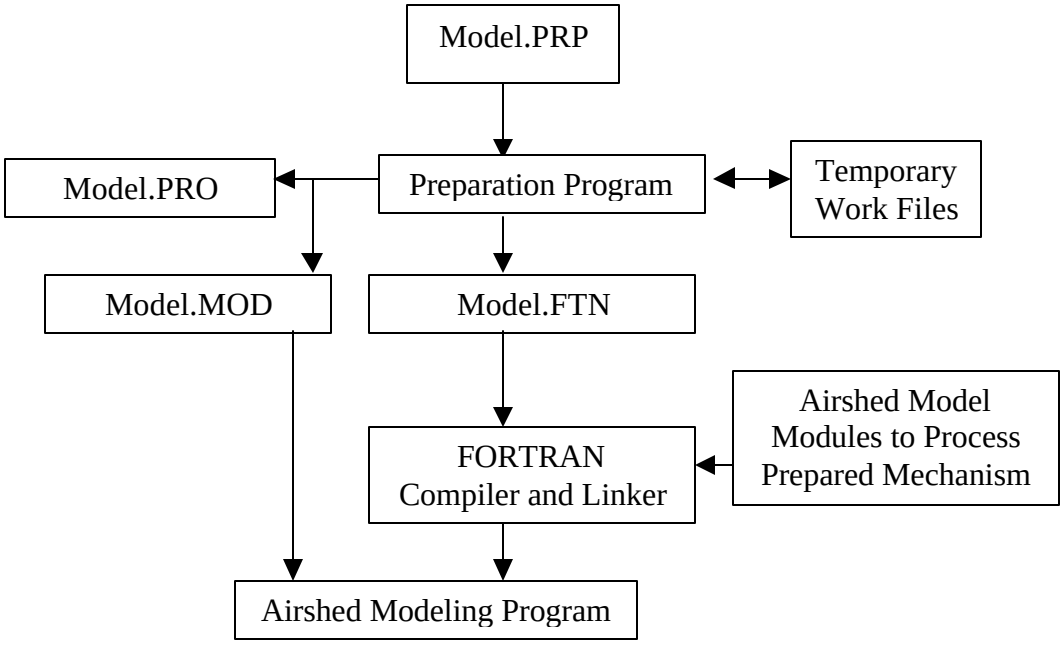

Figure 3.1. Relationships between programs and data files in the SAPRC model (Carter, 1988).

3.2 Development of the ICEM

For this study, the SAPRC-99 model was modified to include an additional option to simulate indoor air chemistry. The resulting model is referred to as the Indoor Chemistry and Exposure Model (ICEM). The additional option allows simulation of transport processes between indoor and outdoor environments, indoor emissions, chemical reactions, and deposition. The building interior was modeled as a single well-mixed environment with homogeneous chemistry and irreversible

heterogeneous deposition. The model can be used to evaluate the effects of building environmental conditions, outdoor air pollutants, and transport parameters on indoor air pollutants. In its simplest mathematical form, the governing equation of the ICEM model can be represented by:

$$\frac{dC_i}{dt} = \kappa_i \lambda C_{oi} - \lambda C_i + F\frac{E_i}{V} + \sum_{j=1}^{n} R_{ij} - V_{di} C_i a \qquad (3.1)$$

where, C_i is the indoor concentration of pollutant i (ppm), C_{oi} is the outdoor concentration of pollutant i (ppm), κ_i is the outdoor-to-indoor penetration factor for pollutant i (unitless; 0 to 1), λ is the fresh air exchange rate (min^{-1}), E_i is the whole-building emission rate (all sources) for pollutant i (mmol/min), F is the molar gas volume (m^3/kmol), R_{ij} is the reaction rate between pollutant i and pollutant j (ppm/min), V_{di} is the deposition velocity for pollutant i to indoor materials (m/min), a is the surface area to volume ratio (m^{-1}) for the indoor environment under question, V is the volume of the indoor environment (m^3), and t is time (min).

The first term in equation 3.1 corresponds to the time rate of change of pollutant concentration (C_i) within a building environment. For example, this might correspond to an increasing O_3 concentration during the course of a summer day or the increasing and decreasing concentration of specific volatile organic compounds after the use of a cleaning product. The model solves for indoor air pollutant concentrations (C_i) as a function of time.

The second and third terms in equation 3.1 correspond to the effects of fresh air exchange. The second term represents the transport of pollutants from outdoors to indoors, i.e., penetration through the building envelope. The third term represents the removal of pollutants from indoors to outdoors. The pollutant penetration factor (κ_i)

used in the second term is a unitless parameter that is intended to account for fractional penetration through the building envelope. Very limited work has been done to establish penetration factors for reactive pollutants in buildings. Only one publication on penetration of reactive pollutants was identified. Liu and Nazaroff (2001) performed a detailed modeling investigation and estimated O_3 penetration factors for different scenarios. The predicted penetration factor ranged from 0.1 to greater than 0.9. However, the authors also cautioned the use of these values for real buildings. In the absence of any measured penetration factors for O_3 and other reactive pollutants in real buildings, a value of 1.0 was used for all gaseous pollutants in this study. Reviewing the results of the PTEAM study, Wallace (1996) reported that a penetration factor of unity is reasonable for fine particles. The results of Liu and Nazaroff (2001) also indicate that essentially all fine particles penetrate through building envelopes. Mosley *et al*. (2001) also reported similar penetration factors for particles with aerodynamic diameters less than 2.0 μm. Thus, a penetration factor of unity for fine particles was also used in this study. The ICEM can be revised to include penetration factors of less than unity as such data become available.

Outdoor pollutant concentrations (C_{oi}) are supplied to the model as input parameters, and are allowed to vary with time. The fresh air exchange rate is defined as the ratio of fresh airflow to the volume of the building and is provided to the model as an input parameter.

The fourth term in equation 3.1 corresponds to the whole-building emission rate for pollutant i (from all sources). A literature search was conducted to evaluate studies where simultaneous measurements of indoor and outdoor pollutant concentrations were performed. For purposes of illustration and definition of a "base case" scenario that will be used later in the dissertation, these values have been used to estimate "reasonable" values of E_i using equation (3.2):

$$E_i = \lambda C_i \left(1 - \frac{1}{R_i}\right) V / (1000\, MW_i) \qquad (3.2)$$

where, E_i is the whole-building emission rate from all sources for pollutant i (mmol/min), C_i is the indoor concentration of pollutant i ($\mu g/m^3$), R_i is the indoor/outdoor concentration ratio of pollutant i (unitless), λ is the fresh air exchange rate (min^{-1}), V is the volume of indoor environment (m^3), MW_i is the molecular weight of pollutant i (mg/mmol), and 1000 is a conversion factor, i.e., from μg to mg.

As an example, average indoor and outdoor pollutant concentrations, indoor/outdoor pollutant concentration ratios, and "reasonable" residential/commercial indoor pollutant emission rates (E_i) are listed in Table 3.1. A geometric mean value of 0.53 hr^{-1} for λ was used to estimate E_i for this example (Wallace, 1996). A value of 500-m^3 was used for the building volume. This value corresponds roughly to a 2,000 square foot home. The data cited in Table 3.1 indicate that average indoor pollutant concentrations are higher than average outdoor pollutant concentrations for many compounds. Average indoor concentrations of nitrogen dioxide, in the absence of combustion appliances, and sulfur dioxide are less than the corresponding outdoor concentrations. Therefore, E_i for these two compounds were assumed to be zero, although transient emissions of NO_x can occur in homes with gas burners and can be simulated with the ICEM model. Indoor emission rates for all other pollutants were assigned values of zero.

"Typical" outdoor pollutant levels and indoor emission rates shown in Table 3.1 were used in the ICEM model for this study. However, it is acknowledged that there are wide variations in VOC concentrations between homes. This is due to transient sources such as cigarettes, cleaners, or the application of architectural coatings that can lead to highly transient VOC concentrations. Newer homes often

have higher VOC concentrations due to off-gassing from building materials. While the ICEM is capable of simulating episodic source events and building-specific source fingerprints, an attempt to describe all possible emission scenarios is not possible.

Table 3.1. Typical Indoor/Outdoor Pollutant Levels, I/O Ratios, and Indoor Emission Rates

Compounds	Typical Indoor Levels (ppb)	Typical Outdoor Levels (ppb)	I/O (-)	Typical Emission Rates (mmol/min)
Inorganic Compounds				
NO_2 [a, b, c, d]	30	38	0.78	0
NH_3 [a, e]	10	0.74	13	0.001
SO_2 [a, e]	1	4.6	0.22	0
CO [a, b, d]	1000	125	8	0.16
Alkanes and Related Compounds				
Methane [a]	2000	1000	2.0	0.18
Ethane [a]	2.5	0.83	3.0	0.0003
Propane [a]	1.5	0.5	3.0	0.00018
N-C4[a]	4.0	1.33	3.0	0.00048
N-C5[a]	2.0	0.67	3.0	0.00024
N-C6[a]	0.7	0.23	3.0	0.00008
N-C7[a]	0.3	0.1	3.0	0.00004
N-C8 [a]	0.9	0.3	3.0	0.00011
N-C9 [f]	1.2	0.4	3.0	0.00014
N-C10 [f]	0.8	0.27	3.0	0.0001
N-C11 [f]	0.8	0.27	3.0	0.0001
N-C12 [f]	0.8	0.27	3.0	0.0001
N-C13 [f]	1.5	0.5	3.0	0.00018
N-C14 [f]	0.8	0.27	3.0	0.0001
N-C15 [f]	0.2	0.07	3.0	0.00002
Cyclohexane [f]	1.4	0.47	3.0	0.00017
1,1,1-Trichloroethane [a]	10	3.33	3.0	0.0012
Dichloromethane [g, h]	0.4	0.04	10.0	0.00007
Chloroform [f, h]	0.8	0.16	5.0	0.00012
Aldehydes, Ketones, and Alcohols				
Formaldehyde [a, i]	30	4.17	7.2	0.00466
Acetaldehyde [a, h]	5	1	5.0	0.00072
Benzaldehyde [a]	1.6	0.5	3.0	0.00019
Acetone [f]	10	3.3	3.0	0.0012

Table 3.1. Typical Indoor/Outdoor Pollutant Levels, I/O Ratios, and Indoor Emission Rates (Continued)

Compounds	Typical Indoor Levels (ppb)	Typical Outdoor Levels (ppb)	I/O (-)	Typical Emission Rates (mmol/min)
Methyl ethyl ketone [a, h]	9.2	2.3	4.0	0.00125
Methanol [a]	10	3.3	3.0	0.0012
Ethanol [a]	100	33.3	3.0	0.01204
2-Propanol (Isopropanol) [g]	2.27	0.76	3.0	0.00027
2-Butoxy ethanol [f]	0.2	0.07	3.0	0.00002
Aromatics				
Benzene [a, h]	5	2.5	2.0	0.00045
Toluene [a, h]	10	2	5.0	0.00144
m-Xylene [a]	2	1	2.0	0.00018
o-Xylene [a]	3	1.5	2.0	0.00027
p-Xylene [a, h]	2	1	2.0	0.00018
Ethylbenzene [a, h]	2	0.7	3.0	0.00024
Phenol [f]	2.3	0.8	3.0	0.00028
1,2,4-Trimethylbenzene [a]	2	1.7	1.2	0.00006
1,3,5-Trimethylbenzene [a, c]	1	0.8	1.2	0.00003
1,4 Dichlorobenzene [f]	4	0.8	5.0	0.00058
Isopropylbenzene [j]	0.18	0.06	3.0	0.00002
Alkenes and Terpenes				
Ethene [a]	1.5	0.5	3.0	0.00018
Propene [a]	0.5	0.17	3.0	0.00006
Trans-2-Butene [a]	0.3	0.1	3.0	0.00004
Cis-2-Butene [a]	0.3	0.1	3.0	0.00004
Isobutene [a]	0.5	0.17	3.0	0.00006
1,3-Butadiene [a]	0.3	0.1	3.0	0.00004
2-Methyl 2-Butene [a]	0.4	0.13	3.0	0.00005
Isoprene [a]	2	0.67	3.0	0.00024
α-Pinene [a, k]	0.5	0.04	12.4	0.00008
Limonene [a, k]	4	0.27	14.7	0.00067
3-Carene [a, k]	0.23	0.02	10.7	0.00004
Styrene [a, h]	0.5	0.1	5.0	0.00007

Notes: a - Weschler and Shields, 1996; b - Lee and Chan, 1998; c – Baek *et al*., 1997; d - Phillips *et al*., 1993; e - Brauer *et al*., 1991; f - Weschler, 1992; g - Weschler, 2000; h - The US Environmental Protection Agency, 1998; i - Zhang *et al*., 1994; j - Shah & Singh, 1988; k - Gebefuegi, *et al*., 1995.

Instead, average VOC concentrations from the published literature were used to predict whole building emission rates. These are meant solely for purposes of

illustration and reflect what might be considered as "reasonable" background emission rates for purposes of prescribing a reasonable base case condition. Alkene emisisons were also varied around the base case condition and the dynamic response of indoor OH· to episodic releases of specific VOCs are also described later in this dissertation.

The fifth term in equation 3.1 corresponds to the summed results of all reactions involving pollutants i and j. The SAPRC-99 model contains detailed chemistry for both inorganic and organic compounds, with some lumped compounds. Lumping of similar primary VOC species, a feature of the SAPRC-99 model, was not used in the ICEM model. Instead, the ICEM model started with the SAPRC-99 base mechanism and then added the chemistry of approximately forty additional organic compounds from the SAPRC-99 model. These compounds are shown in Table 3.1 and are consistent with those chemicals that are often observed at much higher concentrations indoors than outdoors.

The limonene/O_3 and limonene/OH· reactions in the SAPRC-99 model were modified based on the experimental investigations of Hakola *et al*. (1994), Ruppert *et al*. (1999), and Clausen *et al*. (2001). Specifically, RCHO, a lumped C_{3+} aldehyde, was removed from the products of limonene/O_3 and limonene/OH· reactions. 4-Acetyl-1-methyl-cyclohexene (AMCYCHEX) and 3-isopropenyl-6-oxoheptanal (IPOH) were added to products of the limonene/OH· reaction with yields of 0.20 and 0.29, respectively, and AMCYCHEX was added to the products of the limonene/O_3 reaction with a yield of 0.04 following Hakola *et al*. (1994). Grosjean *et al*. (1992) reported that the limonene/O_3 reaction also produces 3-isopropenyl-6-oxoheptanal; however, no yield was reported. Recently, Clausen *et al*. (2001) reported a yield of 0.02-0.04 for IPOH resulting from the limonene/O_3 reaction; a yield of 0.04 was used for IPOH in this study. Glasius *et al*. (2000) reported formation of several other

compounds including limonic acid, limononic acid and 7-hydroxy-limononic acid from the limonene/O_3 reaction with a total yield of less than 0.03. These compounds were not included in the model. Finally, the yield of HCHO in the limonene/O_3 reaction was revised from 0.058 to 0.19 following Ruppert *et al*. (1999). The resulting limonene/O_3 and limonene/$OH^{\cdot}$ reactions are shown in Equations 6.13 and 6.33 in Chapter 6. The reactions of 4-acetyl-1-methyl-cyclohexene and 3-isopropenyl-6-oxoheptanal with $OH^{\cdot}$ were also included in ICEM (Equations 6.34 and 6.35 in Chapter 6). All chemical reactions currently included in the ICEM are shown in Appendix A.

Photolysis in outdoor environments is driven by solar radiation, the intensity of which is greater than light energy in indoor environments. To estimate the spectral photon energy distribution in a "typical" indoor environment, a light intensity of 1,600 lumen/m^2 was assumed to exist in the hypothetical indoor environment. This is the average light intensity recommended by the Illuminating Engineering Society of North America for reading purposes, which may result from a combination of daylight diffused through windows and from fluorescent light (Kaufman and Christensen, 1987).

For the purpose of this study, it was assumed that 50% of the indoor light intensity is contributed by daylight, and the other 50% contributed by fluorescent light. Spectral power distributions of daylight and fluorescent light were obtained from the literature, and were then combined with the assumed light intensity to estimate the spectral photon energy for daylight and fluorescent light (Kaufman and Christensen, 1987). The summation of the spectral photon energies of daylight and fluorescent light is the total spectral photon energy distribution that drives photolysis in indoor environments. The spectral photon energy distributions of daylight,

fluorescent light, and the total indoor spectral photon energy distribution are shown in Table 3.2.

Table 3.2. Estimated Spectral Photon Energies of Daylight, Fluorescent Light, and the Total Indoor Spectral Photon Energy Distribution

Wavelength (nm)	Average Wavelength (nm)	Daylight (photon/cm^2/sec)	Flourescent Light (photon/cm^2/sec)	TOTAL (photon/cm^2/min)
300-310	305	0.00E+00	0.00E+00	0.00E+00
310-320	315	7.99E+13	9.99E+13	1.08E+16
320-330	325	0.00E+00	0.00E+00	0.00E+00
330-340	335	4.52E+13	4.52E+13	5.42E+15
340-350	345	2.40E+13	2.40E+13	2.88E+15
350-360	355	4.06E+13	4.06E+13	4.87E+15
360-370	365	2.15E+14	2.41E+14	2.74E+16
370-380	375	5.66E+13	4.53E+13	6.12E+15
380-390	385	7.16E+13	5.37E+13	7.52E+15
390-400	395	9.43E+13	6.28E+13	9.43E+15
400-410	405	7.93E+14	5.95E+14	8.32E+16
410-430	420	5.33E+14	1.42E+14	4.05E+16
430-440	435	1.83E+15	1.60E+15	2.06E+17
440-450	445	8.77E+14	1.60E+14	6.22E+16
450-470	460	1.02E+15	2.13E+14	7.41E+16
470-480	475	1.27E+15	2.73E+14	9.27E+16
480-500	490	1.21E+15	3.38E+14	9.28E+16
500-530	515	1.28E+15	6.41E+14	1.15E+17
530-540	535	1.27E+15	9.22E+14	1.31E+17
540-550	545	2.39E+15	2.45E+15	2.91E+17
550-580	565	1.93E+15	1.93E+15	2.31E+17
580-590	585	2.48E+15	2.62E+15	3.06E+17
590-600	595	2.14E+15	2.57E+15	2.82E+17
600-630	615	1.37E+15	2.74E+15	2.47E+17
630-650	640	9.90E+14	2.80E+15	2.28E+17
650-680	665	5.34E+14	2.14E+15	1.60E+17
680-700	690	3.83E+14	1.53E+15	1.15E+17
700-760	730	1.07E+14	1.07E+15	7.08E+16

Paulson *et al*. (1999) performed extensive studies on alkene and O_3 homogeneous reactions and subsequent hydroxyl radical ($OH^{\cdot}$) formation. For this study, $OH^{\cdot}$ yields for alkene and O_3 reactions in the original SAPRC-99 model were

replaced by the respective yields from Paulson *et al.*'s work and are shown in Table 3.3.

Table 3.3. $OH^{\cdot}$ Yields for Alkene/O_3 Reactions in the SAPRC-99 and the ICEM Models

Compound	$OH^{\cdot}$ Yields SAPRC-99 Model	$OH^{\cdot}$ Yields ICEM Model
Ethene	0.12	0.18
Propene	0.32	0.35
trans-2-Butene	0.965	0.64
cis-2-Butene	0.52	0.37
Isobutene	0.07	0.67
1,3-Butadiene	0.06	0.13
2-Methyl 2-Butene	0.856	1.0
Isoprene	0.266	0.25
α-pinene	0.7	0.7
Limonene	0.7	0.86
3-Carene	0.7	1.0
Styrene	0.0	0.07
Methyl vinyl ketone	0.164	0.16
Methacrolein	0.208	0.2

The sixth term in equation 3.1 corresponds to the removal of pollutant i by irreversible deposition on indoor materials. Deposition velocity (V_{di}) data for common compounds (O_3, NO, $HO_2^{\cdot}$, etc.) are available in the literature. However, data are scarce for most compounds needed for the ICEM model. Deposition velocities obtained from the literature are shown in Table 3.4, all of which were taken from Nazaroff and Cass (1986), except for the value for sulfur dioxide (SO_2) which was taken from Weschler (1992). The deposition velocity of acetaldehyde (CH_3CHO) was assumed to be equal to that of lumped aldehyde (RCHO) based on Nazaroff and Cass (1986). The deposition velocity of ammonia (NH_3) was assigned a value equal to that of nitric acid (HNO_3). Gaseous compounds for which deposition velocities were not available in the literature were assigned values of zero. The ICEM does not currently account for reversible adsorption/desorption phenomena.

The SAPRC-99 model utilizes the Livermore Solver for Ordinary Differential Equations (LSODE). The LSODE subroutine was also used in the ICEM model. The LSODE can solve stiff and non-stiff ordinary differential equations using a backward differentiation formula method (Gear method).

Table 3.4. Deposition Velocities of Gaseous Compounds Used in the ICEM

Pollutant Symbol	Pollutant Name	Deposition Velocity (cm/s)
O_3	Ozone	0.036
NO_2	Nitrogen Dioxide	0.006
CO	Carbon Monoxide	0.00
NO	Nitric Oxide	0.00
HONO	Nitrous Acid	0.07
HNO_3	Nitric Acid	0.07
HO_2NO_2	Peroxynitric Acid	0.07
H_2O_2	Hydrogen Peroxide	0.07
$NO_3^{\cdot}$	Nitrate Radical	0.07
N_2O_5	Nitrogen Pentaoxide	0.07
$HO_2^{\cdot}$	Hydroperoxy Radicals	0.07
$OH^{\cdot}$	Hydroxyl Radicals	0.07
HCHO	Formaldehyde	0.005
CH_3CHO	Acetaldehyde	0.005
RCHO	Lumped higher Aldehydes	0.005
NH_3	Ammonia	0.07
SO_2	Sulfur Dioxide	0.036

Note: Deposition Velocities were taken from Nazaroff and Cass, 1986; Weschler, 1992

3.3 Particle Chemistry of a -Pinene

Kamens *et al.* (1999) conducted experiments in a 190-m^3 outdoor Teflon film chamber under dark conditions and used the results to develop the particle formation chemistry of α-pinene. An overview of the particle chemistry of α-pinene is provided here; details can be found in Kamens *et al.* (1999). Particle chemistry for α-pinene can be divided into two parts: (1) gas-phase chemistry leading to semi-volatile products and (2) particle growth by partitioning of semi-volatile products onto existing particles. The particle chemistry of α-pinene consists of six semi-volatile model compounds: *pinald, pinacid*, *diacid*, *oxy-pinald, p3gas*, and *oxy-pinacid*. The

model compound *pinald* represents pinonaldehyde and nor-pinonaldehyde, *pinacid* represents pinonic and nor-pinonic acids, *diacid* represents pinic and nor-pinic acids, *oxy-pinald* represents hydroxy and aldehyde substituted pinonaldehydes, *p3gas* represents - a pinic acid precursor (2,2-dimethylcyclobutane-3-acetylcarboxylic acid - $C_9H_{14}O_3$), and *oxy-pinacid* represents hydroxy and aldehyde substituted pinonic acids. A schematic diagram of the chemistry of the α-pinene/O_3 reaction system is shown in Figure 3.2.

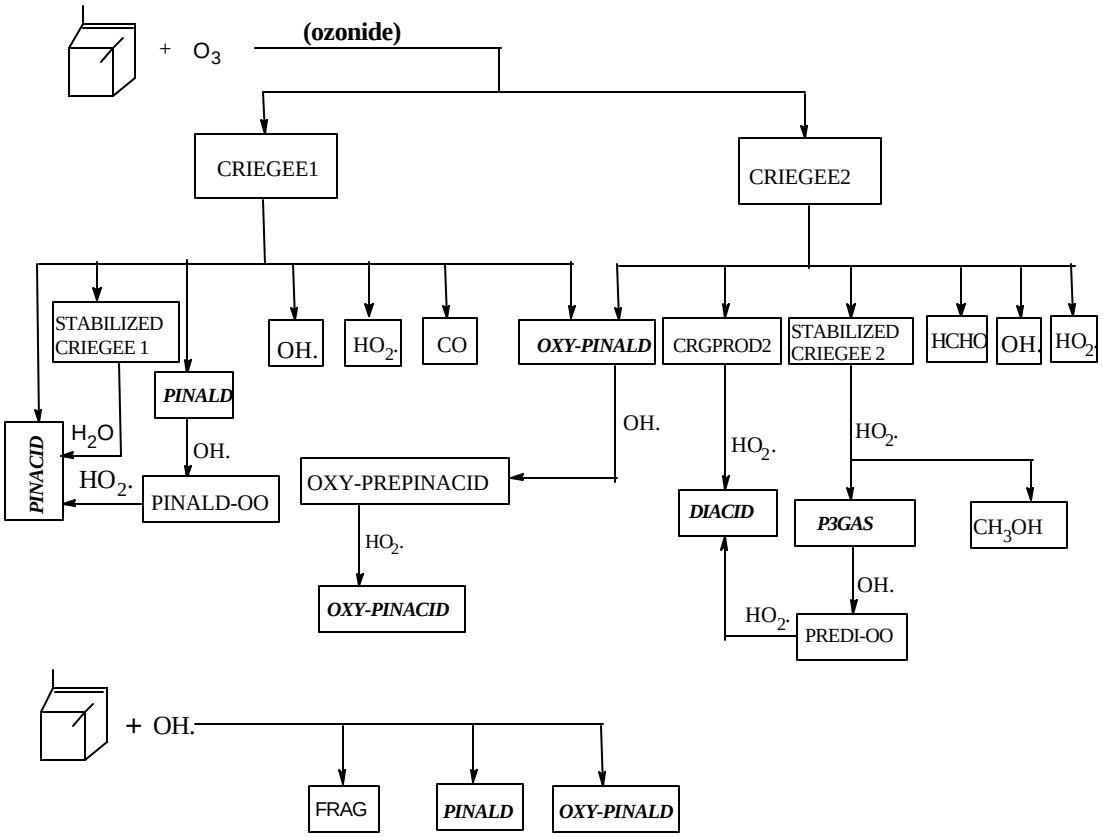

Figure 3.2. Reaction between α-Pinene and O_3

Gas Phase Chemistry

α-Pinene reacts with O_3 to produce an ozonide. However, the ozonide is a highly unstable compound and rapidly decomposes into two Criegee biradicals (CRIEGEE1 and CRIEGEE2). Several reaction pathways are available for the decomposition of these Criegee biradicals. The decomposition of CRIEGEE1 leads to *pinacid*, stabilized criegee 1 radical, *pinald*, *oxy-pinald*, $OH^{\cdot}$, $HO_2^{\cdot}$, and CO. Stabilized Criegee 1 biradicals react with H_2O to form *pinacid*. In the presence of O_2, *pinald* reacts with $OH^{\cdot}$ to form a peroxyacyl radical (PINALD-OO), which is subsequently oxidized via $HO_2^{\cdot}$ to produce *pinacid*. *Oxy-pinald* is oxidized to *oxy-pinacid* via $OH^{\cdot}$ and $HO_2^{\cdot}$.

The decomposition of CRIEGEE2 leads to *oxy-pinald*, CRGPROD2 (a generalized intermediate product), a stabilized criegee 2 radical, HCHO, $OH^{\cdot}$ and $HO_2^{\cdot}$. Stabilized Criegee 2 radicals can react with H_2O to produce *p3gas* and methanol (CH_3OH). The compound *p3gas* reacts with $OH^{\cdot}$ producing a peroxyacyl radical (PREDI-OO), which in turn produces *diacid* via oxidation with $HO_2^{\cdot}$. The compound CRGPROD2 reacts with $HO_2^{\cdot}$ to form *diacid*. α-Pinene also reacts with $OH^{\cdot}$ to produce *pinald*, *oxy-pinald*, and volatile oxygenated products called FRAG. Six semi-volatile products are shown in bold and italic letters in Figure 3.2.

Partitioning of Semi-Volatile Products on to "Seed" Particles

The six semi-volatile products described above can partition on to "seed" particles. Some of these products have very low vapor pressures and can self-nucleate to form new particles and are designated as "seed1" in the model. Partitioning was treated as sorption to, and desorption of semi-volatile products from, particles. The ratio of the sorption rate ($k_{on,i}$) and desorption rate ($k_{off,i}$) constants was taken as the equilibrium constant ($K_{p,i}$) for gas-particle equilibrium:

$$K_{p,i} = k_{on,i} / k_{off,i} \quad (3.3)$$

Here, $K_{p,i}$ represent the ratio of the sorbed-phase concentration of species i (ng/μg) to the gas-phase concentration of i (ng/m^3) and has unit of m^3/μg. It was estimated from knowledge of the vapor pressure and molecular weight of a product according to:

$$K_{p,i} = 7.501\ RT / (10^9\ MW_{om}\ {}^{i}p^{0}_{L}) \quad (3.4)$$

where, $K_{p,i}$ is the equilibrium constant (m^3/μg) for compound i, R is the universal gas constant (8.31 J/K/mol), T is the temperature (K), MW_{om} is the average molecular weight of the organic particles (g/mol), ${}^{i}p^{0}_{L}$ is the vapor pressure of the product (torr), and 7.51 is a conversion factor (Kamens *et al*. 1999). The original expression for the equilibrium constant, $K_{p,i}$ was developed by Pankow (1994):

$$K_p = \frac{F_i}{A_i\ TSP} = \frac{7.51\,RT\ f_{om}}{10^9 MW_{om}\ \xi_i\ {}^{i}p^{o}_{L}} \quad (3.5)$$

where, F_i is the particle phase concentration of compound i (ng/m^3), A_i is the gas phase concentration of compound i (ng/m^3), TSP is the total suspended particle concentration (μg/m^3), R is the universal gas constant (8.31 J/K/mol), T is the temperature (K), f_{om} is the mass fraction of the TSP that absorbs the organic particles, MW_{om} is the average molecular weight of the organic particles (g/mol), ξ is the activity coefficient of compound i in the liquid medium, ${}^{i}p^{0}_{L}$ is the vapor pressure of the product (torr), and 7.51 is a conversion factor. Kamens *et al*. (1999) used a value of 1 for f_{om} and ξ and developed the relationship presented in equation 3.4.

Absorption of semi-volatile products on to particles is a weak function of temperature; thus it was assumed that sorption rates ($k_{on,i}$) are independent of

temperature. Desorption rate constants ($k_{off,i}$) of semi-volatile products from particles are strongly dependent on temperature and were estimated using:

$$k_{off,i} = \beta \exp(-E_a/RT) \tag{3.6}$$

where, β is the pre-exponential factor, R is the universal gas constant (8.31 J/K/mol), T is the temperature (K), and E_a is the activation energy (J/mol). A general equation for evaporation from a liquid surface was used to estimate values of β and E_a (Kamens *et al*., 1999):

$$I_{evap} = \eta \theta \frac{k_b T}{h} \exp(-\frac{\Delta\phi}{k_b T}) \equiv \eta k_{evap} \tag{3.7}$$

where, I_{evap} refers to the flux of molecules (molecules/cm^2 sec), η refers to the exposed molecule numbers on the surface of the liquid (number/cm^2), θ refers to the coefficient of transmission and was taken as unity, k_b refers to the Bolzmann's constant (1.4×10^{-23} Joules/K); T is the temperature (K), h refers to Planck's constant (6.6×10^{-34} Joules sec), $\Delta\phi$ refers to the energy needed by an individual molecule to evaporate from the liquid surface (Joules). The parameter, k_{evap}, was divided by particle radius to obtain the value of desorption rate constant ($k_{off,i}$) in equation 3.6. The value of β becomes k_bT/h and has a numerical value of 6.21×10^{-12} (sec^{-1}) at 298 K (Kamens *et al*. 1999). The estimated values of E_a were shown to be close to the pure liquid enthalpy values of the compound being desorped. Sorption rates ($k_{on,i}$) for semi-volatile products were estimated as the product of equilibrium constant, $K_{p,i}$, and the desorption rate constant (k_{off}) for any given compound.

Secondary particle mass associated with α-pinene reactions can be estimated by keeping track of all seven products (six semi-volatile products and "seed1", the

self-nucleated product) in the particle phase. An average molecular weight of 120 g/mol was used to convert secondary particle concentrations from volumetric units (ppm) to mass units ($\mu g/m^3$). Detailed α-pinene particle chemistry is presented in Appendix B. α-Pinene chemistry published by Kamens *et al*. (1999) was combined with the homogeneous reactions of SAPRC-99 in the ICEM. "Seed" particles needed for the model were estimated based on outdoor-to-indoor transport. An average molecular weight of 90 g/mol was used to convert "seed" particle concentrations from volumetric units (ppm) to mass units ($\mu g/m^3$).

Kamens *et al*. (1999) also determined losses of semi-volatile reaction products and particles to Teflon film chamber walls. Several reactions were included in the particle formation mechanism of α-pinene to account for these wall losses. The ICEM estimates surface removal rates using prescribed deposition velocities, the surface area to volume ratio, and pollutant concentrations in indoor environments. Thus, reactions that account for chamber wall losses in the α-pinene particle formation mechanism were switched off, allowing the ICEM to estimate surface removal rates of these compounds based on prescribed deposition velocities. Determination of deposition velocities for these compounds are discussed in Chapter 4.

Losses of the semi-volatile products to the Teflon film chamber walls at 298K are shown in Table 3.5. The average wall loss of these semi-volatile products was 0.0016 min^{-1}, twice the wall loss rate of 0.0008 min^{-1} for particles. Deposition velocity data for these semi-volatile products in actual building environments are not known. In the absence of any measured data in indoor environments, deposition velocities for semi-volatile organic products of α-pinene were assigned twice the deposition velocity of fine particles following Kamens *et al*. (1999). As discussed in Chapter 4, the average deposition rate of particles in the chamber was 0.34 hr^{-1}, thus

the average deposition rate of these semi-volatile products in the chamber was assumed to be 0.68 hr^{-1}. With the surface to volume ratio of 2.7 m^{-1}, the average deposition velocity of semi-volatile products in the chamber was 0.007 cm/sec.

Table 3.5. Wall Loss Rates of the Semi-Volatile Compounds of a -Pinene/O_3 Reactions (Kamens *et al*., 1999)

Compounds	Wall Loss Rate at 298K (min^{-1})
Diacid	2.19×10^{-3}
Pinacid	2.19×10^{-3}
Oxy-pinacid	1.46×10^{-3}
Oxy-pinald	1.46×10^{-3}
Pinald	9.15×10^{-4}
Average	**1.65×10^{-3}**

3.4 Input Parameters Required for the ICEM

The ICEM requires the following input parameters: outdoor pollutant concentrations, indoor pollutant emission rates, building volume, fresh air flow rate to the building, temperature, relative humidity, photon energy distribution, pollutant deposition velocities, surface area to volume ratio, and simulation start and end times. Outdoor pollutant concentrations and indoor pollutant emission rates are allowed to vary with time. The model also requires a set of chemical reactions. The mechanism currently used in the ICEM is shown in Appendices A and B. The photon energy distribution used in the ICEM is shown in Table 3.2. A typical input file for the simulation of indoor secondary particle mass concentrations is shown in Appendix C.

3.5 Limonene/O_3 Reaction Mechanism and Associated Products

Several studies have been completed to characterize the gas and particle phase products of O_3/limonene reactions (Schuetzle and Rasmussen, 1978; Arey *et al.*, 1990; Grosjean *et al*., 1992; Grosjean *et al*., 1993; Hakola *et al.*, 1994; Eusebi, 1996; Calogirou *et al.*, 1999; Ruppert *et al.*, 1999; Glasius *et al*., 2000; and Clausen *et al*., 2001). All of the reaction products are yet to be identified; consequently accurate

reaction pathways for O_3/limonene reactions are not currently known. The author of this dissertation is currently working on development of a complete set of reactions to predict particle formation and growth following O_3/limonene reactions. These reactions will ultimately be included in the ICEM.

Reactions between limonene and O_3 can proceed via the attack of O_3 on the double bonds forming two ozonides. These ozonides are very unstable and readily decompose to other products. The detailed pathways via which these decomposition processes occur are not currently known. The reaction between limonene and O_3 also produces $OH^{\cdot}$ with a yield of 0.86 (Paulson *et al.*, 1999). Limonene also reacts with $OH^{\cdot}$ to form a host of products. Calogirou *et al.* (1999) has recently proposed detailed reaction pathways leading to various products via the oxidation of limonene by $OH^{\cdot}$. However, many of the proposed reaction products are yet to be experimentally identified. A list of the products that have been measured from O_3/limonene reactions is provided in Table 3.6 (Grosjean *et al*., 1992; Grosjean *et al*., 1993; Hakola *et al.*, 1994; Glasius *et al*., 2000; and Clausen *et al*., 2001). Molecular weight and vapor pressures of these products are also presented in Table 3.6. These products have low vapor pressure and should effectively partition into particles. Vapor pressures shown in Table 3.6 were estimated using the MPVPWIN^{TM} program of the USEPA. The MPVPWIN^{TM} estimates vapor pressures using three different techniques and recommends the most suitable vapor pressure. All three techniques use boiling point to estimate vapor pressure. Boiling points are estimated using the group contribution principle.

Table 3.6. Reaction Products of O_3/Limonene Reactions

Product name	Structure	Molecular Weight	Vapor Pressure @ 298 K (mm Hg)
Limonaketone	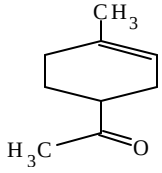	138.21	2.0
Limononaldehyde	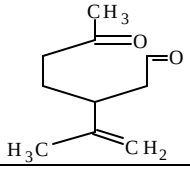	168.24	6.06×10^{-2}
Keto-limononaldehyde	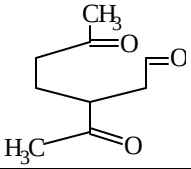	170.21	1.27×10^{-2}
Limononic acid	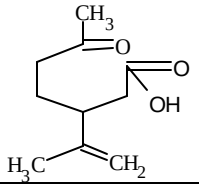	184.24	8.85×10^{-4}
Keto-limononic acid	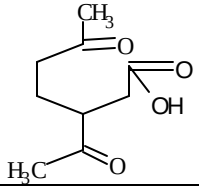	186.21	2.15×10^{-4}
Norlimononic acid	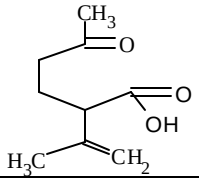	170.21	2.5×10^{-3}
Hydroxy-limononic acid	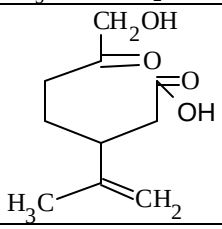	200.24	1.17×10^{-6}

Table 3.6. (Continued)

Product name	Structure	Molecular Weight	Vapor Pressure @ 298 K(mm Hg)
Hydroxy-keto-limononic acid	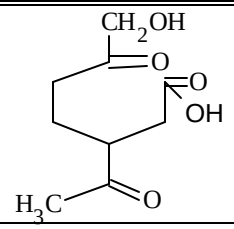	202.21	2.61×10^{-7}
Limonic acid	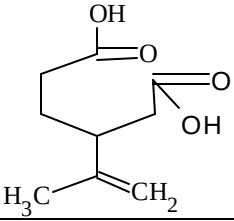	186.21	3.47×10^{-5}
Keto-limonic acid	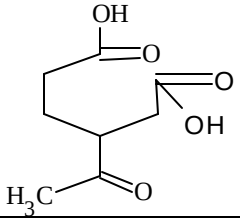	188.18	1.12×10^{-5}
Norlimonic acid	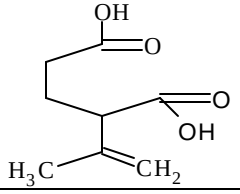	172.18	8.43×10^{-5}

4.0 CHAMBER STUDIES: EXPERIMENTAL APPROACH

Descriptions of the experimental program and systems, sampling and analytical methods, quality assurance procedures, and determination of ozone and particle deposition velocities in the chamber are presented in this chapter.

4.1 Experimental Program

Twenty-seven chamber experiments were completed to assess the effects of O_3/terpene reactions on indoor secondary organic particles. Ten experiments were conducted with pure α-pinene, six with pure limonene, and eleven were conducted with six different consumer products. Experiments involving pure α-pinene and limonene were conducted at different emission rates, air exchange rates, initial particle levels, and temperatures. A summary of the experimental program is shown in Table 4.1. Preliminary experiments were also conducted to determine deposition velocities for O_3 and particles in the chamber.

Table 4.1. Experimental Program

Compound/Consumer Products	No of Experiments	Ozone Levels
Pure α-pinene	1	Low
Pure α-pinene	9	Elevated
Pure limonene	1	Low
Pure limonene	5	Elevated
Liquid Air-Freshener	1	Low
Liquid Air-Freshener	1	Elevated
Solid Air-Freshener	1	Elevated
General Purpose Cleaner	1	Low
General Purpose Cleaner	1	Elevated
Wood Floor Cleaner	1	Low
Wood Floor Cleaner	1	Elevated
Perfume	1	Low
Perfume	1	Elevated
Dishwashing Detergent	1	Low
Dishwashing Detergent	1	Elevated

4.2 Experimental System

Experiments were conducted in a stainless steel chamber (~11m^3) located at the Center for Energy and Environmental Resources (CEER) at the University of Texas at Austin. The chamber has dimensions of 2.4 m x 1.8 m x 2.5 m (L x W x H). A dedicated blower was used to draw air through the environmental chamber and to discharge it outdoors (once through system). Inlet air was provided from within the general occupied space of the building. The inlet air was not conditioned for the experiments described herein. Thus, it contained some amount of common indoor pollutants, including terpenes, O_3, and particles. A diagram of the environmental chamber and associated instrumentation is shown in Figure 4.1.

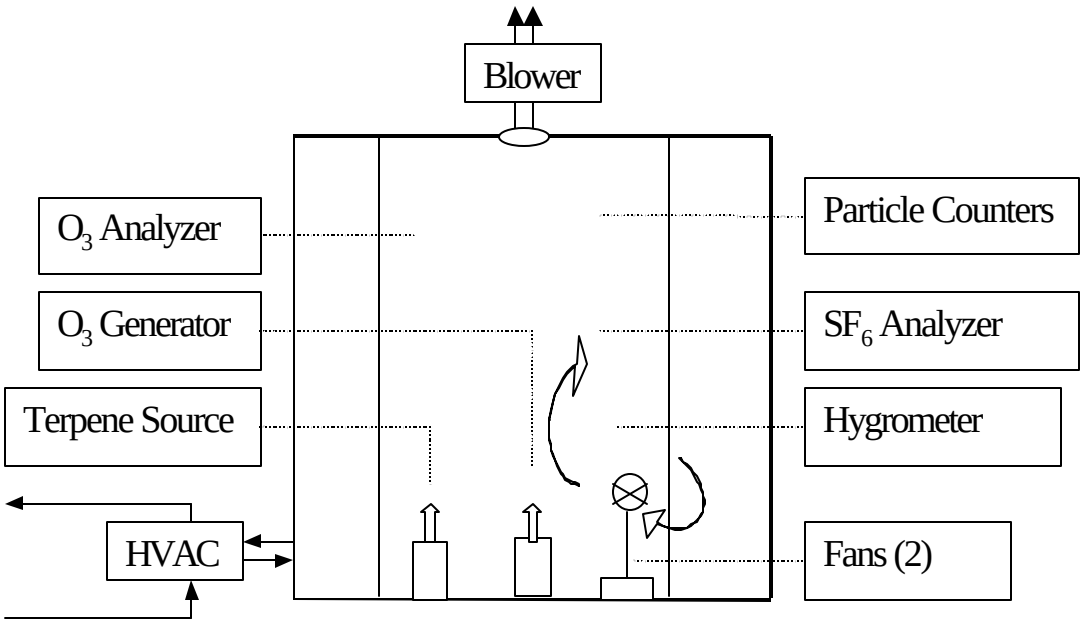

Figure 4.1. Schematic diagram of the environmental chamber

A commercial corona discharge ozone generator (Living Air, BORA-IV) was placed in the middle of the chamber and operated for 10-20 hours to achieve steady-state O_3 concentrations prior to the introduction of terpenes. The rated ozone

emission rate of this system was 70 mg/hr; however, the system was not operated at its rated capacity during experiments. Ozone emission rates during experiments varied from 3-5 mg/hr, with the exception of one experiment during which the ozone emission rate was approximately 10 mg/hr. For most of the experiments, a 4 milliliter (mL) vial containing either pure reagent grade α-pinene or limonene was then placed on the floor of the chamber, allowing for evaporation of α-pinene or limonene. The difference in vial mass before and after each experiment was combined with the duration of the experiment to obtain the average α-pinene or limonene emission rate.

For some experiments, consumer products were sprayed directly into the chamber. For others, a solid air freshener was suspended approximately 180 cm below the ceiling using wiring. All consumer products except perfume and dishwasher detergent were purchased about a month prior to experiments. Perfume was purchased about two years before the experiment. Dishwasher detergent was purchased approximately three months prior to corresponding experiments.

Two fans (SMC®, Model TR12 and Coll-Breeze™, Model EB24925) were operated on the floor of the chamber to enhance mixing. A space heater was used to maintain elevated temperatures in the chamber during two of the twenty-seven experiments.

4.3 Sampling and Analytical Methods

Chamber particle number concentrations were continuously measured using two particle counters (Particle Measuring Systems Inc., LASAIR® - model 1002; and TSI™, P-TRAK™ - model 8525). The P-TRAK™ was used to measure number concentrations of particles between 0.02-1.0 μm in diameter. The P-TRAK™ utilizes alcohol to grow particles, which are then detected using a laser system. The sample

averaging time of the P-TRAK™ was set to 60 seconds. Detailed specifications of the P-TRAK™ are shown in Table 4.2.

Table 4.2. Specifications for P-TRAK™

Criteria	P-TRAK™
Manufacturer	TSI®, Inc.
Concentration Range	0 - 5 x 10^5 #/cm^3
Number of Channels	1
Size Range	0.02 to > 1.0 µm
Sample Flow Rate	100 cm^3/min
Alcohol Requirement	100% reagent grade isopropyl alcohol
Temperature Range	0-38 ^oC
Power Requirement	6 AA Alkaline or AC power
Carrying Size	53 x 36 x 21 (cm)
Weight	1.7 kg

The LASAIR® measures total particle numbers in eight different channels corresponding to diameters of (all in µm) 0.1-0.2, 0.2-0.3, 0.3-0.4, 0.4-0.5, 0.5-0.7, 0.7-1.0, 1.0-2.0, and >2.0 µm. Sample air is drawn by an internal sampling pump in the LASAIR® and is then passed over a laser beam that detects particle number concentrations based on the principle of light scattering. The analyzer has a nominal flow rate of 0.94 cm^3/sec. The sampling interval of the instrument was set at 60 second intervals. The instrument provides total particle numbers in each of the channels for the sampling interval. Total particle number in each channel was divided by the total sampling volume to determine the average particle number concentration during the sampling interval. Particle number concentrations from the first six channels of the LASAIR® were added to obtain the total particle number concentrations for the size range of 0.1-1.0 µm. This total particle number concentration was then subtracted from the particle number concentration detected by the P-TRAK™ to obtain the particle number concentration in the range of 0.02-0.1 µm. Thus, the two particle analyzers collectively provided particle number concentrations in nine different diameter ranges. This subtraction technique

introduces some levels of uncertainty for concentrations in the 0.02-0.1 μm diameter range. Nevertheless, the results provided useful information in the ultrafine range of particles.

Mass concentration was estimated from particle number concentrations and particle density. Two different approaches were employed as described below.

Method 1:

A geometric mean diameter was estimated from the minimum and maximum particle diameters in each of the size range. The average volume of particles in each size range was determined by assuming that each particle was a sphere with a diameter equal to the geometric mean diameter. The total particle volume in each of the size ranges was estimated by multiplying the average volume of the particle by the particle number concentration in that size range. Particle volumes in each of the size ranges were summed to obtain the total particle volume.

Total particle volume was multiplied by particle material density to obtain particle mass concentration. Turpin and Lim (2001) analyzed reported atmospheric particle density data and suggested a material density of 1.2 g/cm^3 for atmospheric organic aerosols. A particle density of 1.2 g/cm^3 was used in this study.

This method has been shown to produce reasonable particle mass concentrations in previous studies. For example, Fan (2002) has concurrently measured particle number and mass concentrations during experiments involving reactions of O_3 with VOCs. Particle mass concentrations were measured using a filter-based technique. Particle mass concentrations were also estimated using measured particle number concentrations and the geometric mean diameters as described above. The estimated particle mass concentrations were 25% lower than

the results obtained using the filter-based technique. A particle density of 1.0 g/cm^3 was used in that study. If a particle density of 1.2 g/cm^3 had been used, the estimated particle mass concentration would have been within 5% of results obtained using the filter-based technique.

For experiments with pure α-pinene and limonene, the experimental mass concentrations obtained using this Method 1 contained initial oscillations due to growth wave kinetics and the coarseness of particle size analyzers. Therefore, this method was not used to derive particle mass concentrations for experiments with pure α-pinene and limonene. It was used to derive particle mass concentrations for experiments with consumer products.

Method 2 (functional fit to data):

The particle size ranges and number concentrations measured by the LASAIR® were used to develop an exponential best-fit curve through the data. As discussed earlier, particle number concentrations in the 0.02-0.1 μm had potentially high uncertainties and were not included in the curve fitting. For purposes of curve fitting, each size range was represented by the geometric mean diameter estimated from the minimum and maximum particle diameters in each of the size range. For example, particle number concentrations in the 0.1-0.2 μm size range were represented by a geometric mean diameter of 0.14 μm.

The resulting curve was used to estimate particle number concentrations in small size increments, starting from 0.1 μm and ending at 0.7 μm (1.0 μm for experiment #12) with an increment of 0.01 μm. The resulting particle number concentrations were used to estimate particle mass concentrations using the procedure described in Method 1. For each experiment, this procedure was repeated for each

time step. This method was used to derive particle mass concentrations for experiments with pure α-pinene and limonene.

The LASAIR® and P-TRAK™ particle counters were located outside of the chamber during each experiment. The LASAIR® and P-TRAK™ sample tubing were located in the middle of the chamber approximately 1.5-meter above the floor. The LASAIR® sample tube inlet was placed within about 20 cm of the P-TRAK™ sample tube inlet. The LASAIR® drew sample air from within the chamber through a 3.5-meter long (3 mm OD) urethon tube. The P-TRAK™ pulled air through a 5-meter long (6 mm OD) tygon tube. Particle losses in tubing were determined by running the analyzers with and without tubing. For analysis without tubing, samples were collected outside the chamber. For analysis with tubing the sample inlet was placed near the instrument outside the chamber. The length and configuration of tubing was identical to that used for actual experiments. The average loss of particles was 25% in the 5-meter tube used for the P-TRAK™ and 14% in the 3.5-meter tube used for the LASAIR®. Measured particle number concentrations were adjusted to account for losses in tubing; particle number concentrations measured by the LASAIR® and P-TRAK™ were multiplied by a factor of 1.17 and 1.34, respectively, to obtain the actual particle number concentrations in the chamber.

Chamber O_3 (inside and outside) was measured using an ozone analyzer (Dasibi Environmental Corporation, model 1003-AH). This instrument measures O_3 using the principle of ultra-violet light absorption. A solenoid valve was used to switch the intake of the O_3 analyzer between the interior and exterior of the chamber. The solenoid valve was programmed to maintain the intake of the ozone analyzer inside the chamber for 50 minutes before switching to outside the chamber for a period of 10-minutes for each hour of the experiment. The analyzer was placed outside of the chamber and drew sample air through approximately 3 meter (6 mm

OD) of teflon tubing. Loss of O_3 in the teflon tubing is expected to be small and therefore was not accounted for. Clausen *et al.* (2001) conducted mouse bioassay experiments in which a teflon tube (length = 4.9 meter, ID = 22 mm) was used to introduce O_3 into a chamber. They also reported that the O_3 concentration loss in the teflon tube used in their experiment was less than 1%. A data logger (Agilent Technologies, model 34970A) was connected to the ozone analyzer to record data.

The chamber air exchange rate was measured by injecting sulfur hexa-fluoride (SF_6) and monitoring its decay using a GC/ECD optimized for analysis of SF_6 (Lagus Applied Technology, Inc., model 101, Autotrac). A small amount (<10 mL) of high purity SF_6 (Air Liquid, electronic grade, purity 99.96%) was mixed with ambient air in a 2-liter Tedlar bag and the resulting mixture was then manually injected into the chamber at the beginning of each experiment via a 6 mm OD teflon tube. The SF_6 was allowed to mix in the chamber for 20-30 minutes before any measurements were taken. The SF_6 analyzer pulled sample air from about 1.5-meter above the chamber floor through a 3 mm OD tube and was programmed to take samples every two minutes. The initial chamber SF_6 concentrations ranged from 10-35 ppb. Equation 3.1 was used to determine the air exchange rate in the chamber. The decay of SF_6 concentrations in the chamber occurred only due to air exchange. Thus, the slope of a plot of natural logarithm of the normalized SF_6 concentration versus time provided the air exchange rate in the chamber. A typical plot of the decay of chamber SF_6 and the resulting air exchange rate is provided in Figure 4.2.

Chamber temperature and relative humidity were measured during each experiment using a portable digital hygrometer (VWR, model 35519-041). The sample probe of the hygrometer was placed inside the chamber approximately 0.75 meter above the floor. Temperature and relative humidity were recorded every 30-60 minutes during each experiment.

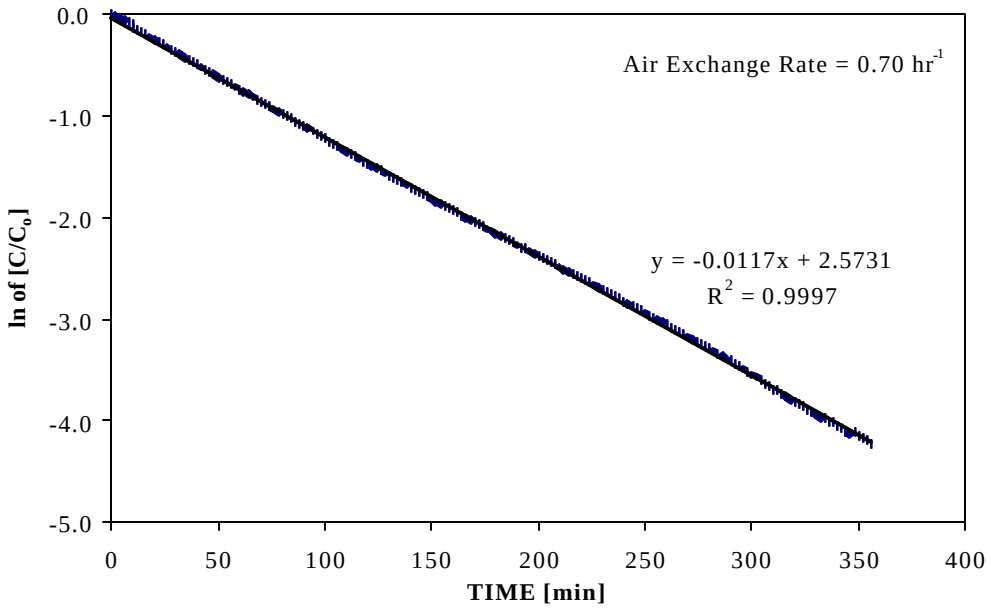

Figure 4.2. A typical plot of the decay of SF_6 in the chamber. 'C' is SF_6 concentration at time t and Co is the initial SF_6 concentration.

To determine terpene concentrations in the chamber, air samples were collected on Tenax® adsorption tubes. Samples were drawn through a 1 meter length (from sample inlet to adsorbent tube) of teflon tubing (6 mm OD), with the inlet located about 0.75 meter above the chamber floor. A portable air-sampling pump (SKC® AIRCHECK, Model 224-PCXR4) was used to draw air to the sorbent tubes. The sample flow rate was measured using a primary gas flow calibrator (SKC, UltraFlo™, model 709) located downstream of the sample pump and ranged from 100-400 mL/min. Sample time varied from 2 to 7 minutes, with total sample volume varying from 0.7 to 2 liters. One or two samples were taken prior to the introduction of terpenes into the chamber. For experiments #17 to #27, samples were collected at about 15-60 minute intervals after the introduction of consumer products.

Adsorption tubes were capped using stainless steel swagelok end plugs and stored in a laboratory refrigerator at 4 ^{o}C until analysis was performed, always within three days of sample collection. The adsorption tubes were analyzed using a thermal desorber (Tekmar 1600 Aerotrap) and purge and trap controller (Tekmar 3000) followed by gas chromatographic (GC) separation (Hewlett Packard, model 5890) and mass selective detection (MSD, Hewlett Packard, model 5971A). The thermal desorber was equipped with an autosampler, which allowed a maximum of 16 samples. Two blank tubes (one in the 1st and the other in the 9th position) were used for purposes of quality assurance. Each tube was heated for 8 minutes at 225 ^{o}C during which time a carrier gas (helium) was passed through the tube. Compounds removed during thermal desorption were then conveyed to the purge and trap controller via a transfer line maintained at 200 ^{o}C. A Tenax concentrating trap located in the purge and trap concentrated the compounds, which were then desorbed for two minutes at 225 ^{o}C. The desorbed compounds were then transported to the GC/MSD by the carrier gas. The total run time for the GC was 16 minutes and the final temperature of the GC oven was 170 ^{o}C. The GC oven started with an initial temperature of 35 ^{o}C, ramped at a rate of 7 ^{o}C per minute for 5 minutes, and then ramped at a rate of 20 ^{o}C per minute for another 5 minutes until the final temperature was reached. MSD parameters included a solvent delay of 6 minutes, scans of masses from 35 to 350 amu, and 1.45 scans/second. Hewlett Packard ChemStation Version B.02.05 and EnviroQuant ChemStation G1701BA Version B.01.00 were used to perform chromatographic analyses.

Each experiment began with the measurement of particle number concentrations outside of the chamber for 10-30 minutes followed by measurements inside the chamber for another 10-30 minutes before the introduction of terpenes into the chamber. Experiments involving α-pinene or limonene continued for a period of 10-12 hours after source introduction into the chamber. Experiments involving

consumer products lasted 2-10 hours. Particle number concentrations outside the chamber were measured for 10-30 minutes at the end of each experiment.

Operation of the P-TRAK™ requires an isopropanol supply, which needed to be replenished every 5-6 hours. Replenishing the P-TRAK™ with alcohol required about 5-10 minutes, during which time measurements were not collected. Particle number concentrations in the 0.02-0.1 μm size range during this period were estimated by interpolation of data collected immediately before and after alcohol replenishment.

4.4 Quality Assurance Procedures

Periodic zero checks were conducted on the LASAIR® by connecting the inlet of the sampler to the exhaust of the LASAIR® analyzer; the exhaust of the LASAIR® contains a particle filter. Thus, recycling sample air through the LASAIR® analyzer should produce a zero particle count. The operation of the LASAIR® with recycling the sample air indeed produced a zero particle count. The recommended annual calibration was performed by the manufacturer within twelve months of the experiments discussed herein. Periodic zero checks on the P-TRAK™ were performed by connecting a zero-kit analyzer to the inlet system in accordance with manufacturer specifications. The system was calibrated by the manufacturer three months prior to the beginning and six months prior to the end of experiments.

A five-point calibration was performed on the ozone analyzer using primary standards two weeks prior to all experiments. The analyzer responses were within 1% of the primary standards; thus the ozone analyzer data were used without any further correction. The calibration was also repeated at the end of these experiments; analyzer responses were also within 1% of the standards.

A five-point calibration was performed on the GC/MSD system using known standards. The standards were made by sequentially diluting known amounts of organic compounds in 1 mL of high purity methanol. Ten microliters (μL) of pure reagent grade α-pinene or limonene was mixed with 1 mL of high purity methanol in a 2 mL vial. Ten μL of the resulting mixture was then further mixed with 1 mL of high purity methanol in a second vial. The diluted mixture from the second vial was injected into five different clean sorbent tubes, with corresponding mass injections of 50, 100, 200, 400, and 800 nanograms (ng). These standards were then analyzed using the GC/MSD described in section 4.3. The resulting calibration curves were linear. A typical calibration curve for limonene is shown in Figure 4.3.

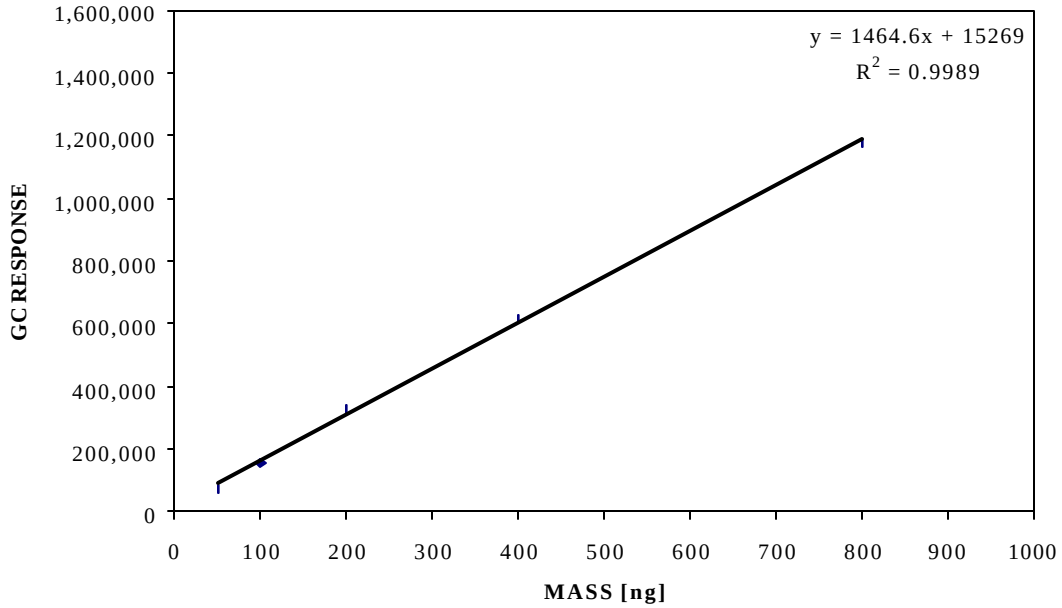

Figure 4.3. A typical calibration curve for limonene

Air samples were initially collected on three adsorption tubes in series and analyzed via the GC/MSD as discussed above. Target volatile organic compounds were not detected in the second and third tubes, which ensured that breakthrough did

not occur in the first tube. Adsorption tubes were also analyzed twice in succession to ensure that trace organic compounds were not left on the tubes after thermal desorption. Analysis indicated that all target organic compounds were removed by thermal desorption during the first run; no compound was detected in the second run.

A vial was tested in a fume hood for constant α-pinene emission rate. A 4-mL vial containing pure α-pinene was placed in a fume hood and vial weight was taken at different time intervals. Analysis of the lost materials indicated that the α-pinene emission rate was indeed constant over time. A typical experimental result is shown in Figure 4.4. Mass emission rates during these preliminary hood experiments were comparable to those observed for actual chamber experiments.

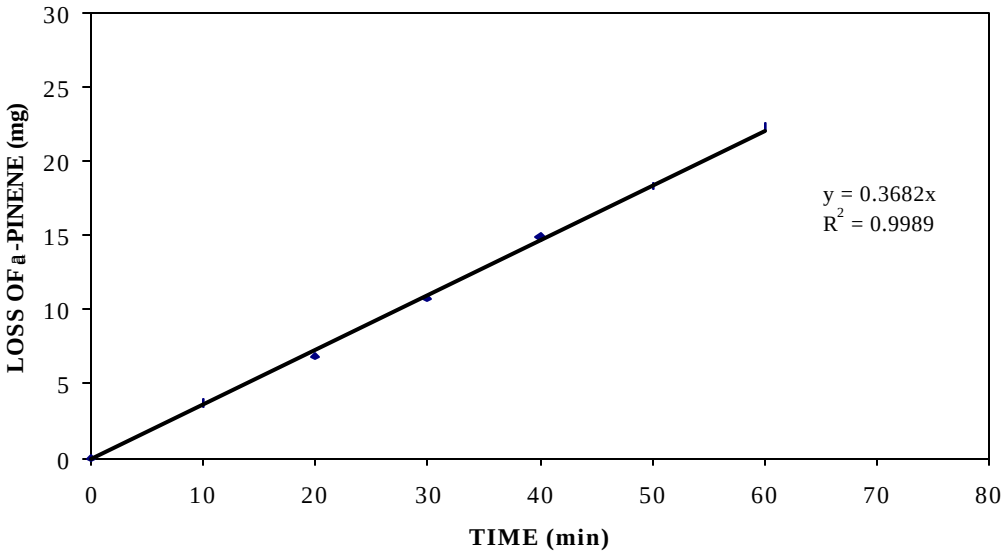

Figure 4.4. A typical result showing a constant a -pinene emission rate

4.5 Deposition Velocities of Ozone and Particles in the Chamber

The ICEM requires deposition velocities of pollutants in indoor environments to estimate surface removal rates. Preliminary deposition velocities of O_3 and particles were measured by measurement of decay rates in the chamber. Ozone concentrations in the chamber were initially raised to an elevated level by operating the ozone generator. The ozone generator was then switched off and the decay of O_3 in the chamber was measured by the ozone analyzer. Equation 3.1 was used to determine the O_3 deposition rate in the chamber. The decay of O_3 concentrations occurred due to deposition on surfaces in the chamber and air exchange. The elevated initial O_3 concentration in the chamber was much higher than the typical O_3 concentrations in the chamber due to outdoor-to-indoor transport; therefore, the effect of the transport of outdoor O_3 on the decay of O_3 concentration was negligible. Thus, the slope of a plot of natural logarithm of the normalized O_3 concentration versus time provided the O_3 decay rate in the chamber. The air exchange rate was also measured during the experiment and was subtracted from the O_3 decay rate to obtain the O_3 deposition rate in the chamber.

A typical plot of the O_3 decay rate in the chamber is shown in Figure 4.5. The ozone decay rate for the experiment shown in Figure 4.5 was 1.39 hr^{-1}, and the air exchange rate was 0.91 hr^{-1}. Thus, the O_3 deposition rate in the chamber was 0.48 hr^{-1}. The measured O_3 deposition rate is much lower than the reported average O_3 deposition rate of 3.6 hr^{-1} for indoor environments (Nazaroff and Cass, 1986). However, the environmental chamber used for this study was constructed of stainless steel and thereby had a much lower O_3 deposition rate. The measured O_3 deposition rate is closer to the deposition rate of 1.5 hr^{-1} reported by Mueller *et al.* (1973) for a stainless steel room. The surface area to volume ratio of the environmental chamber used in this study was 2.7 m^{-1}. With this surface area to volume ratio, the deposition

velocity of O_3 in the chamber was 0.005 cm/sec. This deposition velocity was used in the ICEM for purposes of comparing experimental and predicted results.

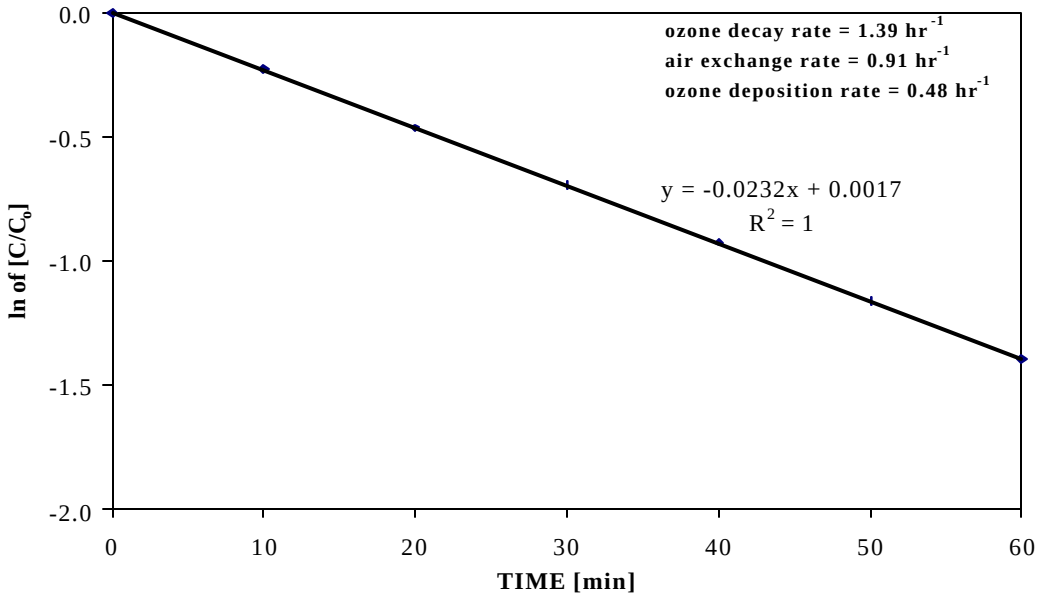

Figure 4.5. Ozone decay rate in the experimental chamber. 'C' is O_3 concentration at time t and Co is the initial O_3 concentration.

Particle concentrations in the chamber were initially raised to elevated levels by directly injecting a commercial air-freshener containing aerosols into the chamber. The decay rates of particles were measured by the P-TRAK™ and the LASAIR®. Equation 3.1 was used to determine the particle deposition rate in the chamber. The decay of particle concentrations occurred due to deposition of particles on surfaces in the chamber and due to air exchange. The elevated initial particle number concentration in the chamber was much higher than the typical particle number concentrations in the chamber due to outdoor-to-indoor transport; therefore, the effect of the transport of particles from outdoors on the decay of particle concentrations was negligible. Thus, the slope of a plot of natural logarithm of the normalized particle number concentration versus time provided the particle decay rate in the chamber. The air exchange rate was also measured during the experiment and was subtracted

from the particle decay rate to obtain the particle deposition rate in the chamber. A typical plot of the particle (0.5-0.7 μm size range) decay rate in the chamber is shown in Figure 4.6. The particle decay rate during this experiment was 1.36 hr^{-1} and the air exchange rate was 1.0 hr^{-1}. The deposition rate of the particles was obtained by subtracting the air exchange rate from the particle decay rate, and was 0.36 hr^{-1} for particles in the 0.5-0.7 μm size range. Deposition rates of particles in the 0.2-0.3 μm and 0.7-1.0 μm ranges were measured to be 0.30 hr^{-1} and 0.37 hr^{-1}, respectively. The average value of these deposition rates was 0.34 hr^{-1} and was used in ICEM. The measured particle deposition rate compares favorably with the fine particle deposition rate of 0.33 hr^{-1} reported by Wainman (1999) and 0.39 hr^{-1} reported by Wallace (1996). The average deposition velocity of particles in the chamber was 0.0035 cm/sec.

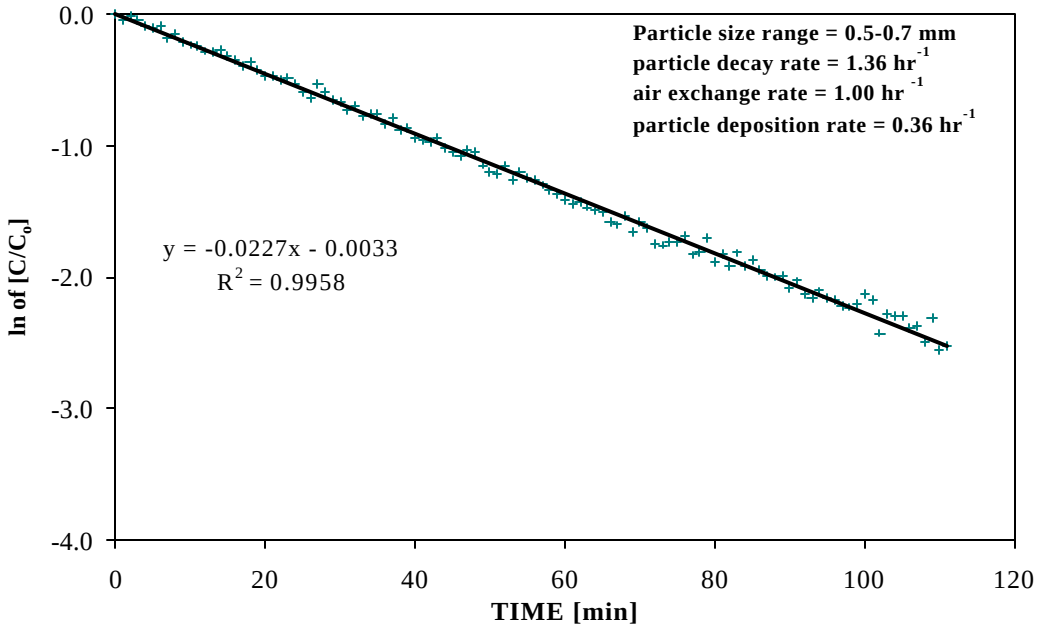

Figure 4.6. Particle decay rate in the experimental chamber. 'C' is particle concentration at time t and Co is the initial particle concentration.

5.0 CHAMBER STUDIES: EXPERIMENTAL RESULTS

Experiments were conducted in an 11-m^3 environmental chamber to evaluate the effects of homogeneous reactions between O_3 and terpenes on formation/growth of indoor secondary particles. Experimental results are presented in this chapter.

5.1 Particle Growth from the Release of Pure a -Pinene

A summary of the ten experiments involving α-pinene is presented in Table 5.1. Number concentrations represent particles in the 0.02-0.7 μm diameter range and mass concentrations represent particles in the 0.1-0.7 μm diameter range. Results of all chamber experiments involving α-pinene are included in Appendix D; selected results are presented here.

Table 5.1. Summary of Chamber Results from the Release of Pure a -Pinene

Expt No.	l	E	Initial O_3	T	Initial Particle	Max Particle	Time	Final Particle	M_i	$M_{f,e}$	SOA	$M_{f,p}$	Difference
	(hr^{-1})	(mg/min)	(ppb)	(C)	(#/cc)	(#/cc)	(min)	(#/cc)	(mg/m^3)	(mg/m^3)	(mg/m^3)	(mg/m^3)	(%)
1	1.25	196	15	25	2,760	3,423	108	1,997	3.6	4.3	0.7	5.0	-16
2	0.55	75	132	24	7,047	96,989	17	10,004	3.1	38.5	35.4	55.3	-43
3	0.68	81	134	26	1,383	34,662	34	7,227	2.2	21.0	18.8	26.5	-26
4	1.06	78	111	24	9,202	11,852	39	6,774	4.3	16.2	11.9	19.7	-21
5	0.70	70	136	25	4,138	18,529	31	7,324	9.2	28.9	19.7	29.9	-3
6	0.70	91	170	24	10,391	14,532	48	9,511	5.4	48.7	43.3	65.9	-26
7	0.75	98	142	25	2,836	30,114	26	6,327	10.8	33.2	22.4	52.2	-57
8	1.34	89	157	32	8,472	31,062	48	35,975	6.9	17.1	10.2	20.5	-20
9	1.50	102	144	33	12,529	37,729	48	25,332	3.3	6.5	3.2	8.8	-35
10	0.71	185	159	25	4,438	25,131	32	9,180	2.7	73.7	71.0	181	-145

Note:
λ = air exchange rate, E = α-pinene emission rate, Time = time at which the maximum particle number concentrations occurred in the chamber, M_i = initial particle mass concentration in the chamber, $M_{f,e}$ = final experimental particle mass concentration in the chamber, $M_{f,p}$ = final predicted particle mass concentration in the chamber, SOA = secondary organic aerosol = $M_{f,e} - M_i$, Difference = $(M_{f,e} - M_{f,p})/M_{f,e}$

The ozone generator was not operated during experiment #1, so for this experiment the O_3 levels were in the range of 10-15 ppb and were derived from outdoor-to-indoor penetration at the CEER. The evolution of particle number concentrations for experiment #1 is presented in Figure 5.1. Time zero in Figure 5.1

refers to the instant when α-pinene was introduced into the chamber. The P-TRAK™ was not operated after about 500 minutes from the introduction of α-pinene into the chamber. The α-pinene emission rate for experiment #1 was much higher than for other experiments. Despite the higher α-pinene emission rate, the particle level increase was small relative to experiments with elevated O_3 levels.

The evolutions of experimental and predicted particle mass and O_3 concentrations during experiment #1 are presented in Figure 5.2. The initial particle mass concentration was 3.6 μg/m^3, and mass concentrations increased slightly after the introduction of *α*-pinene into the chamber.

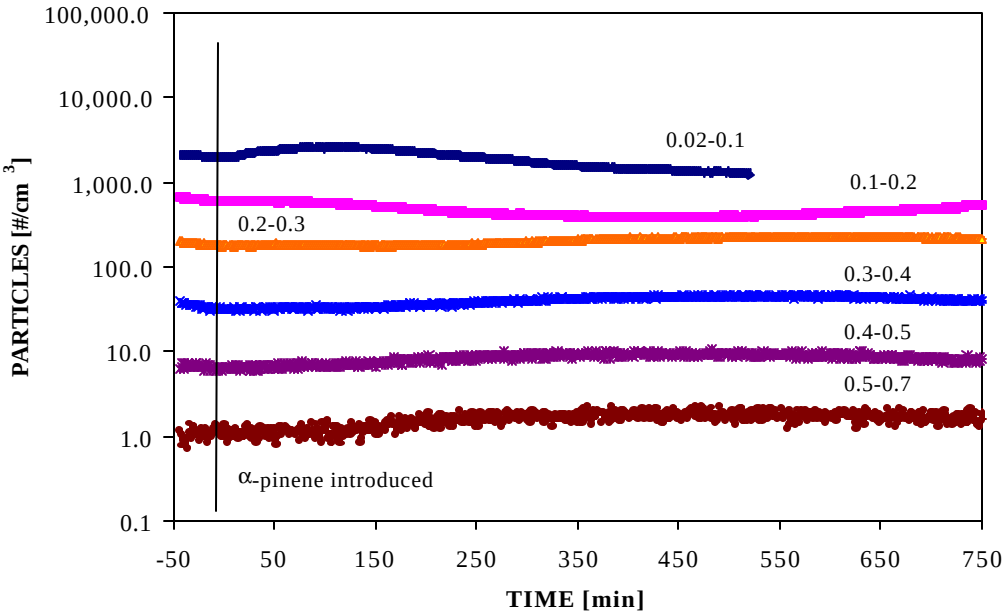

Figure 5.1. Evolution of particle number concentrations during experiment #1. l = 1.25 hr^{-1}

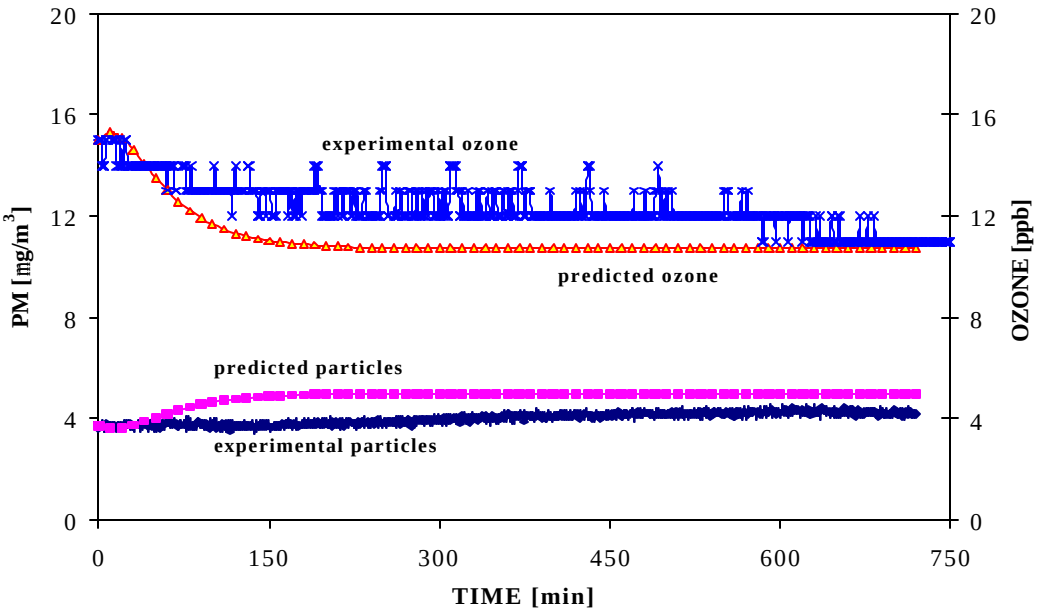

Figure 5.2. Experimental and predicted particle mass and O_3 concentrations during experiment #1. $l = 1.25\ hr^{-1}$

Particle mass concentration in the chamber eventually reached a steady-state level of about 4.3 $\mu g/m^3$. The difference between the steady-state and initial particle mass concentration is the secondary organic aerosol (SOA) mass concentration. The SOA was only 0.7 $\mu g/m^3$ for the conditions used in experiment #1. The predicted particle mass concentrations for experiment #1 were in good agreement with experimental results and were within 16% of the experimental results at steady-state conditions. The O_3 concentration in the chamber was initially about 15 ppb and decreased slightly after the introduction of α-pinene into the chamber before reaching a steady-state concentration. The decrease in O_3 concentration and subsequent increase in particle mass concentrations most likely occurred due to reaction of O_3 with α-pinene.

Experiment #3 involved α-pinene and elevated O_3 levels; the evolution of particle number concentrations for this experiment is shown in Figure 5.3. A rapid "burst" of small particles in the 0.02-0.1 μm size range was detected shortly after the introduction of α-pinene into the chamber. Particle numbers in the 0.02-0.1 μm size range then decreased before attaining a steady concentration of approximately four times the initial concentration. Particle numbers in the next size range then increased and subsequently decreased before attaining a steady concentration. This process continued for particles with diameters up to 0.5-0.7 μm, after which no appreciable increase in particle numbers was observed. The initial "burst" of small particles followed by a decrease in particle numbers in a given size range and increase in particle numbers in subsequent size ranges created an effective particle growth "wave" that was observed for all experiments. Ultimately, particle number concentrations reached steady-state conditions controlled primarily by the reaction rate of O_3 with α-pinene and the prevailing air exchange rate.

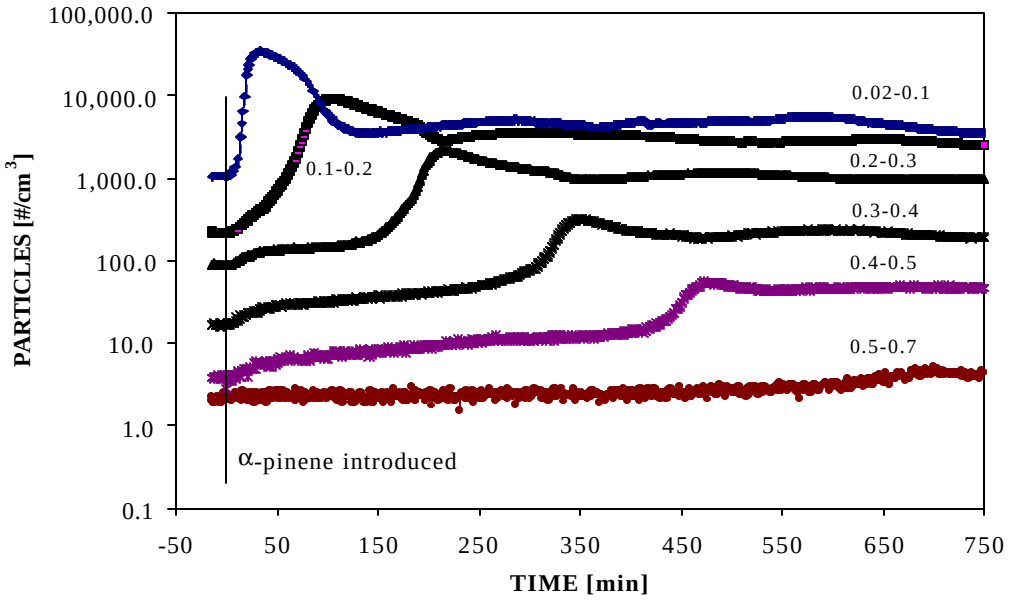

Figure 5.3. Evolution of particle number concentrations during experiment #3. l = 0.68 hr^{-1}

Particle surface area and volume based on Method 1, at time zero for experiment #3 are shown in Figures 5.4 and 5.5, respectively. The maximum particle surface area and particle volume occurred in the 0.2-0.3 μm size range. The bulk of the particle surface area was contained among the 0.02-0.1, 0.1-0.2, 0.2-0.3, and 0.3-0.4 μm size ranges. While there was some initial growth of larger size particles, the initial "burst" of particles was observed in the 0.02-0.1 μm size range. This suggests that the initial "burst" of small particles may not be solely the result of condensation/absorption of semi-volatile particles onto smaller seed particles, in which case an initial "burst" would be expected in the larger size ranges. The initial "burst" of small particles may be the result of the nucleation of very low vapor pressure products of the O_3/α-pinene reactions, as well as the growth of smaller particles to the detectable particle range.

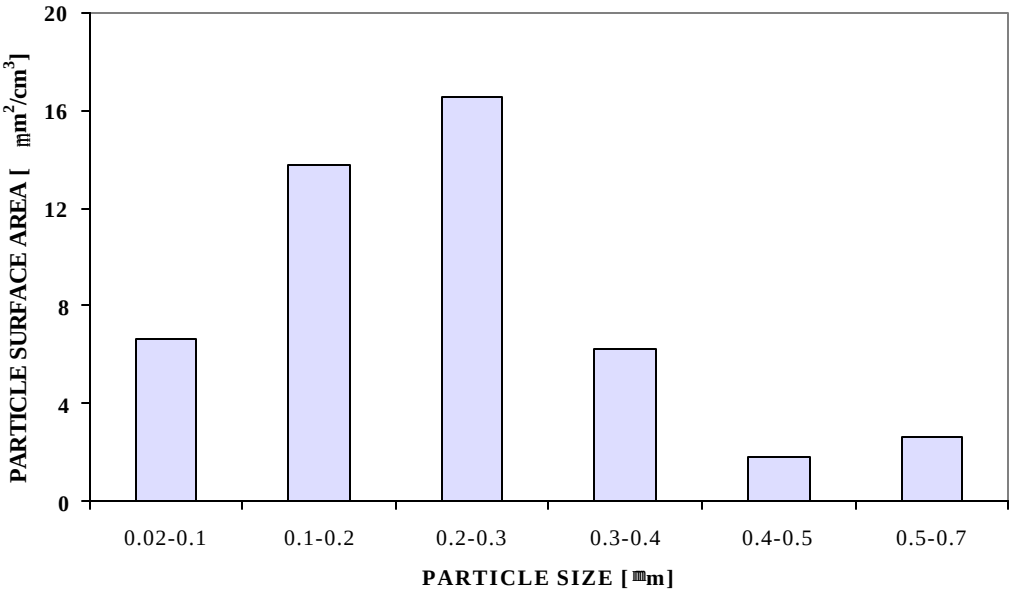

Figure 5.4. Particle surface area as a function of particle size at time zero during experiment #3. l = 0.68 hr^{-1}

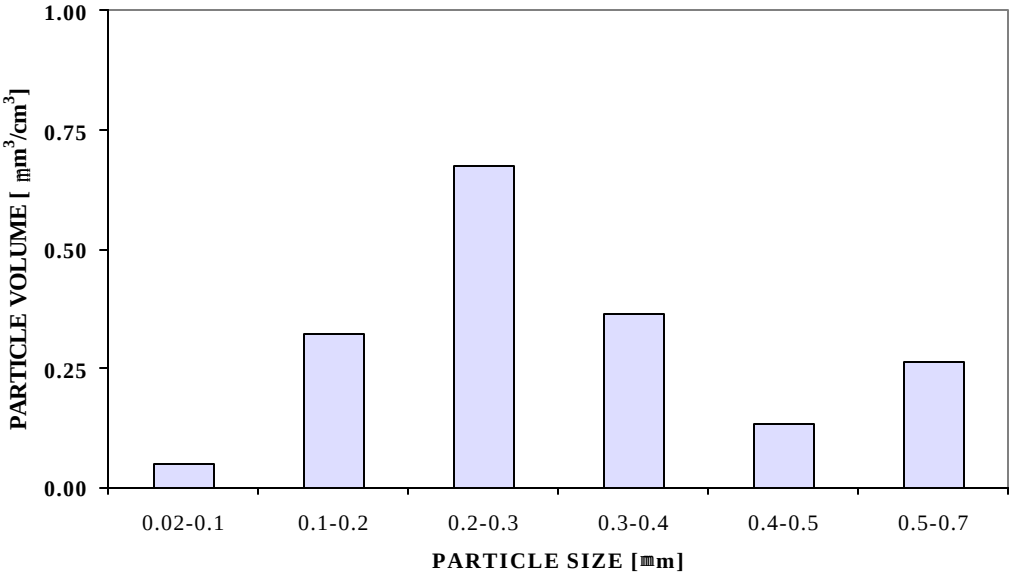

Figure 5.5. Particle volume as a function of particle size at time zero during experiment #3. l = 0.68 hr^{-1}

Details of the reaction products that can form new particles via nucleation are not currently known. However, Kamens *et al.* (1999) suggested two possible mechanisms for the nucleation process to occur. Stabilized Criegee biradicals can react with products containing carbonyl groups to form a secondary ozonide. It also has been suggested that Criegee biradicals can react with dicarboxylic acid to form an anhydride. These products were suggested to have high molecular weights (~350) and very low vapor pressures (10^{-15} torr) (Kamens *et al.* (1999), with significant potential for self-nucleation.

It is, however, also possible that initial particles in the chamber during experiment #3 were bimodally distributed and particles in the smaller size range (lower than the detectable range of 0.02 μm) may contain higher surface area or volume. Thus, the initial "burst" of particles may have been a result of the growth of smaller particles via partitioning of the semi-volatile reaction products alone.

The initial particle number concentration during experiments # 4 and #6 were relatively high compared to experiment #3. Particle surface area and volume at time zero for experiment #4 are shown in Figures 5.6 and 5.7, respectively. The maximum particle surface area and volume occurred in the 0.1-0.2 μm size range and the bulk of the particle surface area and volume was contained among the 0.02-0.3 μm size range. The evolution of particle number concentrations for experiment #4 is shown in Figure 5.8. The initial "burst" of particles in the 0.02-0.1 μm size range was negligible compared to experiment #3. The initial increases in particle number concentrations occurred in the 0.1-0.2, 0.2-0.3, and 0.3-0.4 μm size ranges and reflects particle growth from the immediate lower size ranges containing the bulk of the particle surface area and volume. This suggests that the initial particles in the chamber were not bimodally distributed for experiment #4, and the initial particle growth occurred via condensation and/or absorption of semi-volatile particles. Similar results were observed for experiment #6.

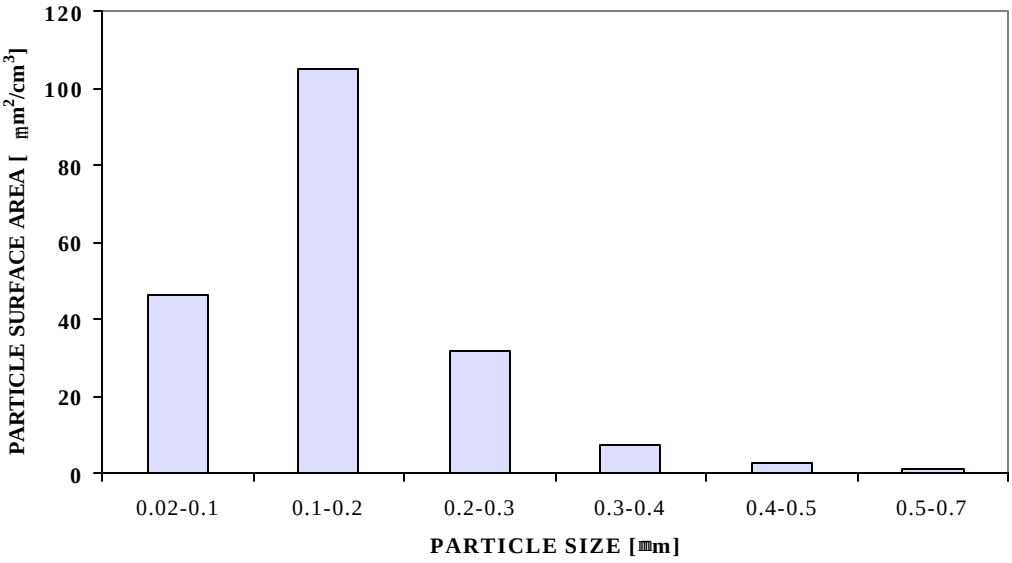

Figure 5.6. Particle surface area as a function of particle size at time zero during experiment #4. l = 1.06 hr^{-1}

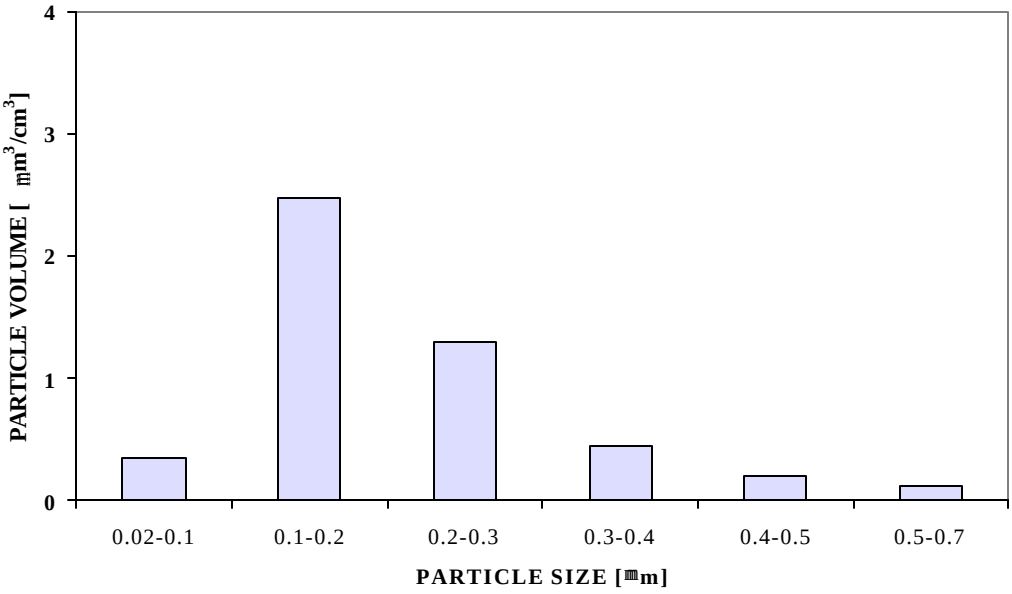

Figure 5.7. Particle volume as a function of particle size at time zero during experiment #4. l = 1.06 hr^{-1}

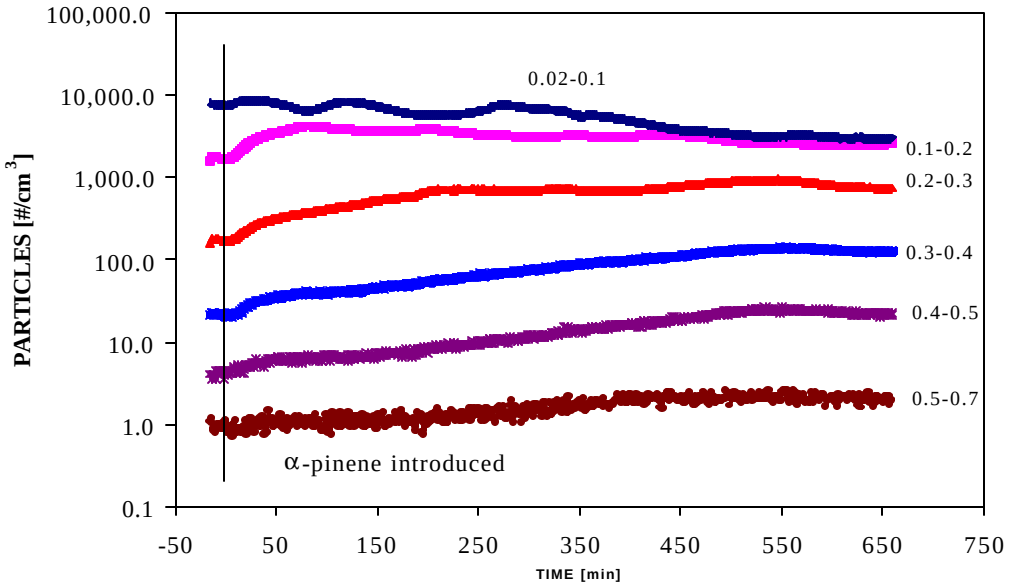

Figure 5.8. Evolution of particle number concentrations during experiment #4. l = 1.06 hr^{-1}

Thus, it is conceivable that initial particles during experiment #3 were not bimodally distributed and the initial "burst" of small particles may have occurred via nucleation of very low vapor pressure products of O_3/α-pinene reactions, and via the growth of smaller particles into the detectable size range.

Unfortunately, the limited number of particle size ranges associated with the instruments used for this study lend enough uncertainty to surface area calculations to preclude a definitive statement regarding the relative importance of particle formation versus growth. Therefore, the issue of particle nucleation/growth during the initial phase of the experiment should be further explored using particle analyzers that can measure much finer size distributions.

For all experiments, particles were observed to grow up to about 450 minutes after the introduction of α-pinene into the chamber. Similar results were also observed by Weschler and Shields (2002).

Over the entire experimental program there was a constant time lag of between 2-15 minutes prior to rapid increase in particle number concentration. The initial burst of particles was not detected by the P-TRAK™ until about 2-10 minutes after the introduction of α-pinene in the chamber for all experiments except #8 and #9. Experiment #8 and #9 were performed at 8-9 ^{o}C higher temperature than other experiments. The burst of particles during these two experiments was detected by the P-TRAK™ after about 10-15 minutes after the introduction of α-pinene in the chamber. These observations were not due to conveyance times between sample inlet and particle instruments. The estimated travel time for particles from the chamber to the P-TRAK™ was only about 0.5 minute. The travel time for particles from the chamber to the LASAIR® was even shorter.

It takes a finite amount of time for the α-pinene to evaporate and to mix into the chamber. The effective time to evaporate to and mix into the chamber should have been fairly similar for all experiments, and likely contributed partly to the delay in the initial burst of particles in the chamber.

However, the primary reason for the delay in the initial burst of particles was likely due to the time needed for the reaction between O_3 and α-pinene to raise concentrations of low vapor pressure semi-volatile products to sufficient levels for nucleation to occur, or for condensation on existing smaller particles. The elevated temperatures during experiment # 8 and #9 caused the vapor pressures of these products to be higher than that of other experiments. Thus, it should have taken longer to raise the concentrations of these products to sufficient levels for nucleation, a plausible reason why the initial burst of particles was further delayed during each of these two experiments.

The particle size distribution during experiment #3 at the time of α-pinene introduction into the chamber (time = 0) and at a steady-state condition (time = 700 minutes) is shown in Figure 5.9. Particle number concentrations in all size ranges at steady state were consistently higher than the particle number concentrations at time zero. Similar results were also observed for other experiments. The increase in particle number concentrations occurred via the O_3/α-pinene reactions and partitioning of subsequent reaction by-products.

The evolutions of experimental and predicted particle mass and O_3 concentrations for experiment #3 are presented in Figure 5.10. Particle mass concentration in the chamber was initially 2.2 $\mu g/m^3$ and increased after the introduction of α-pinene into the chamber.

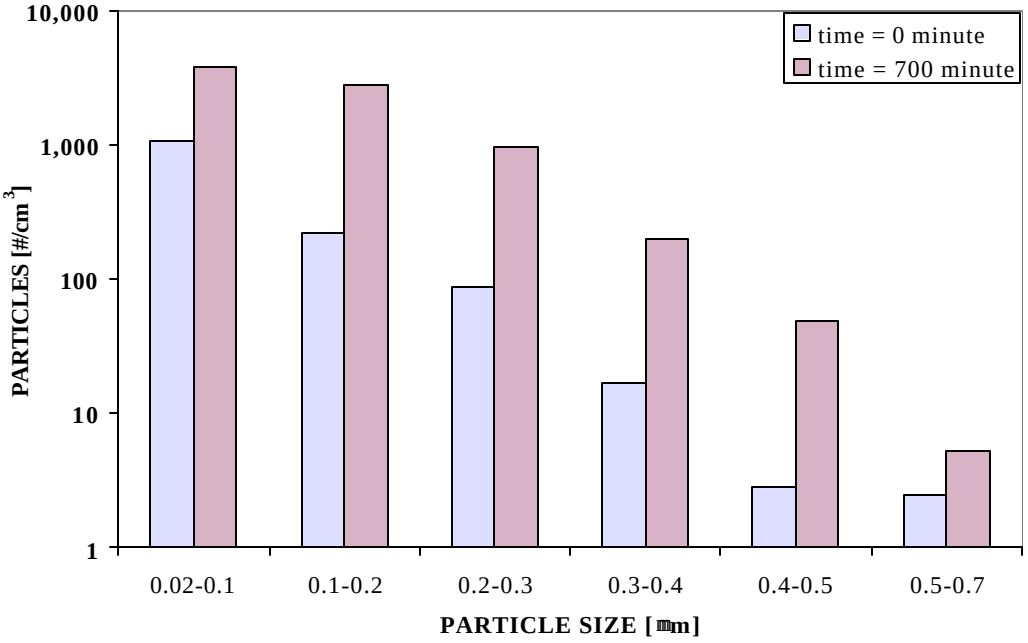

Figure 5.9. Particle size distribution at time 0 and 700 minutes for experiment #3 . l = 0.68 hr^{-1}

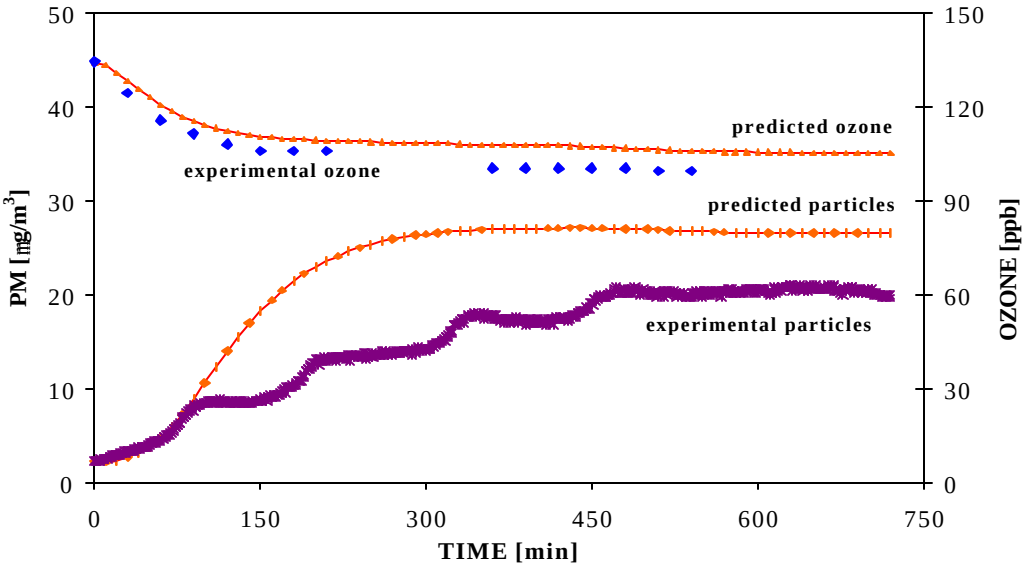

Figure 5.10. Experimental and predicted particle mass and O_3 concentrations during experiment #3. l = 0.68 hr^{-1}

Particle mass concentration eventually reached a steady-state level of 21.0 $\mu g/m^3$; thus the SOA concentration was 18.8 $\mu g/m^3$. The predicted and measured particle mass concentrations for experiment #3 were in good agreement; predicted mass concentrations were within 26% of experimental results at steady-state conditions.

Predicted (using ICEM) constituents of the particles are shown in Figure 5.11 for experiment #3. Model compounds *diacid*, *oxy-pinald*, and *oxy-pinacid* were the three highest contributors and represented almost 90% of the predicted SOA mass concentrations. Model simulations suggest that O_3 and $OH^{\cdot}$ initiated reaction pathways produced approximately 92% and 8% of the predicted secondary particle mass concentrations, respectively. Similar results were predicted for other experiments.

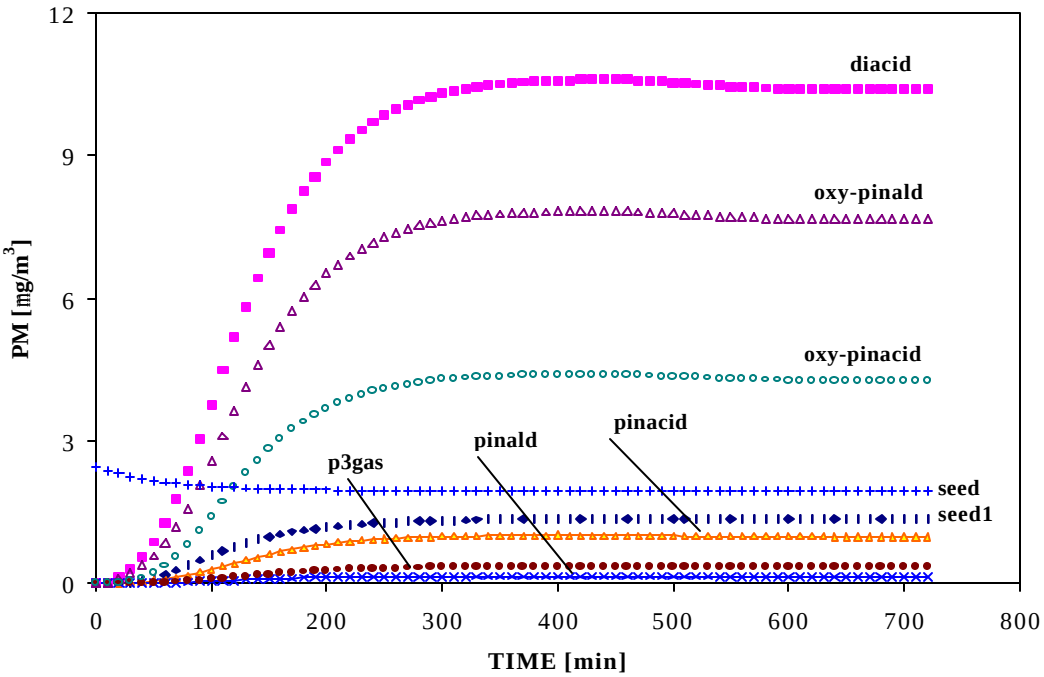

Figure 5.11. Constituents of the predicted particle mass concentrations for experiment #3. $l = 0.68\ hr^{-1}$

The evolution of particle number concentrations for experiment #2 is shown in Figure 5.12. Experiment #2 was also conducted at elevated O_3 levels. Similar to experiment #3, a rapid "burst" of small particles in the 0.02-0.1 μm size range was detected shortly after the introduction of α-pinene into the chamber. A particle growth "wave" similar to experiment #3 was also observed.

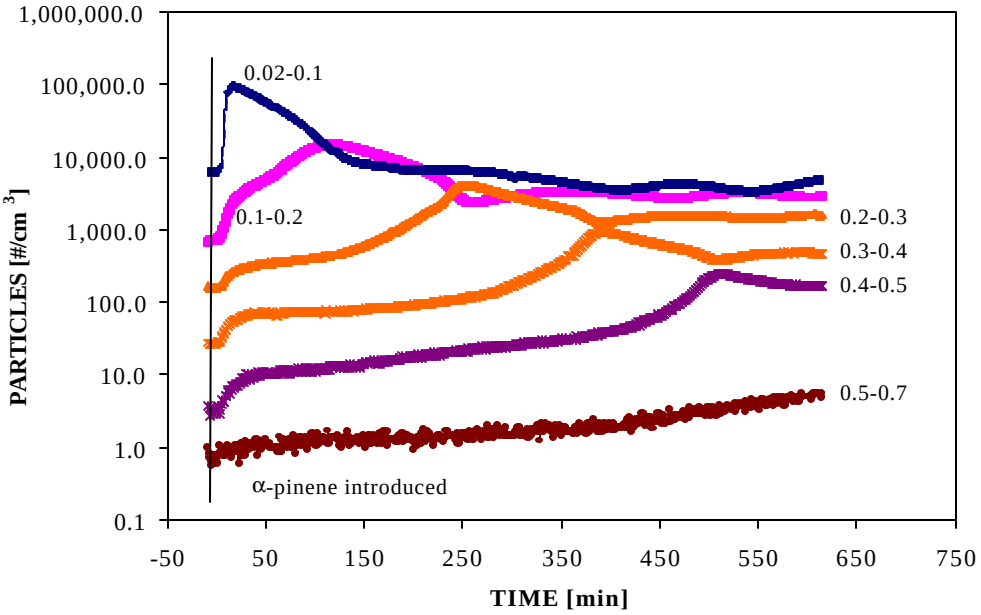

Figure 5.12. Evolution of particle number concentrations during experiment #2. $l = 0.55\ hr^{-1}$

A sample analysis of relative time scales suggests that coagulation phenomena play an insignificant role in defining the particle growth wave. Hinds (1982) provided an equation to relate particle number concentrations for coagulation:

$$N(t) = N_o / (1 + N_o K t) \qquad (5.1)$$

where, K is the coagulation coefficient, N(t) is the particle number concentration at time t, and N_o is the initial particle concentration. The coagulation coefficient, K, for polydisperse particles was estimated using the following equation (Hinds, 1982; Lee and Chan, 1984):

$$K = \frac{2kT}{3\eta}\{1 + \exp(\ln^2 \sigma_g) + \frac{2.49\lambda}{CMD}[\exp(0.5\ln^2 \sigma_g) + \exp(2.5\ln^2 \sigma_g)]\} \quad (5.2)$$

where, k is the Boltzmann constant (1.38 x 10^{-16} dyne-cm/K), T is the temperature (298 K), η is the viscosity of air (1.90 x 10^{-4} dyne-s/cm^2), σ_g is the geometric standard deviation of the particles, and CMD is the count median diameter. The count median diameter (CMD) and the geometric standard deviation (σ_g) were estimated by the following equations (Hinds, 1982):

$$\ln(CMD) = \frac{\sum n_i \ln d_i}{N} \quad (5.3)$$

$$\ln \sigma_g = \left[\frac{\sum n_i (\ln d_i - \ln CMD)^2}{N-1}\right]^{\frac{1}{2}} \quad (5.4)$$

where, n_i is the particle number concentrations in each of the particle size range, d_i is the geometric mean particle diameter of each size range, and N is the total particle number concentration.

Equation 5.3 and 5.4 were used to estimate particle count median diameter (CMD) and the geometric standard deviation (σ_g) for experiment #2. Equation 5.2 was used to estimate the coagulation coefficient (K) for polydisperse particles. Equation 5.1 was used to estimate the time (t_1) needed for the reduction in peak

number concentration of smaller particles to peak number concentration of larger particles via coagulation. The estimated (t_1) and observed times (t_2) are presented in Table 5.2 for experiment #2, and are consistent in magnitude with other experiments.

Table 5.2. Estimated (t_1) and Observed Time (t_2) for the Reduction in Peak Particle Number Concentrations during Experiment #2.

Range	d	K	N_o	N(t)	t_1	t_2
μm	μm	cm^3/s	$\#/cm^3$	$\#/cm^3$	min	min
0.02-0.1	0.045	1.3E-09	92,870	14,816	725	98
0.1-0.2	0.141	1.4E-09	14,816	4,129	2,059	140
0.2-0.3	0.245	1.8E-09	4,129	926	7,723	136
0.3-0.4	0.346	1.6E-09	926	244	3.1×10^4	118
0.4-0.5	0.447	1.7E-09	244	5	1.9×10^6	106

The diameter "d" in Table 5.2 represents the geometric mean diameter of each size range. Estimated times for coagulation were greater than the observed times by 1-4 orders of magnitude. Thus, coagulation was not the dominant process via which number concentrations of smaller particles decreased after the initial burst of 0.02-0.1 μm particles. More importantly, chamber particle mass concentrations continued to increase until a stable condition was attained, reinforcing that coagulation was not the dominant growth process in the system; coagulation would lead to changes in particle number concentrations but a relatively constant mass concentration.

The evolutions of experimental and predicted particle mass and O_3 concentrations during experiment #2 are presented in Figure 5.13. The initial ozone concentration was 132 ppb. It decreased after the introduction of α-pinene into the chamber, and ultimately attained a relatively steady-state level. The predicted O_3 concentrations were within 5% of experimental results. Particle mass concentration was initially 3.1 $\mu g/m^3$ and increased after the introduction of α-pinene into the chamber. Particle mass concentration eventually reached a steady-state level of 39 $\mu g/m^3$. The SOA concentration was therefore 35 $\mu g/m^3$. The predicted and measured

particle mass concentrations were within 43% of one another at steady-state conditions.

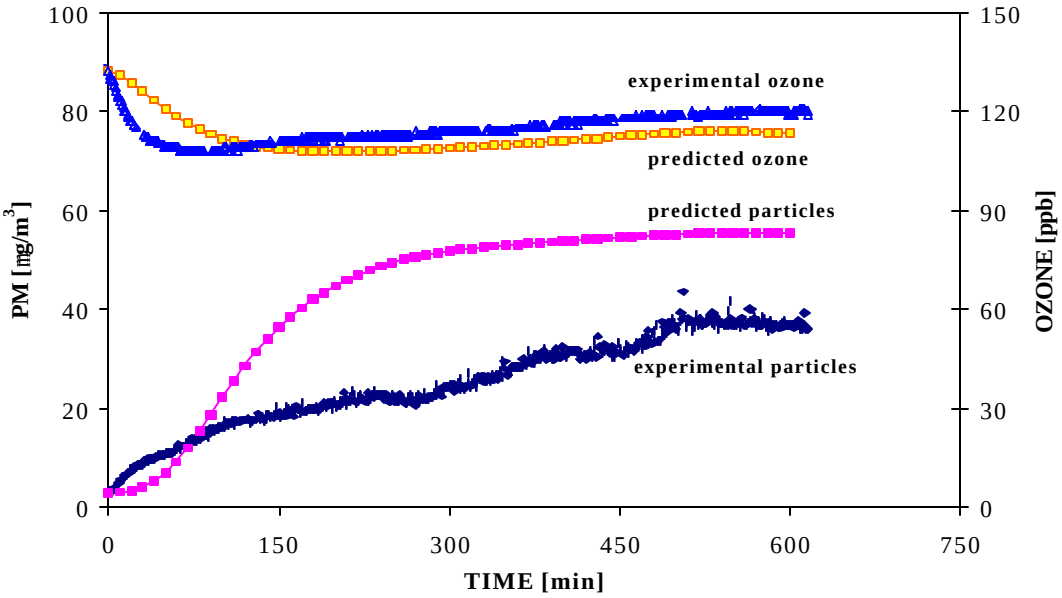

Figure 5.13. Experimental and predicted particle mass and O_3 concentrations during experiment #2. λ = 0.55 hr^{-1}

The air exchange rate for experiment #2 was lower than all other experiments and the resulting SOA mass concentration was also higher than all experiments except for experiments #6 and #10. The air exchange rate during experiment #6 was higher than experiment #2; however, the initial particle number concentrations and the initial O_3 concentrations during experiment #6 were also higher than experiment #2. The higher initial O_3 and particle concentrations resulted in higher SOA mass concentration during experiment #6 compared to experiment #2.

Experiment #10 was conducted at a much higher α-pinene emission rate than experiment #2. However, the lower air exchange rate during experiment #2 increased the time for O_3/α-pinene reactions to proceed and the residence time of particles in

the chamber. The combination of longer reaction time for the O_3/α-pinene reaction and longer particle residence time raised the particle mass concentrations to greater than most of the other experiments.

A comparison of predicted and experimental steady-state particle mass concentrations associated with O_3/α-pinene reactions is presented in Figure 5-14. Predicted particle mass concentrations were within 3 to 57% higher than measured concentrations for all experiments except experiment #10. Experiment #10 was conducted at a much higher α-pinene emission rate than other experiments; it would have produced a steady-state α-pinene concentration of about 250 ppb in the absence of O_3. α-Pinene emissions for other experiments would have resulted in steady-state α-pinene concentrations of 60-130 in the absence of O_3. While experiment #10 suggests that the ICEM may overpredict fine particle mass concentrations by a factor of two or more for episodic releases of α-pinene, it is not possible to draw such a conclusion based on only one experiment.

The current ICEM does not include adsorption/desorption phenomena that may occur in indoor environments. The adsorption/desorption phenomena may have played a role in over-estimating the particle mass concentrations during experiment #10. However, the exact reason of much higher predicted particle mass concentrations compared to experimental results could not be ascertained from the experiments described herein.

Experiments #8 and #9 were conducted at elevated chamber temperatures. Temperatures during these two experiments were 32-33 ^{o}C, about 8-9 ^{o}C higher than other experiments. The lower particle growth observed during these experiments can not be entirely attributed to elevated temperature, since the air exchange rates during

these experiments were also higher than for other experiments; operation of the space heater tended to increase the air exchange rate in the chamber.

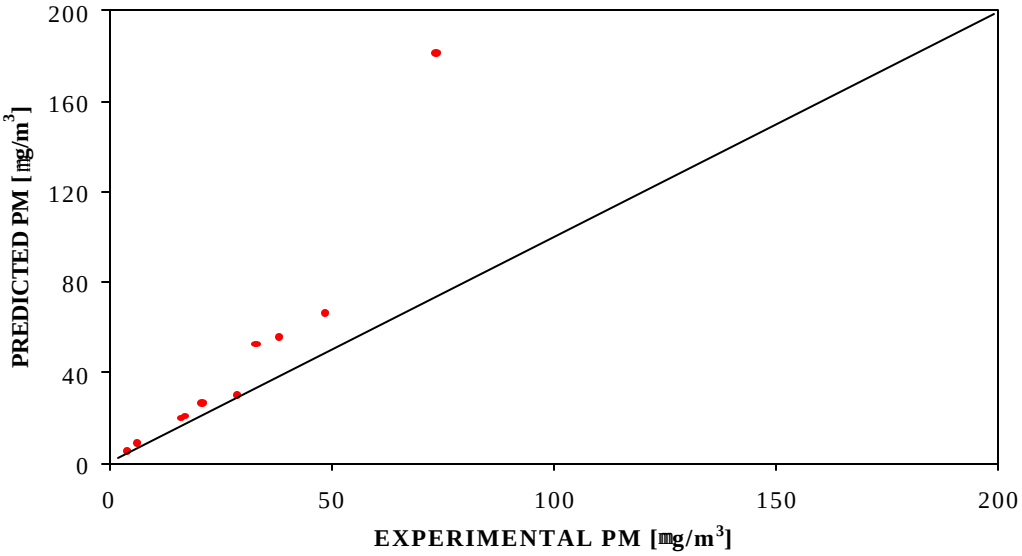

Figure 5.14. Comparisons of experimental and predicted steady state particle mass concentrations

The results of experiments involving α-pinene and O_3 are consistent with the results of Rohr *et al.* (2001) described in Chapter 2. Rohr *et al.* (2001) also reported significant increases in indoor particle number concentrations when α-pinene and O_3 were allowed to react in a plexiglas chamber.

Over all experiments, the reasonably close agreements between predicted and experimental particle mass concentrations are encouraging. The model appears to capture processes associated with particle formation and/or growth. However, additional research will be needed to improve model performance.

5.2 Particle Growth from the Release of Pure Limonene

A summary of the six experiments involving limonene is presented in Table 5.3. Number concentrations represent particles in the 0.02-0.7 μm diameter range, except experiment #12 for which particles in the 0.02-1.0 μm diameter range are shown. Mass concentrations represent particles in the 0.1-0.7 μm diameter range, except experiment #12 for which particles in the 0.1-1.0 μm diameter range are shown. Results of all chamber experiments involving limonene are included in Appendix E; selected results are presented here.

Table 5.3. Summary of Chamber Results from the Release of Pure Limonene

Expt No.	l	E	Initial O_3	T	Initial Particle	Max Particle	Time	Final Particle	M_i	$M_{f,e}$	SOA
	(hr^{-1})	(mg/min)	(ppb)	(C)	(#/cc)	(#/cc)	(min)	(#/cc)	(mg/m^3)	(mg/m^3)	(mg/m^3)
11	NA	113	11	25	3,833	3,833	1	1,805	2.9	2.8	NONE
12	0.71	110	163	25	4,560	90,244	15	11,453	7.3	153	146
13	0.95	85	114	23	7,131	55,987	25	13,628	2.9	68.7	66
14	1.00	88	327	23	3,413	160,285	13	14,940	1.8	78.7	77
15	1.17	84	151	23	2,661	79,174	19	15,061	1.3	63.8	63
16	1.21	91	85	24	6,297	24,643	33	13,362	5.5	68.9	63

Note:
λ = air exchange rate, E = limonene emission rate, Time = time at which the maximum particle number concentration occurred in the chamber, M_i = initial particle mass concentration in the chamber, $M_{f,e}$ = final experimental particle mass concentration in the chamber, and SOA = secondary organic aerosol = $M_{f,e} - M_i$

The ozone generator was not operated during experiment #11, so for this experiment chamber O_3 levels were 11 ppb and were derived from outdoor-to-indoor penetration. The evolution of particle number concentrations for experiment #11 is presented in Figure 5.15. Time zero in Figure 5.15 refers to the instant when limonene was introduced into the chamber. Particle number concentrations did not increase during this experiment. The air exchange rate during this experiment was not measured; however it is expected to be 1-3 hr^{-1} based on experience with other experiments.

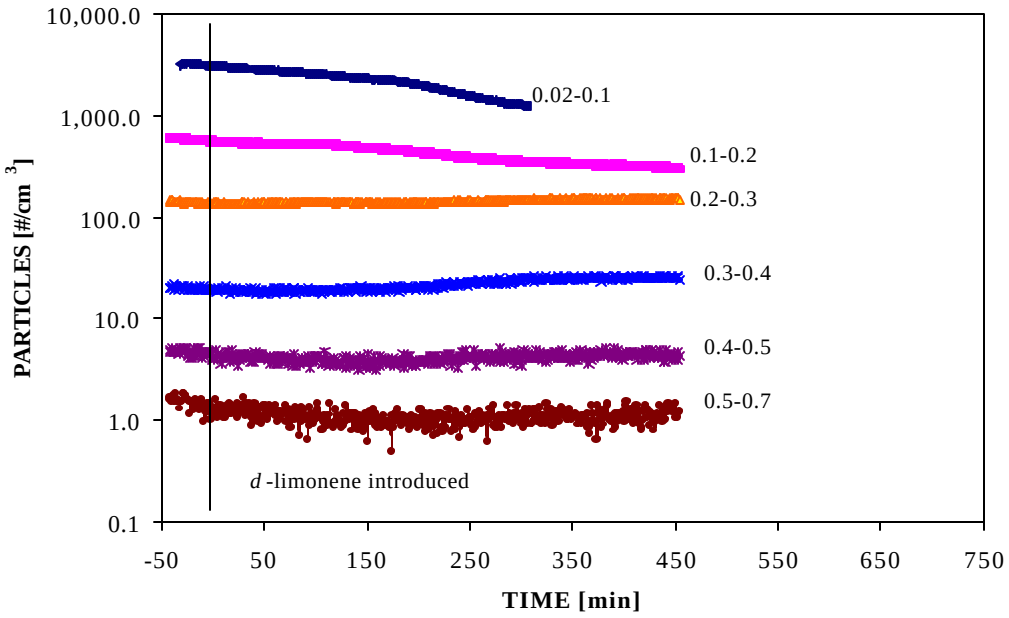

Figure 5.15. Evolution of particle number concentrations during experiment #11.

It was not possible to predict particle mass concentrations from O_3/limonene reactions since a detailed set of reaction and partitioning mechanisms does not currently exist; these reaction mechanisms are currently being developed by the author.

The evolutions of experimental particle mass concentrations and O_3 concentrations during experiment #11 are presented in Figure 5.16. The chamber O_3 concentration was initially 11 ppb and did not appreciably change after the introduction of limonene into the chamber. Particle mass concentration in the chamber was initially 2.9 $\mu g/m^3$ and did not increase after the introduction of limonene into the chamber. These results suggest that no appreciable SOA formation

or growth occurs due to O_3/limonene reactions at relatively low indoor O_3 concentrations.

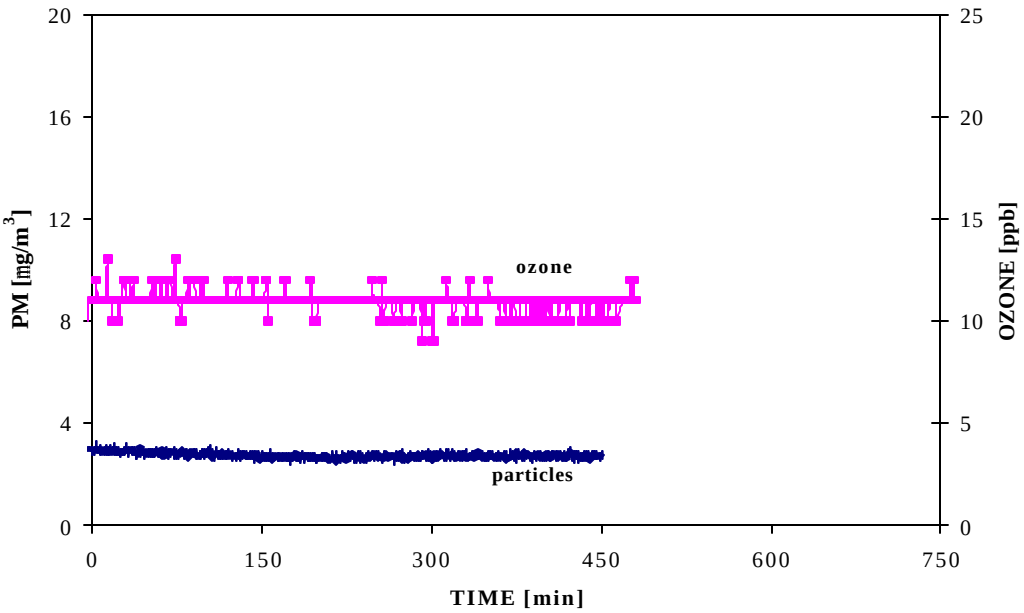

Figure 5.16. Evolution of particle mass and O_3 concentrations during experiment #11.

Experiment #12 involved limonene and elevated chamber O_3 concentrations, high limonene emissions and a relatively low air exchange rate, i.e., long reaction time. Under these conditions, a relatively large increase in final particle number concentration was achieved. The evolution of particle number concentrations for this experiment is shown in Figure 5.17. Similar to experiments with α-pinene, a rapid "burst" of particles in the 0.02-0.1 μm size range was detected shortly after the introduction of limonene into the chamber. Particle numbers in the 0.02-0.1 μm size range then decreased before attaining a steady concentration of approximately 25% higher than the initial concentration. The particle growth "wave" was more pronounced than it was for α-pinene experiments. The rate constant for the O_3/limonene reaction is higher than the rate constant of the O_3/α-pinene reaction. Additionally, the partitioning rates of the semi-volatile products of O_3/limonene

reactions are different than the partitioning rates of semi-volatile products related to O_3/α-pinene reactions. The higher rate constant and different partitioning rates of semi-volatile products produced increased particle levels during experiments with O_3 and limonene, i.e., relative to experiments #1-10 (O_3/α-pinene experiments).

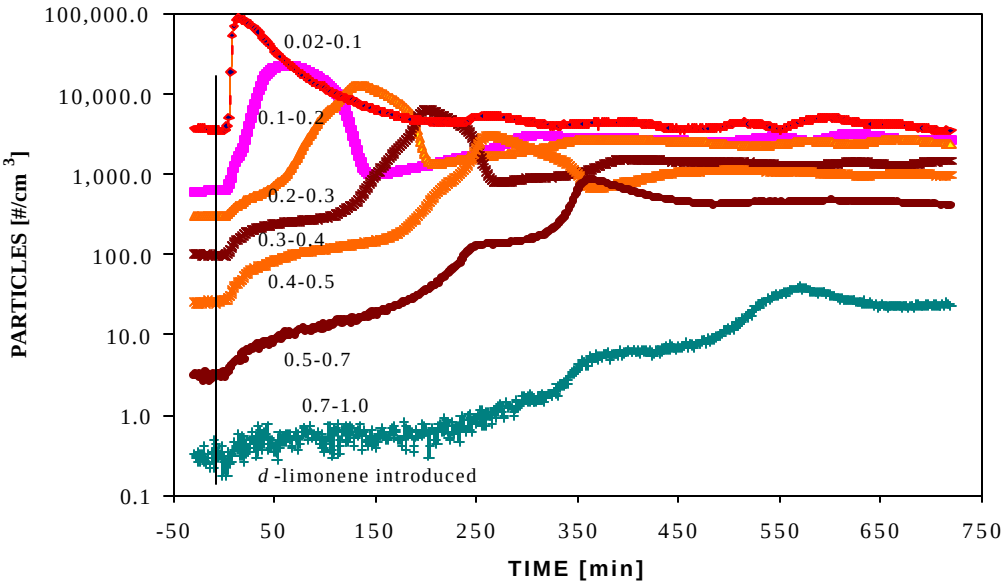

Figure 5.17. Evolution of particle number concentrations during experiment #12. l = 0.71 hr^{-1}

Particle surface area and volume at time zero for experiment #12 are shown in Figures 5.18 and 5.19, respectively. The maximum particle surface area and volume occurred in the 0.2-0.3 μm size range. The bulk of the particle surface area and volume were contained in the 0.02 to 0.5 μm size ranges. However, the initial "burst" of particles was observed in the 0.02-0.1 μm size range. This suggests that the initial "burst" of small particles may not be solely the result of condensation/absorption of reaction products onto smaller particles. It is conceivable that nucleation of very low vapor pressure reaction products also contributed to the particle burst.

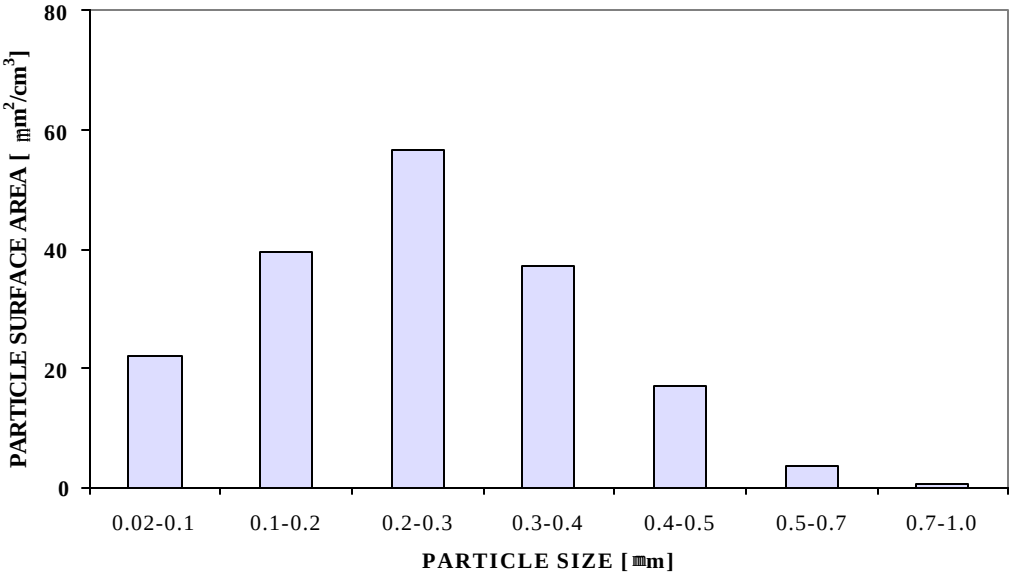

Figure 5.18. Particle surface area as a function of particle size at time zero during experiment #12

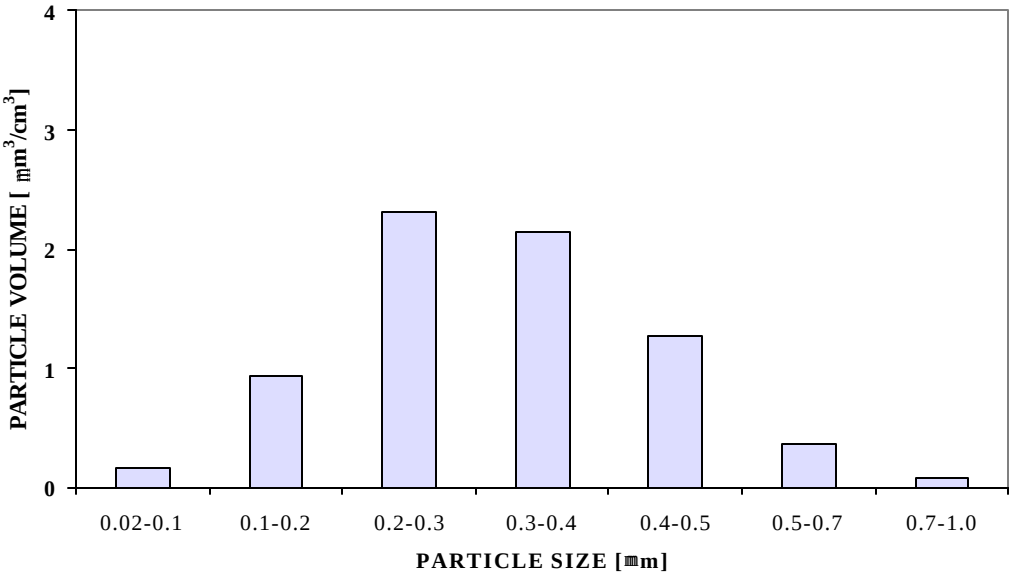

Figure 5.19. Particle volume as a function of particle size at time zero during experiment #12

Exact products that participate in the nucleation process are not known; however, the products are expected to be similar to those associated with O_3/*α*-pinene reactions. In the case of O_3/limonene reactions the analogous low vapor pressure products that might nucleate would include secondary ozonides and anhydrides. Secondary ozonides may result from reactions between stabilized Criegee biradicals and products containing carbonyl groups, and anhydrides may result from reactions between Criegee biradicals and dicarboxylic acids.

However, it is also possible that initial particles in the chamber during experiment #12 were bimodally distributed and particles in the smaller size range (lower than the detectable range of 0.02 μm) may have contained higher surface area or volume. Thus, the initial "burst" of particles may have been the result of the growth of smaller particles via partitioning of semi-volatile reaction products.

Particles were observed to grow up to about 350 minutes after the introduction of limonene into the chamber during experiment #12. This trend was observed for all experiments. Similar experimental results were observed by Weschler and Shields (2002).

As with particles generated by O_3/α-pinene reactions, an analysis of relative time scales suggests that coagulation plays an insignificant role in defining the particle growth wave. The estimated time (t_1) needed for the reduction in peak number concentration of smaller particles to peak concentration of larger particles via coagulation and the observed time (t_2) are presented in Table 5.4 for experiment #12. Consistent with the observations during experiments with α-pinene, estimated times for coagulation were greater than the observed times by 1-3 orders of magnitude. Thus, coagulation was not the dominant process for the reduction of smaller particle

number concentrations (after the initial burst of 0.02-0.1 μm size particles) and subsequent increases in larger particle number concentrations.

Table 5.4. Estimated (t_1) and Observed Time (t_2) for the Reduction in Peak Particle Number Concentrations during Experiment #12

Range	D	K	N_o	N(t)	t_1	t_2
μm	μm	cm^3/s	$\#/cm^3$	$\#/cm^3$	min	min
0.02-0.1	0.045	1.3E-09	86,926	22,874	408	45
0.1-0.2	0.141	1.4E-09	22,874	12,905	390	72
0.2-0.3	0.245	1.5E-09	12,905	6,265	927	68
0.3-0.4	0.346	2.0E-09	6,265	3,065	1.4×10^3	63
0.4-0.5	0.447	2.8E-09	3,065	848	5.0×10^3	100
0.5-0.7	0.592	2.0E-09	848	40	2.0×10^5	211

The particle size distribution during experiment #12 at the time of limonene introduction into the chamber (time = 0) and at the steady-state condition (time = 700 minutes) are shown in Figure 5.20. Particle number concentrations in all size ranges (except 0.02-0.1 μm) at steady-state were consistently higher than particle number concentrations at the time of limonene introduction into the chamber.

The evolutions of experimental particle mass and O_3 concentrations during experiment #12 are presented in Figure 5.21. The initial O_3 concentration in the chamber was 163 ppb and decreased with the introduction of limonene into the chamber. During the course of the experiment, O_3 levels in the chamber increased to more than the initial level. The emission rate of the O_3 generator was found to depend on many factors, including environmental conditions e.g., relative humidity. Higher O_3 emissions rates coupled with higher outdoor O_3 concentrations raised the chamber O_3 levels to more than the initial concentrations.

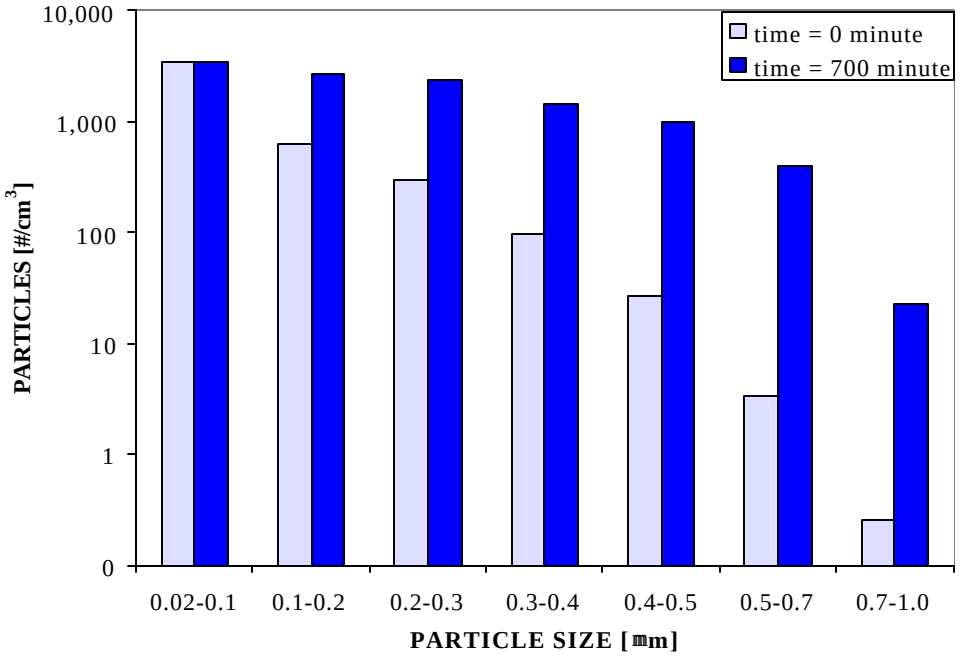

Figure 5.20. Particle size distribution at 0 and 700 minutes for experiment #12

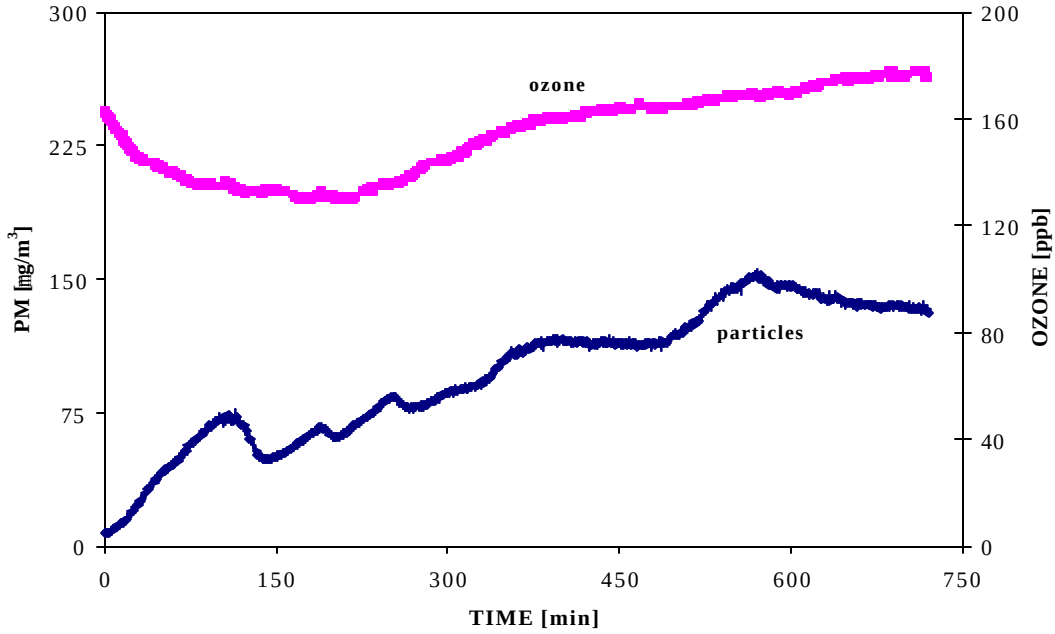

Figure 5.21. Evolution of particle mass and O_3 concentrations during experiment #12. l = 0.71 hr^{-1}

The initial particle mass concentration in the chamber for experiment #12 was 7.3 $\mu g/m^3$ and increased with the introduction of limonene into the chamber. The particle mass concentration in the chamber eventually reached a steady-state value of 153 $\mu g/m^3$. The SOA mass concentration was, therefore, 146 $\mu g/m^3$.

The evolution of particle number concentrations for experiment #16 is shown in Figure 5.22, which was also conducted at elevated O_3 levels. The air exchange rate for this experiment was higher than experiment #12. Similar to experiment #12, a rapid "burst" of small particles in the 0.02-0.1 µm size range was detected shortly after the introduction of limonene into the chamber. Particle numbers in the 0.02-0.1 µm size range then decreased before attaining a steady-state concentration of approximately 10% higher than the initial concentration. A particle growth "wave" was also observed during this experiment. Ultimately, particle number concentrations reached steady-state and were controlled primarily by the reaction rate of O_3 with limonene and the prevailing air exchange rate.

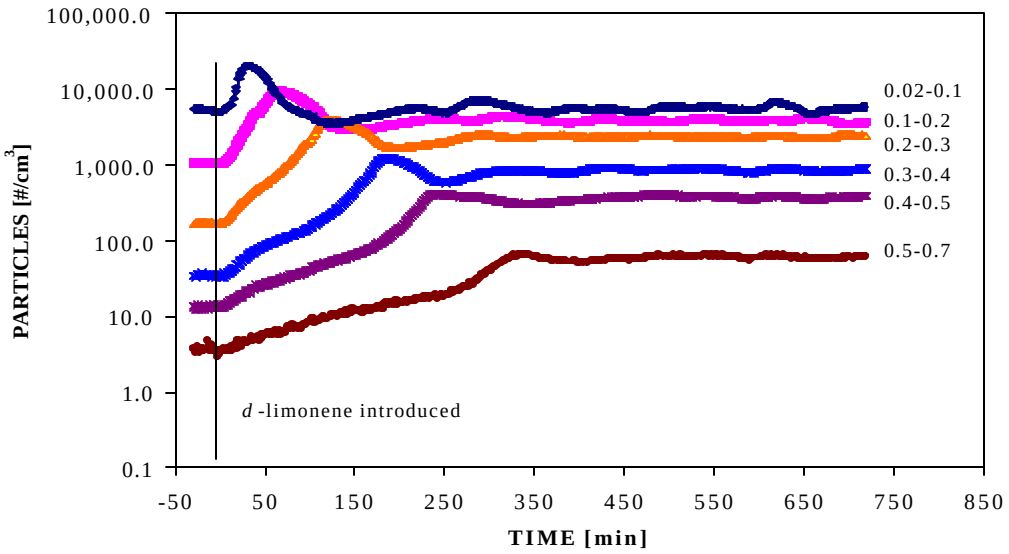

Figure 5.22. Evolution of particle number concentrations during experiment #16. l = 1.21 hr^{-1}

The particle size distributions during experiments #12 and #16 at the time of limonene introduction into the chamber (time = 0) and at steady-state (time = 600 minutes) are shown in Figures 5.23 and 5.24, respectively. Particle number concentrations in the 0.02-0.1 and 0.1-0.2 μm size ranges during experiment #12 at time zero were 30-40% lower than the corresponding particle number concentrations during experiment #16. Particle number concentrations in the 0.2-0.3, 0.3-0.4, and 0.4-0.5 μm size ranges during experiment #12 at time zero were 2-3 times as high as the corresponding particle number concentrations during experiment #16. Particle number concentrations in the 0.5-0.7 and 0.7-1.0 μm size range during experiment #12 at time zero was close to the corresponding particle number concentration during experiment #16.

Particle number concentrations in the 0.02-0.1 μm and 0.1-0.2 μm size ranges during experiment #12 at steady state were also about 10-25% lower than the corresponding particle number concentrations during experiment #16. Particle number concentration in the 0.2-0.3 μm size range during experiment #12 at steady state was close to the corresponding particle number concentration for experiment #16. However, particle number concentrations in the 0.3-0.4, 0.4-0.5, 0.5-0.7 and 0.7-1.0 μm size ranges during experiment #12 at steady-state were 2-30 times as high as the corresponding particle number concentrations for experiment #16. Despite the lower initial particle concentrations during experiment #12, particles were distributed into the larger size ranges due to the lower air exchange rate, i.e., greater reaction time for experiment #12. These results are consistent with recent observations by Weschler and Shields (2002).

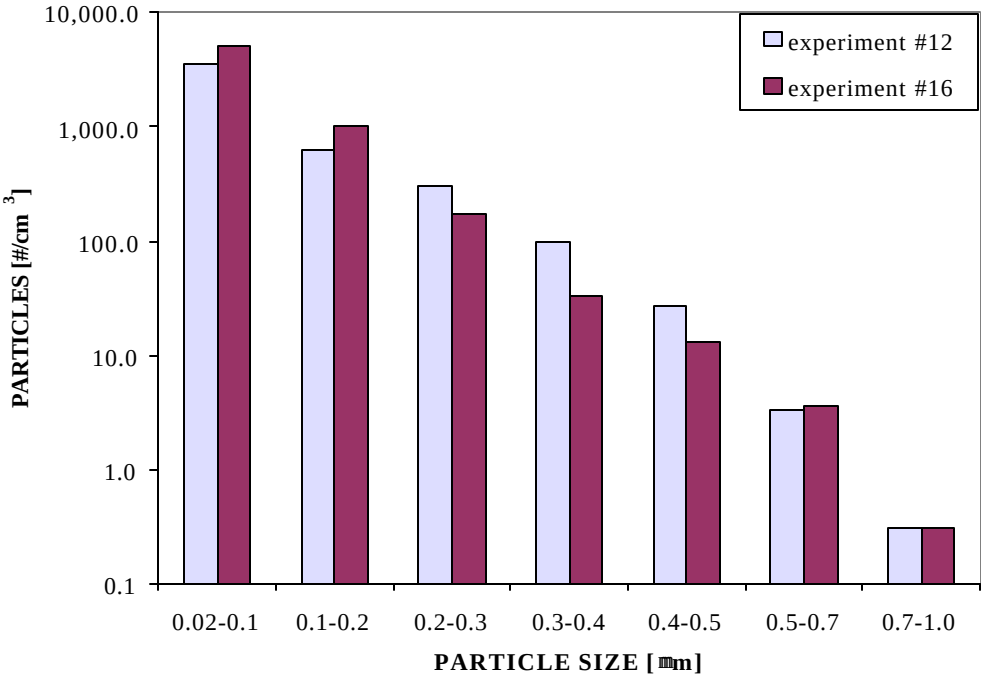

Figure 5.23. Particle size distribution during experiment #12 and #16. Time = 0 minutes

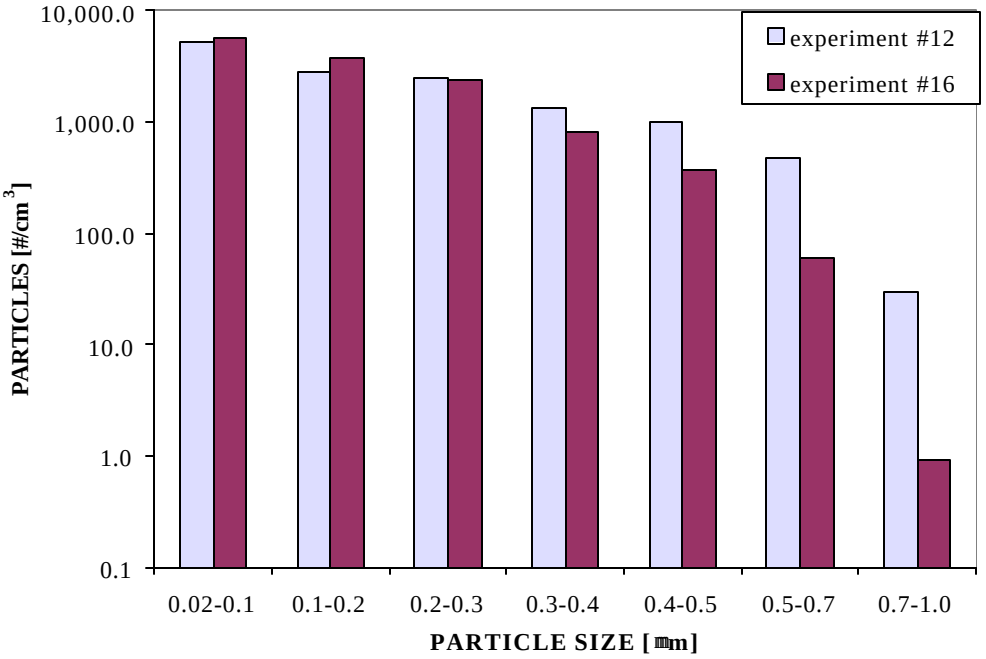

Figure 5.24. Particle size distribution during experiment #12 and #16. Time = 600 minutes

The resulting particle mass concentrations during experiments #12 and #16 are shown in Figure 5.25. As seen in Figure 5.25, particle mass concentrations during experiment #12 were significantly higher than during experiment #16. The higher reaction rate and longer reaction time produced larger particles, which contribute significantly to particle mass concentration.

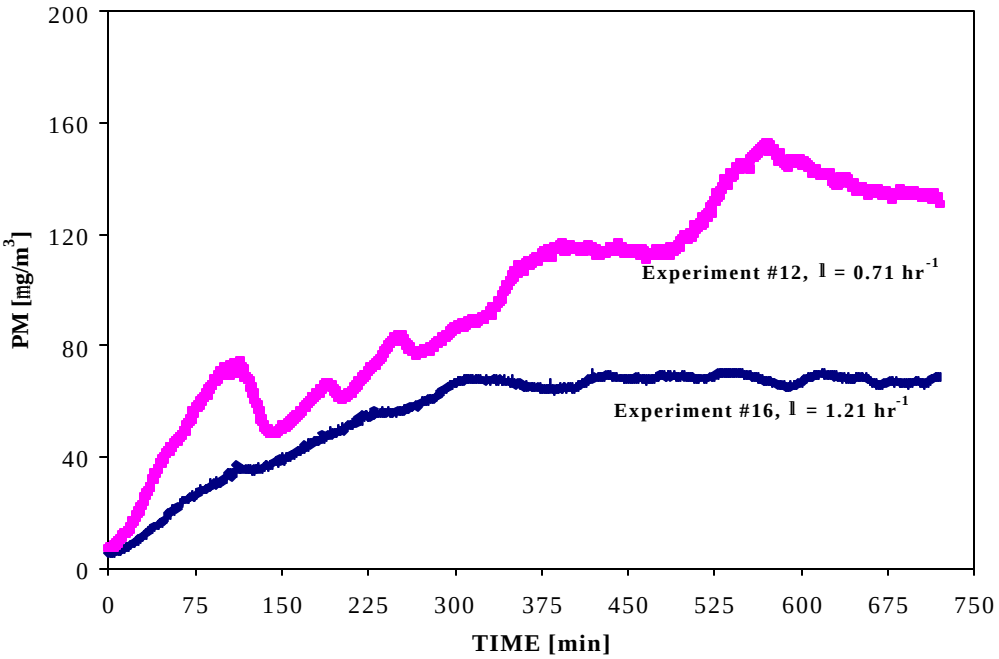

Figure 5.25. Evolutions of particle mass concentrations during experiment #12 and #16.

Experiment #14 involved limonene and a chamber O_3 concentration that was a factor of two or more greater than other experiments. Particle concentrations during experiment #14 were higher than particle concentrations observed during other experiments with similar air exchange rates. The concentration used for experiment #14 was unrealistically high for outdoor-to-indoor penetration, even in the world's most polluted urban areas. However, such an O_3 concentration could occur with the use of commercial ozone air "purifiers", and underscores the potential for occupant exposures to significant fine particle concentrations during the use of such devices.

The results obtained herein for O_3/limonene reactions are consistent with recent findings by Weschler and Shields (1999), Wainman *et al*. (2000), and Weschler and Shields (2002), as discussed in Chapter 2. In all cases, significant increases in particle number concentrations were reported when limonene and O_3 were allowed to react at elevated concentrations in indoor environments.

5.3 Comparisons of Secondary Organic Aerosol Concentrations between O_3/a -Pinene and O_3/Limonene Reactions

Experiment #4 involved the reaction of α-pinene with O_3. The initial O_3 level was 111 ppb, and the air exchange rate was 1.06 hr^{-1}. Experiment #13 involved limonene with an initial O_3 level of 114 ppb, and an air exchange rate of 0.95 hr^{-1}. The α-pinene emission rate during experiment #4 was 8% lower than the limonene emission rate during experiment #13. The initial particle levels between these experiments were within 30%. Therefore, conditions between these two experiments were not identical; but were reasonably similar. The indoor SOA mass concentration during experiment #4 was 11.9 $\mu g/m^3$ compared to a value of 66 $\mu g/m^3$ during experiment #13. Thus, the indoor SOA mass concentration for experiment #13 was 5.5 times as high as experiment #4. If the air exchange rate between these experiments had been equal, the difference between the SOA concentration would have been slightly lower.

Experiment #15 involved the reaction of limonene with O_3. The initial O_3 concentration was 151 ppb and the air exchange rate was 1.17 hr^{-1}. The α-pinene emission rate during experiment #4 was about 10% lower than the limonene emission rate during experiment #15. However, the initial particle concentrations during experiment #4 were at least three times as high as experiment #15. Despite the higher air exchange rate and lower initial particle concentration, experiment #15 produced an indoor SOA mass concentration that was 5.3 times as high as experiment #4. If the

air exchange rate and the initial particle levels between these experiments had been equal, the difference between the indoor SOA mass concentrations would have been greater. Thus, O_3/limonene reactions produced 5.3-5.5 times as much indoor SOA mass concentrations as did O_3/*α*-pinene reactions for reasonably similar conditions.

Limonene contains two carbon-carbon double bonds and is, therefore, more easily attacked by O_3 than is α-pinene. The rate constant for the O_3/limonene reaction at 298 K is 2.0×10^{-16} cm^3/molecule-sec and is approximately two times as high as the reported rate constant of 8.66×10^{-17} cm^3/molecule-sec for the O_3/α-pinene reaction (Atkinson, 1994). The rate constant for the OH·/limonene reaction at 298 K is 1.71×10^{-10} cm^3/molecule-sec, and is about three times as high as the reported rate constant of 5.37×10^{-11} cm^3/molecule-sec for the OH·/α-pinene reaction (Atkinson, 1994). The primary reaction products generated via oxidation of limonene undergo further reaction producing secondary reaction products. Partitioning rates of the primary and secondary products of the O_3/limonene reactions will be different than the semi-volatile products of O_3/α-pinene reactions. The combination of higher rate constants and different partitioning rates clearly lead to higher SOA levels for O_3/limonene reactions, i.e., in contrast to O_3/α-pinene reactions.

5.4 Particle Growth from the Release of Terpenes from Consumer Products

The following consumer products were investigated: a liquid air-freshener, a solid air-freshener, a general-purpose cleaner, a wood floor cleaner, a perfume, and a dishwasher detergent. A summary of experiments involving these consumer products is shown in Table 5.5. A parameter referred to as "particle formation potential" (PFP) was defined to compare indoor secondary particles resulting from different consumer products:

$$PFP = \frac{(\text{maximum } SOA_1 - \text{maximum } SOA_2) * \lambda}{\text{initial elevated } O_3 \text{ conccentration}} \qquad (5.5)$$

where, maximum SOA_1 is the maximum SOA concentration during experiment with elevated O_3 levels and maximum SOA_2 is the maximum SOA concentration during experiment with low O_3 levels. For solid air freshener, maximum SOA_2 was taken as zero.

Table 5.5. Summary of Experiments from the Release of Terpenes in Consumer Products

Expt No.	l	Product	Initial O_3	T	Initial Particle	Max Particle	Initial PM	Max PM	SOA	Max Terpene	Particle Formation Potential
	(hr^{-1})		(ppb)	(C)	(#/cc)	(#/cc)	(mg/m^3)	(mg/m^3)	(mg/m^3)	(ppb)	(hr^{-1})
17	0.66	A	126	24	11,481	670,000	13.3	216	203	691	0.53
18	0.71	A	15	23	4,953	30,799	9.5	14.5	5.0	NA	-
19	0.62	B	112	24	7,320	670,000	5.9	116	110	396	0.27
20	0.79	C	95	24	4,990	211,004	8.1	23.9	15.8	10	0.06
21	0.80	C	15	24	6,966	12,747	9.1	10.4	1.3	NA	-
22	0.71	D	207	24	8,205	670,000	3.1	72.6	69.5	46	0.10
23	0.71	D	14	24	7,560	8,258	3.8	16.1	12.3	NA	-
24	0.70	E	184	25	5,215	362,312	3.0	24.8	21.8	13	0.04
25	0.83	E	15	24	3,551	5,981	6.6	8.5	1.9	NA	-
26	1.16	F	156	26	7,095	11,602	5.4	21.1	15.7	6	0.01
27	0.97	F	16	27	3,467	3,988	5.6	18.1	12.5	7	-

Note:
A = liquid air-freshener, B = solid air-freshener, C = general purpose cleaner, D = special purpose cleaner, E = perfume, F = detergent, and, λ = air exchange rate
Particle number concentrations refer to particles in the 0.02-0.7 μm diameter range for all experiments except experiments #22, #23, #26 and #27. For experiments #22, #23, #26 and #27, particle number concentrations refer to particles in the 0.02-1.0 μm diameter range.
SOA is the difference between maximum and initial particle mass concentrations
Terpene concentration is the sum of α-pinene and limonene concentrations

5.4.1 Liquid Air-Freshener

Two experiments were conducted with a lime scented liquid air-freshener [SHADOW LAKE^{TM} INC., Air Sense]. Experiment #17 was performed at an initial O_3 concentration of 126 ppb and experiment #18 was performed at an initial O_3 concentration of 15 ppb. One spray of air freshener was introduced into the chamber during each experiment. The evolution of particle number concentrations during experiment #17 (elevated O_3 level) is shown in Figure 5.26. The air freshener was introduced into the chamber at time zero. The total number concentration of particles

in the 0.02-0.7 μm diameter range was initially 11,481 #/cm^3, and increased to over 670,000 #/cm^3 immediately after the introduction of the air freshener into the chamber. The increase in number concentration was highest for particles with the smallest diameter range, and increases were successively smaller for larger diameter particles. After the initial increase, number concentrations of particles in each size range between 0.2 and 0.7 μm continued to increase, reaching peak concentrations in succession, and then decreasing.

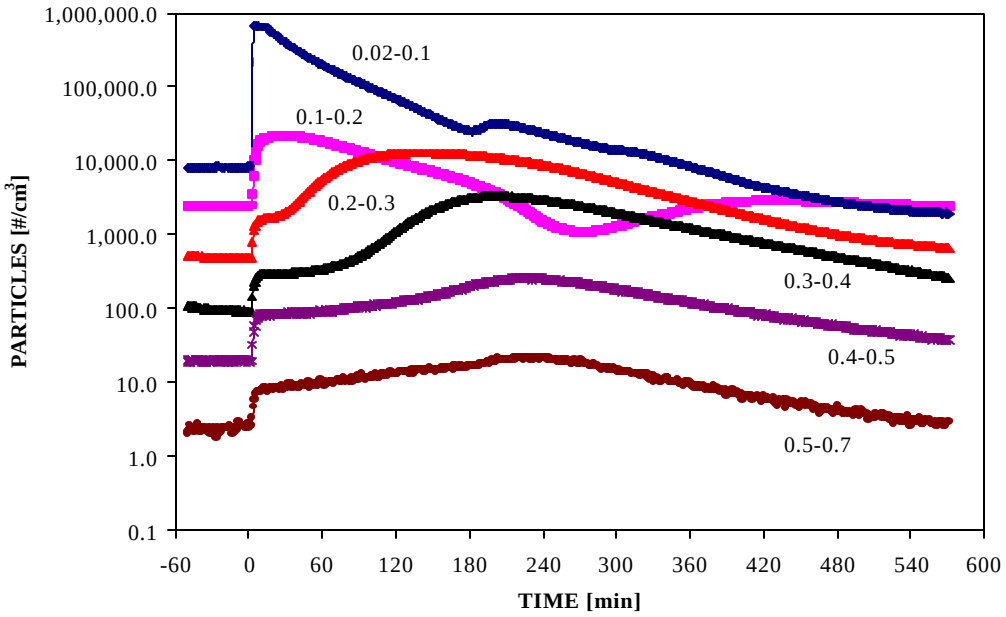

Figure 5.26. Particle number concentrations during experiment #17 (liquid air freshener and elevated O_3 levels). l = 0.66 hr^{-1}

Particle number concentrations during experiment #18 are shown in Figure 5.27. Ozone concentrations were only in the range of 15-20 ppb and were derived from outdoor-to-indoor penetration. The particle number concentration in the 0.02-0.7 μm diameter range was initially 4,953 #/cm^3 and increased to 30,799 #/cm^3 after the introduction of the air freshener. This result indicates that little SOA mass is

formed at low O_3 concentration, and also that particle results observed at higher O_3 concentrations were not due to the aerosol spray.

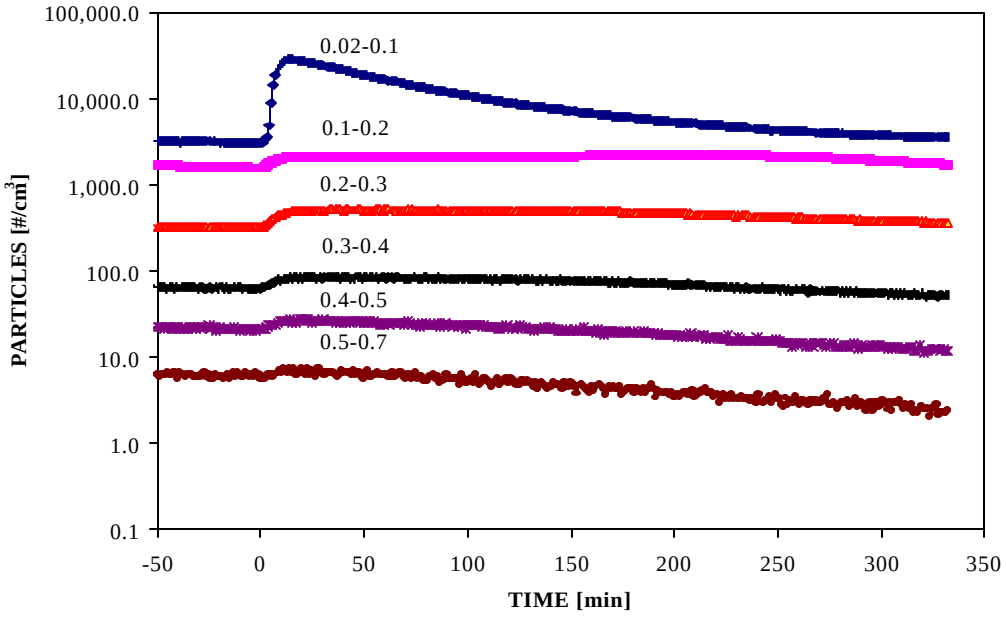

Figure 5.27. Particle number concentrations during experiment #18 (liquid air freshener and lower O_3 levels). $l = 0.71\ hr^{-1}$

Particle mass and O_3 concentrations for experiment #17 (elevated O_3 level) are shown in Figure 5.28. Particle mass concentrations during experiment #18 are also shown in Figure 5.28. For experiment # 17 (elevated O_3 level), the O_3 concentration was initially over 125 ppb and decreased sharply with the introduction of the air-freshener, highlighting the importance of O_3/terpene reactions. Ozone concentrations then slowly increased to more than the original levels. The emission rate of the ozone generator was found to depend on many factors including environmental conditions e.g., relative humidity. Higher O_3 emission rates coupled with higher outdoor O_3 levels are believed to have raised the chamber O_3 levels to more than the initial levels.

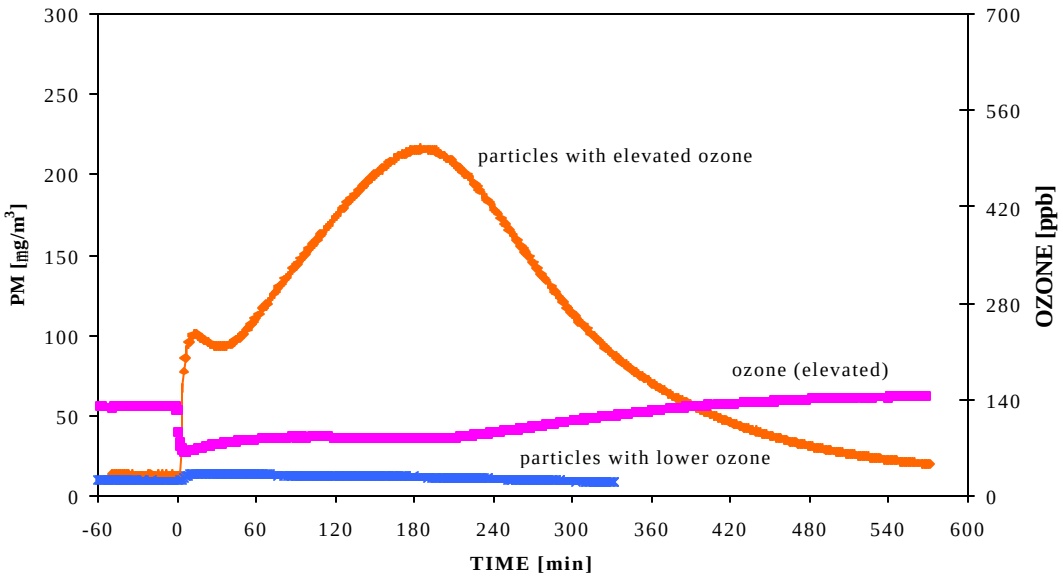

Figure 5.28. Particle mass and O_3 concentrations during experiment 17 and 18 (liquid air freshener). l = 0.66 hr^{-1}

Air samples were collected and analyzed using GC/MSD during experiment #18 (elevated O_3 level). The analysis indicated the presence of α-pinene and limonene during the experiment. However, the amount of organic mass reported by the GC/MSD was much higher than the highest calibration point and is therefore not reported here. Terpene concentrations increased with the introduction of the air freshener and then gradually decreased over the course of the experiment due to air exchange and reactions with O_3.

The initial particle mass concentration (diameter < 0.7 μm) for experiment #17 (elevated O_3) was 13.3 $\mu g/m^3$. Particle mass concentrations increased sharply immediately after the introduction of the air freshener and continued to increase up to about 190 minutes after the introduction of the air-freshener. The peak particle mass

concentration was 216 $\mu g/m^3$. Particle mass concentrations then slowly decreased, approaching the original level due to the decay of terpenes in the chamber.

The initial particle mass concentration for experiment #18 (lower O_3) was 9.5 $\mu g/m^3$. The growth of particles during this experiment was significantly less than that of experiment #17. The peak particle mass concentration for experiment #18 reached only 14.5 $\mu g/m^3$. The air exchange rate during experiment #18 (lower O_3 level) was 0.71 hr^{-1}, slightly higher than the experiment with elevated O_3 levels. The difference in air-freshener mass before and after the spray indicated that the amount of air-freshener released during experiment #18 (lower O_3) was only about one-third of the air-freshener released during experiment #17 (elevated O_3). Somewhat higher particle mass concentrations would have resulted if the air exchange rate and the amount of air-freshener released during experiment #18 had been equal to that of experiment #17.

As discussed earlier in this dissertation, the growth of indoor particles is a two-step process. First, the gas phase reactions between O_3 and terpenes produce semi-volatile products. Second, these semi-volatile products partition onto existing "seed" particles and lead to increases in particle mass concentrations. Initially, the O_3/terpene reaction rates are high and produce large concentrations of semi-volatile products. Some of these semi-volatile products then partition onto available "seed" particles and result in increased particle mass concentrations, e.g., as shown in Figure 5.28. For short-term releases of terpenes, the O_3/terpene reaction rate then decreases with time primarily due to the decay of terpene in the chamber. Consequently less semi-volatile products are produced. However, more particles become available with time and serve as "seed" particles on which semi-volatile products partition. As shown in Figure 5.28, this can lead to a continued increase in particle mass concentration even as terpene levels decline. For experiment #17, this process lead to

a particle mass concentration increase up to 190 minutes after the introduction of the spray air-freshener into the chamber. Particles, terpenes as well as O_3 were also removed from the chamber due to air exchange. As a result, terpene and particle concentrations gradually decreased and approached original levels. The average particle concentration during experiment #17 (~ 9 hours) was 106 $\mu g/m^3$. This result underscores the potential for prolonged and significant human exposures to fine particle mass following the use of some indoor consumer products when outdoor ozone levels are episodic. The particle formation potential of the liquid air freshener was 0.53 hr^{-1} - the highest among the consumer products that were investigated, which also reflects the very high terpene levels present in the product.

5.4.2 Solid Air-Freshener

Experiment #19 was conducted with a commercial solid air-freshener [CAR-FRESHENER Corporation, Royal Pine®] with an initial chamber O_3 concentration of 112 ppb. The solid air freshener was suspended in the chamber using wiring at time zero. The subsequent evolution of particle number concentrations is shown in Figure 5.29. The total number concentration of particles in the 0.02-0.7 μm diameter range was initially 7,320 $\#/cm^3$ and increased to over 670,000 $\#/cm^3$ shortly after the introduction of the air freshener into the chamber. The increase in number concentration was highest for particles with the smallest diameter range (0.02-0.1 μm). Increases were successively smaller for larger particles. After the initial increase, number concentrations in the 0.02-0.1 μm diameter range decreased over the course of the experiment. Number concentrations in other diameter ranges continued to increase, reaching peak concentrations in succession, before decreasing to approximate steady-state values. The continued growth of particles in different diameter ranges suggests that O_3/terpene reactions persisted throughout the course of the experiment.

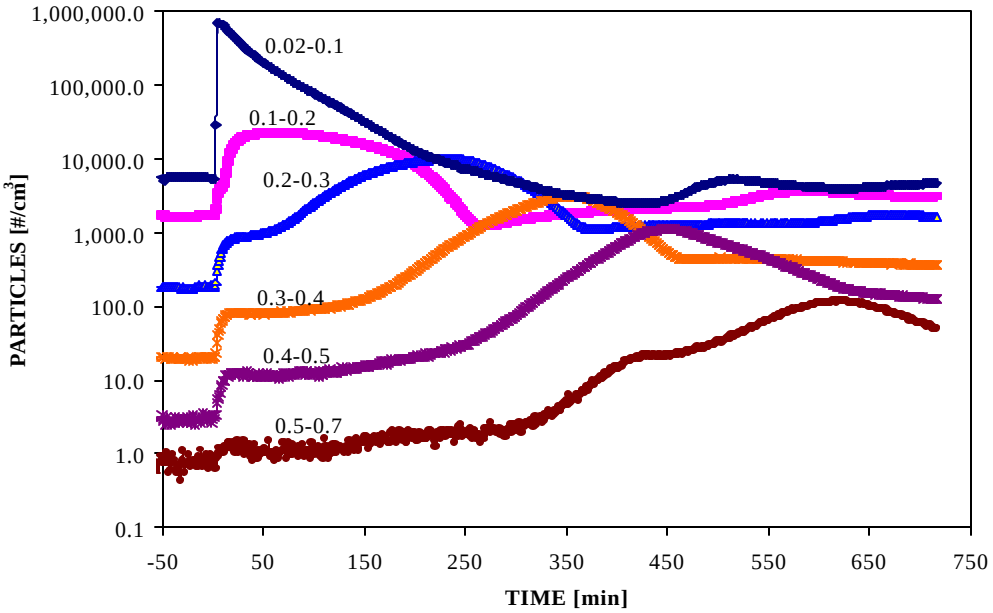

Figure 5.29. Particle number concentrations during experiment #19 (solid air freshener). $l = 0.62\ hr^{-1}$

Air samples were also collected and analyzed using GC/MSD during experiment #19. The analysis indicated the presence of α-pinene, limonene, β-pinene, camphene, and 3-carene during the experiment. However, the amount of organic mass reported by the GC/MSD was much higher than the highest calibration point, and is therefore not reported here. Terpene concentrations increased with the introduction of the air freshener and then gradually decreased over the course of the experiment due to air exchange, decay of terpene emission rates from the air-freshener, and reactions with O_3.

Particle mass and O_3 concentrations for experiment #19 are presented in Figure 5.30. The O_3 concentration decreased sharply with the introduction of the air-freshener, reinforcing the significance of O_3/terpene reactions. The lower O_3 concentration was persistent and constant throughout the course of the experiment.

Due to varying terpene content and vapor pressures of individual terpenes, it is likely that the source fingerprint for this product varied significantly over the course of the experiment. The constant O_3 concentration throughout the experiment suggests that organic compounds were continuously released from the solid air-freshener.

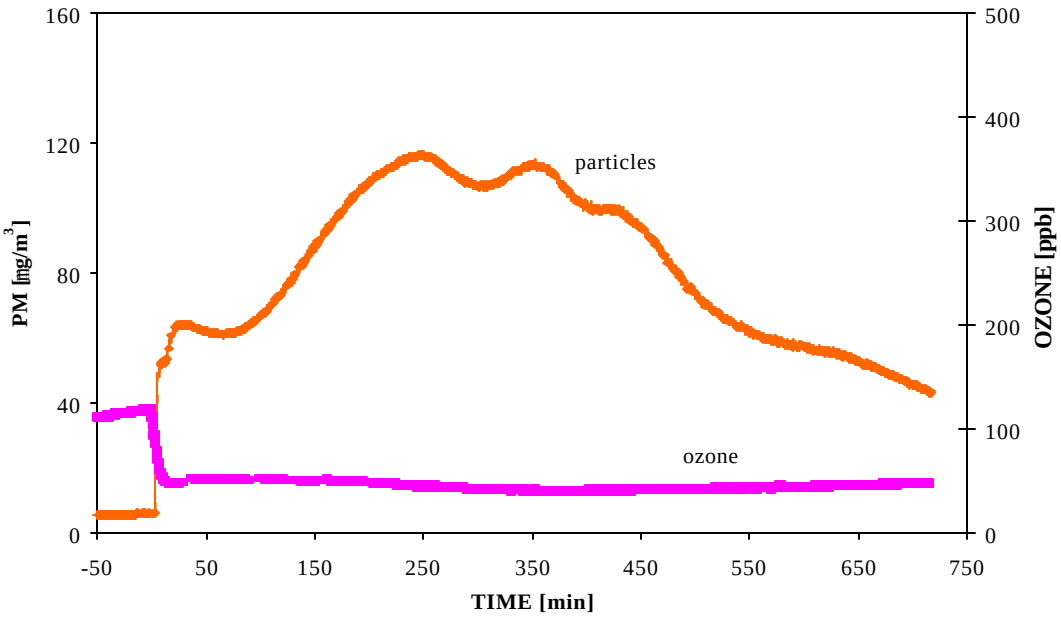

Figure 5.30. Particle mass, O_3, and terpenes concentrations during experiment # 19 (solid air freshener). $1 = 0.62\ hr^{-1}$

Solid air-freshener is designed to continuously release scent over a long period of time, which can cause elevated indoor terpene concentrations. These indoor terpenes, in turn, can react with indoor O_3 producing elevated levels of indoor secondary particles and other gaseous pollutants.

The initial particle mass concentration for experiment #19 was 5.9 $\mu g/m^3$. Particle mass concentrations increased sharply immediately after the introduction of the air freshener and continued to increase for approximately four hours after the introduction of the air-freshener. Several local peaks were observed in Figure 5.30

and correspond to peak number concentrations of different size particles in Figure 5.29. Total terpene concentrations decreased with time and ultimately resulted in the decrease in particle mass concentrations. The average particle concentration during the experiment was 81 $\mu g/m^3$. The particle formation potential of the solid air-freshener was 0.27 hr^{-1} - the second highest among the consumer products that were investigated, reflecting the presence of high terpene levels in the product.

The product tested for experiment #19 is normally used inside the cabin of motor vehicles (hung on rear-view mirrors). The high mass concentrations observed for experiment #19 indicates that individuals who use such products may be exposed to significant levels of fine particles during urban commutes in summertime O_3 seasons. On average, Americans spend approximately as much time in transit as they do outdoors (Jenkins *et al*., 1992; Klepeis and Tsang, 1996), the environment for which significant regulatory attention has been given to fine particles.

5.4.3 General Purpose Cleaner

Two experiments were conducted with a lemon scented commercial general purpose cleaner [The Clorox Company, Pine-Sol®]. Experiment #20 was performed with an initial O_3 level of 95 ppb and experiment #21 was performed with an initial O_3 level of 15 ppb. The evolution of particle number concentrations during experiment #20 (elevated O_3 level) is shown in Figure 5.31.

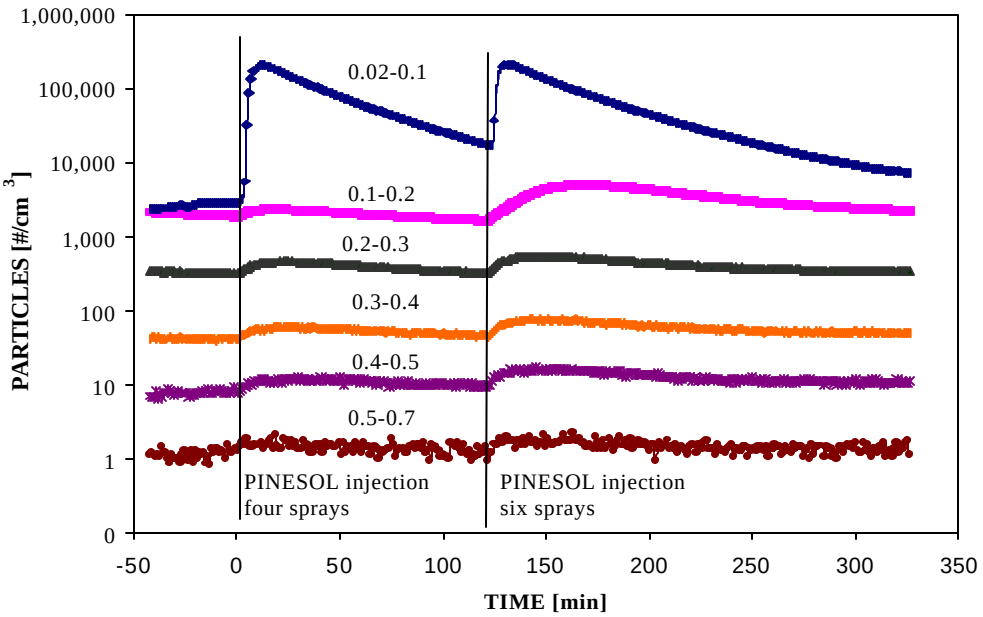

Figure 5.31. Particle number concentrations during experiment #20 (PINESOL® and elevated O_3 levels). l = 0.79 hr^{-1}

Four sprays of the cleaner were introduced into the chamber at time zero and six sprays of the cleaner were introduced at time 120 minute. The total number concentration of particles in the 0.02-0.7 µm diameter range was initially only 4,990 #/cm^3 and increased to 205,422 #/cm^3 after the first introduction of the cleaner, and to 211,004 #/cm^3 after the second introduction of the cleaner. Particle number concentrations for every diameter range up to 0.7 µm increased with the introduction of the cleaner. The increase in number concentration was highest for particles in the smallest diameter range. Increases were successively smaller for larger diameter particles. After the initial increase, number concentrations in all diameter ranges continually decreased over the course of the experiment.

Particle mass, O_3, and terpene concentrations for experiment #20 are shown in Figure 5.32. The O_3 concentration decreased with the introduction of the cleaner.

The decrease in O_3 concentration was larger following six sprays than following the four sprays. Chamber O_3 concentrations slowly increased to near the original levels both times.

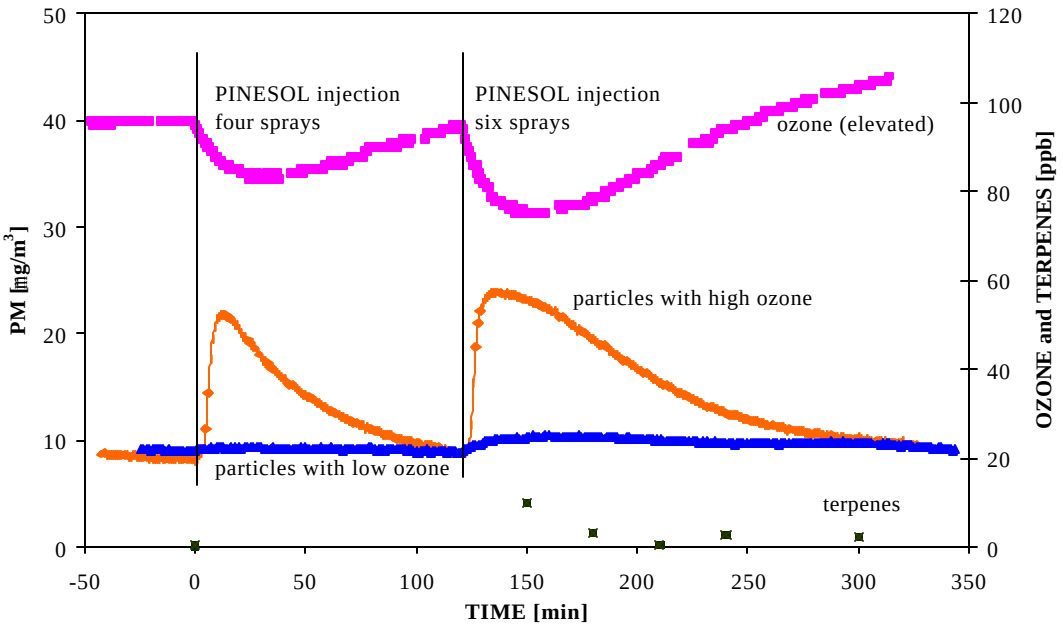

Figure 5.32. Particle mass, O_3, and terpene concentrations during Experiment #20 and #21 (PINESOL®). l = 0.79 hr^{-1}

The terpene concentration in the chamber was close to zero before the introduction of the cleaner. The concentration increased with the introduction of the cleaner and then decreased over the course of the experiment due to removal by air exchange and reactions with O_3. The peak terpene concentration following six sprays was about 10 ppb. Terpene concentrations were not measured following the application of four sprays. On average, limonene represented about 80% of the total terpene concentration. The remaining 20% of the total terpene concentration was α-pinene.

The initial particle mass concentration for experiment #20 (elevated O_3 level) was 8.1 $\mu g/m^3$. Particle mass concentrations increased sharply immediately after the introduction of the cleaner and then slowly decreased over the course of the experiment, primarily due to the decay of terpenes in the chamber. The peak particle mass concentration was 21.7 $\mu g/m^3$ when four sprays were introduced, and was about 23.9 $\mu g/m^3$ when six sprays were introduced. It is possible that each spray did not release an equal amount of cleaner; thus the amount of cleaner sprayed during the six sprays may not have been proportionately higher than the case of four sprays. Consequently, particle level increases during the case of six sprays were not proportionately higher than the case of four sprays. The average particle concentration (<0.7 μm) during the experiment was 14.5 $\mu g/m^3$.

Ozone concentrations were only in the range of 15-25 ppb during experiment #21 (lower O_3 level) and were derived from outdoor-to-indoor penetration. Particle mass concentrations for experiment #21 are also shown in Figure 5.32. Particle mass concentrations increased only slightly during experiment #21, indicating that particle levels during experiment #20 (high O_3 level) were indeed due to O_3/terpene reactions as opposed to aerosol spray. The air exchange rate during the experiment with lower O_3 levels was 0.8 hr^{-1}, close to the experiment with elevated O_3 levels. Thus, most of the increases in particle mass concentrations during the experiment with elevated O_3 concentrations can be attributed to O_3/terpene reactions.

Results of these experiments are consistent with the results of Long *et al*. (2000). They also observed significant increases in indoor particle levels after the application of Pinesol® during mopping and cleaning operations in a home. The particle formation potential of the general purpose cleaner was 0.06 hr^{-1} - the fourth highest among the consumer products that were investigated.

5.4.4 Wood Floor Cleaner

Two experiments were conducted with a commercial wood floor cleaner [S. C. Johnson & Son. Inc., Pledge®]. Experiment #22 was performed at an initial O_3 concentration of 207 ppb and experiment #23 was performed at an initial O_3 concentration of 14 ppb. Four sprays of the wood floor cleaner were introduced into the chamber during each experiment. The evolution of the particle number concentrations during experiment #22 (elevated O_3 level) is shown in Figure 5.33. The total number concentration of particles in the 0.02-1.0 μm diameter range was initially 8,205 #/cm^3, and increased to 670,000 #/cm^3 immediately after the introduction of the wood floor cleaner into the chamber. Number concentrations for particles with diameters up to 1.0 μm increased with the introduction of the wood floor cleaner. The increase in number concentration was highest for particles in the smallest diameter range, and decreased with successively larger particles.

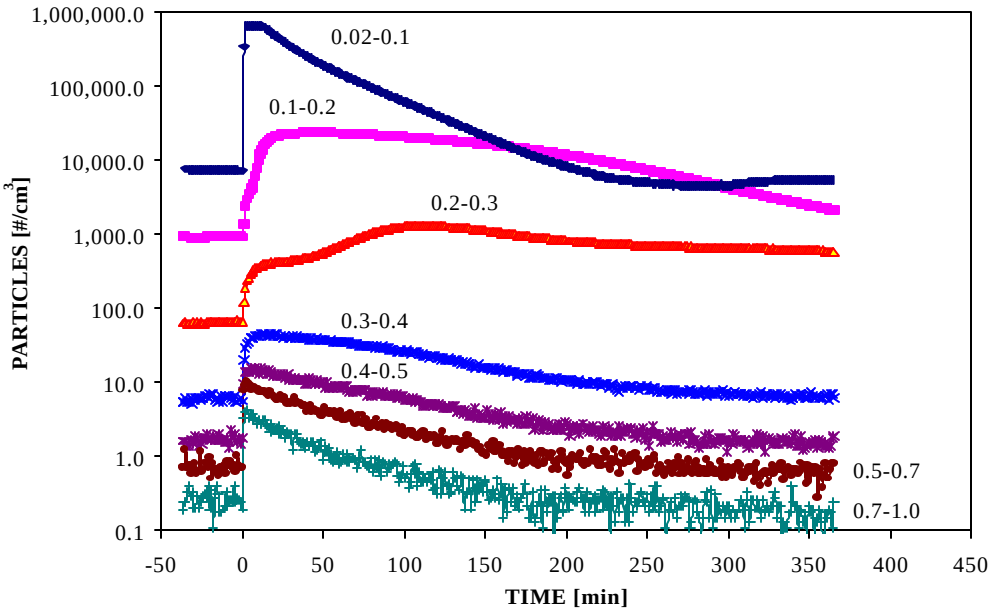

Figure 5.33. Particle number concentrations during experiment #22 (wood floor cleaner and elevated O_3 levels). 1 = 0.71 hr^{-1}

After the initial increase, number concentrations in all diameter ranges except 0.1-0.2 and 0.2-0.3 μm continually decreased over the course of the experiment. After the initial increase, number concentrations in the 0.1-0.2 μm remained relatively constant for about 50 minutes before slowly decreasing toward the original level. The relatively constant concentration for about 50 minutes suggests that smaller particles continued to grow into 0.1-0.2 μm ranges during this time period. Number concentrations in the 0.2-0.3 μm diameter range continued to increase with a peak concentration at around 110 minutes after the introduction of the wood floor cleaner.

Particle mass, O_3, and terpene concentrations for experiment #22 (elevated O_3 level) are shown in Figure 5.34. The initial O_3 concentration in the chamber decreased sharply with the introduction of the wood floor cleaner. Ozone concentrations then slowly increased to greater than the original levels due to higher O_3 emission rates and higher outdoor O_3 levels.

The initial terpene concentration was about 1-2 ppb. The terpene concentration increased with the introduction of the wood floor cleaner and then gradually decreased over the course of the experiment due primarily to the air exchange and reaction with O_3. The peak terpene concentration was 46 ppb. On average, limonene represented over 80% of the total terpene concentration. The remaining 20% of the total tepene concentration was contributed by α-pinene.

The initial particle mass concentration for experiment # 22 (elevated O_3) was 3.1 $\mu g/m^3$. Particle mass concentrations increased sharply immediately after the introduction of the wood floor cleaner and then slowly decreased over the course of the experiment primarily due to the decay in terpene concentrations.

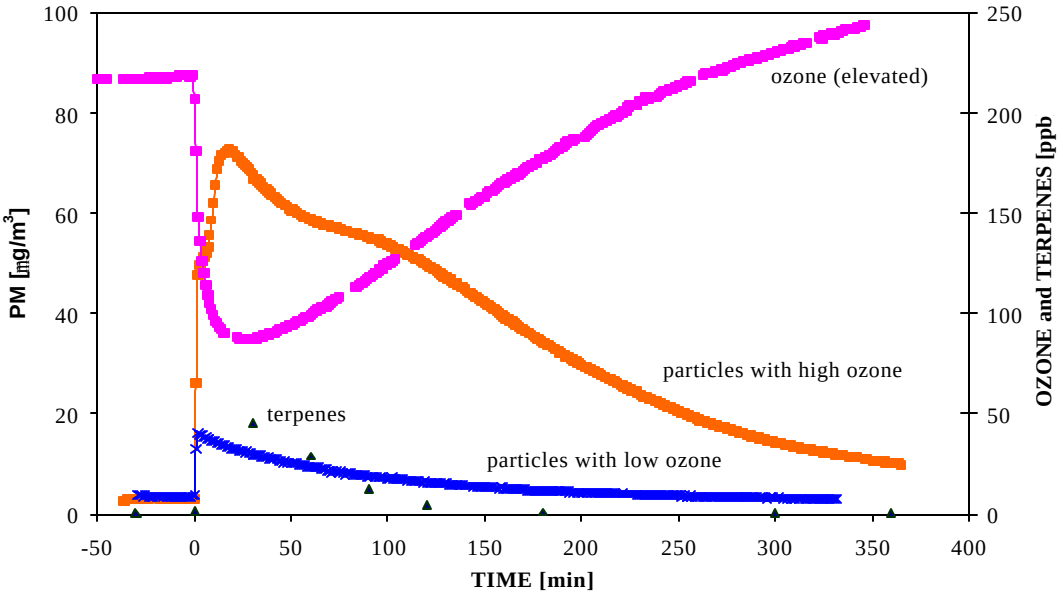

Figure 5.34. Particle mass, O_3, and terpenes concentrations during experiment #22 and #23 (wood floor cleaner). $l = 0.71\ hr^{-1}$

However, a "hump" in particle mass concentration was also observed around 110 minutes after the introduction of the wood floor cleaner. This hump corresponded to an increase in number concentrations for particles in the 0.2-0.3 µm diameter range. The peak particle mass concentration was 72 $\mu g/m^3$. The experiment was terminated at 350 minutes after the introduction of the wood floor cleaner. At termination, the particle mass concentration was still about 3 times as much as the original particle mass concentration. The average particle concentration (<1.0 µm) during the experiment was 36 $\mu g/m^3$.

Particle mass concentrations during experiment #23 (lower O_3 level) are also shown in Figure 5.27. The initial particle mass concentration was 3.8 $\mu g/m^3$ and the peak particle mass concentration was 16.1 $\mu g/m^3$. The particle formation potential of

the wood floor cleaner was 0.10 hr^{-1} - the third highest among the consumer products that were investigated.

5.4.5 Perfume

Two experiments were conducted with a retail perfume (POLO SPORT, RALPH LAUREN). Experiment #24 was performed at an initial O_3 concentration of 184 ppb and experiment #25 was performed at an initial O_3 concentration of 15 ppb. Five sprays of the perfume were introduced into the chamber during both experiments. The evolution of the chamber particle number concentrations during experiment #24 (elevated O_3 level) is shown in Figure 5.35.

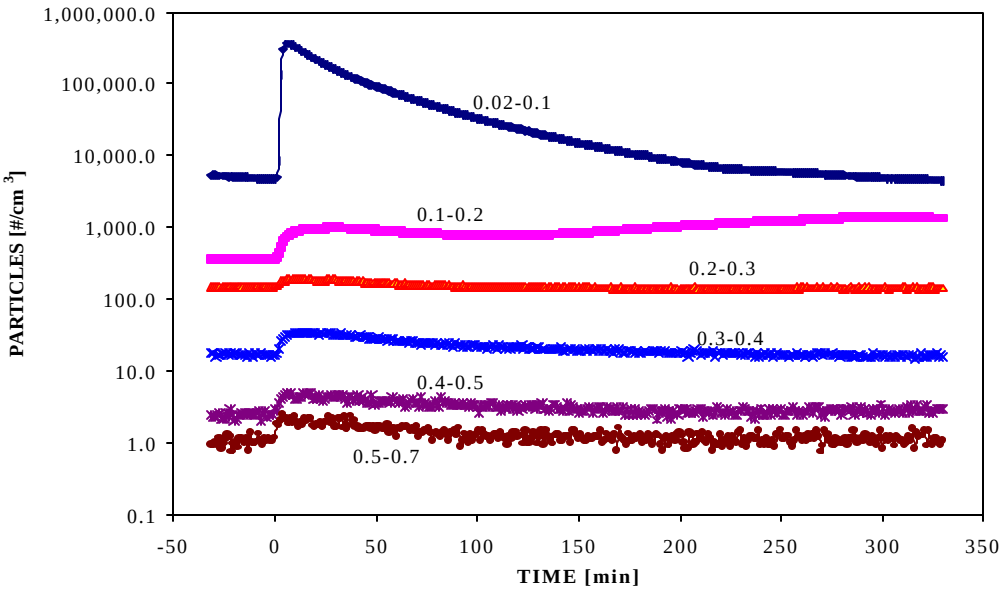

Figure 5.35. Particle number concentrations during experiment #24 (perfume and elevated O_3 levels). 1 = 0.70 hr^{-1}

The total number concentration of particles in the 0.02-0.7 µm diameter range was initially 5,215 #/cm^3, and increased to over 362,000 #/cm^3 immediately after the introduction of perfume into the chamber. Particle number concentrations for all diameter ranges up to 0.7 µm increased with the introduction of the perfume. The

increase in number concentration was highest for small particles and increases were successively smaller for larger particles. After the initial increase, number concentrations in all diameter ranges continually decreased over the course of the experiment.

Particle mass, O_3, and terpene concentrations for experiment #24 (elevated O_3 level) are shown in Figure 5.36. The O_3 concentration decreased sharply with the introduction of the perfume, reinforcing the importance of O_3/terpene chemistry. The O_3 concentrations then slowly increased to more than the original levels due to higher emission rates.

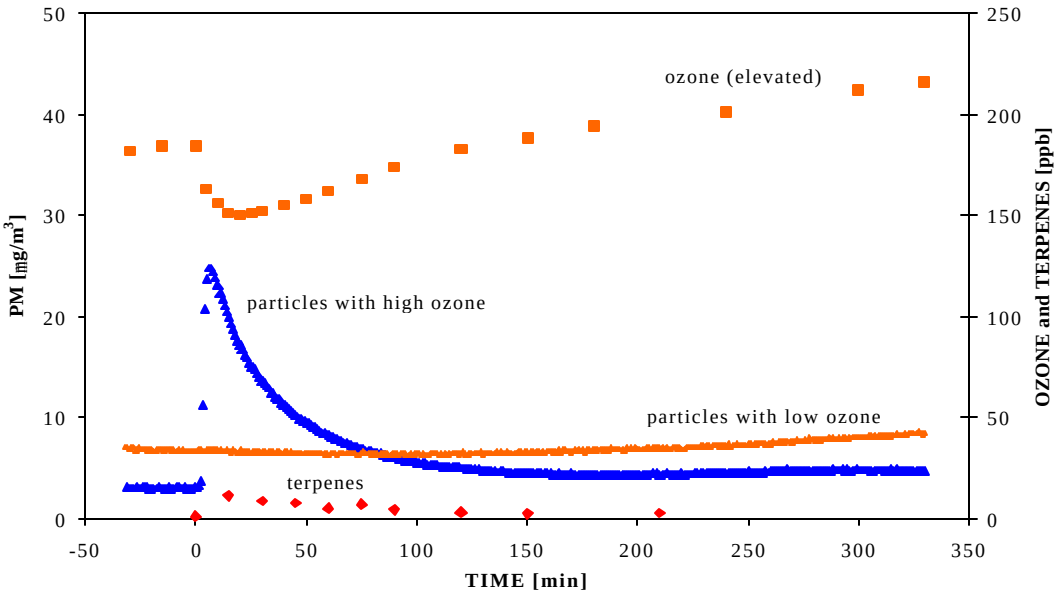

Figure 5.36. Particle mass, O_3, and terpenes concentrations during experiment #24 and #25 (perfume). l = 0.70 hr^{-1}

The initial terpene concentration was about 1.0 ppb. It increased with the introduction of the perfume and then gradually decreased over the course of the experiment due to air exchange and reactions with O_3. The peak terpene concentration was close to 11 ppb. On average, limonene contributed over 90% of

the terpene concentration. The remaining 10% of the total tepene concentration was contributed by α-pinene.

The initial particle mass concentration for experiment #24 (elevated O_3 level) was 3.0 $\mu g/m^3$. Particle mass concentrations increased sharply immediately after the introduction of perfume with a peak concentration of 25 $\mu g/m^3$. Particle mass concentrations then slowly decreased to initial levels, due primarily to the decay in terpene concentrations. The average particle concentration for the first 150 minutes of the experiment was 9.0 $\mu g/m^3$.

Ozone concentrations for experiment #25 (lower O_3) were only in the range of 10-15 ppb and were derived from outdoor-to-indoor penetration. Particle mass concentrations during this experiment are also shown in Figure 5.36. Increases in particle concentrations during this experiment (lower O_3 level) were insignificant. Thus, the increase in particle concentrations during the experiment with elevated O_3 level can be attributed to O_3/terpene reactions. The air exchange rate for experiment #25 (lower O_3 level) was 0.8 hr^{-1}, higher than for experiment #24. Somewhat higher particle mass concentrations would have resulted if the air exchange rate had been equal to the experiment with elevated O_3 levels. The particle formation potential of this product was 0.04 hr^{-1} - the second lowest among the consumer products that were investigated.

5.4.6 Dishwashing Detergent

Two experiments were conducted with a commercial lemon scented dishwasher detergent [Benckiser Consumer Products Inc., Electrasol]. A residential dishwashing machine (Kenmore™, Model 17651) using this detergent was operated in the experimental chamber during both experiments. Experiment #26 was performed at an initial O_3 concentration of 156 ppb and experiment #27 was

performed at an initial O_3 concentration of 16 ppb. The evolutions of particle number concentrations during both experiments are shown in Figure 5.37. The dishwasher was started at time zero during experiment #26 (elevated O_3 level) and at 175 minutes during experiment #27 (lower O_3 level).

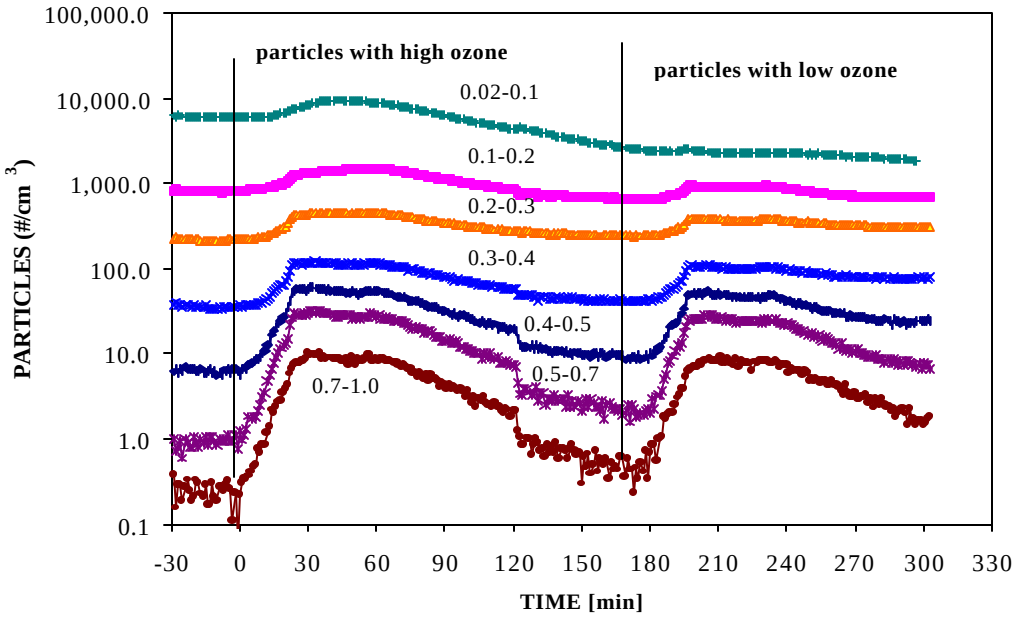

Figure 5.37. Particle number concentrations during experiment #26 (detergent with elevated O_3 levels, $l = 1.16\ hr^{-1}$) and #27 (detergent with lower O_3 levels, $l = 0.97\ hr^{-1}$)

Particle number concentrations increased during both experiments; however, the increases were higher for experiment #26 (elevated O_3 level). The O_3 concentration was initially 156 ppb for experiment #27 and decreased sharply with the start of the dishwashing machine. The operation of the dishwashing machine increased the relative humidity in the chamber causing a sharp decrease in the emission rate of the ozone generator. Thus, the reduction in O_3 concentration due to O_3/terpene reactions could not be ascertained. The peak terpene concentration was 6

ppb during experiment #26 (elevated O_3 level) and the peak terpene concentrations during experiment #27 (lower O_3 level) was 7 ppb.

Particle mass concentrations for these experiments are shown in Figure 5.38. Particle mass concentrations were higher during experiment #26 (elevated O_3 level). The peak particle mass concentrations were 21.1 and 18.1 $\mu g/m^3$ for experiment #26 (elevated O_3 level) and #27 (lower O_3 level), respectively. The average particle mass concentrations were 14.0 and 12.5 $\mu g/m^3$ for experiment #26 (elevated O_3 level) and #27 (lower O_3 level), respectively. The air exchange rate for experiment #27 (lower O_3 level) was lower than the air exchange rate for experiment #26 (elevated O_3 level). If the air exchange rates were equal, the difference in particle mass concentrations would have been greater. The particle formation potential of the dishwasher detergent was 0.01 hr^{-1} - the lowest among the consumer products that were investigated.

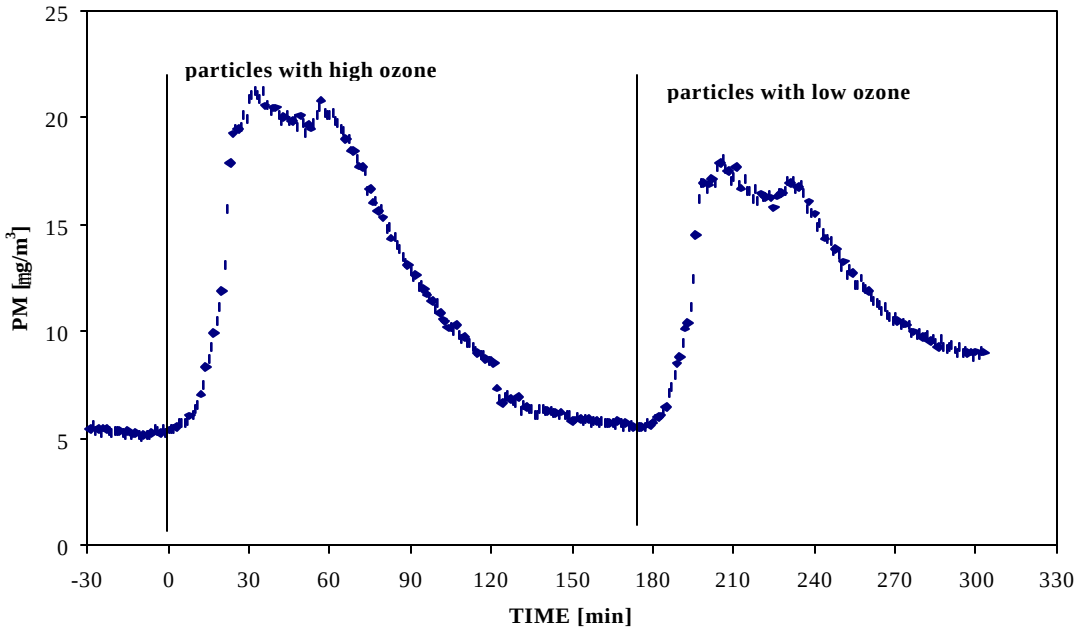

Figure 5.38. Particle mass concentrations during experiment #26 (detergent with elevated O_3 levels and #27 (detergent with lower O_3 levels)

5.5 Summary

Experimental results indicate that significant particle formation/growth occurs indoors due to reactions between O_3 and terpenes. The particle growth occurs through an initial "burst" of small particles followed by a decrease in particle numbers in a given size range and increase in particle numbers in subsequent size ranges. This process leads to an effective particle growth "wave". If the initial indoor particle levels are low, the initial "burst" of particles may be the result of nucleation of O_3/terpene reaction products and the growth of smaller particles into larger detectable sizes. If the initial indoor particle levels are high, the initial "burst" of particles becomes small and particle growth appears to occur via partitioning of O_3/terpene reaction products. Additional research is recommended to resolve the issue of particle formation/growth during the initial phase of the experiment using particle analyzers that can measure finer size distributions.

The O_3/limonene reactions produce approximately five times as much indoor SOA mass concentrations as do O_3/α-pinene reactions. Air exchange rate plays a significant role on secondary particle levels. Particles are distributed toward larger sizes leading to higher particle mass concentrations at lower air exchange rate.

The ICEM predicted indoor secondary particle mass concentrations were generally in good agreement with experimental results, which suggests that the model is capturing the essence of particle formation/growth processes.

Terpenes are present in many common consumer products. Results of the experiments involving consumer products clearly demonstrate that fine particle formation/growth can occur from the application of these products in indoor environments. Indoor secondary particle concentrations from the application of these

consumer products can be significant at times of elevated indoor O_3 concentrations. A liquid air freshener produced the highest particle formation potential among the consumer products that were investigated in this study. The solid air freshener produced the second highest particle formation potential, and the dishwasher detergent produced the lowest particle formation potential among the consumer products that were investigated.

The results presented in this chapter suggest that O_3/terpene reactions can lead to significant exposures to fine particles with diameters <1.0 μm. This is particularly true for conditions involving elevated concentrations of limonene, e.g., from any of a large number of consumer products, and elevated levels of indoor O_3, e.g., during elevated outdoor O_3 concentrations or the use of indoor ozone generators.

6.0 APPLICATION OF THE ICEM

The ICEM was applied to investigate the levels and dynamic nature of indoor secondary particles and free radicals. Model applications and results are described in this chapter.

6.1 Effects of Selected Parameters on Indoor Secondary Organic Aerosol Levels

Model simulations were performed to investigate the effects of the following parameters on indoor SOA mass concentrations: air exchange rate, outdoor fine particle concentration, outdoor O_3 concentration, indoor α-pinene emission rate, and indoor temperature. A base-case scenario was defined as follows:

Indoor α-pinene emission rate = 2.3 mg/min

Outdoor O_3 concentration = 100 ppb and,

Outdoor fine particle concentration ($PM_{2.5}$) = 15 $\mu g/m^3$

An indoor volume of 500 m^3 was used for this analysis. The prescribed indoor emission rate would produce an indoor α-pinene concentration of about 100 ppb at an air exchange rate of 0.5 hr^{-1} in the absence of O_3. For simplicity, it was also assumed that no pollutants other than O_3, α-pinene, associated gaseous by-products, and fine particles existed in the indoor environment.

Pollutant deposition velocities shown in Table 3.4 were used in the model. A surface removal rate of 0.39 hr^{-1} was used for fine particles (Wallace, 1996). Surface removal rates of the semi-volatile organic products of α-pinene were assigned twice the surface removal rate of fine particles following Kamens *et al*. (1999). It was also assumed that no other sources of fine particles were present in the building, and that transport of outdoor fine particles provided "seed" particles in the model.

All model simulations were performed with an assumed indoor relative humidity of 50%, indoor temperature of 297^0K (except when the effects of temperature were investigated), and an air exchange rate of 0.5 hr^{-1} (except when the effects of air exchange rate were investigated).

The predicted indoor O_3 concentration for the base-case scenario was 11 ppb. The total indoor fine particle concentration was predicted to be 12.1 $\mu g/m^3$. The predicted indoor SOA concentration resulting from reactions between O_3 and α-pinene for the base-case scenario was 3.7 $\mu g/m^3$. The predicted indoor "seed" particle concentration resulting from the transport of outdoor fine particles was 8.4 $\mu g/m^3$.

6.1.1 Effects of Air Exchange Rate on Indoor Secondary Organic Aerosol Concentrations

The air exchange rate was varied from 0.1 to 3.0 hr^{-1}. Resulting steady-state indoor SOA concentrations are shown in Figure 6.1. Indoor seed and outdoor particle concentrations are also shown in Figure 6.1. Predicted indoor SOA concentrations increased with lower air exchange rates (above 0.4 hr^{-1}). Lower air exchange rates were associated with lower indoor O_3 and "seed" particle levels. However, indoor α-pinene concentrations also increased with lower air exchange rates. The O_3/α-pinene reaction rate and time available for reactions increased with the reduction in the air exchange rate (above 0.4 hr^{-1}). The combination of higher reaction rates and longer reaction times resulted in increased indoor SOA concentrations. The predicted indoor SOA concentrations decreased with further reductions in air exchange rate below 0.4 hr^{-1}, primarily due to a decrease in the O_3/α-pinene reaction rate below an air exchange rate of 0.4 hr^{-1}. Interestingly, at air exchange rates of 0.3 hr^{-1} to 1.0 hr^{-1}, i.e., typical of many residential dwellings, SOA was predicted to account for approximately 20 to 35% of the total indoor fine particles. Such contributions are similar to the unexplained fraction previously described by Wallace (1996) and Santannam *et al*. (1990).

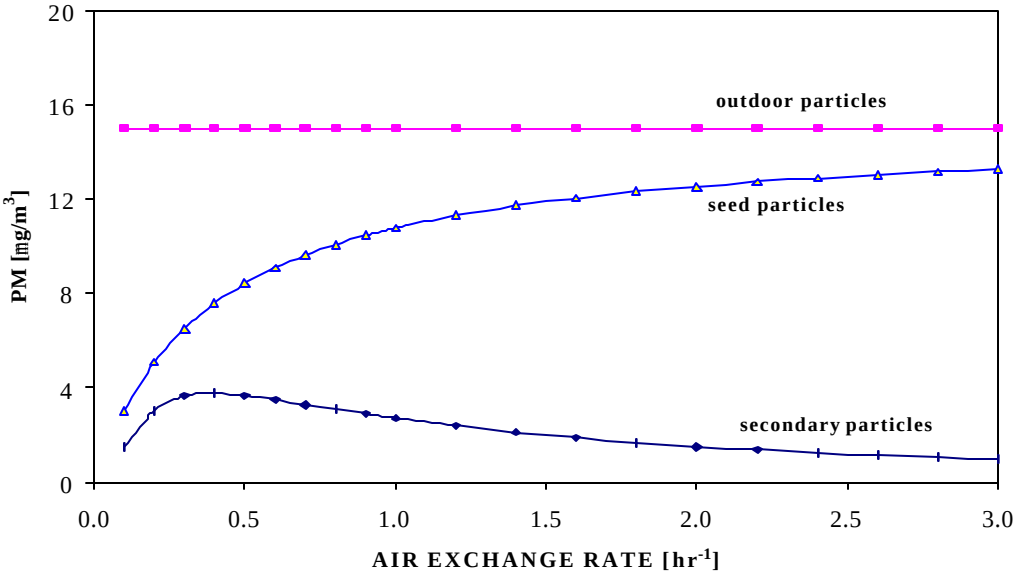

Figure 6.1. Indoor fine particle concentration as a function of air exchange rate

6.1.2 Effects of Outdoor Fine Particle Concentration on Indoor Secondary Organic Aerosol Concentrations

Outdoor fine particle concentrations were varied from 0 to 100 µg/m^3. The resulting steady-state indoor SOA concentrations are shown in Figure 6.2. Indoor seed concentrations are also shown in Figure 6.2. Higher outdoor fine particle concentrations caused higher indoor "seed" particle concentrations. Higher indoor "seed" particles increased the partitioning of semi-volatile products and resulted in increased indoor SOA concentrations. The predicted indoor SOA concentration was only 0.4 µg/m^3 when the outdoor particle level was zero and resulted from self-nucleation of low vapor pressure reaction products. However, the predicted indoor SOA concentration increased to almost 12 µg/m^3 at an outdoor fine particle concentration of 100 µg/m^3, a very high concentration in outdoor environments.

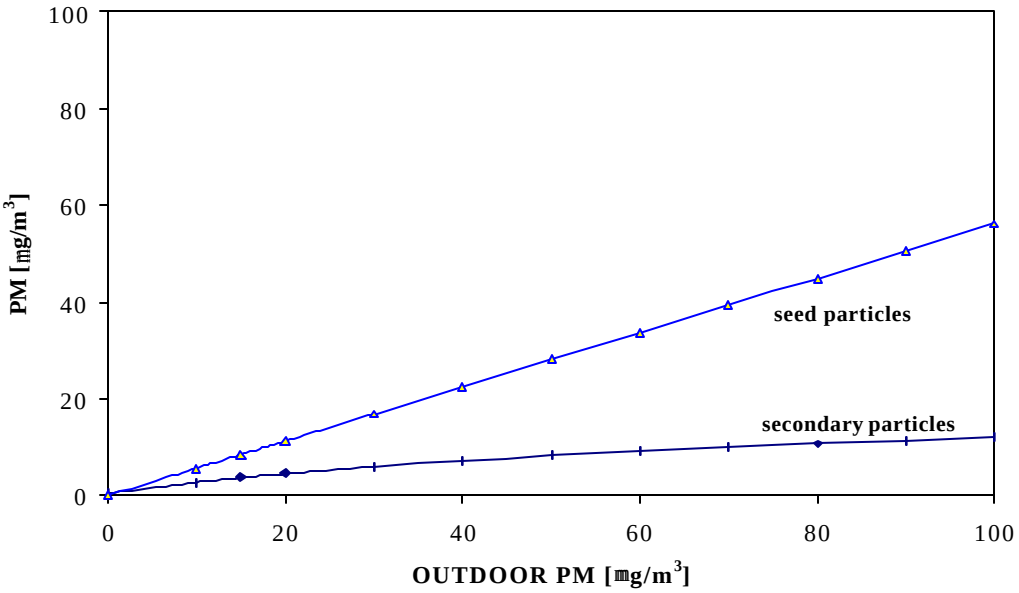

Figure 6.2. Indoor fine particle concentration as a function of outdoor fine particle concentration

6.1.3 Effects of Outdoor O_3 Concentration on Indoor Secondary Organic Aerosol Concentrations

The outdoor O_3 concentration was varied from 0 to 200 ppb. The resulting steady-state indoor SOA concentrations are shown in Figure 6.3. Indoor seed, total, and outdoor particle concentrations are also shown in Figure 6.3. Indoor SOA mass concentrations increased with higher outdoor O_3 concentrations. The higher outdoor O_3 concentrations caused an increase in indoor O_3 concentrations, which in turn increased the O_3/α-pinene reaction rate. Increased amounts of reaction products were available due to the higher O_3/α-pinene reaction rate, and resulted in increased indoor SOA mass concentrations. The predicted indoor SOA mass concentration at an outdoor O_3 concentration of 200 ppb was almost 50% of the total indoor fine particle concentration.

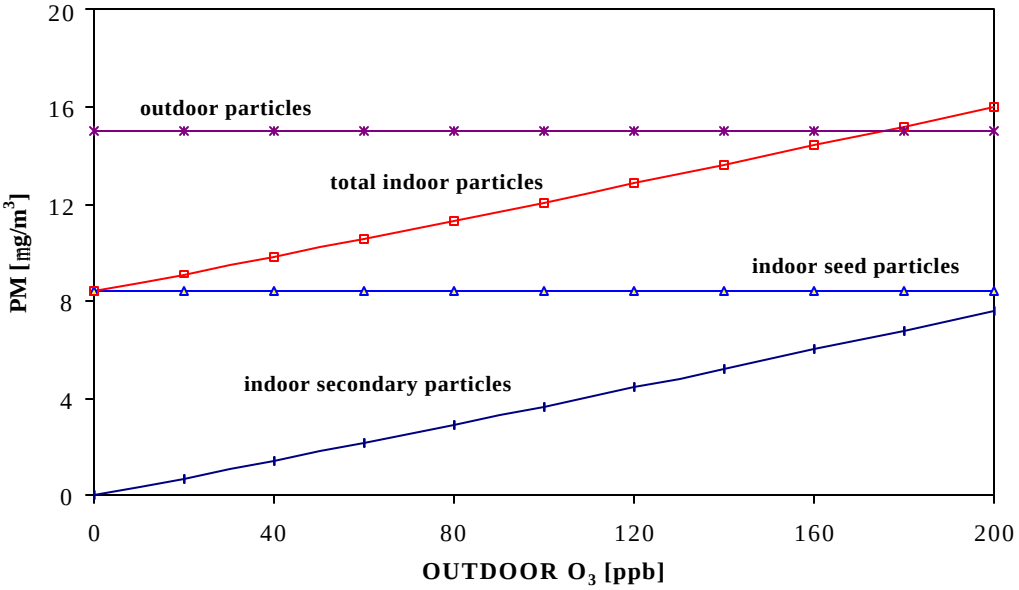

Figure 6.3. Indoor fine particle concentration as a function of outdoor O_3 concentrations

6.1.4 Effects of Indoor a -Pinene Emission Rate on Indoor Secondary Organic Aerosol Concentrations

The indoor α-pinene emission rate was varied from 0 to 3 times the base-case emission rate. The resulting steady-state indoor SOA concentrations are shown in Figure 6.4. Indoor seed and outdoor particle concentrations are also shown in Figure 6.4. Increased indoor α-pinene emission rates increased the O_3/α-pinene reaction rate and resulted in elevated indoor SOA concentrations. The contribution of SOA to indoor fine particle mass equaled that of outdoor-to-indoor penetration for an α-pinene emission rate of 4.6 mg/min.

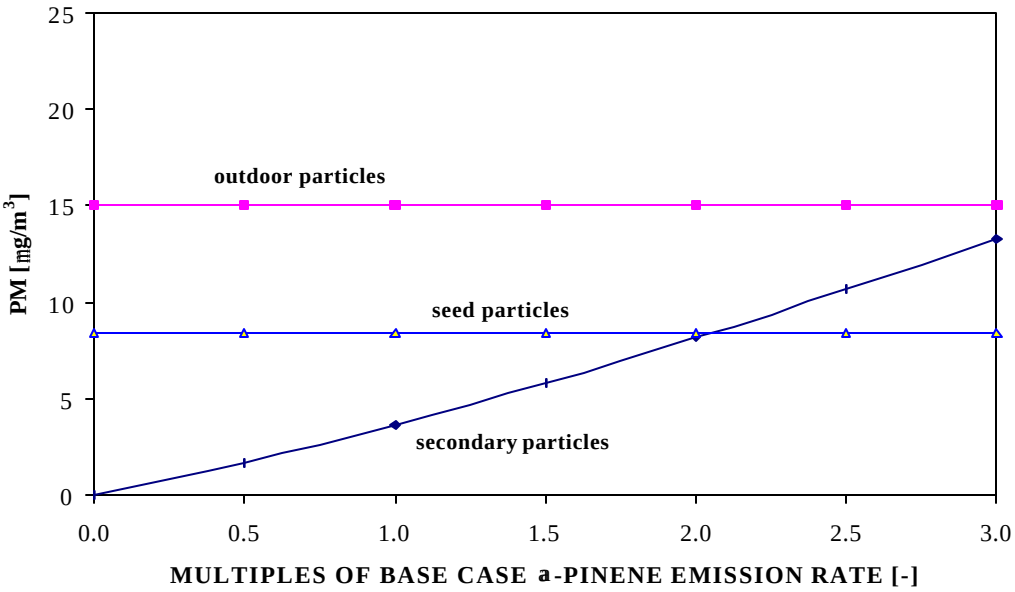

Figure 6.4. Indoor fine particle concentration as a function of indoor base-case a -pinene emission rate

6.1.5 Effects of Indoor Temperature on Indoor Secondary Organic Aerosol Concentrations

The indoor temperature was varied from 280 to 315K (45 ^{o}F to 108 ^{o}F). The resulting steady-state indoor SOA concentrations are shown in Figure 6.5. Indoor seed and outdoor particle concentrations are also shown in Figure 6.5. The indoor SOA concentrations increased dramatically as indoor temperature was reduced.

Lower temperatures reduced the rates of homogeneous chemical reactions. However, this effect was more than compensated for by an increase in gas-to-particle partitioning of reaction products at lower temperatures. Predicted indoor SOA concentrations increased by more than a factor of two for every 10 ^{o}C decrease in indoor temperature.

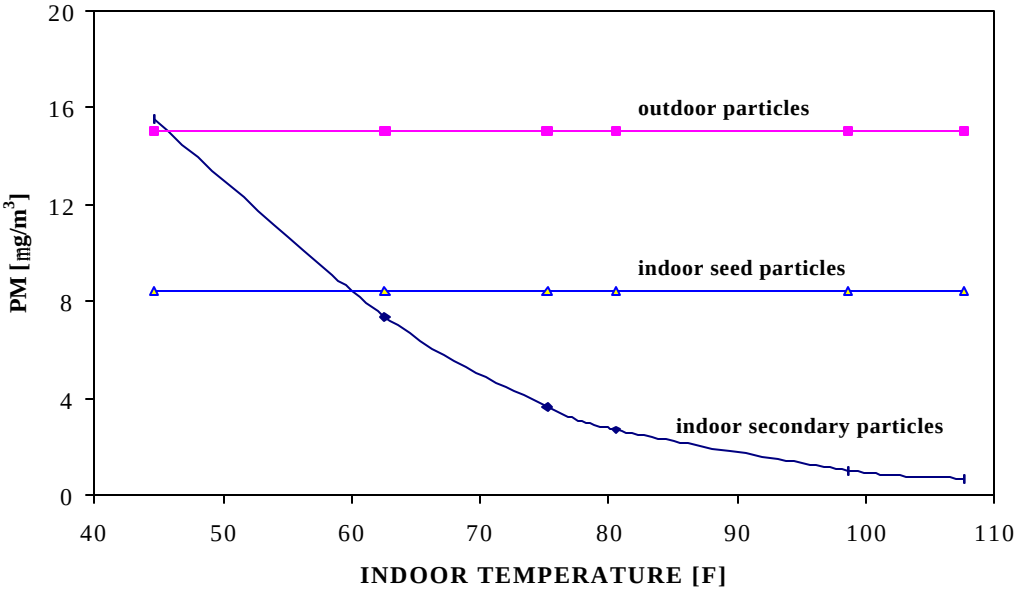

Figure 6.5. Indoor fine particle concentration as a function of indoor temperature

6.2 Predictions of Indoor Hydroxyl Radicals

Hydroxyl radicals (OH·) react with most atmospheric trace compounds. In fact, the fate of many atmospheric compounds is determined solely by reaction with atmospheric OH· (Finlayson-Pitts and Pitts, 1986). For this reason, outdoor OH· concentrations and chemistry have been subject to active research for many years. In contrast, the presence of OH· in indoor environments has received far less attention. It has been implicitly or explicitly assumed that outdoor transport is the only source of indoor OH·, and that since OH· is highly reactive, indoor levels of OH· are negligible. Consequently, indoor chemistry has received far less attention than has outdoor atmospheric chemistry. Ironically, production of OH· inside buildings was suggested as early as 1986 in a model of indoor air chemistry (Nazaroff and Cass, 1986). However, indoor OH· production did not receive detailed attention for another 10 years (Weschler and Shields, 1996).

Numerous organic compounds, including alkenes, have been measured in residential and commercial buildings, with indoor concentrations generally being significantly higher than outdoors (Shah and Singh, 1988; Brown *et al*., 1994; Gebefuegi *et al*., 1995; Brickus *et al*., 1998). Ozone (O_3) can be transported from outdoors to indoors, allowing indoor alkene/O_3 reactions to produce $OH^{\cdot}$. Weschler and Shields (1996) demonstrated that certain alkene/O_3 reactions proceed at rates faster than air exchange rates in typical residential and commercial buildings, and thus provide a source of $OH^{\cdot}$ in indoor environments. They estimated indoor $OH^{\cdot}$ concentrations using average concentrations of O_3 and other compounds commonly found in indoor environments, and reported that indoor $OH^{\cdot}$ concentrations are lower than typical day-time urban outdoor $OH^{\cdot}$ concentrations, but can be higher than typical night-time urban outdoor $OH^{\cdot}$ concentrations. Weschler and Shields (1997b) also validated the conclusions of their previous studies by performing experiments in a manipulated but realistic indoor setting. The authors continuously injected O_3, limonene and 1,3,5-trimethylbenzene in an unoccupied office, and derived indoor $OH^{\cdot}$ concentrations up to 7×10^5 molecules/cm^3 from the decrease in indoor 1,3,5-trimethylbenzene concentrations.

To explore the effects of several factors on indoor $OH^{\cdot}$, a base-case scenario was defined as follows: indoor emission rates equal to "typical" indoor emission rates and outdoor pollutant levels equal to "typical" outdoor pollutant levels. In addition to the "typical" levels shown in Table 3.1, the following values were taken as typical of urban summertime conditions, and were assigned to outdoor pollutants for the base-case scenario: NO = 7 ppb, N_2O_5 = 20 ppt, HONO = 4.5 ppt, HNO_3 = 10 ppb, H_2O_2 = 2 ppb, HO_2NO_2 = 50 ppt, $OH^{\cdot} = 5 \times 10^6$ molecules/cm^3 (0.2 ppt), $CH_3OO^{\cdot}$ = 10 ppt, $NO_3^{\cdot}$ = 1 ppt, $HO_2^{\cdot}$ = 4 ppt, and O_3 = 100 ppb. All model simulations were performed with an assumed indoor relative humidity of 50%, indoor temperature of 297 ^{o}K

(except when the effects of temperature were investigated), and an air exchange rate of 0.5 hr^{-1} (except when the effects of air exchange rates were investigated).

Reactions producing OH· in the ICEM are shown in Table 6.1 (Equations 6.1-6.20). As discussed later, indoor photolysis only moderately affects indoor OH·. Consequently, all photolysis reactions have been omitted from Table 6.1. Transport from the outdoor environment is a source of OH· to indoor environments. However, model results were insensitive to outdoor OH· levels, indicating that the outdoor-to-indoor transport term is not a significant contributor to indoor OH· concentrations.

The α-pinene/O_3 and α-pinene/OH· reactions in the SAPRC-99 model were replaced by the α-pinene fine particle formation mechanism reported by Kamens *et al*. (1999). Criegee biradicals 1 and 2 are produced from the reaction of α-pinene with O_3 (Kamens *et al.*, 1999). The species "PINALD" in Equations 6.15, 6.37, and 6.38 represent pinonaldehyde and norpinonaldehyde that are formed from α-pinene. The yield of "PINALD" in the α-pinene/OH· reaction was adjusted to 0.34 based on recent work by Wisthaler *et al*. (2001). Methacrolein, methyl vinyl ketone, and lumped isoprene product species are generated from isoprene/O_3 and isoprene/OH· reactions. Reactive aromatic fragmentation products are generated from aromatic/OH· reactions.

Reactions that consume OH· are listed in Table 6.1 (Equations 6.21-6.50). In addition, OH· can also be consumed by alkanes, and other organic compounds in the model. Collectively, these compounds are referred to as "other organic compounds", and are not shown here. Other possible sinks of indoor OH· include: (1) deposition to (heterogeneous reactions with) indoor surfaces, and (2) transport to the outdoor environment. The final indoor OH· concentration is determined by the competing effects of all sources and sinks.

Table 6.1. Reactions Producing and Consuming $OH^{\cdot}$ in the ICEM

No	Reactions that produce $OH^{\cdot}$	No	Reactions that consume $OH^{\cdot}$
6.1	$NO + HO_2^{\cdot} = OH^{\cdot} +$	6.21	$NO + OH^{\cdot} =$
6.2	$O_3 + HO_2^{\cdot} = OH^{\cdot} +$	6.22	$O_3 + OH^{\cdot} =$
6.3	$NO_3^{\cdot} + HO_2^{\cdot} = 0.8\ OH^{\cdot} +$	6.23	$NO_3^{\cdot} + OH^{\cdot} =$
6.4	Ethene + O_3 = 0.18 $OH^{\cdot}$ +	6.24	Ethene + $OH^{\cdot}$ =
6.5	Isoprene + O_3 = 0.25 $OH^{\cdot}$ +	6.25	Isoprene + $OH^{\cdot}$ =
6.6	Propene + O_3 = 0.35 $OH^{\cdot}$ +	6.26	Propene + $OH^{\cdot}$ =
6.7	Isobutene + O_3 = 0.72 $OH^{\cdot}$ +	6.27	Isobutene + $OH^{\cdot}$ =
6.8	Cis-2-Butene + O_3 = 0.37 $OH^{\cdot}$ +	6.28	cis-2-Butene + $OH^{\cdot}$ =
6.9	Trans-2-Butene + O_3 = 0.64 $OH^{\cdot}$ +	6.29	trans-2-Butene + $OH^{\cdot}$ =
6.10	2-Methyl 2-Butene + O_3 = 1.0 $OH^{\cdot}$ +	6.30	2-Methyl 2-Butene + $OH^{\cdot}$ =
6.11	1,3-Butadiene + O_3 = 0.13 $OH^{\cdot}$ +	6.31	1,3-Butadiene + $OH^{\cdot}$ =
6.12	3-Carene + O_3 = 1.0 $OH^{\cdot}$ +	6.32	3-Carene + $OH^{\cdot}$ =
6.13	Limonene + O_3 = 0.86 $OH^{\cdot}$ + 0.04 AMCYCHEX + 0.04 IPOH + 0.19 HCHO	6.33	Limonene + $OH^{\cdot}$ = 0.2 AMCYCHEX + 0.29 IPOH +
	Intentionally left blank	6.34	AMCYCHEX + $OH^{\cdot}$ =
	Intentionally left blank	6.35	IPOH + $OH^{\cdot}$ =
6.14	Styrene + O_3 = 0.07 $OH^{\cdot}$ +	6.36	Styrene + $OH^{\cdot}$ =
6.15	Criegee biradical 1 = 0.8 $OH^{\cdot}$ + 0.3 PINALD	6.37	α-Pinene + $OH^{\cdot}$ = 0.34 PINALD +
6.16	Criegee biradical 2 = 0.8 $OH^{\cdot}$ +	6.38	PINALD + $OH^{\cdot}$ =
6.17	Methacrolein + O_3 = 0.20 $OH^{\cdot}$ +	6.39	Methacrolein + $OH^{\cdot}$ =
6.18	Methyl vinyl ketone + O_3 = .16 $OH^{\cdot}$ +	6.40	Methyl vinyl ketone + $OH^{\cdot}$ =
6.19	Lumped isoprene product species + O_3 = 0.285 $OH^{\cdot}$	6.41	Lumped isoprene product + $OH^{\cdot}$ =
6.20	Reactive aromatic fragmentation products + O_3 = 0.5 $OH^{\cdot}$ +	6.42	Reactive aromatic fragmen- tation productS + $OH^{\cdot}$ =
		6.43	HONO + $OH^{\cdot}$ =
		6.44	NO_2 + $OH^{\cdot}$ =
		6.45	HNO_3 + $OH^{\cdot}$ =
		6.46	CO + $OH^{\cdot}$ =
		6.47	HO_2NO_2 + $OH^{\cdot}$ =
		6.48	H_2O_2 + $OH^{\cdot}$ =
		6.49	$HO_2^{\cdot}$ + $OH^{\cdot}$ =
		6.50	SO_2 + $OH^{\cdot}$ =

6.2.1 Comparison with Previous Studies

The predicted steady-state indoor $OH^{\cdot}$ concentration of 1.2×10^5 molecules/cm^3 for the base-case scenario was within 37% of the estimate of 1.65×10^5 molecules/cm^3 reported by Weschler and Shields (1996). However, there were some differences in the base-case scenarios used in the two studies. To compare the

ICEM predictions with the estimates of Weschler and Shields, separate simulations were performed using reactions reported in their study.

Weschler and Shields (1996) used average indoor concentrations of 39 organic and inorganic compounds that are commonly found in indoor air to estimate the indoor OH· concentration for an air exchange rate of 1.0 hr^{-1}. An indoor O_3 concentration of 20 ppb was used in their study. Average pollutant concentrations reported by Weschler and Shields could not be directly used in the ICEM, as the model predicts indoor pollutant concentrations based on prescribed emission rates. Therefore, average indoor pollutant emission rates were estimated using the average indoor pollutant concentrations reported by Weschler and Shields, and were used as input to the ICEM. The source of indoor O_3 was the transport of outdoor air into the indoor environment. An outdoor O_3 concentration of 95 ppb was assigned to the ICEM to match the indoor O_3 concentration of 20 ppb reported by Weschler and Shields (1996). The ICEM then led to an indoor OH· concentration of 1.6×10^5 molecules/cm^3 for the base-case, i.e., within 0.5% of the estimate of Weschler and Shields.

Weschler and Shields (1996) also performed a sensitivity analysis to assess the influence of several key parameters on predicted indoor OH· concentrations. A similar analysis was also completed using the ICEM. Comparative results are shown in Table 6.2. Indoor OH· concentrations predicted by ICEM are in good agreement with those of Weschler and Shields (1996). Details about case 1 through 11 can be found in Weschler and Shields (1996).

Weschler and Shields (1997b) performed experiments to measure OH· concentrations in an unoccupied office in which ozone, limonene and 1,3,5-trimethylbenzene were continuously injected. The authors measured indoor

concentrations of ozone, limonene and 1,3,5-trimethylbenzene, and derived indoor $OH^{\cdot}$ concentrations from the decrease in indoor 1,3,5-trimethylbenzene concentrations. In one of the experiments, the indoor ozone and limonene concentrations were 62 and 109 ppb, respectively, and the measured indoor $OH^{\cdot}$ concentration was 6.0×10^5 molecules/cm^3.

Table 6.2. Comparisons of ICEM predicted Indoor $OH^{\cdot}$ Levels to that of Weschler and Shields

Cases	Description	Indoor $OH^{\cdot}$ (molecules/cm^3) ICEM	Indoor $OH^{\cdot}$ (molecules/cm^3) (Weschler & Shields, 1996)	Difference (%)
Case 1	Base-case	1.64×10^5	1.65×10^5	- 0.3
Case 2	1/10 [VOC] base-case	2.41×10^4	2.27×10^4	+ 6.5
Case 3	3 times [VOC] base-case	2.98×10^5	3.08×10^5	- 3.2
Case 4	No VVOC	1.56×10^5	1.55×10^5	+ 0.4
Case 5	Only Limonene	1.05×10^5	1.03×10^5	+ 1.8
Case 6	Only Terpinene	6.27×10^4	6.16×10^4	+ 1.8
Case 7	Only 2-Methyl-2-Butene	2.26×10^4	2.19×10^4	+ 3.0
Case 8	Only α-Pinene	8.84×10^3	7.88×10^3	+ 12.2
Case 9	Low Ozone	2.56×10^4	2.46×10^4	+ 4.0
Case 10	No Ozone	1.76×10^1	1.72×10^1	+ 2.2
Case 11	No Alkenes	7.62×10^2	7.46×10^2	+ 2.1

In the other experiments, the indoor ozone and limonene concentrations were 106 and 72 ppb, respectively, and the measured indoor $OH^{\cdot}$ concentration was 7.1×10^5 molecules/cm^3. Measured air exchange rates, office volume, indoor temperature, and indoor emission rates for ozone, limonene and 1,3,5-trimethylbenzene were taken from the Weschler and Shields study (1997b) and provided as input data to the ICEM. For the experiments with the O_3 concentration of 62 ppb, the model predicted an indoor $OH^{\cdot}$ concentration of 1.1×10^6 molecules/cm^3, approximately double the experimental result. For the experiments with the O_3 concentration of 106 ppb, the predicted indoor $OH^{\cdot}$ concentration was 1.7×10^6 molecules/cm^3, slightly more than

double the experimental result. Considering the lack of information regarding the other organic and inorganic compounds present during the experiments, the agreement between the model and experimental results is satisfactory. The over-predictions suggest that the model, not surprisingly, did not fully capture the type and concentrations of compounds present in the office, particularly compounds that serve as $OH^{\cdot}$ sinks.

6.2.2 Results of Base-Case Application

Predicted steady-state indoor $OH^{\cdot}$ concentrations are discussed in sections 6.2.2-6.2.8. Dynamic indoor $OH^{\cdot}$ concentrations are presented in section 6.2.9. For the base-case scenario, the predicted indoor $OH^{\cdot}$ reached steady-state within 360 minutes. At higher air exchange rates, the predicted indoor $OH^{\cdot}$ reached steady-state faster than the base-case scenario, and at lower air exchange rates the predicted indoor $OH^{\cdot}$ reached steady-state slower than the base-case scenario. These results are consistent with basic reactor theory.

The predicted steady-state indoor $OH^{\cdot}$ concentration for the base-case scenario was 1.2×10^5 molecules/cm^3. This value is lower than the typical outdoor summertime urban $OH^{\cdot}$ levels of $5\text{-}10 \times 10^6$ molecules/cm^3 (Seinfeld and Pandis, 1998), but greater than typical nighttime outdoor $OH^{\cdot}$ levels, e.g., approximately 5×10^4 molecules/cm^3 (Tanner and Eisele, 1995).

Selected production and consumption rates of indoor $OH^{\cdot}$ for the base-case scenario are shown in Table 6.3. The combined $OH^{\cdot}$ production rate of all alkene/O_3 reactions (Equations 6.4-6.20) is 9.2 ppt min^{-1}, while the combined $OH^{\cdot}$ consumption rate of all alkene/$OH^{\cdot}$ reactions (Equations 6.24-6.42) is 5.4 ppt min^{-1}. For base-case conditions, the set of these reactions is a net source of $OH^{\cdot}$ in indoor environments. Reactions of NO with $HO_2^{\cdot}$ and $OH^{\cdot}$ (Equations 6.1 and 6.21) were predicted to

produce and consume indoor $OH^{\cdot}$ at the rates of 6.8 ppt min^{-1} and 0.006 ppt min^{-1}, respectively. Interestingly, the net $OH^{\cdot}$ generation rate from basic NO_x chemistry was predicted to be more significant than alkene/O_3 reactions for base-case conditions.

Table 6.3. Selected Production and Consumption Rates of Indoor $OH^{\cdot}$ for Base-Case Conditions at Steady-State

Compounds	Eqn Nos.	$OH^{\cdot}$ Production Rate (ppt/min)	Eqn Nos.	$OH^{\cdot}$ Consumption Rate (ppt/min)	Net $OH^{\cdot}$ Production Rate (ppt/min)
Alkenes	6.4 - 6.20	9.2	6.24-6.41	5.4	+ 3.8
NO	6.1	6.8	6.21	0.006	+ 6.8
O_3	6.2	0.1	6.22	0.005	+ 0.1
$NO_3^{\cdot}$	6.3	0.003	6.23	0.00002	+ 0.003
Summed	-	16.1	-	5.4	+ 10.7

As seen in Table 6.3, reactions of O_3 with $HO_2^{\cdot}$ and $OH^{\cdot}$ (Equations 6.2 and 6.22) and reactions of $NO_3^{\cdot}$ with $HO_2^{\cdot}$ and $OH^{\cdot}$ (Equations 6.3 and 6.23) were also net contributors to indoor $OH^{\cdot}$ for the base-case scenario. However, the collective indoor $OH^{\cdot}$ production rates by Reactions 6.1-6.3 were lower than the production rates of alkene/O_3 reactions.

Interestingly, the rate at which $OH^{\cdot}$ was predicted to be transported from outdoors was only 0.002 ppt min^{-1}, which is negligible compared to the combined alkene/O_3 production rate. The rate at which hydroxyl radicals were predicted to be deposited on indoor surfaces was 0.0003 ppt min^{-1}, which is also negligible compared to the combined alkene/$OH^{\cdot}$ consumption rate.

Predicted indoor $OH^{\cdot}$ production and consumption rates by individual alkenes are presented in Table 6.4. The reaction between O_3 and limonene was predicted to account for 40% of the total $OH^{\cdot}$ production rate for base-case conditions, underscoring the potential importance of limonene sources on indoor air chemistry.

Both limonene and isoprene were predicted to be the major sinks for OH· removal. It should be noted that in addition to the production and consumption of OH· by alkenes as shown in Table 6.4, other sources and sinks of OH· were also present in the model.

Table 6.4. Indoor OH· Production and Consumption Rates by Individual Alkenes for Base-Case Conditions

Compound	OH· Production Rate (ppt/min)	Compound	OH· Consumption Rate (ppt/min)
Limonene	6.4	Limonene	2.6
2-Methyl 2-Butene	1.3	Isoprene	1.3
Trans-2-Butene	0.5	Styrene	0.2
α-pinene	0.4	Isobutene	0.17
Cis-2-Butene	0.2	1,3-Butadiene	0.14
3-Carene	0.11	α-pinene	0.14
Isoprene	0.10	2-Methyl 2-Butene	0.12
Isobutene	0.07	3-Carene	0.11
Propene	0.03	Trans-2-Butene	0.10
Styrene	0.01	Cis-2-Butene	0.10
Ethene	0.01	Propene	0.09
1,3-Butadiene	0.004	Ethene	0.09
Reactive aromatic fragmentation products	0.0025	3-isopropenyl-6-Oxoheptanal	0.09
Lumped isoprene product species	0.0018	4-acetyl-1-methyl-cyclohexene	0.08
Methyl vinyl ketone	0.0007	Reactive aromatic fragmentation products	0.05
Methacrolein	0.0002	Lumped isoprene product species	0.04
		Methacrolein	0.01
		Methyl vinyl ketone	0.01
Total	**9.2**	Total	**5.4**

6.2.3. Effects of Indoor Alkene Emission Rates on Indoor OH· Concentrations

The effects of indoor alkene emission rates on steady-state indoor OH· are shown in Figure 6.6. Alkene emission rates were varied from 0 to 10 times the base-case condition shown in Table 3.1. Indoor OH· concentrations increased non-linearly

with increasing indoor alkene emission rates. The predicted indoor OH· concentration at an indoor alkene emission rate of zero was 3.5 x 10^4 molecules/cm^3; some alkenes are transported from outdoors to indoors even when the indoor alkene emission rate is zero. For base-case conditions, the mass flow of alkenes from outdoors to indoors was only 15% of total alkene input to the indoor system. When all indoor sources were set to zero, the contribution to the indoor OH· production rate by the NO/HO_2· reaction (Equation 6.1) was dominant and accounted for over 70% of the total indoor OH· production rate. The collective contribution of alkene/O_3 reactions was about 28% of the total indoor OH· production rate.

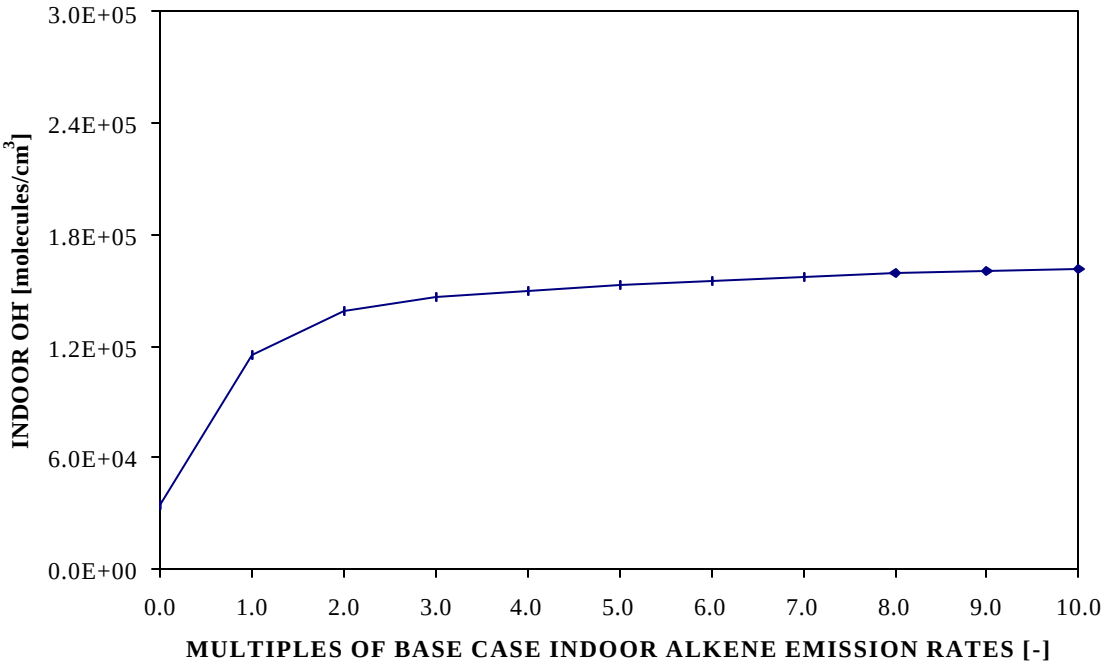

Figure 6.6. Effects of indoor alkene emission rate on steady-state indoor OH· concentration

The collective contribution to indoor OH· production by Reactions 6.1-6.3 decreased, and the contribution by alkene/O_3 reactions increased, as the indoor alkene emission rates were increased. The collective contribution of alkene/O_3 reactions was over 99% of the total indoor OH· production rate when the indoor alkene emission

rate was 10 times the base-case emission rate. However, the combined $OH^{\cdot}$ consumption rate by alkene/$OH^{\cdot}$ reactions also increased with increased indoor alkene emission rates. Estimated indoor $OH^{\cdot}$ concentrations increased by a factor of almost five between the lowest and highest indoor alkene emission rates.

6.2.4. Effects of Outdoor O_3 Levels on Indoor $OH^{\cdot}$ Concentrations

Outdoor O_3 concentrations were varied from 20 to 200 ppb to determine the effect on indoor $OH^{\cdot}$ concentrations. Ozone reacts with NO at a very high rate; thus outdoor NO concentrations would be lower than 7 ppb (used for the base-case scenario) with higher O_3 concentrations. Outdoor NO concentrations were adjusted for various outdoor O_3 concentrations using the following equation:

$$[NO] = k_1 [NO_2] / k_3 [O_3] \quad (6.51)$$

where, k_1 is the rate constant for NO_2 photolysis in the troposphere [0.5 min^{-1} corresponding to the solar noon photolysis rate (Seinfeld and Pandis, 1998)], k_3 is the rate constant for the NO/O_3 reaction (26.51 ppm^{-1} min^{-1} at 297 ^{0}K) (Carter, 2000), $[NO_2]$ is the outdoor NO_2 concentration (0.0385 ppm in this study), [NO] is the outdoor NO concentration, and $[O_3]$ is the outdoor O_3 concentration. The resulting outdoor NO concentrations were utilized in the model with outdoor O_3 concentrations.

The effects of outdoor O_3 concentrations on indoor $OH^{\cdot}$ concentrations are illustrated in Figure 6.7. The predicted indoor $OH^{\cdot}$ concentration at an outdoor O_3 level of 20 ppb was only 3.0 x 10^4 molecules/cm^3 and was dominated by the NO/$HO_2^{\cdot}$ reaction (Equation 6.1). Reaction 6.1 contributed about 90% and alkene/O_3 reactions contributed about 10% of the total indoor $OH^{\cdot}$ production rate at an outdoor O_3 concentration of 20 ppb.

For the base-case air exchange rate, higher outdoor O_3 concentrations were accompanied by higher indoor O_3 and lower indoor NO concentrations. The contribution to indoor $OH^{\cdot}$ production by alkene/O_3 reactions increased with increasing outdoor O_3 concentrations, accounting for 87% of the contribution at the outdoor O_3 level of 200 ppb. The contribution to indoor $OH^{\cdot}$ production by Reaction 6.1 initially increased and then decreased with higher outdoor O_3 concentrations. Reaction 3 accounted for about 10% of the total indoor $OH^{\cdot}$ contribution at an outdoor O_3 concentration of 200 ppb. The estimated indoor $OH^{\cdot}$ concentration increased by a factor of almost four between the lowest and highest outdoor O_3 levels. However, the predicted indoor $OH^{\cdot}$ concentration varied little for outdoor O_3 concentrations greater than 60 ppb under otherwise base-case conditions. This result is potentially significant as it may lead to simplifications in indoor air chemistry models for cities like Houston, where summertime O_3 concentrations often exceed 60 ppb for much of the day.

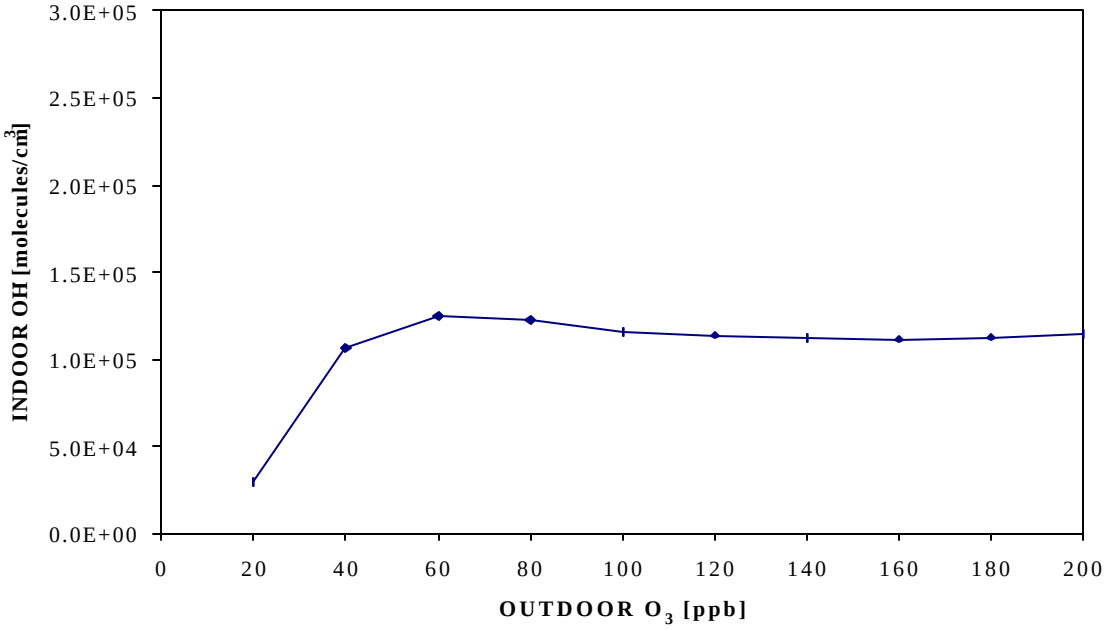

Figure 6.7. Effects of outdoor O_3 concentration on steady-state indoor $OH^{\cdot}$ concentration

6.2.5. Effects of Outdoor NO Levels on Indoor OH· Concentrations

The outdoor NO concentration was varied from 4 to 30 ppb to determine its effects on indoor OH· concentrations. Outdoor O_3 concentrations were adjusted for higher outdoor NO concentrations using Equation 6.51. The effects of outdoor NO concentrations on indoor OH· concentrations are shown in Figure 6.8. The predicted indoor OH· concentration at an outdoor NO concentration of 4 ppb was 1.1 x 10^5 #/cm^3. Alkene/O_3 reactions were predicted to account for 86% of the total indoor OH· production rate when the outdoor NO level was 4 ppb. The NO/HO_2· reaction contributed about 14% of the total indoor OH· production rate.

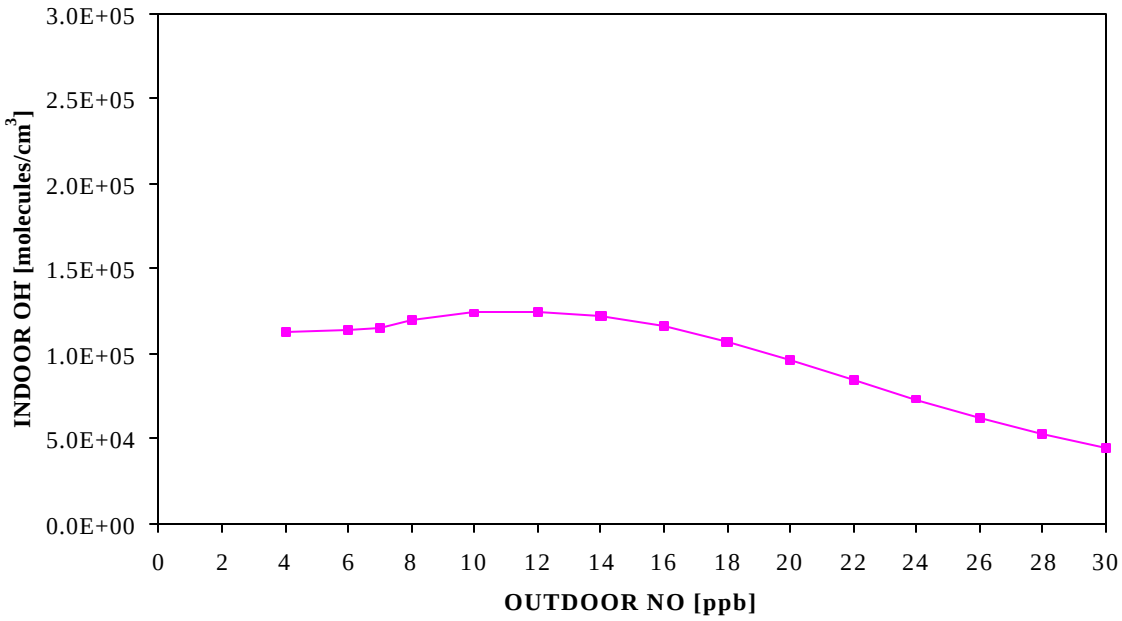

Figure 6.8. Effects of outdoor NO concentration on steady-state indoor OH· concentration

The predicted indoor OH· concentrations increased slightly from the initial concentration, reaching a peak level at an outdoor NO concentration of 12 ppb. The contribution of the NO/HO_2· reaction to the total indoor OH· production rate increased up to the outdoor NO concentration of 16 ppb, and then decreased. The contribution

of alkene/O_3 reactions to the total indoor OH· production rate decreased with increased outdoor NO concentrations.

6.2.6 Effects of Air Exchange Rate on Indoor OH· Concentrations

The effects of air exchange rate on indoor OH· concentrations are shown in Figure 6.9. The air exchange rate was varied from 0.1 to 3.0 hr^{-1}, a range consistent with very "tight" to very leaky homes. The indoor OH· concentration increased with increasing air exchange rate. At lower air exchange rates, indoor OH· production rates were dominated by alkene/O_3 reactions, while the contribution by Reactions 6.1-6.3 was lower. The NO/HO_2· reaction accounted for only 15% of the total indoor OH· production rate at an air exchange rate of 0.1 hr^{-1}. The contribution to indoor OH· by alkene/O_3 reactions decreased with increasing air exchange rates; while the contribution to indoor OH· by Reactions 6.1-6.3 increased. Reactions 6.1-6.3 collectively accounted for about 50% of the indoor OH· production rate while alkene/O_3 reactions collectively accounted for the other 50% at an air exchange rate of 3.0 hr^{-1}. The predicted indoor OH· concentration increased by a factor of approximately nine between the air exchange rates of 0.1 and 3.0 hr^{-1}.

The net contribution to indoor OH· by reactions of alkenes with O_3 and OH· increased with air exchange rates. The net contribution to indoor OH· by reactions of NO with HO_2· and OH· also increased with air exchange rates. However, at lower air exchange rates, the net contribution to indoor OH· by reactions of alkenes with O_3/OH· was higher than that of reactions of NO with HO_2·/OH·. At higher air exchange rates, the net contribution to indoor OH· by reactions of NO with HO_2·/OH· exceeded the net contribution by reactions of alkenes with O_3/OH·. Thus, basic NO_x chemistry plays an important role in determining the net indoor OH· concentrations at higher air exchange rates.

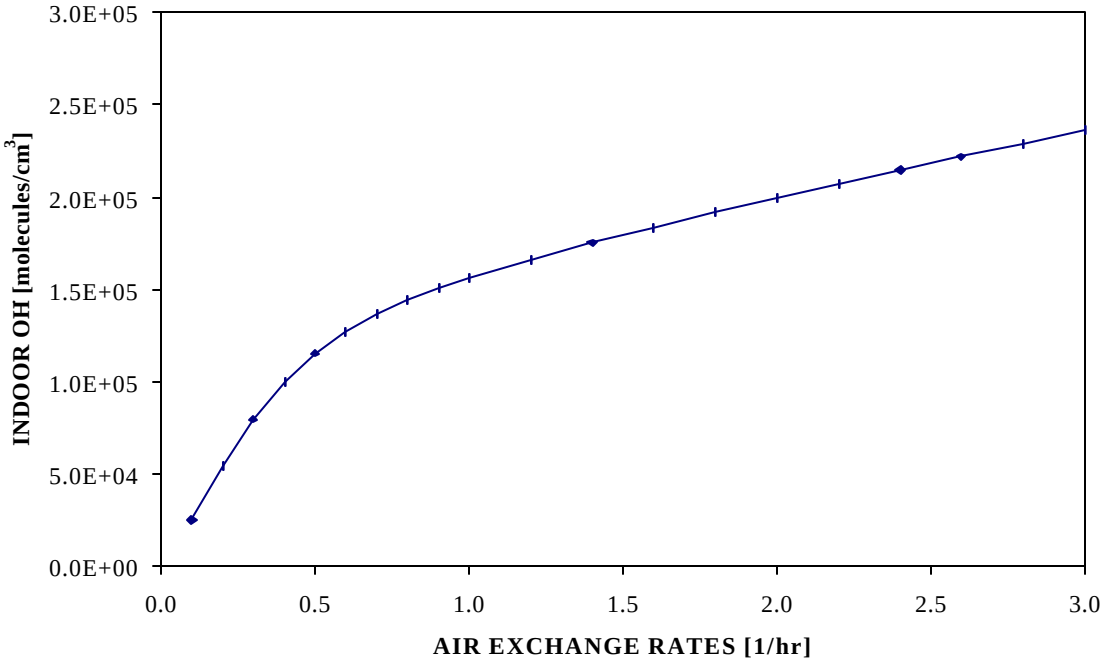

Figure 6.9. Effects of air exchange rate on steady-state indoor OH· concentration

6.2.7 Effects of Indoor Light Intensity and Indoor Temperature on Indoor OH· Concentrations

Model simulations were performed by varying indoor light intensity and indoor temperature. Indoor light intensity was varied from zero to twice the value used for the base-case conditions (i.e., 3,200 lumen m^{-2}). The predicted indoor OH· concentrations increased by only 20% when indoor light intensity was varied within the specified range. Thus, indoor light intensity should have only a moderate effect on indoor OH· concentrations. The estimated indoor OH· concentrations increased by only 66% when indoor temperature was increased from 290 to 315 ^{o}K, a relatively large range of indoor temperatures. Thus, indoor temperature should also have only a moderate effect on indoor OH· concentrations.

6.2.8 Effects of Other Factors on Indoor $OH^{\cdot}$ Concentrations

Model simulations were performed by varying hydroxyl radical deposition velocity, outdoor $OH^{\cdot}$ concentration, outdoor $NO_3^{\cdot}$ concentration, and outdoor $HO_2^{\cdot}$ concentration. Hydroxyl radical deposition velocity was varied from 0 to 0.14 cm/sec. Even when the deposition velocity was doubled relative to the base-case condition, hydroxyl radicals deposited on indoor surfaces at a rate of only 0.0006 ppt/min, compared to a combined alkene/$OH^{\cdot}$ consumption rate of approximately 10 ppt/min. Consequently, indoor $OH^{\cdot}$ concentrations did not change appreciably with variations in deposition velocity.

Outdoor $OH^{\cdot}$ concentrations were varied from 0 to 5 x 10^7 molecules/cm^3. The transport of hydroxyl radicals from outdoors occurred at a maximum rate of approximately 0.02 ppt/min, which is much lower than the combined alkene/O_3 production rate of approximately 10 ppt/min; consequently indoor $OH^{\cdot}$ concentrations did not change with higher outdoor $OH^{\cdot}$ concentrations.

Outdoor $NO_3^{\cdot}$ concentrations were varied from 0 to 10 ppt. Nitrate radicals were transported from outdoors at a maximum rate of approximately 0.08 ppt/min, which is much lower than the $NO_3^{\cdot}$ production rate of approximately 10 ppt/min by the O_3/NO_2 reaction alone. Additionally, the ICEM includes other reactions that can produce indoor $NO_3^{\cdot}$. Thus, indoor $OH^{\cdot}$ concentrations did not change appreciably with higher outdoor $NO_3^{\cdot}$ concentrations.

Outdoor $HO_2^{\cdot}$ concentrations were varied from 0 to 100 ppt. Hydroperoxy radicals were transported from outdoors at a maximum rate of approximately 1.0 ppt/min, which is much lower than the $HO_2^{\cdot}$ production rate of 134 ppt/min generated by the breakdown of HO_2NO_2 alone. Additionally, the ICEM includes multiple reactions, including alkene/O_3 reactions, that were predicted to produce indoor $HO_2^{\cdot}$.

Thus, indoor $OH^{\cdot}$ concentrations did not change appreciably with higher outdoor $HO_2^{\cdot}$ concentrations.

6.2.9 Indoor $OH^{\cdot}$ Dynamics

Two cases were investigated to study the dynamics of $OH^{\cdot}$ in indoor environments. The first case involved a typical cleaning operation with a commercial cleaner that contains 4% by weight α-pinene and 5% by weight limonene. Two ounces of the cleaner were assumed to be used in the cleaning operation, releasing approximately 2.74 mmol of emissions into the hypothetical building atmosphere. Simulations were performed with an air exchange rate of 0.5 hr^{-1}. It was assumed that base-case conditions existed in the hypothetical building during the cleaning operation. For simplicity, the outdoor O_3 concentration was assumed to be constant at 100 ppb.

The predicted indoor O_3, $OH^{\cdot}$, α-pinene, and limonene concentrations during the cleaning operation are shown in Figure 6.10. Cleaning started at time zero and lasted for 10 minutes. The maximum predicted α-pinene and limonene concentrations in the building during the cleaning operation reached approximately 56 ppb and 72 ppb, respectively. These concentrations are significantly less than odor thresholds for either compounds, and are thus considered to be well within the realm of reality.

The indoor O_3 concentration before the cleaning operation was 11.4 ppb. The indoor O_3 concentration decreased during the cleaning operation, reaching a minimum value of 9.2 ppb at 30 minutes, and then increased to its pre-cleaning value over a 10 hour time period. The maximum indoor $OH^{\cdot}$ concentration during the cleaning operation reached 2.4 x 10^5 molecules/cm^3.

Predicted indoor OH· concentrations were produced primarily via reactions of α-pinene and limonene with indoor O_3. Reactions of α-pinene with O_3 (Equations 6.15 and 6.16) and limonene with O_3 (Equation 6.13) contributed 3% and 40%, respectively, of the total indoor OH· production rate before the cleaning operation. However, α-pinene/O_3 and limonene/O_3 reactions contributed up to 24% and 75% of the total indoor OH· production rate during the cleaning operation. The contributions of the α-pinene/O_3 and limonene/O_3 reactions to the total indoor OH· production rate returned to pre-cleaning levels over a 10 hour time period, due primarily to decay in the concentrations of the two tepene precursors.

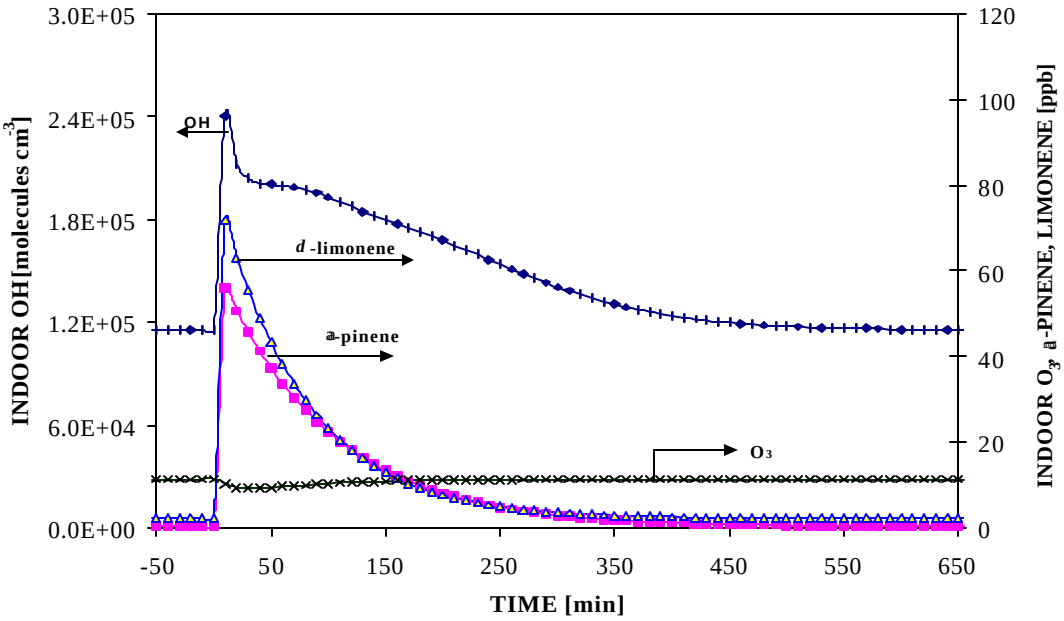

Figure 6.10. Predicted indoor O_3, OH·, a -pinene, and limonene concentrations during a typical cleaning operation

In the second case, time varying outdoor NO, NO_2, and O_3 concentrations measured at monitoring station 411 in Houston, Texas (May 25, 2001) were incorporated into the model. Other parameters associated with the base-case condition were unchanged. During the May 25 episode, two O_3 peaks were observed

at monitoring station 411 as shown in Figure 6.11. The maximum ambient O_3 concentration was 166 ppb. Predicted indoor NO, O_3 and $OH^{\cdot}$ concentrations are shown in Figure 6.12.

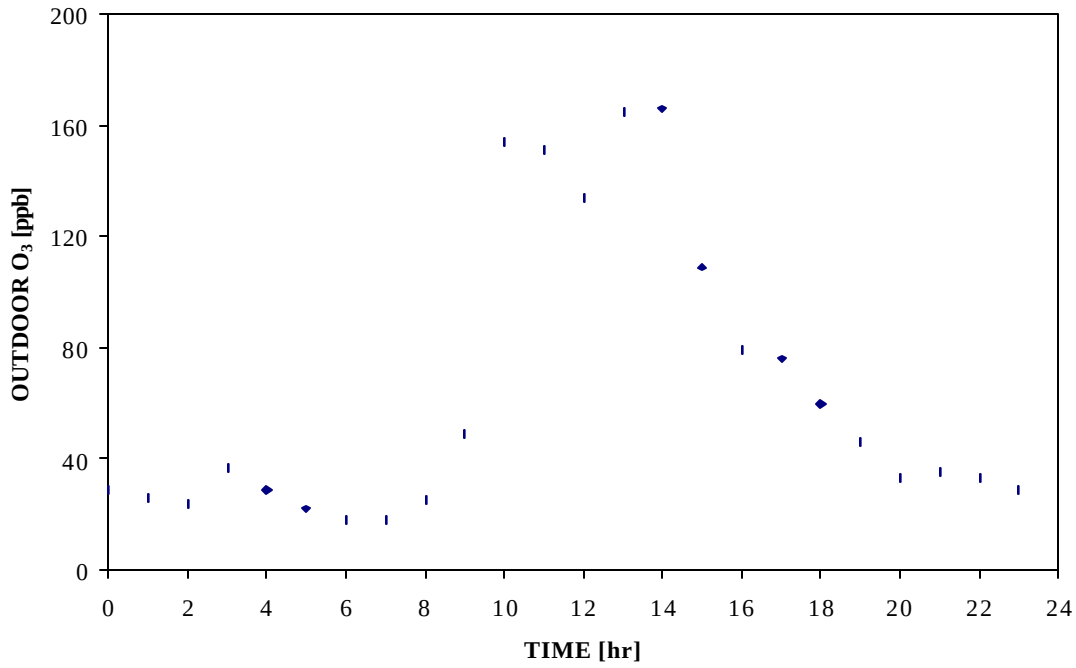

Figure 6.11. Outdoor O_3 for monitoring station 411 in Houston, Texas

The predicted indoor O_3 and $OH^{\cdot}$ concentrations followed the outdoor O_3 concentrations. The predicted indoor $OH^{\cdot}$ concentration at hour zero was 5.4×10^4 #/cm^3 and was the result of alkene/O_3 reactions. The indoor NO concentration was negligible from 0 to 5:00 hours; thus the predicted indoor $OH^{\cdot}$ concentrations followed the indoor O_3 concentrations.

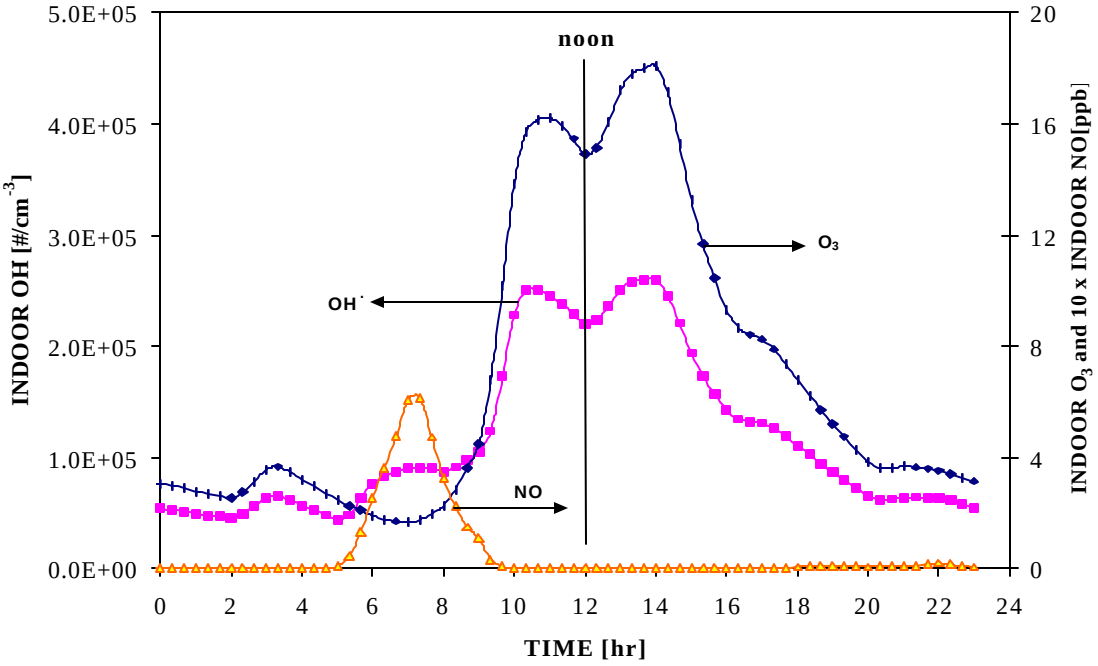

Figure 6.12. Predicted indoor O_3 and $OH^{\cdot}$ concentrations during a high outdoor O_3 day

After 5:00 a.m, the indoor O_3 continued to decrease and the indoor NO concentrations started to increase reaching a peak level at 7:00 a.m due to commuter traffic exhaust. The $NO/HO_2^{\cdot}$ reaction became important after 5:00 a.m. The contribution of the $NO/HO_2^{\cdot}$ reaction to the total indoor $OH^{\cdot}$ formation rate exceeded that of the alkene/O_3 reactions at 7:00 a.m. The predicted indoor $OH^{\cdot}$ concentrations were the combined result of alkene/O_3 and $NO/HO_2^{\cdot}$ reactions during this period. The predicted indoor NO concentrations started to decrease after 7:00 a.m and reached a negligible level around 10:00 a.m. Thus, the contribution of the $NO/HO_2^{\cdot}$ reaction to the total indoor $OH^{\cdot}$ formation rate decreased and also reached a negligible level after 10:00 a.m. From 10:00 a.m to 11:00 p.m (hour 23:00), alkene/O_3 reactions dominated the indoor $OH^{\cdot}$ production rate; thus the predicted indoor $OH^{\cdot}$ concentrations followed the indoor O_3 concentrations.

In reality, neither indoor O_3 nor alkene emission rates are likely to be constant during the course of a day. Indoor O_3 is generally transported from outdoors, which varies not only from day to day, but also from hour to hour of the same day. Indoor alkene emissions also vary with time based on the utilization of consumer products. Thus, indoor $OH^{\cdot}$ levels are expected to reach relatively high concentrations if O_3 and alkenes are simultaneously present indoors at high concentrations. Conversely, indoor $OH^{\cdot}$ concentrations are expected to be low if either O_3 or alkenes are present at low concentrations.

6.2.10 Impacts on Indoor Air Quality

Two examples are presented below in which reactions of limonene and α-pinene with indoor $OH^{\cdot}$ produce compounds that may be of greater concern than the original compounds.

Formation of 3-isopropenyl-6-oxoheptanal (IPOH) from the reactions of limonene with O_3 and $OH^{\cdot}$

Odor thresholds for aldehydes and ketones are generally lower than for many other VOCs. Aldehydes containing unsaturated carbons have even lower odor thresholds (Weschler and Shield, 1997). For example, Jensen and Wolkoff (1996) reported that the odor thresholds of several C_9 aldehydes containing unsaturated carbons range from 1.9-24 ppt. 3-Isopropenyl-6-oxoheptanal contains carbonyl group and unsaturated carbon; thus the odor threshold is expected to be lower.

The indoor emission rate of limonene in ICEM was increased from the base-case condition to an elevated value of 2.3 mg/min (this would produce an indoor limonene concentration of about 100 ppb at an air exchange rate of 0.5 hr^{-1} with no indoor O_3 present). Indoor emission rates and outdoor concentrations of other pollutants were not changed from base-case conditions. Model simulations were

performed to obtain steady-state indoor concentrations of IPOH and results are shown in Figures 6.13.

The first curve represents the net indoor IPOH concentration. The second and third curves represent IPOH concentrations contributed by limonene via $OH^{\cdot}$ and O_3 reaction pathways, respectively. As seen in Figure 6.13, the indoor IPOH concentrations produced via the $OH^{\cdot}$ pathway are predicted to be consistently higher than that of the O_3 pathway. Lower air exchange rates produced higher indoor IPOH concentrations, an interesting result given a continuing trend toward more energy efficient ("tight") buildings.

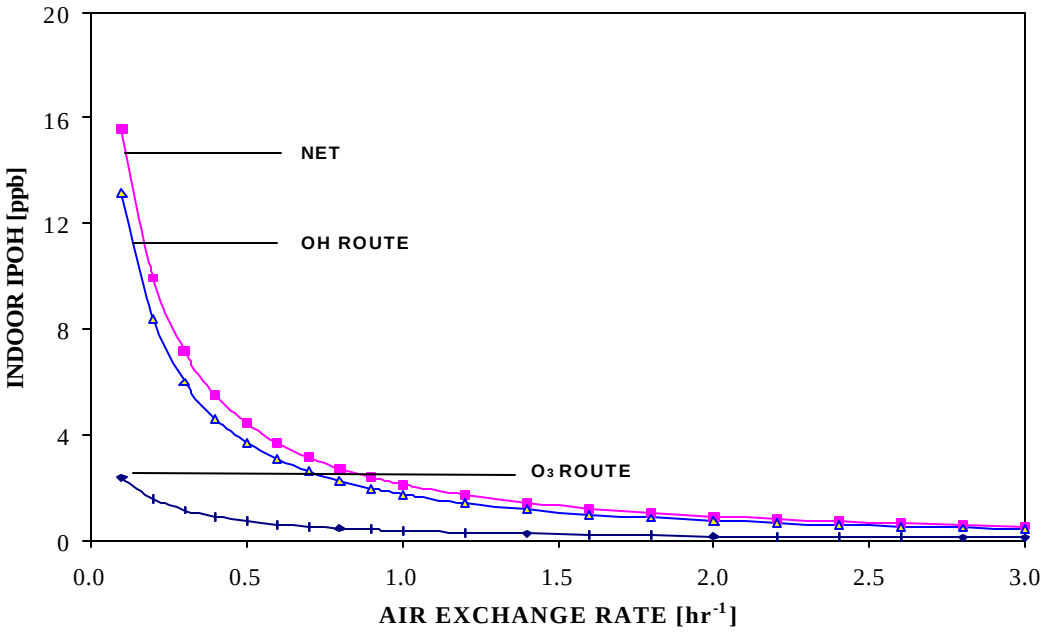

Figure 6.13. Indoor IPOH concentrations for elevated indoor limonene concentration

Formation of pinaldehyde (*PINALD*) from the reaction of* a *-pinene with O_3 and OH

Pinonaldehyde and norpinonaldehyde (PINALD in Equations 6.15, 6.37, 6.38) are low vapor pressure by-products of α-pinene reactions with O_3 and $OH^{\cdot}$. These

by-products are believed to be important intermediates in the formation of secondary organic aerosols.

In this study, the indoor emission rate of α-pinene in ICEM was increased from the base-case condition to an elevated value of 2.3 mg/min. Indoor emission rates and outdoor pollutant concentrations of other pollutants were not changed from base-case conditions. Model predictions are presented in Figure 6.14. The first curve represents the net indoor PINALD concentrations. The second and third curves represent PINALD concentrations contributed by α-pinene via $OH^{\cdot}$ and O_3 reaction pathways, respectively. The indoor PINALD concentration produced via the $OH^{\cdot}$ route was predicted to be consistently higher than that of the O_3 route.

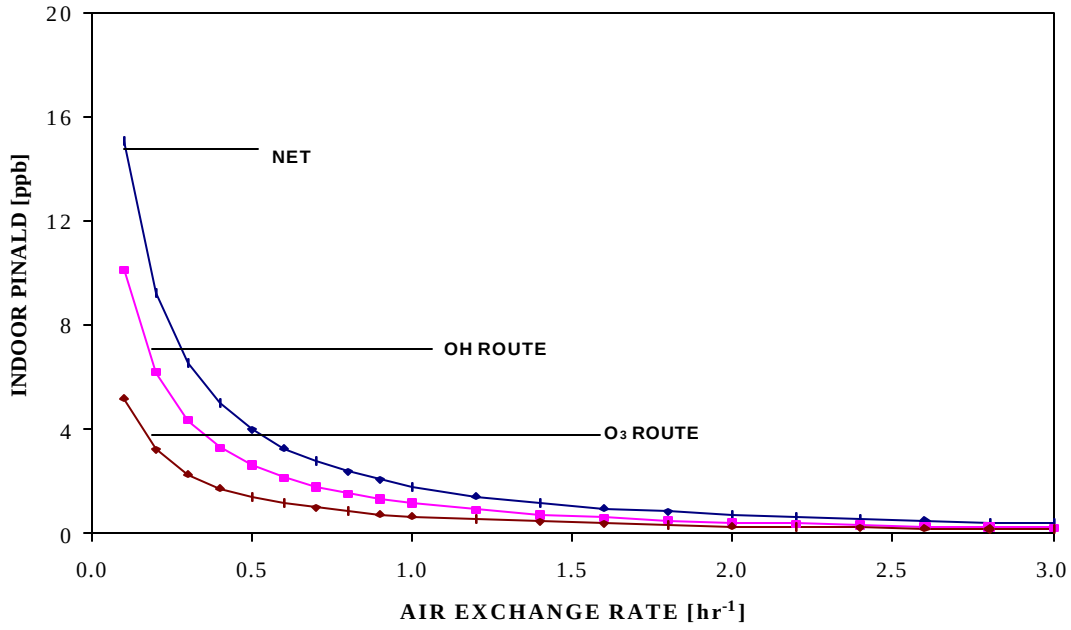

Figure 6.14. Indoor PINALD concentrations for elevated indoor a -pinene concentration

6.3 Summary

The SAPRC-99 atmospheric chemistry model was used in the development of a new indoor air quality model (ICEM) which allows for the simulation of transport

processes between indoor and outdoor environments, indoor emissions, chemical reactions, and deposition. Detailed atmospheric chemistry was incorporated into the ICEM to estimate secondary particle and $OH^{\cdot}$ concentrations in indoor environments.

An estimated base-case indoor secondary fine particle mass concentration resulting from reactions between O_3 and α-pinene is 3.7 $\mu g/m^3$. Indoor secondary particle concentrations are predicted to increase with increased outdoor O_3 levels, lower air exchange rates, increased indoor terpene emission rates, increased outdoor particle levels, and lower indoor temperatures.

A base-case scenario was defined using "reasonable" indoor emission rates and "reasonable" outdoor pollutant levels. The estimated indoor $OH^{\cdot}$ concentration for the base-case scenario was 1.2×10^5 molecules/cm^3. Indoor $OH^{\cdot}$ concentrations were predicted to be lower than typical outdoor summertime urban $OH^{\cdot}$ concentrations, but similar to or greater than typical nighttime outdoor $OH^{\cdot}$ concentrations.

Indoor $OH^{\cdot}$ concentrations were predicted to increase non-linearly with increased outdoor O_3 concentrations, air exchange rates, and indoor alkene emission rates. Indoor $OH^{\cdot}$ concentrations were predicted to decrease with increased outdoor NO concentrations. Indoor temperature and indoor light intensity were predicted to have only moderate effects on indoor $OH^{\cdot}$ concentrations. Hydroxyl radical deposition velocity, outdoor $OH^{\cdot}$ concentrations, outdoor $NO_3^{\cdot}$ concentrations, and outdoor $HO_2^{\cdot}$ concentrations were predicted to have no appreciable impact on indoor $OH^{\cdot}$ concentrations. Production of $OH^{\cdot}$ in indoor environments appears to be controlled primarily by reactions of alkenes with O_3, and NO with $HO_2^{\cdot}$.

Indoor OH· can adversely impact indoor air quality. For example, reactions of terpenes with OH· produce multifunctional (-OH, =O, and –COOH) oxidized products, some of which have low vapor pressures and contribute to fine particle growth in indoor environments. Additional research is needed to verify model predictions and the occurrence of oxidized products in actual building environments.

7.0 IMPLICATIONS OF INDOOR SECONDARY PARTICLES

7.1 General Implications

Terpenes, including α-pinene and limonene, are used as odorants and solvents in a variety of commercial products. They are also emitted from natural and engineered wood products. As such, they are commonly observed at detectable levels in most indoor environments. The reported odor thresholds of α-pinene and limonene are about 700 ppb and 440 ppb, respectively (Molhave *et al.*, 2000). Odors of pine and lemon can often be detected following application of many consumer products, indicating that indoor concentrations of pinenes and limonene indeed exceed their odor thresholds. Indoor concentrations reported in the literature have typically not been measured during the application of consumer products and are often based on long-term averaging, thereby yielding concentrations much lower than expected during applications of such products. Indoor α-pinene concentrations over 400 ppb have been reported by Brown *et al.* (1994). Indoor limonene concentrations of 175 ppb have been reported by Wainman *et al.* (2000).

Ozone typically originates outdoors and is transported indoors. Indoor O_3 levels depend on outdoor O_3 concentrations, and building design and operational parameters. However, indoor O_3 levels typically range between 20-70% of outdoor O_3 levels (Weschler, 2000). Additional sources of O_3 can occur indoors, e.g., ozone air "purifiers" and photocopy machines. The presence of ozone air “purifiers” can raise indoor O_3 levels to well over 100 ppb.

The results presented in this dissertation clearly demonstrate that homogeneous reactions between O_3 and terpenes lead to increases in fine particle mass concentrations. This increase can be significant during periods of elevated

outdoor O_3 concentrations or indoor O_3 releases, coupled with elevated terpene releases, e.g., from cleaners, deodorizers, or new wood products.

Elevated outdoor O_3 concentrations actually have a dual effect on indoor secondary particles. First, elevated outdoor O_3 concentrations can increase outdoor secondary particle concentrations via oxidation of biogenic and other atmospheric unsaturated compounds. Elevated outdoor O_3 concentrations also result in elevated outdoor $OH^{\cdot}$ levels, which in turn can produce additional outdoor secondary particles by oxidizing saturated and unsaturated organic compounds. Elevated outdoor O_3 and particle concentrations increase indoor concentrations of those pollutants. Elevated indoor O_3 levels can produce enhanced amounts of semi-volatile products via increased O_3/terpene reaction rates. These enhanced semi-volatile products can then partition into the elevated indoor "seed" particles producing additional secondary particle mass.

During elevated outdoor O_3 and high indoor α-pinene concentrations, indoor SOA concentrations of about 3-4 $\mu g/m^3$ can be produced from reactions between O_3 with α-pinene. Reactions between O_3 and limonene produce SOA mass concentrations that are approximately five times greater than via O_3/α-pinene reactions. Thus, for an indoor limonene emission rate of 2.3 mg/min (equal to that of α-pinene emissions in this study), the SOA mass concentrations resulting from O_3/limonene reactions can be 15-20 $\mu g/m^3$. If ozone air "purifiers" and elevated terpene levels are simultaneously present in indoor environments, the resulting SOA concentration can be even higher, exceeding 65 $\mu g/m^3$.

The implications of the findings presented herein, and recently published by others, are significant. It appears that under some conditions, indoor air chemistry can lead to significant increases in human exposure to fine particles. Such exposure

could be reduced by avoiding indoor sources of O_3, e.g., from O_3 generators marketed as air "purifiers", or by reducing the use of consumer products that contain terpenes, especially during the summer O_3 season.

The combination of elevated outdoor O_3 concentrations or the presence of indoor O_3 sources, low air exchange rates, high indoor terpene emission rates, and low indoor temperatures produce the highest secondary particle concentrations. Thus, the building designer/operator should avoid this combination to reduce occupant exposure to fine particles. For example, a control device for O_3 can be installed in buildings to reduce indoor O_3 concentration, which can also prevent the formation of elevated SOA concentrations. Sources of indoor terpenes, especially limonene, should be avoided to reduce indoor secondary particle levels. Buildings can be operated with higher air exchange rates in combination with enhanced particle filters. The use of high efficiency particle filters can reduce the transport of outdoor fine particles in commercial buildings, and higher air exchange rates can reduce SOA levels.

Aromatic compounds have been shown to produce a significant fraction outdoor secondary aerosol particles (Pandis *et al*., 1992). However, the contribution of aromatic compounds to indoor secondary organic aerosol compounds is expected to be small. As shown in Table 3.1, the average indoor concentration of toluene is 10 ppb compared to a value of 4 ppb for limonene. The ICEM predicted steady-state indoor O_3 and $OH^{\cdot}$ concentrations for the base-case scenario as discussed in Chapter 6 were 11 ppb and 4.67×10^{-6} ppb (1.2×10^5 molecules/cm^3), respectively. The rate constant for the reaction between toluene and $OH^{\cdot}$ is 8.8 ppb^{-1}min^{-1} at 297 K (Carter, 2000). Thus, the predicted reaction rate of indoor toluene with indoor $OH^{\cdot}$ is only about 0.4 ppt/min.

The rate constant for the reaction between limonene and OH· and for the reaction between limonene and O_3 are 2.5 x 10^2 and 2.9 x 10^{-4} ppb^{-1} min^{-1} at 297 K, respectively (Carter, 2000). Thus, the predicted reaction rate of limonene with OH·, and O_3 are 4.7 and 12.8 ppt min^{-1}, respectively. The combined reaction rate of indoor limonene with indoor OH· and indoor O_3 is 17.5 ppt min^{-1} compared to the predicted reaction rate of indoor toluene with indoor OH· of 0.4 ppt min^{-1}. Thus, the contribution of aromatic compounds to indoor secondary organic aerosol compounds are expected to be significantly smaller than that of terpenes.

7.2 Application to Houston Airshed Conditions

Houston is a designated non-attainment area for ozone. Atmospheric O_3 concentrations in Houston routinely exceed the National Ambient Air Quality Standard (NAAQS). Hourly averaged outdoor NO, NO_2, and O_3 concentrations measured at monitoring station 411 in Houston (May 25, 2001) were incorporated into the ICEM. Ambient fine particle concentrations for this monitoring station were not available; therefore, ambient fine particle concentrations from a nearby monitoring station were collected for the same day (monitoring station 15) and were incorporated into the model. Other model input parameters were kept similar to the conditions described in section 6.1, i.e., indoor α-pinene emission rate of 2.3 mg/min, air exchange rate of 0.5 hr^{-1}, O_3 deposition rate of 3.6 hr^{-1}, and particle deposition rate of 0.39 hr^{-1}. No other pollutant was assumed to be present in the indoor environment. The transport of outdoor particles provided indoor "seed" particles in the model. The predicted indoor O_3 concentrations along with outdoor O_3 concentrations are shown in Figure 7.1. The predicted indoor O_3 concentrations followed outdoor O_3 concentrations. On average, the predicted indoor O_3 concentration was only 10% of the outdoor O_3 concentration, with the lower indoor concentration due to surface removal of O_3, i.e., heterogeneous reactions.

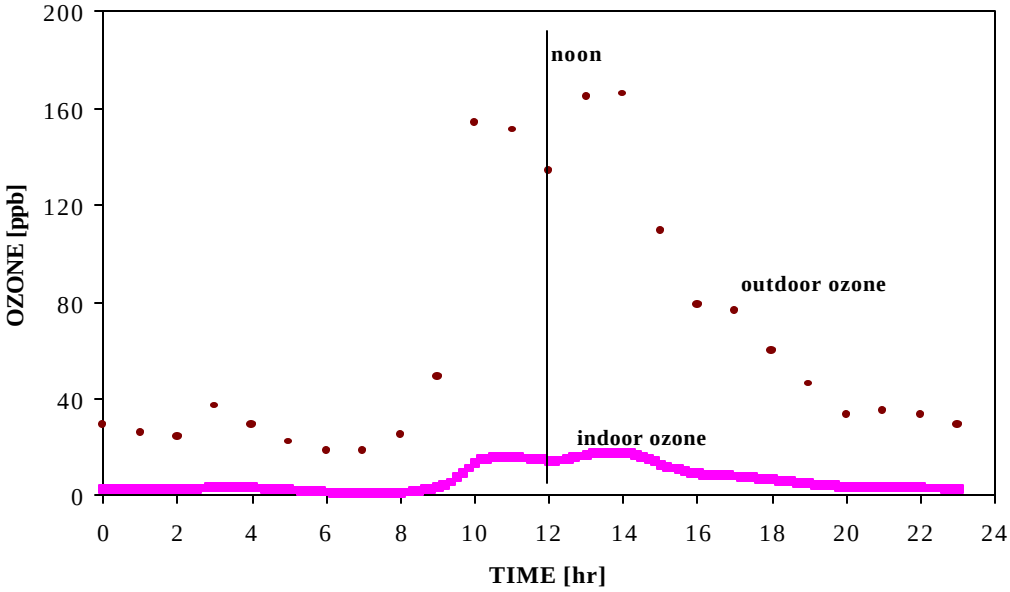

Figure 7.1. Indoor and outdoor O_3 concentrations for Houston

The predicted indoor "seed" particle, secondary particle, and outdoor particle concentrations are shown in Figure 7.2. Indoor "seed" particles are the result of the transport of outdoor particles to indoors and are lower than outdoor particle concentrations due to removal of particles to indoor surfaces. The predicted indoor secondary particle concentrations produced via the O_3/α-pinene reaction are shown in Figure 7.2, marked as "soa (α-pinene)". The predicted indoor secondary particle concentrations were low from 0 to 9:00 due to low indoor O_3 concentrations. After 09:00, indoor O_3 concentrations increased. Consequently, the predicted indoor secondary particle concentrations also increased reaching a peak level immediately after 14:00. The predicted indoor O_3 concentrations decreased after 14:00. The predicted indoor secondary particle concentrations also continuously decreased after 14:00. The predicted indoor secondary particle concentration was about 70% of the indoor "seed" particle concentration at the time of the peak indoor O_3 concentration.

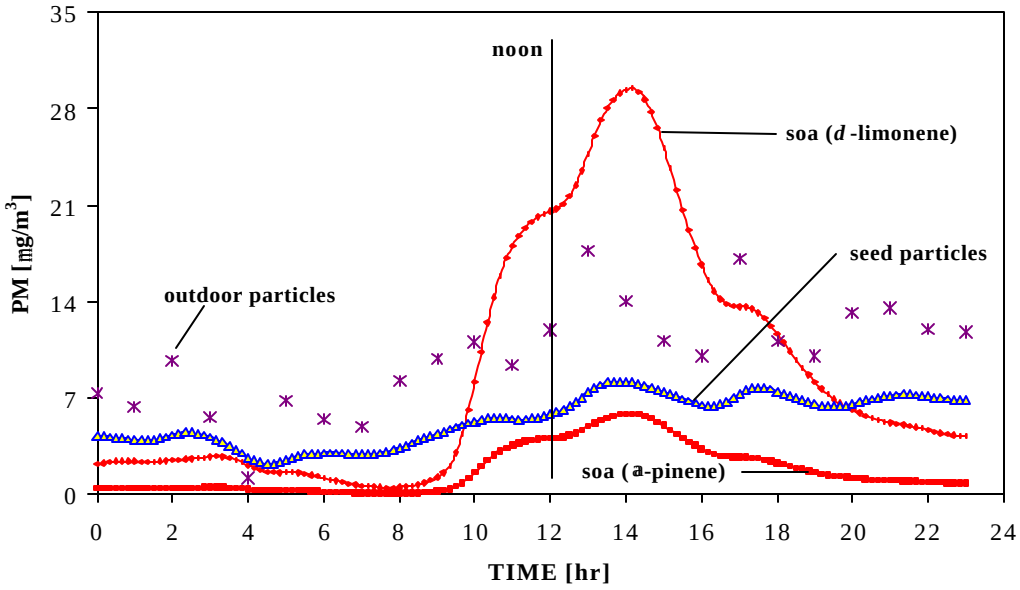

Figure 7.2. Indoor and outdoor particle concentrations for Houston

For limonene emissions identical to those for α-pinene, the indoor secondary particle concentrations were estimated by multiplying the indoor secondary particle concentrations resulting from the O_3/α-pinene reactions by a factor of five; results are shown in Figure 7.2 [marked "soa (limonene)"]. The estimated indoor secondary particle concentrations produced via the limonene/O_3 reactions were about 4 times as high as the peak indoor "seed" particle concentration. The average outdoor particle concentration for the day was 10 μg/m^3, and the average indoor "seed" particle concentration for the day was 5.5 μg/m^3. The average indoor secondary particle concentration produced via the O_3/α-pinene reactions was 1.8 μg/m^3, and the average indoor secondary particle concentration produced via the O_3/limonene reaction was 9.1 μg/m^3. Thus, the predicted daily averaged indoor secondary particle concentration resulting from the O_3/limonene reactions was 65% greater than the

average indoor "seed" particle concentration. Therefore, human exposure to indoor secondary particles, under elevated outdoor O_3 and indoor limonene concentrations, are predicted to exceed human exposure due to the transport of outdoor fine particles to indoors.

The diameters of particles resulting from O_3/terpene reactions are less than 1.0 μm, and a significant fraction are in the ultra-fine range (< 0.1 μm). These particles can penetrate deep into the human lung. Weschler (2001) suggested that hydrogen peroxide also resulting from O_3/limonene reactions can be carried to the deep lung with these particles and can cause tissue damage. Long *et al*. (2001) recently concluded that particles generated indoors may be more bioactive than particles generated outdoors. Wolkoff *et al*. (1999) and Clausen *et al*. (2001) also suggested the formation of strong airway irritants from O_3/terpene reaction mixtures. Thus, the combination of high human exposure to these particles under elevated indoor O_3 and terpene concentrations, and the potential for adverse health effects, warrant additional and immediate attention.

8.0 SUMMARY, CONCLUSIONS, AND RECOMMENDATIONS

8.1 Summary

The research described herein included experimental as well as computational investigations. Twenty-seven chamber experiments were completed to assess the effects of ozone/terpene reactions on indoor secondary organic particles. These experiments were conducted with pure α-pinene, pure limonene, and consumer products. Results of this research have significantly improved the understanding of the effects of ozone/terpene reactions on indoor secondary organic particles. Experimental results indicate that rapid particle formation/growth occurs due to homogeneous reactions between ozone and terpenes, and subsequent gas-to-particle partitioning of reaction products. Experimental results also indicate that many consumer products can emit significant amounts of terpenes that can serve as precursors to the formation/growth of indoor fine particles.

A significant contribution of this research was the prediction of dynamic particle mass concentrations based on detailed homogeneous chemical mechanisms and partitioning of semi-volatile products to particles using a new Indoor Chemistry and Exposure Model (ICEM). The ICEM allows for the simulation of air exchange processes, indoor emissions, chemical reactions, deposition, and variations in outdoor air quality. Predicted indoor secondary particle mass concentrations were in reasonable agreement with experimental results, which suggests that the model is capturing the essence of particle formation/growth processes. The effects of several key parameters on indoor secondary particle levels were studied using the ICEM. The ICEM was also applied to investigate the levels, variations, and dynamics of indoor hydroxyl radicals.

Many uncertainties remain to be resolved. For example, deposition velocities of the semi-volatile products of ozone/α-pinene reactions were assigned twice the deposition velocity of fine particles, which warrants further exploration. However, it has been shown, in principle, that it is possible to reasonably simulate complex indoor chemistry and particle formation/growth dynamics using ICEM.

Indoor air chemistry can lead to significant increases in human exposure to fine particles. Such exposure could be reduced by avoiding indoor sources of ozone, e.g., from ozone generators marketed as air "purifiers", or by reducing the use of consumer products that contain terpenes, especially during the summer ozone season.

8.2 Conclusions

The results stemming from this research led to the following conclusions:

(1) Homogeneous reactions between ozone and terpenes, such as α-pinene and limonene, lead to secondary organic aerosol formation in indoor environments.

(2) Indoor secondary organic particles may account for a large fraction of the previously reported "unexplained" particle mass in indoor environments.

(3) Under conditions of elevated ozone and terpene concentrations, secondary particle mass may dominate total occupant exposure to indoor fine particles.

(4) A significant fraction of indoor secondary particle numbers are in the ultra-fine range (< 0.1 μm). Most of the particle number and mass associated with ozone/terpene reactions is associated with particles less than 1.0 μm in diameter.

(5) Reactions between ozone and limonene produce indoor secondary particles with mass concentrations significantly greater than formed via ozone/α-pinene reactions for identical conditions. As such, reductions in indoor limonene concentrations are particularly important if indoor secondary organic particle levels are to be reduced.

(6) Lower air exchange rates increase indoor secondary particle mass concentrations. Lower air exchange rates increase the ozone/terpene reaction rates and particle residence times. The combination of higher reaction rates and longer particle residence times distributes the resulting particles into larger size ranges and increases particle mass concentrations.

(7) Lower indoor temperatures promote indoor secondary particle mass. Lower indoor temperatures increase gas-to-particle partitioning of low vapor pressure by-products of ozone/terpene reactions and increase particle mass concentrations.

(8) Indoor secondary particle mass concentrations increase with increased outdoor fine particle mass concentrations. Higher outdoor fine particle mass concentrations cause higher indoor "seed" particle concentrations, which in turn increase the partitioning of semi-volatile products and result in increased indoor secondary particle mass concentrations.

(9) Ozone generators that are marketed as indoor air "purifiers" should be avoided, as they can lead to extremely high levels of by-products including fine particles, heavy carbonyls, and carboxylic acids.

(10) Many consumer products can emit significant amounts of terpenes that can serve as precursors to the growth of indoor fine particles. This appears to be particularly true for some liquid and solid air fresheners.

(11) Indoor hydroxyl radical concentrations are likely to be lower than typical outdoor summertime urban hydroxyl radical concentrations, but can be similar to or greater than typical nighttime outdoor hydroxyl radical concentrations.

(12) Indoor hydroxyl radical concentrations increase non-linearly with increased outdoor ozone concentrations, air exchange rates, and indoor alkene emission rates, and decrease with outdoor nitric oxide concentrations.

(13) Indoor temperature and indoor light intensity have only moderate effects on indoor hydroxyl radical concentrations, while hydroxyl radical deposition velocity, outdoor hydroxyl radical concentrations, outdoor nitrate concentrations, and outdoor hydroperoxy radical concentrations are predicted to have no appreciable impact on indoor hydroxyl radical concentrations.

(14) Production of hydroxyl radicals in indoor environments appears to be controlled primarily by reactions of alkenes with ozone, and nitric oxide with hydroperoxy radical.

(15) Indoor air chemistry is important and should be considered during investigations of indoor air quality; secondary products of chemical reactions may be irritating to building occupants and may play a role in sick building syndrome.

8.3 Recommendations for Future Research

Results of this research have enhanced the current knowledge base related to indoor chemistry leading to indoor secondary particles and free radicals. However, it has also generated the need for further research on the following issues:

(1) Particle nucleation/growth during the initial phase of reactions should be further explored using particle size analyzers that can measure much finer size distributions.

(2) Simultaneous measurements of indoor and outdoor ozone, fine particles, and terpenes in cities with high outdoor ozone levels, e.g., Houston, are recommended.

(3) Two terpenes were investigated in this study. Other terpenes can also be present in indoor environments. Studies should be completed to evaluate the impact of other terpenes on indoor fine particle levels.

(4) Reactions between ozone and terpenes can also produce gas phase aldehydes, ketones, and acids. Studies are recommended to evaluate gas-phase indoor concentrations of these pollutants under controlled chamber and field experiments.

(5) Particle chemical reaction mechanisms for a number of aromatic compounds in the outdoor photochemical atmosphere have recently become available. It is recommended that these reaction mechanisms be incorporated into ICEM to evaluate their impacts on indoor fine particle concentrations.

(6) Indoor deposition velocity data are limited, a fact that has been an impediment to the development of indoor air quality models. Studies are recommended to develop a comprehensive database of deposition velocities for common pollutants in indoor environments.

(7) The study focused entirely on homogeneous reactions and associated by-products. Additional research is needed to better understand the role of heterogeneous reactions and associated by-products on indoor air chemistry.

APPENDIX A
Gas Phase Chemistry in the ICEM

NOTE:
'k' is the rate constant. Units are either in ppm^{-1} min^{-1} or min^{-1}
Reactions that contain "HV" are photolytic reactions. Absorption cross-section and quantum yields of the photolysis are given in the files assigned by PHOT.

No.	k	Reactions
1)	PHOT = NO2	NO2 + HV = NO + O3P
2)	2.040E-05	O3P + O2 + M = O3 + M
3)	1.223E+01	O3P + O3 = #2 O2
4)	3.591E-03	O3P + NO + M = NO2 + M
5)	1.422E+04	O3P + NO2 = NO + O2
6)	2.628E+03	O3P + NO2 = NO3 + M
8)	2.748E+01	O3 + NO = NO2 + O2
9)	5.463E-02	O3 + NO2 = O2 + NO3
10)	3.815E+04	NO + NO3 = #2 NO2
11)	6.932E-10	NO + NO + O2 = #2 NO2
12)	2.248E+03	NO2 + NO3 = N2O5
13)	4.047E+00	N2O5 = NO2 + NO3
14)	3.817E-07	N2O5 + H2O = #2 HNO3
17)	9.903E-01	NO2 + NO3 = NO + NO2 + O2
18)	PHOT=NO3NO	NO3 + HV = NO + O2
19)	PHOT=NO3NO2	NO3 + HV = NO2 + O3P
20)	PHOT=O3O3P	O3 + HV = O3P + O2
21)	PHOT=O3O1D	O3 + HV = O*1D2 + O2
22)	3.229E+05	O*1D2 + H2O = #2 HO.
23)	4.212E+04	O*1D2 + M = O3P + M
24)	1.073E+04	HO. + NO = HONO
25)	PHOT=HONO-NO	HONO + HV = HO. + NO
26)	PHOT=HONO-NO2	HONO + HV = HO2. + NO2
27)	9.434E+03	HO. + HONO = H2O + NO2
28)	1.294E+04	HO. + NO2 = HNO3
29)	2.936E+04	HO. + NO3 = HO2. + NO2
30)	2.115E+02	HO. + HNO3 = H2O + NO3
31)	PHOT=HNO3	HNO3 + HV = HO. + NO2
32)	3.054E+02	HO. + CO = HO2. + CO2
33)	9.953E+01	HO. + O3 = HO2. + O2
34)	1.228E+04	HO2. + NO = HO. + NO2
35)	2.003E+03	HO2. + NO2 = HNO4
36)	5.764E+00	HNO4 = HO2. + NO2
37)	PHOT=HO2NO2	HNO4 + HV = #.61{HO2.+NO2} + #.39{HO. + NO3}
38)	7.306E+03	HNO4 + HO. = H2O + NO2 + O2
39)	2.783E+00	HO2. + O3 = HO. + #2 O2
40A)	4.126E+03	HO2. + HO2. = HO2H + O2
40B)	2.163E-01	HO2. + HO2. + H2O = HO2H + O2 + H2O
41)	5.872E+03	NO3 + HO2.=#.8{HO.+NO2 + O2}+#.2 {HNO3 +O2}
42)	3.541E-01	NO3 + NO3 = #2 NO2 + O2

43) PHOT=H2O2 HO2H + HV = #2 HO.
44) 2.497E+03 HO2H + HO. = HO2. + H2O
45) 1.622E+05 HO. + HO2. = H2O + O2
S2OH) 1.419E+03 HO. + SO2 = HO2. + SULF
H2OH) 1.031E+01 HO. + H2 = HO2. + H2O
MER1) 1.062E+04 C-O2. + NO = NO2 + HCHO + HO2.
MER4) 7.510E+03 C-O2. + HO2. = COOH + O2
MEN3) 1.908E+03 C-O2. + NO3 = HCHO + HO2. + NO2
MER5) 3.828E+02 C-O2. + C-O2. = MEOH + HCHO + O2
MER6) 1.589E+02 C-O2. + C-O2. = #2 {HCHO + HO2.}
RRNO) 1.315E+04 RO2-R. + NO = NO2 + HO2.
RRH2) 2.124E+04 RO2-R. + HO2. = ROOH + O2 + #-3 XC
RRN3) 3.376E+03 RO2-R. + NO3 = NO2 + O2 + HO2.
RRME) 2.936E+02 RO2-R. + C-O2. = HO2. + #.75 HCHO + #.25 MEOH
RRR2) 5.138E+01 RO2-R. + RO2-R. = HO2.
R2NO) K SAME AS RXN RRNO R2O2. + NO = NO2
R2H2) K SAME AS RXN RRH2 R2O2. + HO2. = HO2.
R2N3) K SAME AS RXN RRN3 R2O2. + NO3 = NO2
R2ME) K SAME AS RXN RRME R2O2. + C-O2. = C-O2.
R2RR) K SAME AS RXN RRR2 R2O2. + RO2-R. = RO2-R.
R2R3) K SAME AS RXN RRR2 R2O2. + R2O2. =
RNNO)K SAME AS RXN RRNO RO2-N. + NO = RNO3
RNH2) K SAME AS RXN RRH2 RO2-N. + HO2. = ROOH + #3 XC
RNME)K SAME AS RXN RRME RO2-N. + C-O2. = HO2. + #.25 MEOH + #.5 {MEK + PROD2} + #.75 HCHO + XC
RNN3) K SAME AS RXN RRN3 RO2-N. + NO3 = NO2 + O2 + HO2. + MEK + #2 XC
RNRR) K SAME AS RXN RRR2 RO2-N. + RO2-R. = HO2. + #.5 {MEK + PROD2} + O2 + XC
RNR2) K SAME AS RXN RRR2 RO2-N. + R2O2. = RO2-N.
RNRN) K SAME AS RXN RRR2 RO2-N. + RO2-N. = MEK + HO2. + PROD2 + O2 + #2 XC
APN2) 1.526E+04 CCO-O2. + NO2 = PAN
DPAN) 4.226E-02 PAN = CCO-O2. + NO2
APNO) 3.111E+04 CCO-O2. + NO = C-O2. + CO2 + NO2
APH2) 2.023E+04 CCO-O2. + HO2. = #.75 {CCO-OOH +O2} + #.25 {CCO-OH + O3}
APN3) 5.872E+03 CCO-O2. + NO3 = C-O2. + CO2 + NO2 + O2
APME) 1.400E+04 CCO-O2. + C-O2. = CCO-OH + HCHO + O2
APRR) 1.101E+04 CCO-O2. + RO2-R. = CCO-OH
APR2) K SAME AS RXN APRR CCO-O2. + R2O2. = CCO-O2.
APRN) K SAME AS RXN APRR CCO-O2. + RO2-N. = CCO-OH + PROD2
APAP) 2.255E+04 CCO-O2.+CCO-O2.= #2{C-O2. + CO2}+ O2
PPN2) 1.761E+04 RCO-O2. + NO2 = PAN2
PAN2) 3.543E-02 PAN2 = RCO-O2. + NO2
PPNO) 4.084E+04 RCO-O2. + NO = NO2 + CCHO + RO2-R. + CO2

PPH2) K SAME AS RXN APH2 RCO-O2. + HO2. = #.75 {RCO-OOH + O2} + #.25 {RCO-OH + O3}
PPN3) K SAME AS RXN APN3 RCO-O2. + NO3 = NO2 + CCHO + RO2-R. + CO2 + O2
PPME) K SAME AS RXN APME RCO-O2. + C-O2. = RCO-OH + HCHO + O2
PPRR) K SAME AS RXN APRR RCO-O2. + RO2-R. = RCO-OH + O2
PPR2) K SAME AS RXN APRR RCO-O2. + R2O2. = RCO-O2.
PPRN) K SAME AS RXN APRR RCO-O2. + RO2-N. = RCO-OH + PROD2 + O2
PPAP) K SAME AS RXN APAP RCO-O2. + CCO-O2. = #2 CO2 + C-O2. + CCHO + RO2-R. + O2
PPPP) K SAME AS RXN APAP RCO-O2.+ RCO-O2.= #2 {CCHO + RO2-R. + CO2}
BPN2) 2.011E+04 BZCO-O2. + NO2 = PBZN
BPAN) 2.562E-02 PBZN = BZCO-O2. + NO2
BPNO) K SAME AS RXN PPNO BZCO-O2. + NO = NO2 + CO2 + BZ-O. + R2O2.
BPH2) K SAME AS RXN APH2 BZCO-O2. + HO2. = #.75 {RCO-OOH + O2} + #.25 {RCO-OH + O3} + #4 XC
BPN3) K SAME AS RXN APN3 BZCO-O2. + NO3 = NO2 + CO2 + BZ-O. + R2O2. + O2
BPME) K SAME AS RXN APME BZCO-O2. + C-O2. = RCO-OH + HCHO + O2 + #4 XC
BPRR) K SAME AS RXN APRR BZCO-O2. + RO2-R. = RCO-OH + O2 + #4 XC
BPR2) K SAME AS RXN APRR BZCO-O2. + R2O2. = BZCO-O2.
BPRN) K SAME AS RXN APRR BZCO-O2. + RO2-N. = RCO-OH + PROD2 + O2 + #4 XC
BPAP) K SAME AS RXN APAP BZCO-O2. + CCO-O2. = #2 CO2 + C-O2. + BZ-O. + R2O2.
BPPP) K SAME AS RXN APAP BZCO-O2. + RCO-O2. = #2 CO2 + CCHO + RO2-R. + BZ-O. + R2O2.
BPBP) SAME AS RXN APAP BZCO-O2. + BZCO-O2. = #2 {BZ-O. + R2O2. + CO2}
MPN2) K SAME AS RXN PPN2 MA-RCO3. + NO2 = MA-PAN
MPPN) 2.876E-02 MA-PAN = MA-RCO3. + NO2
MPNO) K SAME AS RXN PPNO MA-RCO3. + NO = NO2 + CO2 + HCHO + CCO-O2.
MPH2) K SAME AS RXN APH2 MA-RCO3. + HO2. = #.75 {RCO-OOH + O2} + #.25 {RCO-OH + O3} + XC
MPN3) K SAME AS RXN APN3 MA-RCO3. + NO3 = NO2 + CO2 + HCHO + CCO-O2. + O2
MPME) K SAME AS RXN APME MA-RCO3. + C-O2. = RCO-OH + HCHO + XC + O2
MPRR) K SAME AS RXN APRR MA-RCO3. + RO2-R. = RCO-OH + XC
MPR2) K SAME AS RXN APRR MA-RCO3. + R2O2. = MA-RCO3.
MPRN) K SAME AS RXN APRR MA-RCO3. + RO2-N. = #2 RCO-OH + O2 + #4 XC
MPAP) K SAME AS RXN APAP MA-RCO3. + CCO-O2. = #2 CO2 + C-O2. + HCHO + CCO-O2. + O2
MPPP) K SAME AS RXN APAP MA-RCO3. + RCO-O2. = HCHO + CCO-O2. + CCHO + RO2-R. + #2 CO2
MPBP) K SAME AS RXN APAP MA-RCO3. + BZCO-O2. = HCHO + CCO-O2. + BZ-O. + R2O2. + #2 CO2

```
MPMP) K SAME AS RXN APAP MA-RCO3. + MA-RCO3. = #2 {HCHO +
                                  CCO-O2. + CO2}
TBON) 3.523E+04                  TBU-O. + NO2 = RNO3 + #-2 XC
TBOD) 7.108E+04                  TBU-O. = ACET + C-O2.
BRN2)  5.566E+04                 BZ-O. + NO2 = NPHE
BRH2)  K SAME AS RXN RRH2        BZ-O. + HO2. = PHEN
BRXX) 6.000E-02                  BZ-O. = PHEN
BNN2)  K SAME AS RXN BRN2        BZ(NO2)-O. + NO2 = #2 XN + #6 XC
BNH2)  K SAME AS RXN RRH2        BZ(NO2)-O. + HO2. = NPHE
BNXX) K SAME AS RXN BRXX         BZ(NO2)-O. = NPHE
FAHV)  PHOT=HCHO_R               HCHO + HV = #2 HO2. + CO
FAVS)  PHOT=HCHO_M               HCHO + HV = H2 + CO
FAOH)  1.350E+04                 HCHO + HO. = HO2. + CO + H2O
FAH2)  1.144E+02                 HCHO + HO2. = HOCOO.
FAHR)  1.060E+04                 HOCOO. = HO2. + HCHO
FAHN)  SAME AS RXN MER1          HOCOO. + NO = HCOOH + NO2 + HO2.
FAN3)  8.895E-01                 HCHO + NO3 = HNO3 + HO2. + CO
AAOH)  2.310E+04                 CCHO + HO. = CCO-O2. + H2O
AAHV)  PHOT=CCHO_R               CCHO + HV = CO + HO2. + C-O2.
AAN3)  4.172E+00                 CCHO + NO3 = HNO3 + CCO-O2.
PAOH)  2.936E+04                 RCHO + HO. =  #.034 RO2-R. + #.001 RO2-N. +
                                   #.965 RCO-O2. + #.034 CO + #.034 CCHO +
                                   #-0.003 XC
PAHV)  PHOT=C2CHO                RCHO + HV = CCHO + RO2-R. + CO + HO2.
PAN3)  5.605E+00                 RCHO + NO3 = HNO3 + RCO-O2.
K3OH)  2.855E+02                 ACET + HO. = HCHO + CCO-O2. + R2O2.
K3HV)  PHOT=ACETONE              ACET + HV = CCO-O2. + C-O2.
K4OH)  1.755E+03                 MEK + HO. = #.37 RO2-R. + #.042 RO2-N. +
                                   #.616 R2O2. + #.492 CCO-O2. + #.096 RCO-O2. +
                                  #.115 HCHO + #.482 CCHO + #.37 RCHO +  #.287 XC
K4HV) PHOT=KETONE                MEK + HV = CCO-O2. + CCHO + RO2-R.
MeOH)  1.371E+03                 MEOH + HO. = HCHO + HO2.
MER9)  8.025E+03                 COOH + HO. = H2O + #.35 {HCHO + HO.} + #.65 C-O2.
MERA)  PHOT=COOH                 COOH + HV = HCHO + HO2. + HO.
LPR9)  1.615E+04                 ROOH + HO. = H2O + RCHO + #.34 RO2-R. + #.66 HO.
LPRA)  PHOT=COOH                 ROOH + HV = RCHO + HO2. + HO.
GLHV) PHOT=GLY_R                 GLY + HV = #2 {CO + HO2.}
GLVM) PHOT=GLY_ABS               GLY + HV = HCHO + CO
GLOH) 1.615E+04                  GLY + HO. = #.63 HO2. + #1.26 CO +
                                                #.37 RCO-O2. + #-.37 XC
GLN3)  1.493E+00                 GLY + NO3 = HNO3 + #.63 HO2. + #1.26 CO +
                                              #.37 RCO-O2. + #-.37 XC
MGHV) PHOT=MGLY_ADJ              MGLY + HV = HO2. + CO + CCO-O2.
MGOH)  2.202E+04                 MGLY + HO. = CO + CCO-O2.
MGN3)  3.716E+00                 MGLY + NO3 = HNO3 + CO + CCO-O2.
BAHV)  PHOT=BACL_ADJ             BACL + HV = #2 CCO-O2.
```

```
PHOH)   3.861E+04          PHEN + HO. = #.24 BZ-O. + #.76 RO2-R. +
                                 #.23 GLY + #4.1 XC
PHN3)   5.549E+03          PHEN + NO3 = HNO3 + BZ-O.
CROH)   6.165E+04          CRES + HO. = #.24 BZ-O. + #.76 RO2-R. +
                                 #.23 MGLY + #4.87 XC
CRN3)   2.011E+04          CRES + NO3 = HNO3 + BZ-O. + XC
NPN3)   K SAME AS RXN PHN3 NPHE + NO3 = HNO3 + BZ(NO2)-O.
BZOH)   1.894E+04          BALD + HO. = BZCO-O2.
BZHV)   PHOT=BZCHO         BALD + HV = #7 XC
BZNT)   4.007E+00          BALD + NO3 = HNO3 + BZCO-O2.
MAOH) 4.911E+04            METHACRO + HO. = #.5 RO2-R. + #.416 CO +
                             #.084 HCHO + #.416 MEK + #.084 MGLY +
                             #.5 MA-RCO3. + #-0.416 XC
MAO3) 1.740E-03            METHACRO + O3 = #.008 HO2. + #.1 RO2-R. +
                             #.20 HO. + #.1 RCO-O2. + #.45 CO + #.117 CO2 +
                             #.2 HCHO + #.9 MGLY + #.333 HCOOH + #-0.1 XC
MAN3)   6.984E+00          METHACRO + NO3 = #.5 {HNO3 + RO2-R. + CO +
                             MA-RCO3.} + #1.5 XC + #.5 XN
MAOP)   9.306E+03          METHACRO + O3P = RCHO + XC
MAHV)   PHOT=ACROLEIN      METHACRO + HV = #.34 HO2. + #.33 RO2-R. +
                                 #.33 HO. + #.67 CCO-O2. + #.67 CO + #.67 HCHO +
                               #.33 MA-RCO3. + #-0 XC
MVOH)   2.750E+04          MVK + HO. = #.3 RO2-R. + #.025 RO2-N. +
                             #.675 R2O2. + #.675 CCO-O2. + #.3 HCHO +
                             #.675 RCHO + #.3 MGLY + #-0.725 XC
MVO3)   6.955E-03          MVK + O3 = #.064 HO2. + #.05 RO2-R. + #.16 HO. +
                             #.05 RCO-O2. + #.475 CO + #.124 CO2 + #.1 HCHO +
                             #.95 MGLY + #.351 HCOOH + #-0.05 XC
MVOP)   6.341E+03          MVK + O3P = #.45 RCHO + #.55 MEK + #.45 XC
MVHV)   PHOT=ACROLEIN      MVK + HV = #.3 C-O2. + #.7 CO + #.7 PROD2 +
                               #.3 MA-RCO3. + #-2.4 XC
IPOH)   9.086E+04          ISO-PROD + HO. = #.67 RO2-R. + #.041 RO2-N. +
                             #.289 MA-RCO3. + #.336 CO + #.055 HCHO +
                             #.129 CCHO + #.013 RCHO + #.15 MEK +
                             #.332 PROD2 + #.15 GLY + #.174 MGLY + #-0.504 XC
IPO3)   6.136E-03          ISO-PROD + O3 = #.4 HO2. + #.048 RO2-R. +
                             #.048 RCO-O2. + #.285 HO. + #.498 CO + #.14 CO2 +
                             #.125 HCHO + #.047 CCHO + #.21 MEK +
                             #.023 GLY + #.742 MGLY + #.1 HCOOH +
                             #.372 RCO-OH + #-.33 XC
IPN3)   1.468E+02          ISO-PROD + NO3 = #.799 RO2-R. + #.051 RO2-N. +
                             #.15 MA-RCO3. + #.572 CO + #.15 HNO3 +
                             #.227 HCHO + #.218 RCHO + #.008 MGLY +
                             #.572 RNO3 + #.28 XN + #-.815 XC
IPHV) PHOT=ACROLEIN        ISO-PROD + HV = #1.233 HO2. + #.467 CCO-O2. +
                             #.3 RCO-O2. + #1.233 CO + #.3 HCHO +
```

```
                                  #.467 CCHO + #.233 MEK + #-.233 XC
K6OH)   2.202E+04          PROD2 + HO. = #.379 HO2. + #.473 RO2-R. +
                             #.07 RO2-N. + #.029 CCO-O2. + #.049 RCO-O2. +
                             #.213 HCHO + #.084 CCHO + #.558 RCHO +
                             #.115 MEK + #.329 PROD2 + #.886 XC
K6HV)  PHOT=KETONE    PROD2 + HV = #.96 RO2-R. + #.04 RO2-N. +
                             #.515 R2O2. + #.667 CCO-O2. + #.333 RCO-O2. +
                             #.506 HCHO + #.246 CCHO + #.71 RCHO + #.299 XC
RNOH)   1.145E+04          RNO3 + HO. = #.338 NO2 + #.113 HO2. +
                             #.376 RO2-R. + #.173 RO2-N. + #.596 R2O2. +
                             #.01 HCHO + #.439 CCHO + #.213 RCHO +
                             #.006 ACET + #.177 MEK + #.048 PROD2 +
                             #.31 RNO3 + #.351 XN + #.56 XC
RNHV) PHOT=IC3ONO2    RNO3 + HV = NO2 + #.341 HO2. + #.564 RO2-R. +
                             #.095 RO2-N. + #.152 R2O2. + #.134 HCHO +
                             #.431 CCHO + #.147 RCHO + #.02 ACET +
                             #.243 MEK + #.435 PROD2 + #.35 XC
D1OH)   7.340E+04          DCB1 + HO. = RCHO + RO2-R. + CO
D1O3)   2.936E-03          DCB1 + O3 = #1.5 HO2. + #.5 HO. + #1.5 CO +
                             #.5 CO2 + GLY
D2OH)   7.340E+04          DCB2 + HO. = R2O2. + RCHO + CCO-O2.
D2HV)   PHOT=MGLY_ABS  DCB2 + HV = RO2-R. + #.5 {CCO-O2. + HO2.} +
                             CO + R2O2. + #.5 {GLY + MGLY + XC}
D3OH) 7.340E+04            DCB3 + HO. = R2O2. + RCHO + CCO-O2.
D3HV) PHOT=ACROLEIN DCB3 + HV = RO2-R. + #.5 {CCO-O2. + HO2.} + CO +
                             R2O2. + #.5 {GLY + MGLY + XC}
E1OH)   9.712E+00          CH4 + HO. = H2O + C-O2.
ETOH)   1.238E+04          ETHENE + HO. = RO2-R. + #1.61 HCHO + #.195 CCHO
ETO3)   2.470E-03          ETHENE + O3 = #.18 HO. + #.12 HO2. + #.5 CO +
                             #.13 CO2 + HCHO + #.37 HCOOH
ETN3)   3.202E-01          ETHENE + NO3 = RO2-R. + RCHO + #-1 XC + XN
ETOA)  1.089E+03           ETHENE + O3P = #.5 HO2. + #.2 RO2-R. + #.3 C-O2. +
                             #.491 CO + #.191 HCHO + #.25 CCHO +
                             #.009 GLY + #.5 XC
ISOH)   1.428E+05          ISOPRENE + HO. = #.907 RO2-R. + #.093 RO2-N. +
                             #.079 R2O2. + #.624 HCHO + #.23 METHACRO +
                             #.32 MVK + #.357 ISO-PROD + #-0.167 XC
ISO3)   1.967E-02          ISOPRENE + O3 = #.25 HO. + #.066 RO2-R. +
                             #.008 RO2-N. + #.126 R2O2. + #.192 MA-RCO3. +
                             #.275 CO + #.122 CO2 + #.592 HCHO + #.1 PROD2 +
                             #.39 METHACRO + #.16 MVK + #.204 HCOOH +
                             #.15 RCO-OH + #-0.259 XC
ISN3)   9.995E+02          ISOPRENE + NO3 = #.187 NO2 + #.749 RO2-R. +
                             #.064 RO2-N. + #.187 R2O2. + #.936 ISO-PROD +
                             #-0.064 XC + #.813 XN
ISOP)   5.284E+04          ISOPRENE + O3P = #.01 RO2-N. + #.24 R2O2. +
```

```
                    #.25 C-O2. + #.24 MA-RCO3. + #.24 HCHO +
                    #.75 PROD2 + #-1.01 XC
NH3H)  2.334E+02    NH3 + HO. = NH2. + H2O
L001)  3.821E+02    ETHANE + HO. = RO2-R. + CCHO
L002)  1.678E+03    PROPANE + HO. = #.965 RO2-R. + #.035 RO2-N. +
                    #.261 RCHO + #.704 ACET + #-0.104 XC
L003)  3.617E+03    N-C4 + HO. = #.921 RO2-R. + #.079 RO2-N. +
                    #.413 R2O2. + #.632 CCHO + #.12 RCHO +
                    #.485 MEK + #-0.038 XC
L004)  5.947E+03    N-C5 + HO. = #.855 RO2-R. + #.145 RO2-N. +
                    #.65 R2O2. + #.147 CCHO + #.22 RCHO +
                    #.238 MEK + #.397 PROD2 + #-0.157 XC
L005)  8.056E+03    N-C6 + HO. = #.775 RO2-R. + #.225 RO2-N. +
                    #.787 R2O2. + #.011 CCHO + #.113 RCHO +
                    #.688 PROD2 + #.162 XC
L006)  1.033E+04    N-C7 + HO. = #.705 RO2-R. + #.295 RO2-N. +
                    #.799 R2O2. + #.055 RCHO + #.659 PROD2 + #1.11 XC
L007)  1.283E+04    N-C8 + HO. = #.646 RO2-R. + #.354 RO2-N. +
                    #.786 R2O2. + #.024 RCHO + #.622 PROD2 + #2.073 XC
L008)  1.471E+04    N-C9 + HO. = #.602 RO2-R. + #.398 RO2-N. +
                    #.777 R2O2. + #.018 RCHO + #.584 PROD2 + #3.055 XC
L009)  1.657E+04    N-C10 + HO. = #.572 RO2-R. + #.428 RO2-N. +
                    #.772 R2O2. + #.015 RCHO + #.557 PROD2 + #4.045 XC
L010)  1.894E+04    N-C11 + HO. = #.553 RO2-R. + #.447 RO2-N. +
                    #.771 R2O2. + #.013 RCHO + #.54 PROD2 + #5.038 XC
L011)  2.040E+04    N-C12 + HO. = #.542 RO2-R. + #.458 RO2-N. +
                    #.768 R2O2. + #.011 RCHO + #.53 PROD2 + #6.034 XC
L012)  2.349E+04    N-C13 + HO. = #.535 RO2-R. + #.465 RO2-N. +
                    #.766 R2O2. + #.01 RCHO + #.525 PROD2 + #7.03 XC
L013)  2.642E+04    N-C14 + HO. = #.53 RO2-R. + #.47 RO2-N. +
                    #.765 R2O2. + #.009 RCHO + #.521 PROD2 + #8.027 XC
L014)  3.083E+04    N-C15 + HO. = #.527 RO2-R. + #.473 RO2-N. +
                    #.764 R2O2. + #.008 RCHO + #.519 PROD2 + #9.025 XC
L081)  1.065E+04    CYCC6 + HO. = #.799 RO2-R. + #.201 RO2-N. +
                    #.473 R2O2. + #.203 RCHO + #.597 PROD2 + #.608 XC
AS06)  2.131E+02    CL2-ME + HO. = RO2-R. + #.5 HCHO + #.5 RCHO
AS08)  1.550E+02    CHCL3 + HO. = RO2-R. + #.5 HCHO + #.5 RCHO
AS13)  1.814E+01    111-TCE + HO. = RO2-R. + #.5 HCHO + #.5 RCHO
L118)  4.806E+03    ETOH + HO. = #.95 HO2. + #.05 RO2-R. +
                    #.081 HCHO + #.96 CCHO
L119)  7.807E+03    I-C3-OH + HO. = #.953 HO2. + #.046 RO2-R. +
                    #.001 RO2-N. + #.046 HCHO + #.046 CCHO +
                    #.953 ACET + #-0.003 XC
L170)  3.773E+04    BUO-ETOH + HO. = #.888 RO2-R. + #.112 RO2-N. +
                    #.133 R2O2. + #.55 HCHO + #.013 CCHO +
                    #.318 RCHO + #.508 MEK + #.26 PROD2 + #.211 XC
```

AR01) 1.820E+03 BENZENE + HO. = #.236 HO2. + #.764 RO2-R. + #.207 GLY + #.236 PHEN + #.764 DCB1 + #1.114 XC

AR02) 8.669E+03 TOLUENE + HO. = #.234 HO2. + #.758 RO2-R. + #.008 RO2-N. + #.116 GLY + #.135 MGLY + #.234 CRES + #.085 BALD + #.46 DCB1 + #.156 DCB2 + #.057 DCB3 + #1.178 XC

AR03) 1.042E+04 C2-BENZ + HO. = #.19 HO2. + #.786 RO2-R. + #.024 RO2-N. + #.239 PROD2 + #.094 GLY + #.109 MGLY + #.19 CRES + #.498 DCB1 + #.049 DCB3 + #2.338 XC

AR04) 2.011E+04 O-XYLENE + HO. = #.161 HO2. + #.831 RO2-R. + #.008 RO2-N. + #.084 GLY + #.238 MGLY + #.139 BACL + #.161 CRES + #.054 BALD + #.572 DCB1 + #.06 DCB2 + #.145 DCB3 + #1.697 XC

AR05) 3.464E+04 M-XYLENE + HO. = #.21 HO2. + #.782 RO2-R. + #.008 RO2-N. + #.107 GLY + #.335 MGLY + #.21 CRES + #.037 BALD + #.347 DCB1 + #.29 DCB2 + #.108 DCB3 + #1.628 XC

AR06) 2.099E+04 P-XYLENE + HO. = #.188 HO2. + #.804 RO2-R. + #.008 RO2-N. + #.195 GLY + #.112 MGLY + #.188 CRES + #.083 BALD + #.709 DCB1 + #.012 DCB3 + #2.432 XC

AR08) 4.771E+04 124-TMB + HO. = #.186 HO2. + #.804 RO2-R. + #.01 RO2-N. + #.063 GLY + #.364 MGLY + #.079 BACL + #.186 CRES + #.044 BALD + #.733 DCB1 + #.027 DCB3 + #2.73 XC

AR09) 8.440E+04 135-TMB + HO. = #.186 HO2. + #.804 RO2-R. + #.01 RO2-N. + #.621 MGLY + #.186 CRES + #.025 BALD + #.569 DCB1 + #.097 DCB2 + #.114 DCB3 + #2.273 XC

AR15) 8.147E+02 CL2-BEN + HO. = #.236 HO2. + #.764 RO2-R. + #.207 GLY + #.236 PHEN + #.764 DCB1 + #1.114 XC

AR19) 9.541E+03 I-C3-BEN + HO. = #.19 HO2. + #.786 RO2-R. + #.024 RO2-N. + #.239 PROD2 + #.094 GLY + #.109 MGLY + #.19 CRES + #.498 DCB1 + #.049 DCB3 + #3.338 XC

A001) 3.823E+04 PROPENE + HO. = #.984 RO2-R. + #.016 RO2-N. + #.984 HCHO + #.984 CCHO + #-0.048 XC

A002) 1.546E-02 PROPENE + O3 = #.35 HO. + #.06 HO2. + #.26 C-O2. + #.51 CO + #.135 CO2 + #.5 HCHO + #.5 CCHO + #.185 HCOOH + #.17 CCO-OH + #.07 INERT + #.07 XC

A003) 1.429E+01 PROPENE + NO3 = #.949 RO2-R. + #.051 RO2-N. + #2.693 XC + XN

A004) 5.881E+03 PROPENE + O3P = #.45 RCHO + #.55 MEK + #-0.55 XC

A069) 7.464E+04 ISOBUTEN + HO. = #.9 RO2-R. + #.1 RO2-N. +

#.9 HCHO + #.9 ACET + #-0.2 XC

A070) 1.720E-02 ISOBUTEN + O3 = #.72 HO. + #.04 RO2-R. + #.627 R2O2. + #.667 CCO-O2. + #.167 CO + #.043 CO2 + #1.333 HCHO + #.333 ACET + #.123 HCOOH

A071) 4.873E+02 ISOBUTEN + NO3 = #.644 NO2 + #.039 RO2-N. + #.961 R2O2. + #.316 C-O2. + #.644 HCHO + #.644 ACET + #.87 XC + #.356 XN

A072) 2.481E+04 ISOBUTEN + O3P = #.4 RCHO + #.6 MEK + #.4 XC

A097) 8.190E+04 C-2-BUTE + HO. = #.965 RO2-R. + #.035 RO2-N. + #1.93 CCHO + #-0.07 XC

A098) 1.875E-01 C-2-BUTE + O3 = #.37 HO. + #.52 C-O2. + #.52 CO + #.14 CO2 + CCHO + #.34 CCO-OH + #.14 INERT + #.14 XC

A099) 5.112E+02 C-2-BUTE + NO3 = #.705 NO2 + #.215 RO2-R. + #.08 RO2-N. + #.705 R2O2. + #1.41 CCHO + #.215 RNO3 + #-0.59 XC + #.08 XN

A100) 2.584E+04 C-2-BUTE + O3P = MEK

A101) 9.274E+04 T-2-BUTE + HO. = #.965 RO2-R. + #.035 RO2-N. + #1.93 CCHO + #-0.07 XC

A102) 2.858E-01 T-2-BUTE + O3 = #.64 HO. + #.52 C-O2. + #.52 CO + #.14 CO2 + CCHO + #.34 CCO-OH + #.14 INERT + #.14 XC

A103) 5.768E+02 T-2-BUTE + NO3 = #.705 NO2 + #.215 RO2-R. + #.08 RO2-N. + #.705 R2O2. + #1.41 CCHO + #.215 RNO3 + #-0.59 XC + #.08 XN

A104) 3.200E+04 T-2-BUTE + O3P = MEK

A105) 1.263E+05 2M-2-BUT + HO. = #.935 RO2-R. + #.065 RO2-N. + #.935 CCHO + #.935 ACET + #-0.065 XC

A106) 5.999E-01 2M-2-BUT + O3 = #1.0 HO. + #.7 R2O2. + #.156 C-O2. + #.7 CCO-O2. + #.156 CO + #.042 CO2 + #.7 HCHO + #.7 CCHO + #.3 ACET + #.102 CCO-OH + #.042 INERT + #.042 XC

A107) 1.375E+04 2M-2-BUT + NO3 = #.935 NO2 + #.065 RO2-N. + #.935 R2O2. + #.935 CCHO + #.935 ACET + #-0.065 XC + #.065 XN

A108) 7.486E+04 2M-2-BUT + O3P = MEK + XC

A262) 9.667E+04 13-BUTDE + HO. = #.961 RO2-R. + #.039 RO2-N. + #.48 HCHO + #.48 METHACRO + #.48 ISO-PROD + #-1.039 XC

A263) 9.742E-03 13-BUTDE + O3 = #.13 HO. + #.06 HO2. + #.25 CO + #.19 CO2 + #.5 HCHO + #.125 PROD2 + #.5 METHACRO + #.375 MVK + #.185 HCOOH + #-1.375 XC

A264) 1.468E+02 13-BUTDE + NO3 = #.92 RO2-R. + #.08 RO2-N. + #.92 MVK + #-0.161 XC + XN

A265) 2.906E+04 13-BUTDE + O3P = #.25 HO2. + #.23 RO2-R. + #.02 RO2-N. + #.23 CO + #.75 PROD2 + #.23 METHACRO + #-1.77 XC

TR03) 8.949E+03 A-PINENE + NO3 = #.75 NO2 + #.25 RO2-N. + #.75 R2O2. + #.75 RCHO + #6.25 XC + #.25 XN

TR04) 4.697E+04 A-PINENE + O3P = PROD2 + #4 XC

TR09) 1.275E+05 3-CARENE + HO. = #.75 RO2-R. + #.25 RO2-N. + #.5 R2O2. + #.75 RCHO + #6.25 XC

TR10) 5.554E-02 3-CARENE + O3 = #1.0 HO. + #.161 RO2-N. + #.539 R2O2. + #.482 CCO-O2. + #.058 RCO-O2. + #.058 HCHO + #.482 RCHO + #.3 RCO-OH + #5.492 XC

TR11) 1.336E+04 3-CARENE + NO3 = #.75 NO2 + #.25 RO2-N. + #.75 R2O2. + #.75 RCHO + #6.25 XC + #.25 XN

TR12) 4.697E+04 3-CARENE + O3P = PROD2 + #4 XC

TR17) 2.481E+05 D-LIMONE + HO. = #.75 RO2-R. + #.25 RO2-N. + #.5 R2O2. + #0.2 AMCYCHEX + #.29 IPOH + #6.25 XC

TR18) 2.996E-01 D-LIMONE + O3 = #.86 HO. + #.161 RO2-N. + #.539 R2O2. + #.482 CCO-O2. + #.058 RCO-O2. + #.1 HCHO + #.04 AMCYCHEX + #.04 IPOH + #.3 RCO-OH + #5.492 XC

TR19) 1.791E+04 D-LIMONE + NO3 = #.75 NO2 + #.25 RO2-N. + #.75 R2O2. + #.75 RCHO + #6.25 XC + #.25 XN

TR20) 1.057E+05 D-LIMONE + O3P = PROD2 + #4 XC

AN01) 8.514E+04 STYRENE + HO. = #.87 RO2-R. + #.13 RO2-N. + #.87 HCHO + #.87 BALD + #.26 XC

AN02) 2.510E-02 STYRENE + O3 = #.07 HO. + #.4 HCHO + #.6 BALD + #.6 HCOOH + #.4 RCO-OH + #1.6 XC

AN03) 2.217E+02 STYRENE + NO3 = #.22 NO2 + #.65 RO2-R. + #.13 RO2-N. + #.22 R2O2. + #.22 HCHO + #.22 BALD + #.65 RNO3 + #1.56 XC + #.13 XN

AN04) 2.584E+04 STYRENE + O3P = PROD2 + #2 XC

APPENDIX B
Particle Formation Chemistry of a -Pinene

Note:
'k' is the rate constant. Units are either in ppm^{-1} min^{-1} or min^{-1}

CRIEG1	=	Criegee Biradical 1
CRIEG1	=	Criegee Biradical 2
SCRIEG1	=	Stabilized Criegee Radical Formed from CRIEG1
SCRIEG2	=	Stabilized Criegee Radical Formed from CRIEG2
PINALD	=	Represent pinonaldehyde and nor-pinonaldehyde
PINACID	=	Represent pinonic and nor-pinonic acid
DIACID	=	Represent pinic and nor-pinic acid
O-PINALD	=	Represent hydroxy and aldehhyde substituted pinonaldehydes
O-PINACID	=	Represent hydroxy and aldehhyde substituted pinonic acids
P3GAS	=	Represent a pinic acid precursor 2,2 dimethylcyclo butane-3-acetyl carboxylic acid
SEED	=	Background particles
SEED1	=	Particles formed by self-nucleation
PART	=	Particles formed from DIACID
PART1	=	Particles formed from PINACID
PART2	=	Particles formed from PINALD
PART3	=	Particles formed from O-PINALD
PART4	=	Particles formed from P3GAS
PART5	=	Particles formed from O-PIACID

No.	k	Reactions
AP01)	0.13	A-PINENE + O3 = #0.4 CRIEG1 + #0.6 CRIEG2
AP02)	1.00E+06	CRIEG1 = #0.3 PINACID + #0.15 SCRIEG1 + #0.8 HO. + #0.5 HO2. + #0.3 PINALD + #0.25 O-PINALD + #0.3 CO
AP03)	1.00E+06	CRIEG2 = #0.3 CRGPROD2 + #0.55 O-PINALD + #0.15 SCRIEG2 + #0.8 HO. + #0.5 HO2. + #0.35 HCHO
AP04)	6.00E-03	SCRIEG1 + H2O = PINACID
AP05)	6.00E-03	SCRIEG2 + H2O = P3GAS + CH3OH
AP06)	3.55E+04	P3GAS + HO. = PREDI-OO
AP07)	3.55E+04	O-PINALD + HO. = O-PRACID
AP08)	2.22E+04	PREDI-OO + HO2. = DIACID
AP09)	2.22E+04	CRGPROD2 + HO2. = DIACID
AP10)	2.22E+04	O-PRACID + HO2. = O-PIACID
AP11)	7.93E+04	A-PINENE + HO. = #0.6 PINALD + #0.1 O-PINALD + #0.3 FRAG
AP12)	3.55E+04	PINALD + HO. = PINALDOO
AP13)	2.22E+04	PINALDOO + HO2. = PINACID
!		
! WALL LOSSES		
AP14)	2.19E-03	DIACID = (not used in ICEM, see text for details)
AP15)	2.19E-03	O-PIACID = (not used in ICEM, see text for details)
AP16)	1.46E-03	PINACID = (not used in ICEM, see text for details)
AP17)	1.46E-03	O-PINALD = (not used in ICEM, see text for details)
AP18)	9.15E-04	PINALD = (not used in ICEM, see text for details)
!		
! PARTITIONING REACTIONS		
!		
P01)	29.5	SCRIEG1 + PINALD = SEED1
P02)	29.5	SCRIEG1 + PINACID = SEED1
P03)	29.5	SCRIEG1 + O-PINALD = SEED1
P04)	29.5	SCRIEG1 + P3GAS = SEED1
P05)	29.5	SCRIEG1 + HCHO = O-PINALD
P06)	29.5	SCRIEG1 + O-PIACID = SEED1
P07)	29.5	SCRIEG2 + PINALD = SEED1
P08)	29.5	SCRIEG2 + PINACID = SEED1
P09)	29.5	SCRIEG2 + O-PINALD = SEED1
P10)	29.5	SCRIEG2 + P3GAS = SEED1
P11)	29.5	SCRIEG2 + HCHO = O-PINALD
P12)	29.5	SCRIEG2 + O-PIACID = SEED1
P13)	0.5	DIACID + DIACID = SEED1
P14)	68.0	DIACID + SEED = SEED + PART

P15)	68.0	DIACID + SEED1 = SEED1 + PART
P16	68.0	DIACID + PART = PART + PART
P17)	68.0	DIACID + PART1 = PART1 + PART
P18)	68.0	DIACID + PART2 = PART2 + PART
P19)	68.0	DIACID + PART3 = PART3 + PART
P20)	68.0	DIACID + PART4 = PART4 + PART
P21)	68.0	DIACID + PART5 = PART5 + PART
P22)	0.4	PART = DIACID
P23)	25.0	PINACID + SEED1 = SEED1 + PART1
P24)	25.0	PINACID + PART = PART + PART1
P25)	25.0	PINACID + SEED = SEED + PART1
P26)	25.0	PINACID + PART1 = PART1 + PART1
P27)	25.0	PINACID + PART2 = PART2 + PART1
P28)	25.0	PINACID + PART3 = PART3 + PART1
P29)	25.0	PINACID + PART4 = PART4 + PART1
P30)	25.0	PINACID + PART5 = PART5 + PART1
P31)	3.2	PART1 = PINACID
P32)	20.0	PINALD + SEED1 = SEED1+ PART2
P33)	20.0	PINALD + PART = PART + PART2
P34)	20.0	PINALD + SEED = SEED + PART2
P35)	20.0	PINALD + PART1 = PART1 + PART2
P36)	20.0	PINALD + PART2 = PART2 + PART2
P37)	20.0	PINALD + PART3 = PART3 + PART2
P38)	20.0	PINALD + PART4 = PART4 + PART2
P39)	20.0	PINALD + PART5 = PART5 + PART2
P40)	28.6	PART2 = PINALD
P41)	40.0	O-PINALD + SEED1 = SEED1+ PART3
P42)	40.0	O-PINALD + PART = PART + PART3
P43)	40.0	O-PINALD + SEED = SEED + PART3
P44)	40.0	O-PINALD + PART1 = PART1 + PART3
P45)	40.0	O-PINALD + PART2 = PART2 + PART3
P46)	40.0	O-PINALD + PART3 = PART3 + PART3
P47)	40.0	O-PINALD + PART4 = PART4 + PART3
P48)	40.0	O-PINALD + PART5 = PART5 + PART3
P49)	1.0	PART3 = O-PINALD
P50)	20.0	P3GAS + SEED = SEED + PART4
P51)	20.0	P3GAS + PART = PART + PART4
P52)	20.0	P3GAS + SEED1 = SEED1 + PART4
P53)	20.0	P3GAS + PART1 = PART1 + PART4
P54)	20.0	P3GAS + PART2 = PART2 + PART4
P55)	20.0	P3GAS + PART3 = PART3 + PART4
P56)	20.0	P3GAS + PART4 = PART4 + PART4

```
P57)   20.0        P3GAS + PART5 = PART5 + PART4
P58)   3.8         PART4 = P3GAS
P59)   74.0        O-PIACID + SEED1 = SEED1 + PART5
P60)   74.0        O-PIACID + SEED  = SEED  + PART5
P61)   74.0        O-PIACID + PART  = PART  + PART5
P62)   74.0        O-PIACID + PART1 = PART1 + PART5
P63)   74.0        O-PIACID + PART2 = PART2 +  PART5
P64)   74.0        O-PIACID + PART3 = PART3 + PART5
P65)   74.0        O-PIACID + PART4 = PART4 + PART5
P66)   74.0        O-PIACID + PART5 = PART5 + PART5
P67)   0.32        PART5 = O-PIACID
!
! WALL LOSSES
!
P68)   0.0008      PART   =        (not used in ICEM, see text for details)
P69)   0.0008      PART1 =         (not used in ICEM, see text for details)
P70)   0.0008      PART2 =         (not used in ICEM, see text for details)
P71)   0.0008      PART3 =         (not used in ICEM, see text for details)
P72)   0.0008      PART4 =         (not used in ICEM, see text for details)
P73)   0.0008      PART5 =         (not used in ICEM, see text for details)
P74)   0.0008      SEED   =        (not used in ICEM, see text for details)
P75)   0.0008      SEED1 =         (not used in ICEM, see text for details)
P76)   0.0008      O3      =       (not used in ICEM, see text for details)
```

APPENDIX C
A Typical Input File to the ICEM

```
! title of the simulation
SOA FROM A-PINENE/OZONE REACTIONS
MODEL=SAPRC99P
EPS   5.5E-8
SAVE RATE
MUSTSAVE
!NOCHEM
.
.LBL1 INDOOR, CHEM, DEPOSITION
!
! insert mechanism version
@MODDOC.IN
!
! use "Z1.SDR" – the file for the spectral distribution
.SD-Z1
!
! chamber temperature
.TEMP   297.0
!
! chamber water vapor
H2O     17823  ! RH 50%
!
! chamber volume
VOLUME   500.
!
! volume to surface area ratio, use total surface area is used, not only the floor area
VARATIO  0.357  ! A/V = 2.8
!
! flow rate
FLOW   4.17    ! ACH = 0.5
!
! outside ozone concentration
O#O3     0.10
!
! outside particle concentration
O#SEED  0.00406 (15 ug/m3)
!
! a-pinene emission rate (mmol/min)
E#A-PINENE  0.0170
!
! gaseous deposition velocities (meter/minute)
! average deposition rate for ozone = 3.6/hr
```

```
D#O3            0.0216
D#NO2           0.0036
D#NH3           0.042
D#SO2           0.0216
D#CO            0.000
D#NO            0.000
D#PAN           0.021
D#HONO          0.042
D#HNO3          0.042
D#HNO4          0.042
D#HO2H          0.042
D#NO3           0.042
D#N2O5          0.042
D#HO2.          0.042
D#HO.           0.042
D#HCHO          0.003
D#CCHO          0.003
D#RCHO          0.003
!
! a-pinene and its reaction products
! assume that it is double to that of particles (based on Kamens et al., 1999)
D#DIACID      0.00464
D#O-PIACID    0.00464
D#PINACID     0.00464
D#O-PINALD    0.00464
D#PINALD      0.00464
!
! SEED is the background particles
! SEED1 - particles formed by self-nucleation
! PART through PART5 are secondary particles formed from a-pinene
! average deposition velocity is used
! deposition rate = 0.39/hr
D#SEED    0.00232
D#SEED1   0.00232
D#PART    0.00232
D#PART1   0.00232
D#PART2   0.00232
D#PART3   0.00232
D#PART4   0.00232
D#PART5   0.00232
!
.SETDEF
```

```
!
!    save every 10 minutes
.LBL5 BACKGROUND
.T0     0
.TEND   720.
.DPRN   10.
!
! start simulation
.INT
```

APPENDIX D
Chamber Particle and Ozone Levels
α-Pinene/O_3 Reaction

Table 5.1 (Repeated)
Summary of Chamber Results from the Release of Pure a -Pinene

Expt No.	l	E	Initial O_3	T	Initial Particle	Max Particle	Time	Final Particle	M_i	$M_{f,e}$	SOA	$M_{f,p}$	Difference
	(hr^{-1})	(mg/min)	(ppb)	(C)	(#/cc)	(#/cc)	(min)	(#/cc)	(mg/m^3)	(mg/m^3)	(mg/m^3)	(mg/m^3)	(%)
1	1.25	196	15	25	2,760	3,423	108	1,997	3.6	4.3	0.7	5.0	-16
2	0.55	75	132	24	7,047	96,989	17	10,004	3.1	38.5	35.4	55.3	-43
3	0.68	81	134	26	1,383	34,662	34	7,227	2.2	21.0	18.8	26.5	-26
4	1.06	78	111	24	9,202	11,852	39	6,774	4.3	16.2	11.9	19.7	-21
5	0.70	70	136	25	4,138	18,529	31	7,324	9.2	28.9	19.7	29.9	-3
6	0.70	91	170	24	10,391	14,532	48	9,511	5.4	48.7	43.3	65.9	-26
7	0.75	98	142	25	2,836	30,114	26	6,327	10.8	33.2	22.4	52.2	-57
8	1.34	89	157	32	8,472	31,062	48	35,975	6.9	17.1	10.2	20.5	-20
9	1.50	102	144	33	12,529	37,729	48	25,332	3.3	6.5	3.2	8.8	-35
10	0.71	185	159	25	4,438	25,131	32	9,180	2.7	73.7	71.0	181	-145

Note:
λ = air exchange rate, E = α-pinene emission rate, Time = time at which the maximum particle number concentrations occurred in the chamber, M_i = initial particle mass concentration in the chamber, $M_{f,e}$ = final experimental particle mass concentration in the chamber, $M_{f,p}$ = final predicted particle mass concentration in the chamber, SOA = secondary organic aerosol = $M_{f,e} - M_i$, Difference = $(M_{f,e} - M_{f,p})/M_{f,e}$

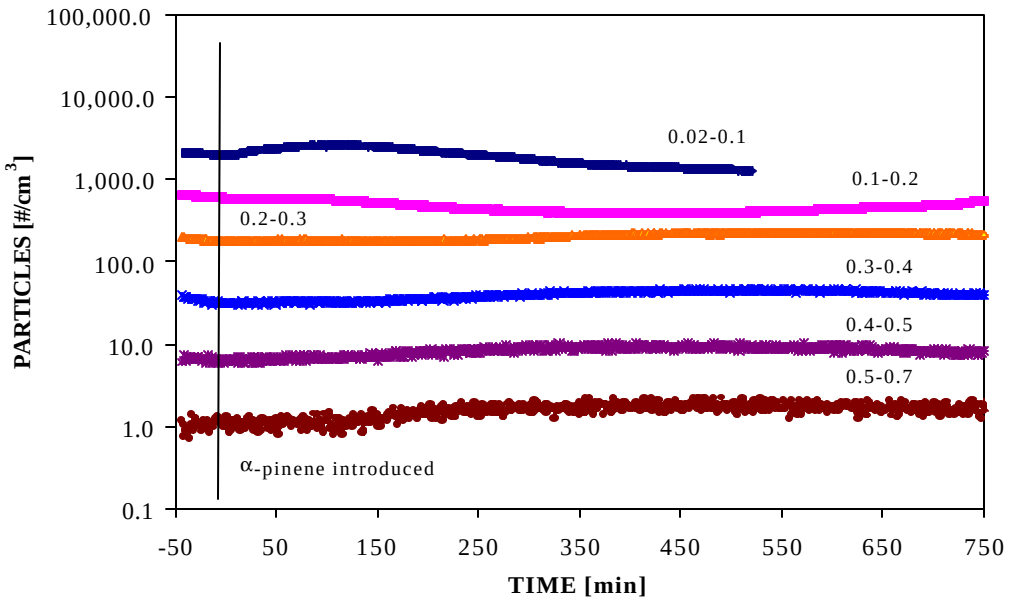

Figure D-1. Evolution of particle number concentrations during experiment #1. l = 1.25 hr^{-1}

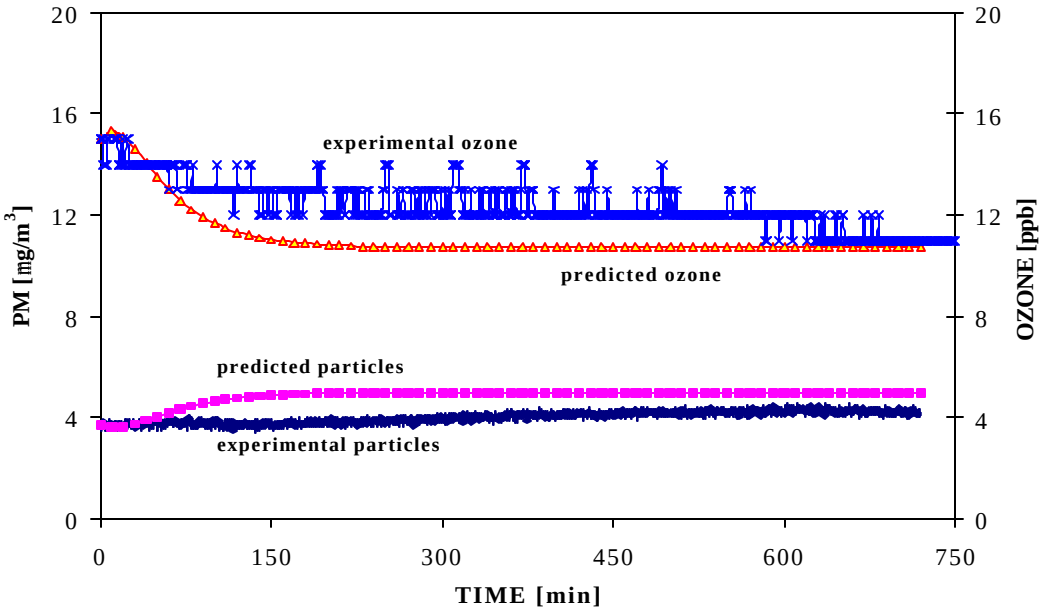

Figure D-2. Evolution of particle mass and ozone concentrations during experiment #1. l = 1.25 hr^{-1}

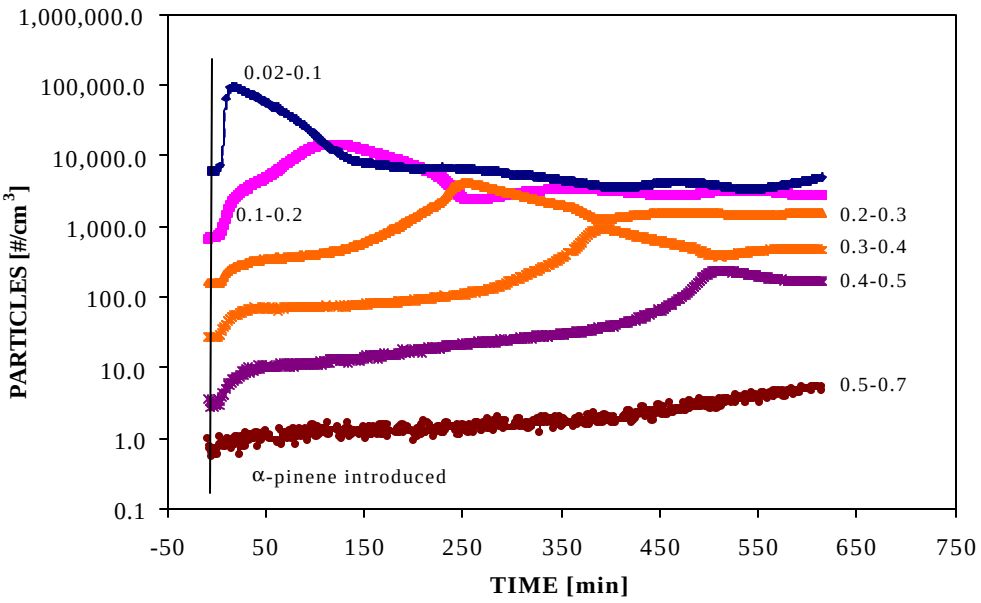

Figure D-3. Evolution of particle number concentrations during experiment #2. $\lambda = 0.55\ hr^{-1}$

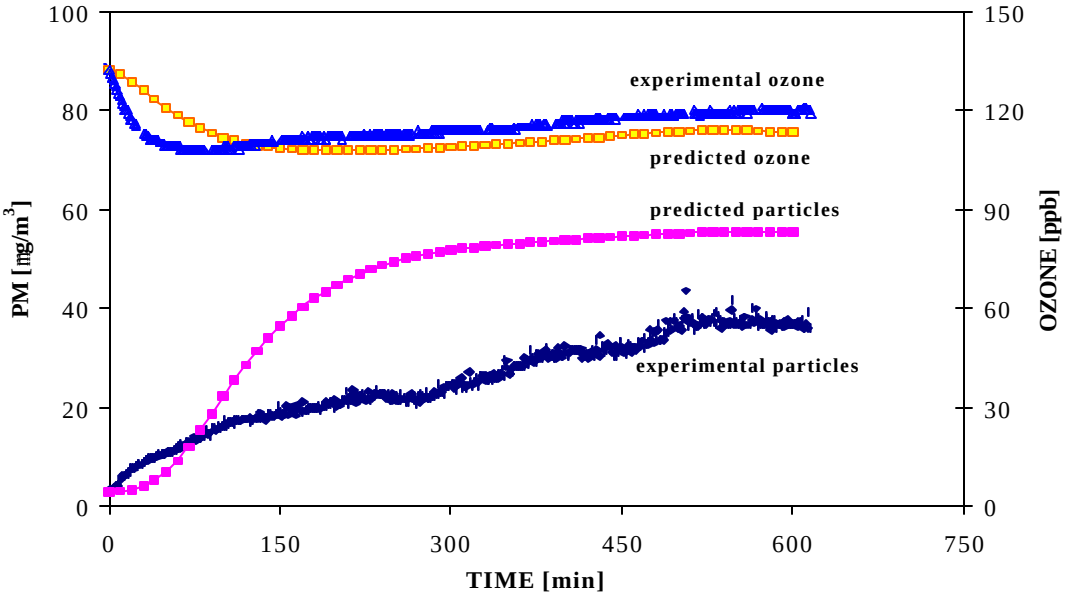

Figure D-4. Evolution of particle mass and ozone concentrations during experiment #2. $\lambda = 0.55\ hr^{-1}$

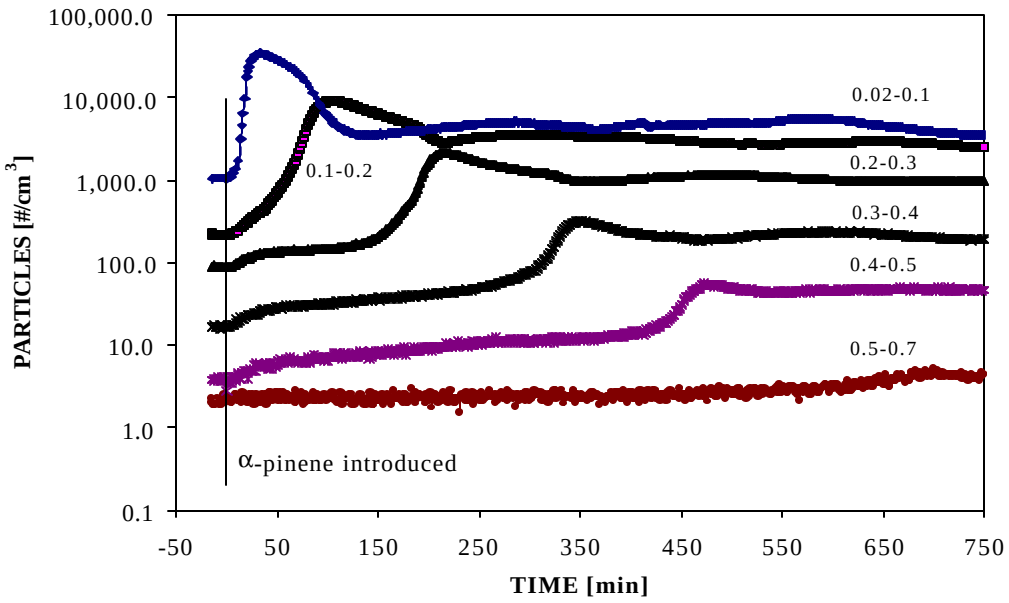

Figure D-5. Evolution of particle number concentrations during experiment #3. l = 0.68 hr^{-1}

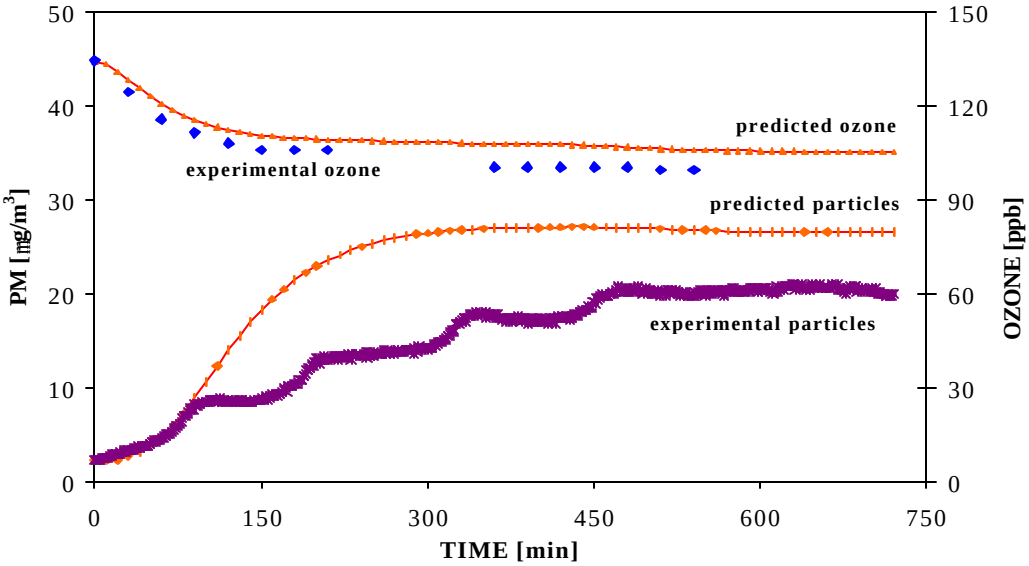

Figure D-6. Evolution of particle mass and ozone concentrations during experiment #3. l = 0.68 hr^{-1}

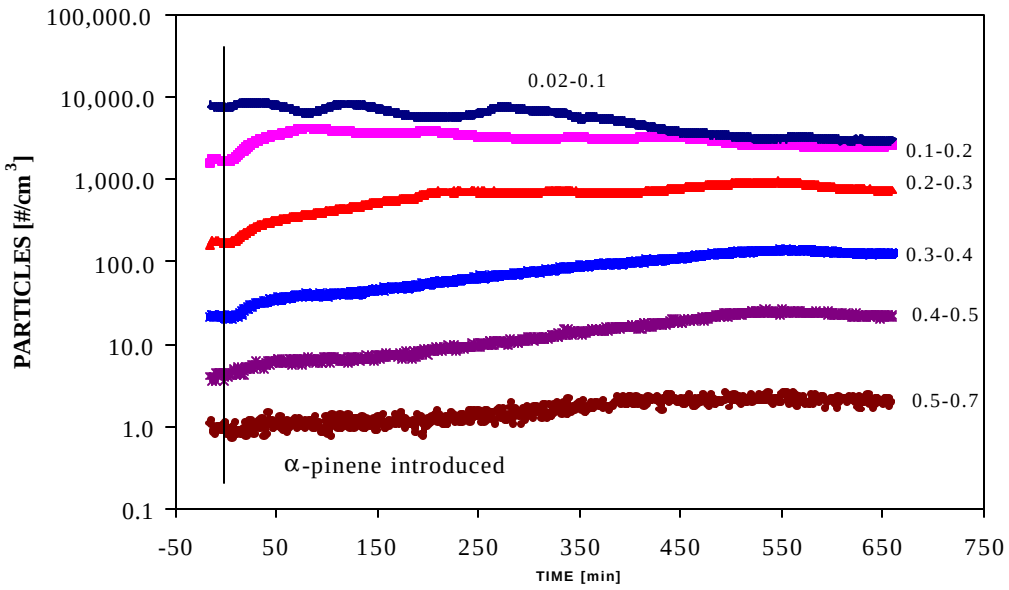

Figure D-7. Evolution of particle number concentrations during experiment #4. l = 1.06 hr^{-1}

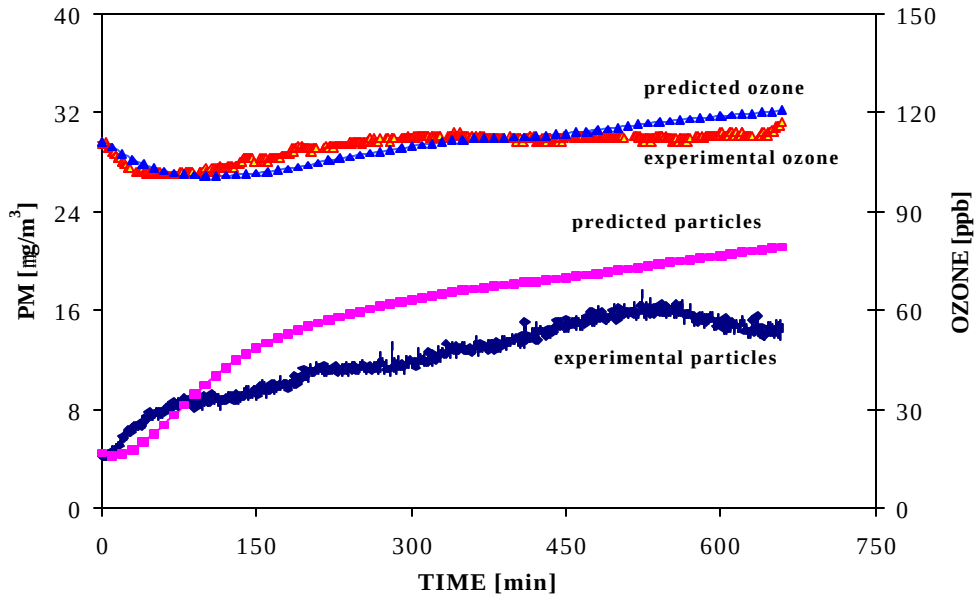

Figure D-8. Evolution of particle mass and ozone concentrations during experiment #4. l = 1.06 hr^{-1}

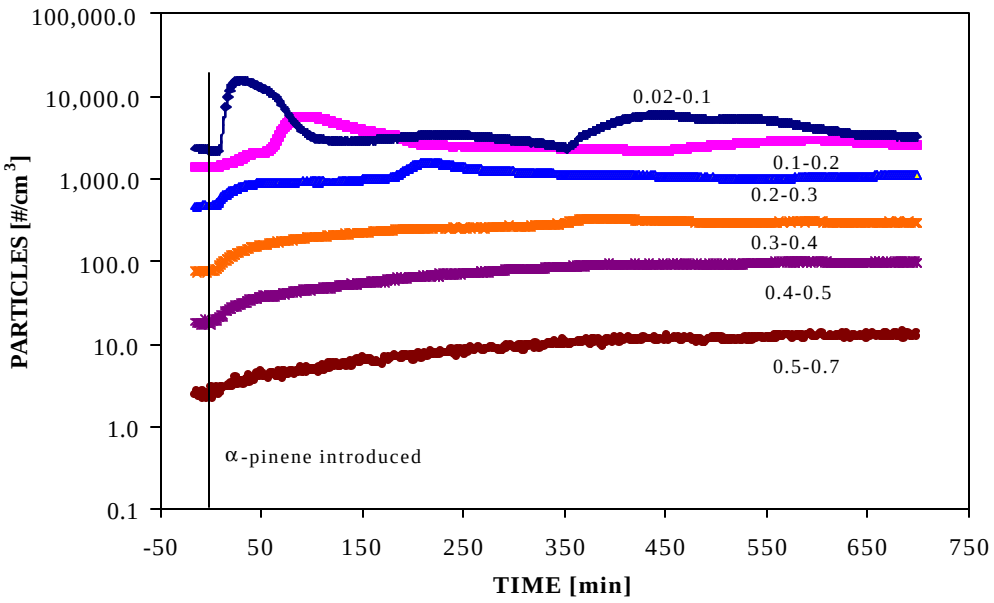

Figure D-9. Evolution of particle number concentrations during experiment #5. l = 0.70 hr^{-1}

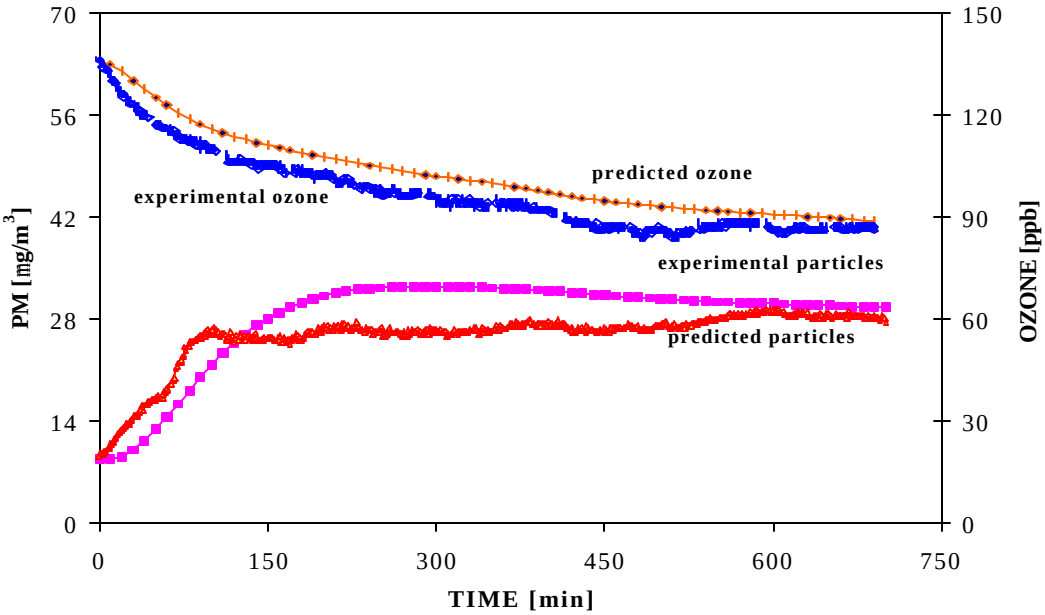

Figure D-10. Evolution of particle mass and ozone concentrations during experiment #5. l = 0.70 hr^{-1}

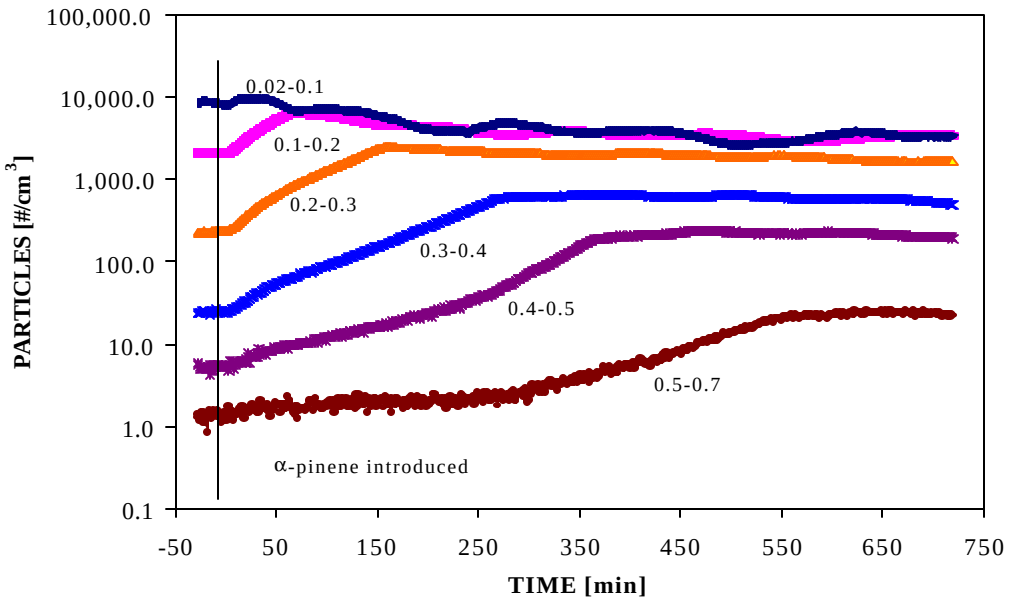

Figure D-11. Evolution of particle number concentrations during experiment #6. l = 0.70 hr^{-1}

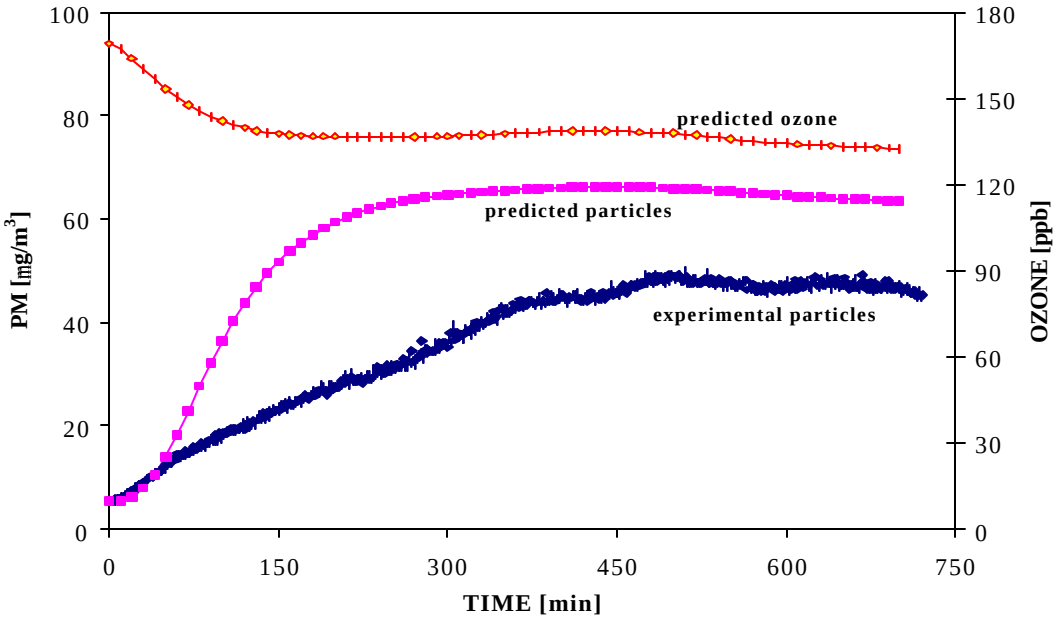

Figure D-12. Evolution of particle mass and ozone concentrations during experiment #6. l = 0.70 hr^{-1}

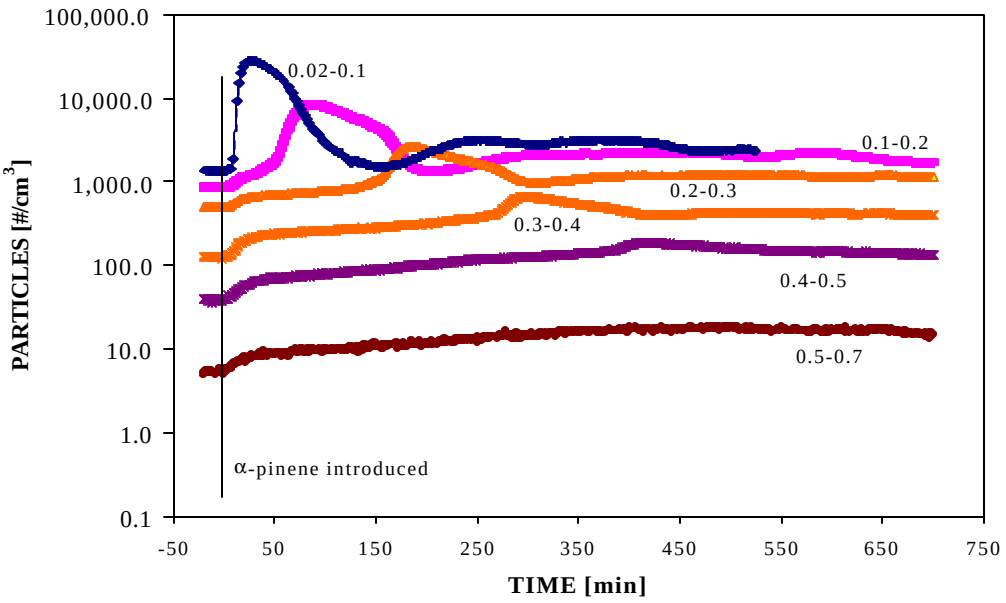

Figure D-13. Evolution of particle number concentrations during experiment #7. l = 0.75 hr^{-1}

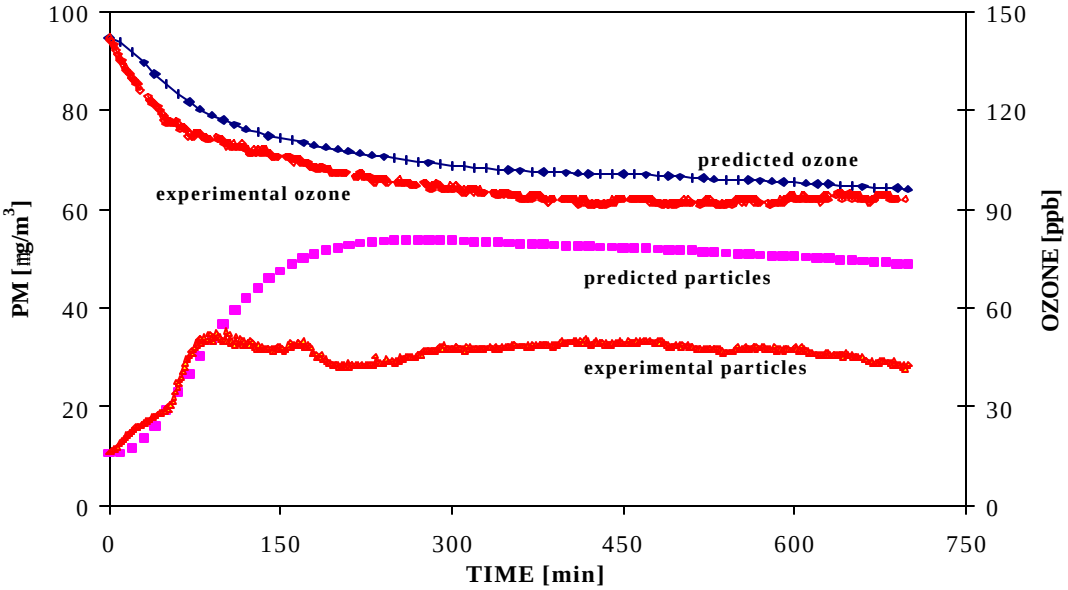

Figure D-14. Evolution of particle mass and ozone concentrations during experiment #7. l = 0.75 hr^{-1}

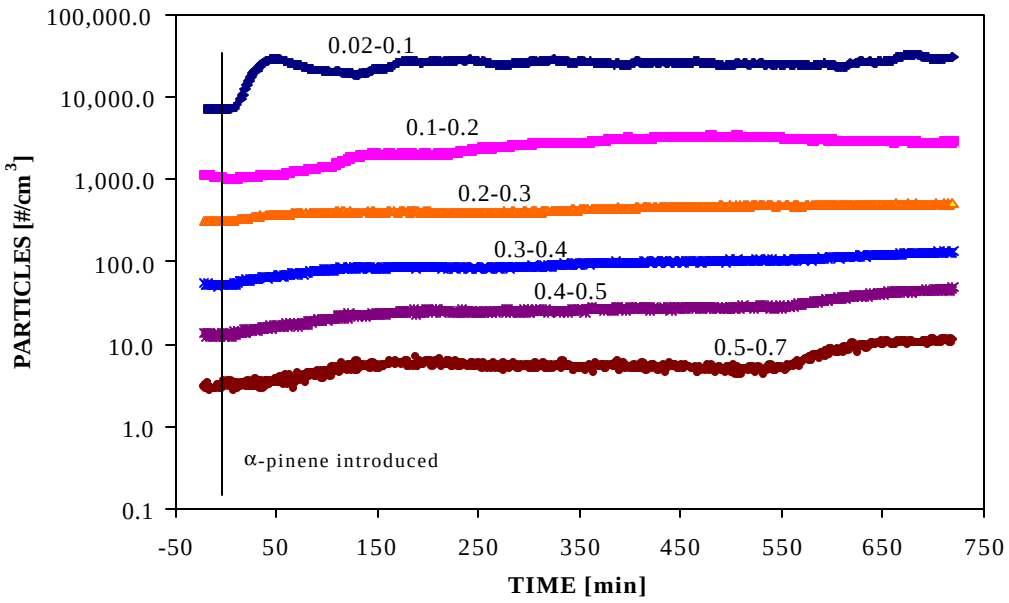

Figure D-15. Evolution of particle number concentrations during experiment #8. l = 1.34 hr^{-1}

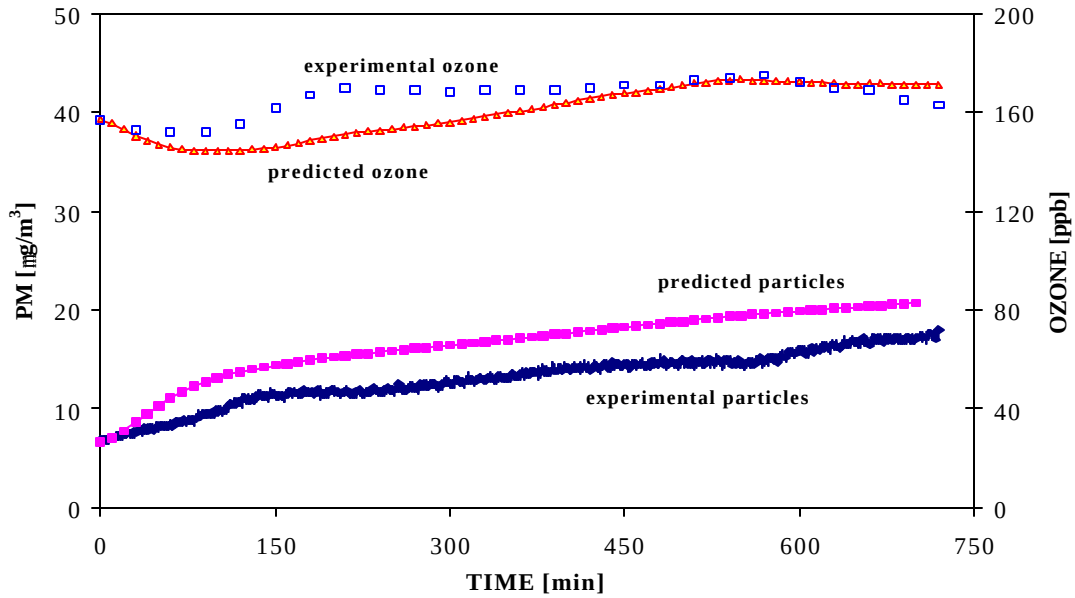

Figure D-16. Evolution of particle mass and ozone concentrations during experiment #8. l = 1.34 hr^{-1}

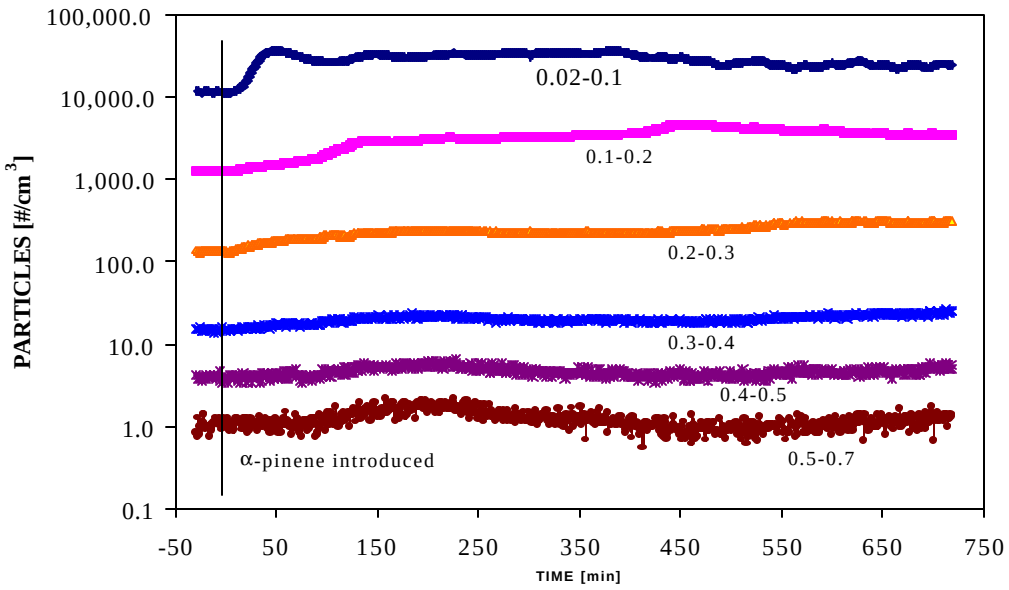

Figure D-17. Evolution of particle number concentrations during experiment #9. l = 1.50 hr^{-1}

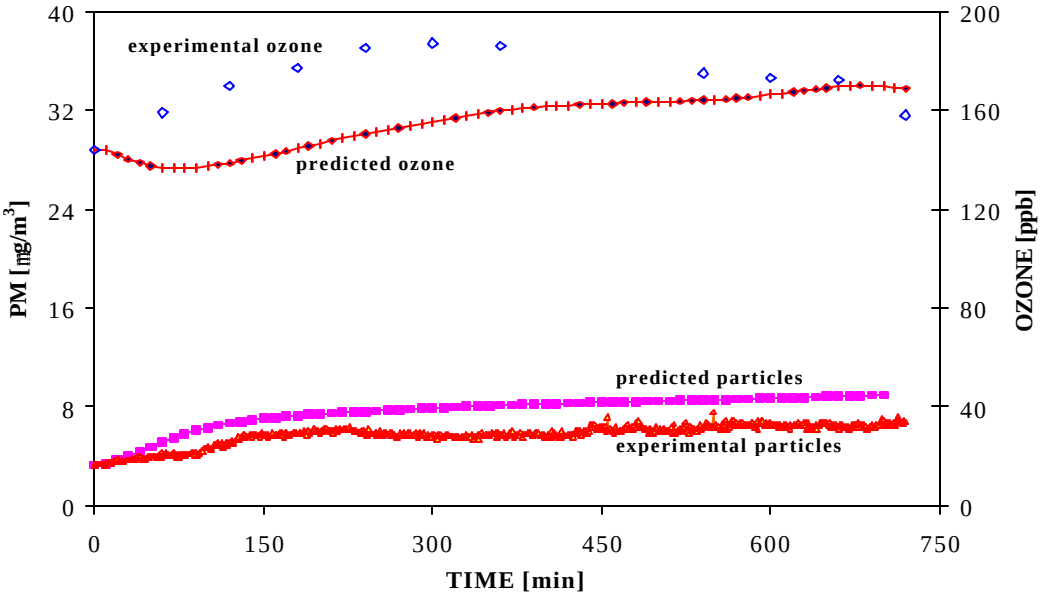

Figure D-18. Evolution of particle mass and ozone concentrations during experiment #9. l = 1.50 hr^{-1}

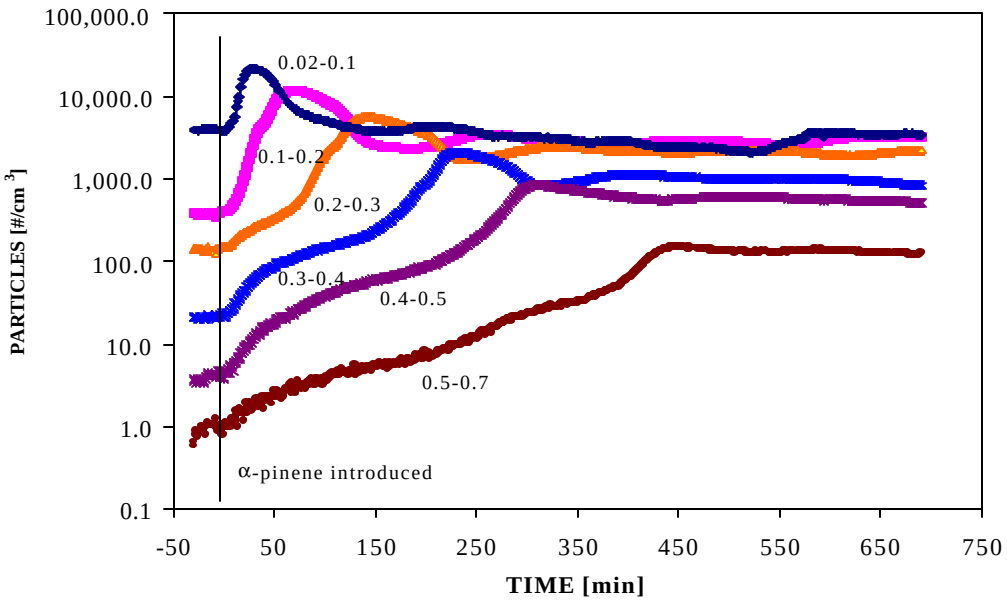

Figure D-19. Evolution of particle number concentrations during experiment #10. l = 0.71 hr^{-1}

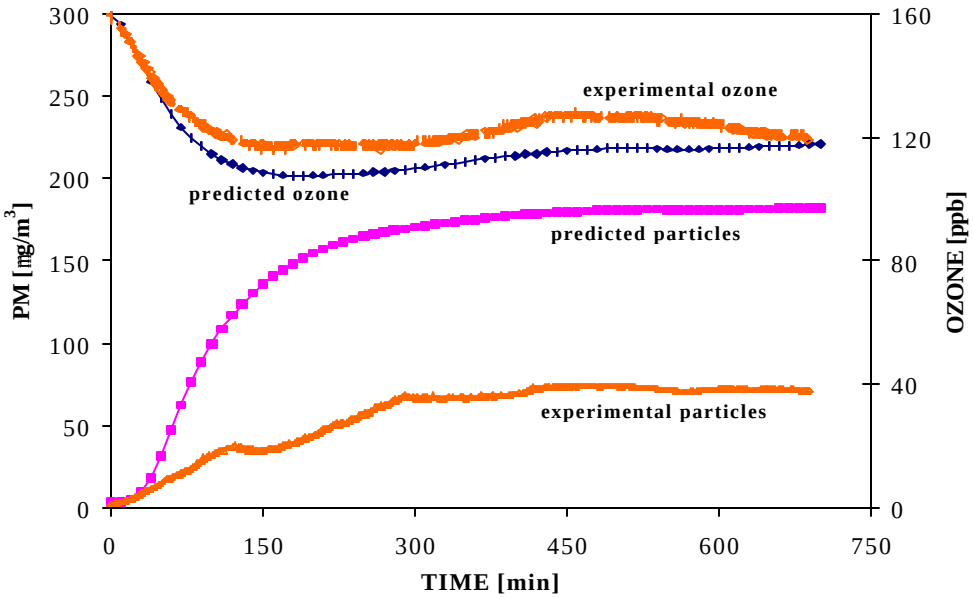

Figure D-20. Evolution of particle mass and concentrations during experiment #10. l = 0.71 hr^{-1}

APPENDIX E
Chamber Particle and Ozone Levels
Limonene/O_3 Reaction

Table 5.3 (Repeated)
Summary of Chamber Results from the Release of Pure Limonene

Expt No.	l	E	Initial O_3	T	Initial Particle	Max Particle	Time	Final Particle	M_i	$M_{f,e}$	SOA
	(hr^{-1})	(mg/min)	(ppb)	(C)	(#/cc)	(#/cc)	(min)	(#/cc)	(mg/m^3)	(mg/m^3)	(mg/m^3)
11	NA	113	11	25	3,833	3,833	1	1,805	2.9	2.8	NONE
12	0.71	110	163	25	4,560	90,244	15	11,453	7.3	153	146
13	0.95	85	114	23	7,131	55,987	25	13,628	2.9	68.7	66
14	1.00	88	327	23	3,413	160,285	13	14,940	1.8	78.7	77
15	1.17	84	151	23	2,661	79,174	19	15,061	1.3	63.8	63
16	1.21	91	85	24	6,297	24,643	33	13,362	5.5	68.9	63

Note:
λ = air exchange rate, E = limonene emission rate, Time = time at which the maximum particle number concentration occurred in the chamber, M_i = initial particle mass concentration in the chamber, $M_{f,e}$ = final experimental particle mass concentration in the chamber, and SOA = secondary organic aerosol = $M_{f,e} - M_i$

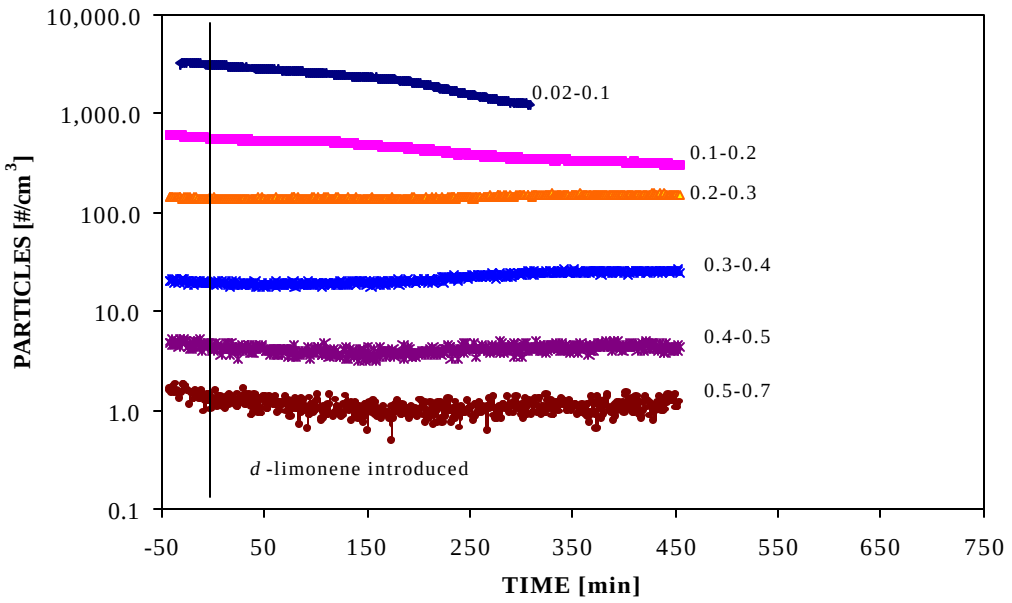

Figure E-1. Evolution of particle number concentrations during experiment #11.

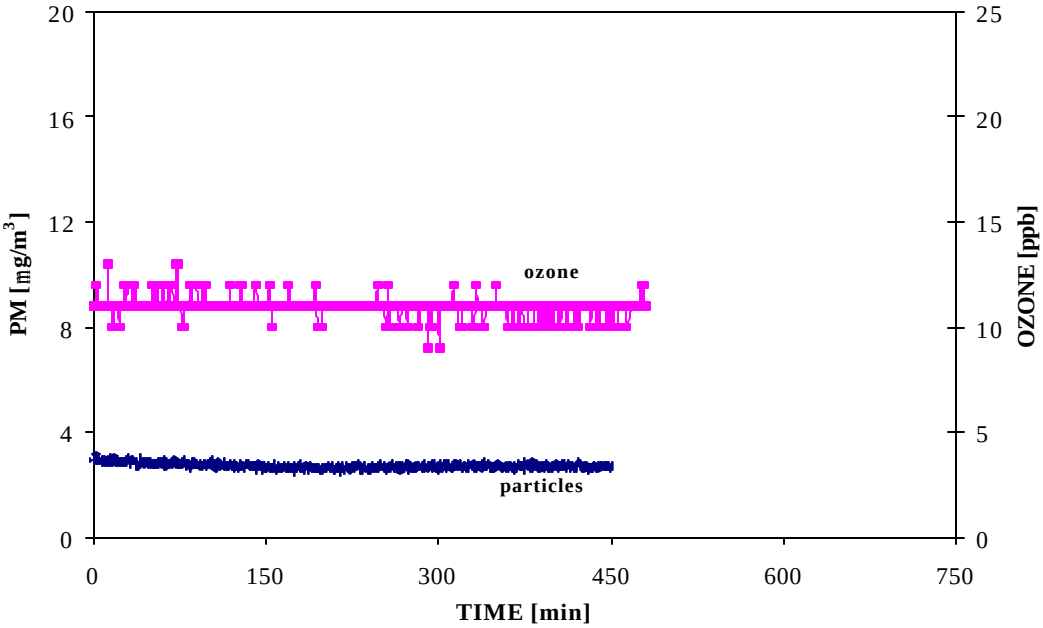

Figure E-2. Evolution of particle mass and ozone concentrations during experiment #11.

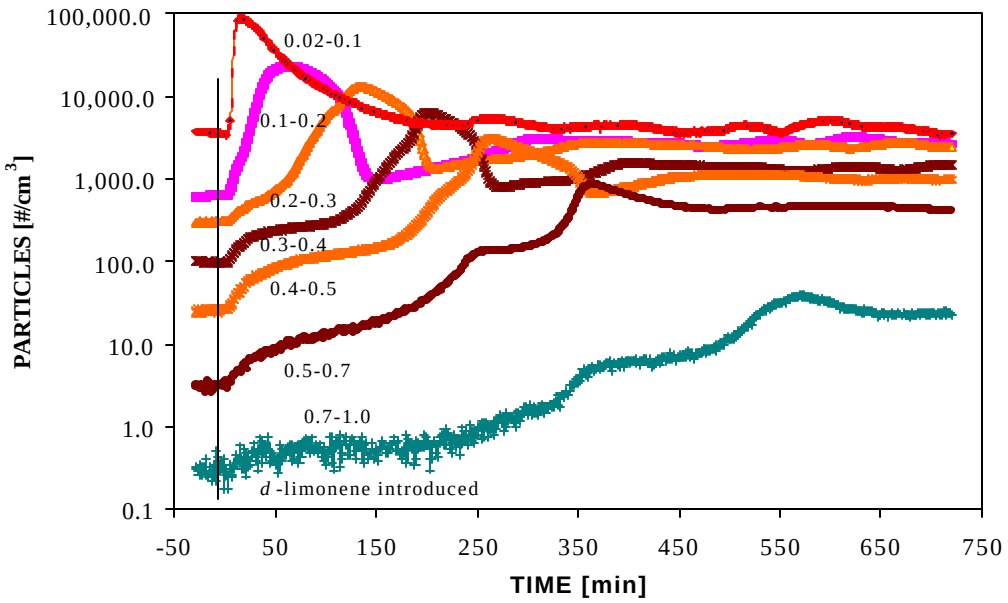

Figure E-3. Evolution of particle number concentrations during experiment #12. l = 0.71 hr^{-1}

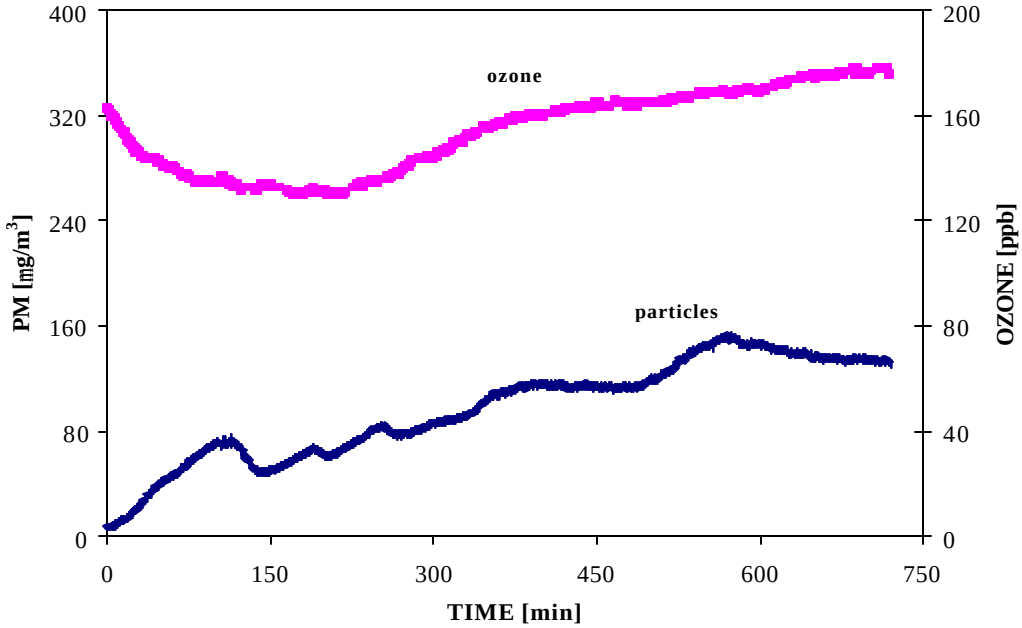

Figure E-4. Evolution of particle mass and ozone concentrations during experiment #12. l = 0.71 hr^{-1}

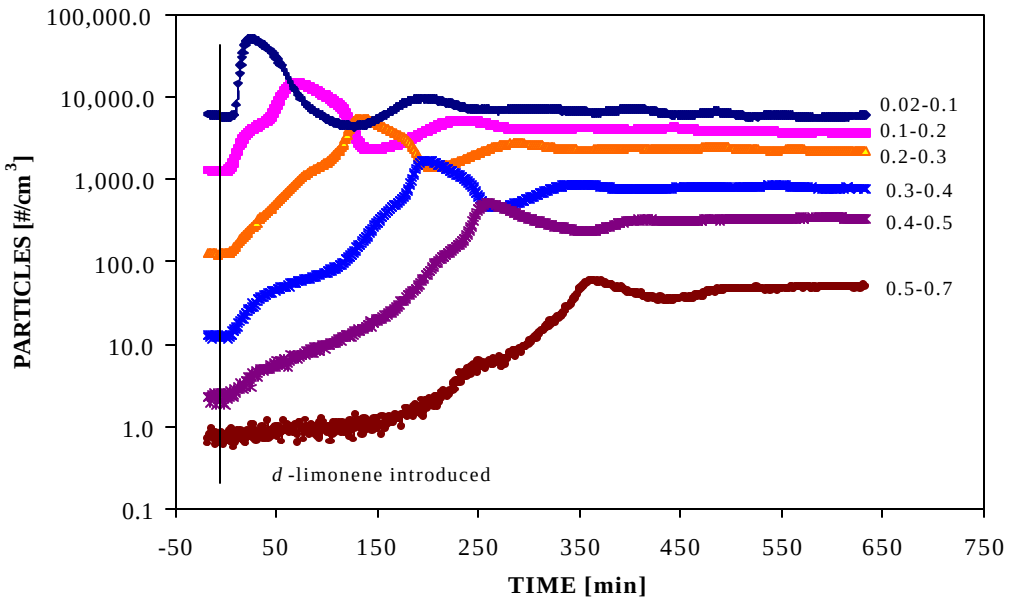

Figure E-5. Evolution of particle number concentrations during experiment #13. l = 0.95 hr^{-1}

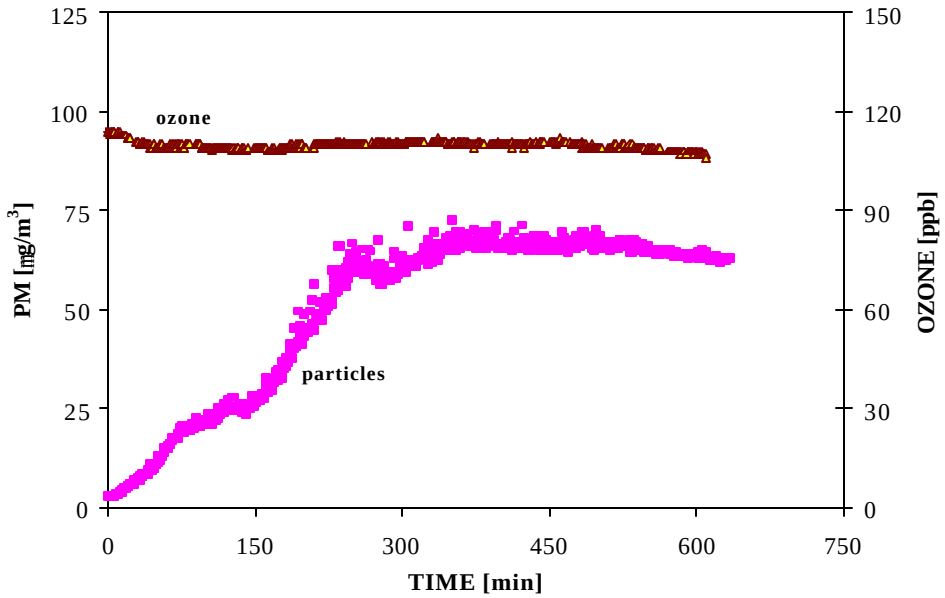

Figure E-6. Evolution of particle mass and ozone concentrations during experiment #13. l = 0.95 hr^{-1}

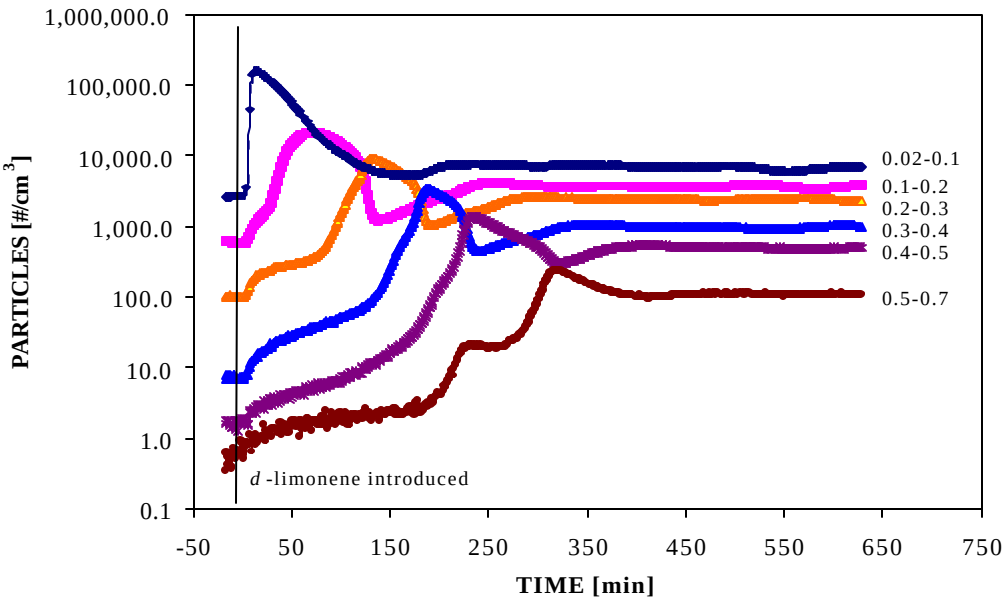

Figure E-7. Evolution of particle number concentrations during experiment #14. l = 1.0 hr^{-1}

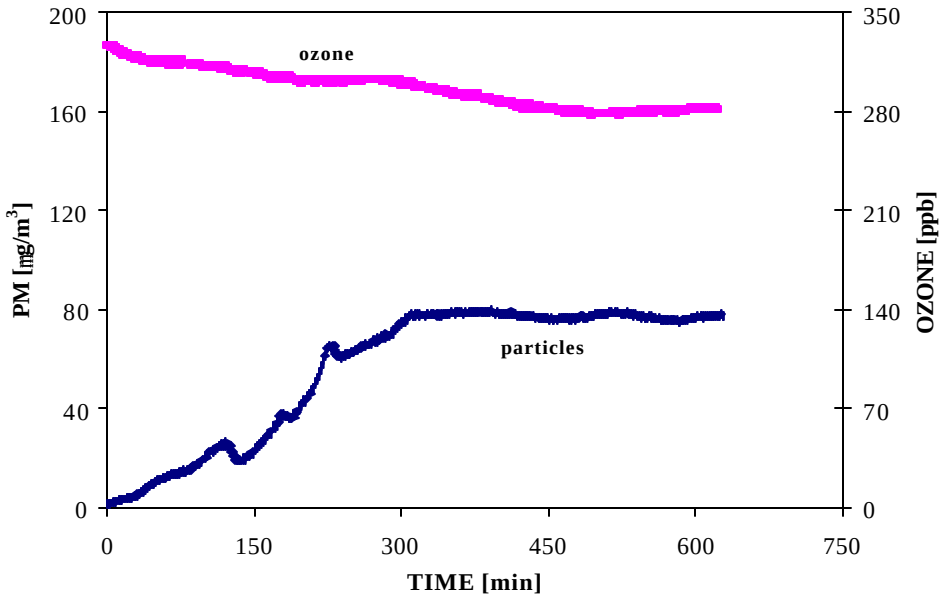

Figure B-8. Evolution of particle mass and ozone concentrations during experiment #14. l = 1.0 hr^{-1}

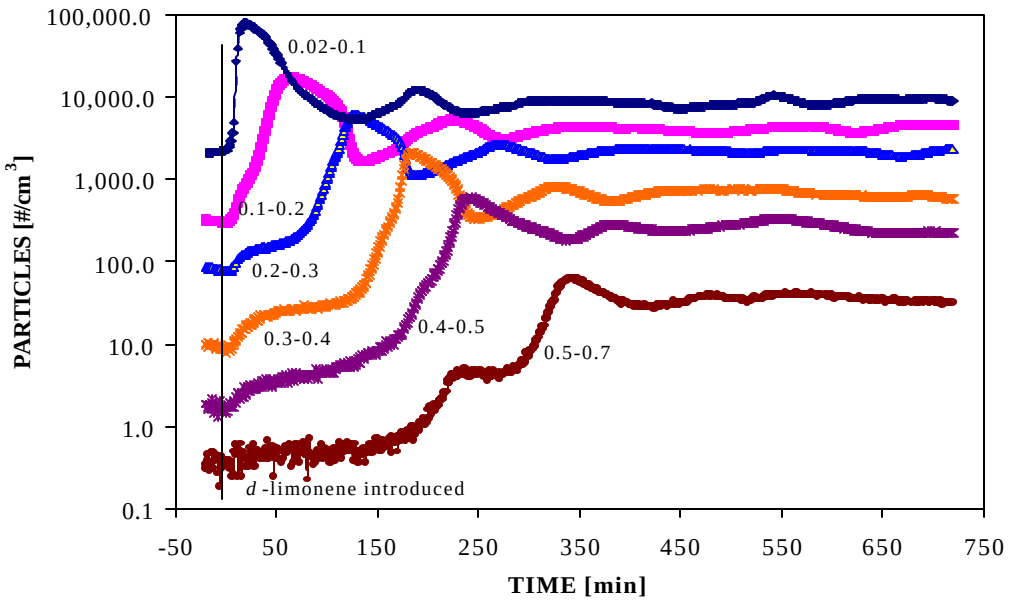

Figure E-9. Evolution of particle number concentrations during experiment #15. l = 1.17 hr^{-1}

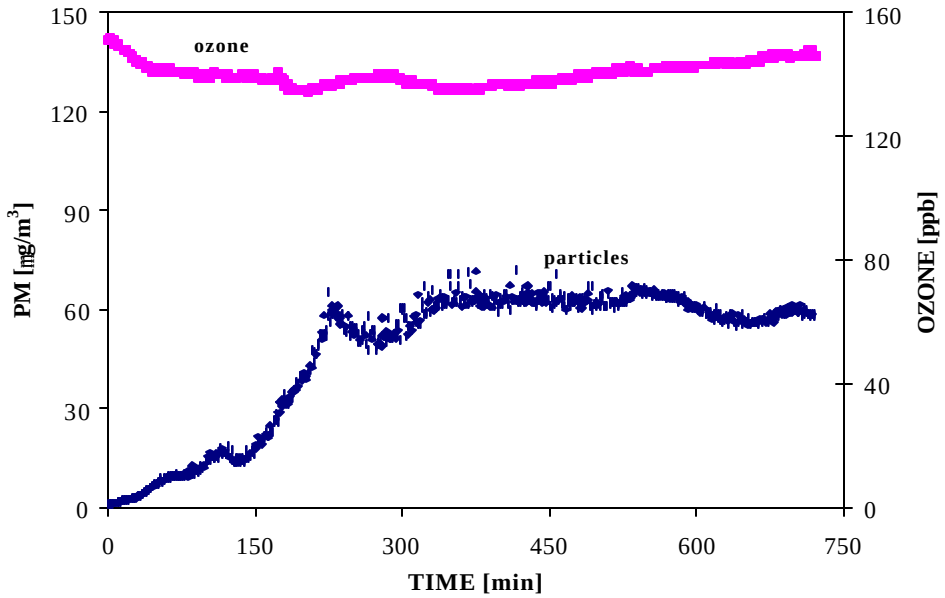

Figure E-10. Evolution of particle mass and ozone concentrations during experiment #15. l = 1.17 hr^{1}

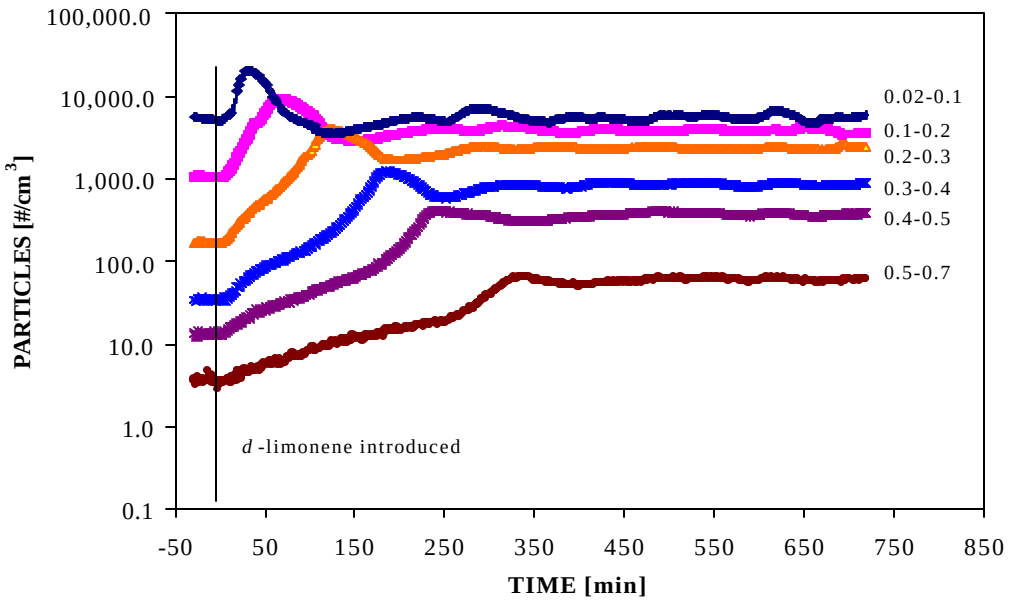

Figure E-11. Evolution of particle number concentrations during experiment #16. l = 1.21 hr^{-1}

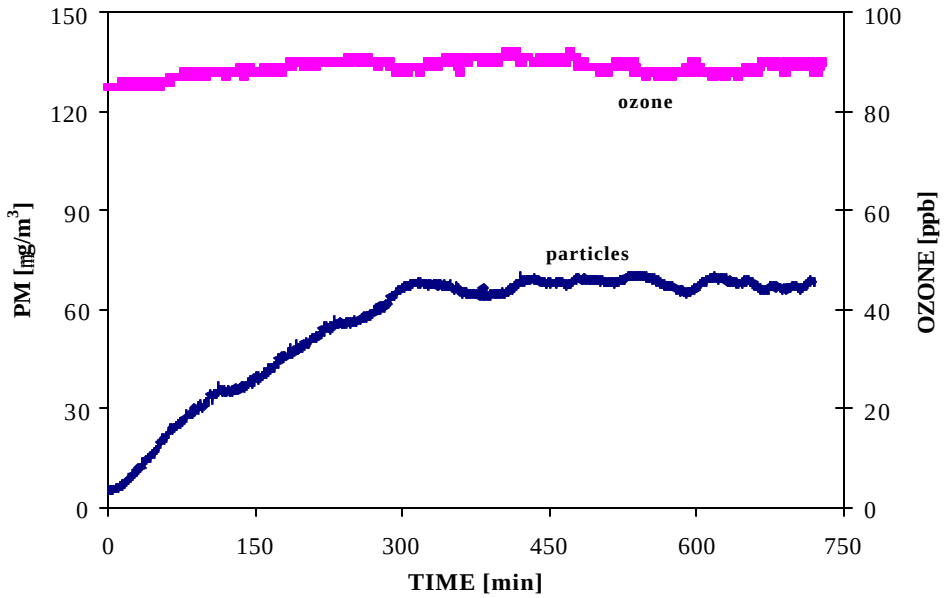

Figure E-12. Evolution of particle mass and ozone concentrations during experiment #16. l = 1.21 hr^{-1}

REFERENCES

Abt, E., Suh, H.H., Catalano, P., and Koutrakis, P., 2000. Relative Contribution of Outdoor and Indoor Particle Sources to Indoor Concentrations. *Environmental Science & Technology*, 34: 3579-3587.

Arey, J., Atkinson, R., Aschmann, A.M., 1990. Product Study of the Gas-Phase Reactions of Monoterpenes With the OH Radical in the Presence of NO_x. *Journal of Geophysical Research*, 95: 18,539-18,546.

Atkinson, R., 1994. Gas-phase Tropospheric Chemistry of Organic Compounds. *Journal of Physical Chemistry, Ref. Data, Monogram No. 2, 1-216.*

Baek, S.O., Kim, Y.S., and Perry, R., 1997. Indoor Air Quality in Homes, Offices, and Restaurants in Korean Urban Areas - Indoor/Outdoor Relationships. *Atmospheric Environment*, 31: 529-544.

Beckett, W.S., Russi, M.B., Haber, A.D., Rivkin, R.M., Sullivan, J.R., Tameroglu, Z., Mohsenin, V., and Leaderer, B.P., 1995. Effects of Nitrous Acid on Lung Function in Asthmatics: A Chamber Study. *Environmental Health Perspectives,* 103: 372-375.

Black, M.S. and Worthman, A.W. 1999. Emissions from Office Equipment. In: Raw, G., Aizlewood, C., and Warren, P. (eds) *Indoor Air 99*. Vol 2, London, Construction Research Communications Ltd., 454-459.

Brauer, M., Koutrakis, P., Keeler, G.J., and Spengler, J.D., 1991. Indoor and Outdoor Concentrations of Inorganic Acidic Aerosols and Gases. *Journal of Air and Waste Management Association*, 41: 171-181.

Brauer, M., Rasmussen, T.R., Kjaergaard, S., and Spengler, J.D., 1993. Nitric Acid Formation in an Exposure Chamber. *Indoor Air 3*:94-105.

Brickus, L.S.R., Cardoso, J.N., and Neto, F.R.D.A., 1998. Distributions of Indoor and Outdoor Air Pollutants in Rio de Janerio, Brazil: Implications to Indoor Air Quality in Bayside Offices. *Environmental Science & Technology*, 32: 3485-3490.

Brown, S.K, Sim, M.R., Abramson, M.J., and Gray, C.N., 1994. Concentrations of Volatile Organic Compounds in Indoor Air - A Review. Indoor Air, 4: 123-134.

Calogirou, A., Larsen, B.R., and Kotzias, D., 1999. Gas Phase Terpene Oxidation Products: a Review. *Atmospheric Environment*, 33: 1423-1439.

Carter, W. P. L., 1988. Documentation for the SAPRC Atmospheric Photochemical Mechanism Preparation and Emissions Processing Programs for Implementation in Airshed Models, Report, California Air Resources Board, Contract A5-122-32, October.

Carter, W. P. L., 2000. Documentation of the SAPRC-99 Chemical Mechanism for VOC Reactivity Assessment, Report to California Air Resources Board, Contract 92-329 and 95-308, May 8.

Carter, W.P.L. and Lurman, F.W., 1991. Evaluation of a Detailed Gas-Phase Atmospheric Reaction Mechanism Using Environmental Chamber Data. *Atmospheric Environment*, 25A, 2771.

Clausen, P.A., Wilkins, C.K., Wolkoff, P., and Nielsen, G.D., 2001. Chemical and Biological Evaluation of a Reaction Mixture of R-(+)-Limonene/Ozone, Formation of Strong Airway Irritants. *Environment International*, 26: 511-522.

Clayton, C.A., Perritt, R.L., Pellizzari, E.D., Thomas, K.W., Whitemore, R.W., Ozkaynak, H., Spengler, J.D., and Wallace, L.A., 1993. Particle Total Exposure Assessment Methodology (PTEAM) Study: Distributions of Aerosols and Elemental Concentrations in Personal, Indoor, and Outdoor Air Samples in a Southern California community. *Journal of Exposure Analysis and Environmental Epidemiology*, 3:227-250.

Daisey, J.M., Hodgson, A.T., Fisk, W.J., Mendell, M.J., and Brinke, J.T., 1994. Volatile Organic Compounds in Twelve California Office Buildings: Classes, Concentrations, and Sources. *Atmospheric Environment*, 28: 3557-3562.

Diemel, J.A.L., Brunekreef, B., Boleji, J.S.M., Biersteker, K., and Veenstra, S.J., 1981. The Arnhem Lead Study II: Indoor Pollution and Indoor-Outdoor Relationship. *Environmental Research*, 25:449-456.

Eusebi, A., 1996. Composition of Aerosol Formed by the Reactions of Hydrocarbons in Urban Atmospheres: Smog Chamber and Field Measurements. PhD Dissertation, University of California, Los Angeles.

Fan, Z., 2002. Environmental and Occupational Health Sciences Institute, UMDNJ-Robert Wood Johnson Medical School, New Jersey, personal communication.

Fellin, P., and Ottson, R., 1994. Assessment of the Influence of Climatic Factors on Concentration Levels of Volatile Organic Compounds in Canadian Homes. *Atmospheric Environment*, 28: 3581-3586.

Finlayson-Pitts, B.J. and Pitts, J.N., 1996. Atmospheric Chemistry, John Wiley & Sons, New York

Finlayson-Pitts, B.J. and Pitts, J.N., 2000. Chemistry of the Upper and Lower Atmosphere : Theory, Experiments, and Applications, Academic Press.

Gebefuegi, I.L., Loerinci, G.L, and Kettrup, A., 1995. Infiltration of VOCs from Outdoor Air: An Indoor-Outdoor Comparison. In: L. Morawska, N.D. Bofinger, and M. Maroni, (eds), Indoor Air: An Integrated Approach, Elsevier Science.

Glasius, M., Lahaniati, M., Calogirou, A., Bella, D., Jensen, N., Hjorth, J., Kotzias, D., and Larsen, B., 2000. Carboxylic Acids in Secondary Aerosols from Oxidation of Cyclic Monoterpenes by Ozone. *Environmental Science & Technology*, 34, 1001-1010.

Gold, D.R., Allen, G., Damokosh, A., Serrano, P., Hayes, C., and Castillejos, M., 1999. Comparison of Outdoor and Classroom Ozone Exposures for School Children in Mexico City. *Journal of Air & Waste Management Association*, 46: 335-342.

Grosjean, D., Williams, E., and Seinfeld, J.H., 1992. Atmospheric Oxidation of Selected Terpenes and Related Carbonyls: Gas Phase Carbonyl Products. *Environmental Science & Technology*, 26: 1526-1533.

Grosjean, D., Williams, E., Grosjean, E., Andino, J.M., and Seinfeld, J.H., 1993. Atmospheric Oxidation of Biogenic Hydrocarbons: Reactions of Ozone with *b*-Pinene, *d*-Limonene and *trans*-Caryophyllene. *Environmental Science & Technology*, 27: 2754-2758.

Hakola, H., Arey, J., Aschmann, S., and Atkinson, R., 1994. Product Formation from the Gas-Phase Reactions of OH Radicals and O_3 with a Series of Monoterpenes. *Journal of Atmospheric Chemistry*, 18, 75-102.

Hales, C.H., Rollinson, A.M., and Shair, F.H., 1974. Experimental Verification of Linear Combination Model for Relating Indoor-Outdoor Pollutant Concentrations. *Environmental Science and Technology*, 8: 452-453.

Hayes, S.R., 1991. Use of an Indoor Air Quality Model (IAQM) to Estimate Indoor Ozone Levels. *Journal of Air & Waste Management Association*, 41: 161-170.

Hinds, W. C., 1982. Aerosol Technology: Properties, Behavior, and Measurements of Aerosol Particles, Wiley-Interscience Publication.

Jenkins, P.L., Philips, T.J., Mulberg, E.J., and Hui, S.P., 1992. Activity Patterns of Californians: Use of and Proximity to Indoor Pollutant Sources. *Atmospheric Environment*, 26A: 2141-2148.

Jensen, B. and Wolkoff, P., 1996. *VOCBASE* Version 2.1, National Institute of Occupational Health, Denmark.

Jones, N.C., Thornton, C.A., Mark, D., and Harrison, R.M., 2000. Indoor/Outdoor Relationships of Particulate Matter in Domestic Homes with Roadside, Urban and Rural Locations. *Atmospheric Environment*, 34: 2603-2612.

Kamens, R., Jang, M., Chien, C. J., and Leach. K., 1999. Aerosol Formation from the Reaction of α-Pinene and Ozone Using a Gas-Phase Kinetics-Aerosol Partitioning Model. *Environmental Science and Technology*, 33:1430-1438.

Kaufman, J.E. and Christensen, J.F., 1987. IES Lighting Handbook, Illuminating Engineering Society of North America.

Kim, Y.S. and Stock, T.H., 1986. House-Specific Characterization of Indoor and Outdoor Aerosols. *Environment International*, 12:75-92.

Klepeis, N.E., and Tsang, T.E., 1996. Analysis of National Human Activity Pattern Survey (NHAPS) Respondents from a Standpoint of Exposure Assessment, Office of Research and Development, US Environmental Protection Agency, EPA/600/R-96/074.

Lee, K.W. and Chen, H., 1984. Coagulation Rate for Polydisperse Particles. *Aerosol Science and Technology*, 3: 327-334.

Lee, S. and Chan, L., 1998. Indoor/Outdoor Air Quality Correlation and Questionnaire Survey at Two Staff Quarters in Hong Kong. *Environment International*, 24: 729-737.

Lee, K., Vallarino, J., Dumyahn, T., Ozkaynak, H., and Spengler, J.D., 1999. Ozone Decay Rates in Residences. *Journal of Air & Waste Management Association*, 49: 1238-1244.

Lee, K., Xue, J., Spengler, J.D., Ozkaynak, H., and Leaderer, BP., 1999. In Indoor Air 99. Vol 3, Raw, G., Aizlewood, C., and Warren, P., Eds. London pp 141-146.

Li, Y. and Harrison, R.M., 1990. Comparison of Indoor and Outdoor Concentrations of Acid Gases, Ammonia and Their Associated Salts. *Environmental Technology*, 11: 315-326.

Li, T.H., Shields, H.C., Turpin, B.J., and Weschler, C.J., 2001. Submitted for publication.

Liu, D. and Nazaroff, W.W., 2001. Modeling Pollutant Penetration across Building Envelopes, *Atmospheric Environment*, 35: 4451-4462.

Long, M.C., Suh, H.H., and Koutrakis, P., 2000. Characterization of Indoor Particle Sources Using Continuous Mass and Size Monitors. *Journal of Air & Waste Management Association*, 50: 1236-1250.

Long, C.M., Suh, H.H., Kobzik, L., Catalano, P.J., Ning, Y.Y., and Koutrakis, P., 2001. A Pilot Investigation of the Relative Toxicity of Indoor and Outdoor Fine Particles: In Vitro Effects of Endotoxin and Other Particulate Properties. *Environmental Health Perspectives*, 109: 1019-1026.

Molhave, L., Kjaergaard, S., Hempel-Jorgensen, A., Juto, J.E., Andersson, K., Stridh, G., and Falk, J., 2000. The Eye Irritation and Odor Potencies of Four Terpenes Which are Major Constituents of the Emissions from Nordic Soft Woods. *Indoor Air*, 10: 315-318

Morrison, G.C. and Nazaroff, W.W., 1999. In *Indoor Air 99*, Vol 4. Raw, G., Aizelwood, C., and Warren, P., eds. London. pp 664-669.

Morrison, G.C. and Nazaroff, W.W., 2000. The Rate of Ozone Uptake on Carpets: Experimental Studies. *Environmental Science & Technology*, 34: 4963-4968.

Mosley, R.B., Greenwell, L.E., Sparks, L.E., Guo, Z., Tucker, W.G., Fortmann, R., and Whitfield, C., 2001. Penetration of Ambient Fine Particles into the Indoor Environment. *Aerosol Science and Technology*, 34: 127-136.

Mueller, F.X., Loeb, L., and Mapes, W.H., 1973. Decomposition Rates of Ozone in Living Areas. *Environmental Science and Technology*, 7: 342-346.

Murray, D.M., and Burmaster, D.E., 1995. Residential Air Exchange Rates in the United States: Empirical and Estimated Parametric Distribution by Season and Climactic Region. *Risk Analysis,* 15: 459-465.

Nazaroff, W.W. and Cass, G.R., 1986. Mathematical Modeling of Chemically Reactive Pollutants in Indoor Air. Environmental Science & Technology, 20: 924-934

Pandis, S.N., Harley, R.A., Cass, G.R., and Seinfeld, J.H., 1992. Secondary Organic Aerosol Formation and Transport. Environmental Science & Technology, 26A: 2269-2282.

Pankow, J., 1994. An Absorption Model of Gas/Particle Partitioning of Organic Compounds in the Atmosphere. *Atmospheric Environment*, 28:185-188.

Paulson S.E., Chung, M.Y., and Hasson, A.S., 1999. OH Radical Formation from the Gas-Phase Reaction of Ozone with Terminal Alkenes and the Relationship between Structure and Mechanism. *The Journal of Physical Chemistry A*, 103: 8125-8138.

Phillips, J.L., Field, R., Goldstone, M., Reynolds, G.L., Lester, J.N., and Perry, R, 1993. Relationships between Indoor and Outdoor Air Quality in Four Naturally Ventilated Offices in the United Kingdom. *Atmospheric Environment*, 27A(11): 1743-1753.

Pitts, J.N., Wallington, T.J., Biermann, H.W., and Winer, A.M., 1985. Identification and Measurement of Nitrous Acid in an Indoor Environment. *Atmospheric Environment,* 19:763-767.

Pope, A. and Dockery, D., 1996. Epidemiology of Chronic Health Effects: cross-sectional Studies. In: Wilson, R., Spengler, J.D., (eds). Particles in Our Air: Concentrations and Health Effects. Harvard University Press.

Rasmussen, T.R., Brauer, M., and Kjaergaard, S., 1995. Effects of Nitrous Acid Exposure on Human Mucous Membranes. *American Journal of Respiratory and Critical Care Medicine,* 151:1504-1511.

Robinson, J.P., Thomas, J., and Behar, J.V. , 1991. Report to the United States Environmental Protection Agency under Contract No. 69-01-7324, Delivery Order 12, Exposure Assessment Research Division, National Exposure Research Center, USEPA, Las Vegas, NV.

Rohr, A.C., Weschler, C.J., Koutrakis, P., and Spengler, J.D., 2001. Generation and Quantification of Ultrafine Particles Through Terpene/Ozone Reactions in a Chamber Setting. *Aerosol Science and Technology*, Submitted.

Rothweiler, H., Wager, P.A., and Schlatter, C., 1992. Volatile Organic Compounds and Some Very Volatile Organic Compounds in New and Recently Renovated Buildings in Switzerland. *Atmospheric Environment*, 26A: 2219-2225.

Ruppert L., Becker K.H., Noziere B., and Spittler M., 1999. Development of Monoterpene Oxidation Mechanisms: Results from Laboratory and Smog Chamber Studies. In: Borrell, P.M., Borrell, P. editors. Proceedings of the EUROTRAC Symposium '98, Southhampton: WIT press, pp 63-68.

Saarela, K., 1999. Emissions from Floor Coverings. In: Salthammer, T., (ed). Organic Indoor Air Pollutants, Occurrence, Measurements, Evaluation, Wiley-VCH.

Sabersky, R.H., Sinema, D.A., and Shair, F.H., 1973. Concentrations, Decay rates, and Removal of Ozone and Their Relation to Establishing Clean Indoor Air. *Environmental Science and Technology*, 7: 347-353.

Salthammer, T., 1999. Volatile Organic Ingredient of Household and Consumer Products. In: Salthammer, T., (ed). Organic Indoor Air Pollutants, Occurrence, Measurements, Evaluation, Wiley-VCH.

Santannam, S., Spengler, J.D., and Ryan, P.B., 1990. *Proceedings of Indoor Air 1990*, 583-588.

Schuetzle, D., and Rasmussen, R.A., 1978. Molecular Composition of Secondary Aerosol Particles Formed from Terpenes. *Journal of Air Pollution Control Association, 28: 236-240*.

Seinfeld, J.H. and Pandis, S.N., 1998. Atmospheric Chemistry and Physics, Wiley Interscience.

Sexton, K., Spengler, J.D., and Trietman, R.D., 1984. Personal Exposure to Respirable Particles: a Case Study in Waterbury, Vermont. *Atmospheric Environment*, 18:1385-1398.

Shah, J. J. and Singh, H. B., 1988. Distribution of Volatile Organic Chemicals in Outdoor and Indoor Air. *Environmental Science & Technology*, 22: 1381-1388.

Shair, F.H. and Heitner, K.L., 1974. Theoretical Model for Relating Indoor Pollutant Concentrations to Those Outside. *Environmental Science and Technology,* 8: 444-451.

Shaughnessey, R.J., Weschler, C.J., Sextro, R.G., and Aglave, R., 1999. Growth of Sub-micron Particles as a Consequence of Ozone/Surface Reactions: Preliminary Data. *Proceedings of Indoor Air 99, the 8th International Conference on Indoor Air Quality and Climate* (Edinburgh, Scotland), 4: 1072-1077.

Shaughnessey, R.J., McDaniels, T.J., and Weschler, C.J., 2001. Indoor Chemistry: Ozone and Volatile Organic Compounds Found in Tobacco Smoke. *Environmental Science & Technology,* 35: 2758-2764.

Sheldon, L.S., Hartwell, T.D., Cox, B.G., Sickles II, J.E., Pellizzari, E.D., Smith, M.L., Perritt, R.L., and Jones, S.M., 1989. An investigation of infiltration and indoor air quality. Final Report. NY State ERDA Contract No. 736-CON-BCS-85. New York State Energy Research and Development Authority. Albany, New York.

Spengler, J.D., Dockery, D.W., Turner, W.A., Wolfson, J. M., and Ferries, B.G., 1981. Long Term Measurements of Respirable Sulfates and Particles Inside and Outside Homes. *Atmospheric Environment*, 15: 123-130.

Spicer, C.W., Kenny, D.V., Ward, G.F., and Billick, I.H., 1993. Transformations, Lifetimes, and Sources of NO_2, HONO, and HNO_3 in Indoor Environments. *Journal of Air & Waste Management Association, 43*:1479-1485.

Stabel, J.R. and Wolkoff, P., 1999. Preliminary Studies on Simulation of the Isoprene Chemistry in Indoor Air. Proceedings of the 8th International Conference on Indoor Air Quality and Climate, 4:743-748, Edinburgh, Scotland.

Tanner, J.D. and Eisele, F.L., 1995. Present OH Measurement Limits and Associated Uncertainties. *Journal of Geophysics*, 100: 2883-2892.

Tropp, R.J., Kohl, S.D., Chow, J.C., and Frazier, C.A., 1998. Final Report for the Texas $PM_{2.5}$ Sampling and Analysis Study, Document No. 6570-685-7770.1F, Prepared for Bureau of Air Quality, City of Houston, December 15.

Turk, B.H., Grimsrud. D.T., Brown, J.T., Geisling-Sobotka, K.L., Harrison, J. and Prill, R.J., 1986. Commercial Building Ventilation Rates and Particle Concentrations. *ASHRE Transaction,* 95:422-433.

Turpin, B.J and Lim, H.J. 2001. Species Contribution to PM2.5 Mass Concentrations: Revisiting Common Assumptions for Estimating Organic Mass. *Aerosol Science and Technology*, 35: 602-610.

United States Environmental Protection Agency, Federal Register, Volume 62, No. 138, Friday July 18, 1997.

United States Environmental Protection Agency, 1998. Inside IAQ, EPA/600/N-98/002.

Wainman, T., 1996. Use of a Two Tiered Dynamic Chamber to Investigate Indoor Air Chemistry, PhD Dissertation. The State University of New Jersey, Rutgers.

Wainman, T, Zhang, J., Weschler, C. J., and Lioy, P. J., 2000. Ozone and Limonene in Indoor Air: A Source of Submicron Particle Exposure. *Environmental Health Perspectives*, 108: 1139-1145.

Wallace, L., Nelson, C.W., and Pellizzari, E., 1991. Identification of Polar Volatile Organic Compounds in Consumer Products and Common Microenvironments. In *Proceedings of the Air and Waste Management Association's 1991 Annual Meeting*.

Wallace, L., 1996. Indoor Particles: a Review. *Journal of Air & Waste Management Association*, 46: 98-126.

Weschler, C.J., Shields, H.C., and Naik, D.V., 1989. Indoor Ozone Exposures. *Journal of Air Pollution Control Association, 39: 1562-1568.*

Weschler, C.J., Shields, H.C., and Rainer, D., 1990. Concentrations of Volatile Organic Compounds at a Building with Health and Comfort Complaints. *American Industrial Hygiene Association Journal, 51: 261-268.*

Weschler, C.J., Brauer, M., and Koutrakis, P., 1992a. Indoor Ozone and Nitrogen Dioxide: A Potential Pathway to the Generation of Nitrate Radicals, Dinitrogen Pentaoxide, and Nitric Acid Indoors. *Environmental Science & Technology*, 26: 179-184.

Weschler, C.J., Hodgson, A.T., and Wooley, J.D., 1992b. Indoor Chemistry: Ozone, Volatile Organic Compounds, and Carpets. *Environmental Science & Technology*, 26: 2371-2377.

Weschler, C.J. and Shields, H.C., 1996. Production of the Hydroxyl Radical in Indoor Air. *Environmental Science & Technology*, 30:3250-3258.

Weschler, C.J. and Shields, H.C., 1997a. Potential Reactions among Indoor Pollutants. *Atmospheric Environment, 31: 3487-3495.*

Weschler, C.J. and Shields, H.C., 1997b. Measurements of the Hydroxyl Radical in a Manipulated but Realistic Environment. *Environmental Science & Technology*, 31: 3719-3722.

Weschler, C.J., and Shields, H.C., 1999. Indoor Ozone/Terpene Reactions as a Source of Indoor Particles. *Atmospheric Environment, 33:* 2301-2312.

Weschler C.J., 2000. Ozone in Indoor Environments: Concentrations and Chemistry. *Indoor Air*, 10: 69-288.

Weschler C.J., 2001. Reactions among Indoor Pollutants. *The Scientific World*, 1: 443-457.

Weschler, C.J. and Shields, H.C., 2002. Experiments Probing the Influence of Air Exchange Rates on Particles Generated by Indoor Chemistry. Submitted to the 9th International Conference on Indoor Air Quality and Climate, Monterey, California.

Wisthaler A., Jensen N.R., Winterhalter, R., Lindinger, W., and Hjorth J., 2001. Measurements of Acetone and Other Gas Phase Product Yields from the OH-Initiated Oxidation of Terpenes by Proton-Transfer-Reaction Mass Spectrometry (PTR-MS). *Atmospheric Environment*, 35: 6181-6191.

Wolkoff, P., Clausen, P.A., Wilkins, C.K., Hougaard, K.S., Larsen, S.T., and Nielsen, G.D., 1999. Formation of Strong Airway Irritants in Terpene/Ozone Mixture. Proceedings of the 8th International Conference on Indoor Air Quality and Climate, 4: 495-498, Edinburgh, Scotland.

Yocum, J.E., 1971. *Journal of Air Pollution Control Association*, 21:251.

Zhang, J, He, Q., and Lioy, P. J., 1994. Characteristics of Aldehydes: Concentrations, Sources, and Exposures for Indoor and Outdoor Residential Microenvironments. *Environmental Science & Technology*, 28:146-152.

VITA

Md Golam Sarwar was born in Pabna, Bangladesh on August 15, 1963, the eldest son of Noor Mohammad and Sahera Khatun. He entered into Bangladesh University of Engineering and Technology in August 1982 and received a Bachelor of Science Degree in Mechanical Engineering in May of 1987. He then entered into the Graduate School of Bangladesh University of Engineering and Technology and received a Master's of Science Degree in Mechanical Engineering in January of 1989. He entered the Gradate School of the University of Texas at Austin in January 1989 and received a Master's of Science Degree in Engineering in December of 1991. He worked as an air quality engineer with the Texas Natural Resource Conservation Commission in Texas and Union Carbide Corporation in Louisiana for eight years. He returned to the Gradate School of the University of Texas at Austin in summer of 2000 as a full-time graduate student. He is a registered professional engineer.

Permanent address: 1000 Brown Drive, Pflugerville, Texas 78660

This dissertation was typed by the author.